



# NUCLEAR ELECTRONICS & COMPUTING

# NEC'2009

Proceedings
of the XXII International Symposium

Joint Institute for Nuclear Research



# NUCLEAR ELECTRONICS & COMPUTING

XXII International Symposium

Varna, Bulgaria, September 7–14, 2009

Proceedings of the Symposium

# NEC'2009

# ЯДЕРНАЯ ЭЛЕКТРОНИКА И КОМПЬЮТИНГ

XXII Международный симпозиум

Варна, Болгария, 7–14 сентября 2009 г.

Труды симпозиума



Дубна, 2010

УДК [539.12+539.14] : [621.38+004.7+004.6] (063)
ББК 22.38я431+22.381.9я431+32.973.2–018я431
N91

The contributions are reproduced directly from the originals presented by the Organizing Committee.

N91 **Nuclear** Electronics & Computing (NEC'2009): Proceedings of the XXII International Symposium (Varna, Bulgaria, September 7–14, 2009). — Dubna: JINR, 2010. — 306 p.

ISBN 978-5-9530-0242-4

The Proceedings of the XXII International Symposium on Nuclear Electronics & Computing (NEC'2009) contain the papers presented at NEC'2009, which was held on 7–14 September 2009 (Varna, Bulgaria). The Symposium is organized by the Joint Institute for Nuclear Research (Dubna), the European Organization for Nuclear Research (CERN) (Geneva) and the Institute for Nuclear Research and Nuclear Energy of the Bulgarian Academy of Sciences (Sofia). It was devoted to the problems of detector & nuclear electronics, computer applications for measurement and control in scientific research, triggering and data acquisition, methods of experimental data analysis, computing & information systems, computer networks for scientific research, and GRID computing.

**Ядерная** электроника и компьютинг (NEC'2009): Труды XXII Международного симпозиума (Варна, Болгария, 7–14 сентября 2009 г.). — Дубна: ОИЯИ, 2010. — 306 с.

ISBN 978-5-9530-0242-4

Труды XXII Международного симпозиума по ядерной электронике и компьютингу (NEC'2009) содержат доклады, представленные на NEC'2009, который проходил 7–14 сентября 2009 г. в Варне (Болгария). Симпозиум организован Объединенным институтом ядерных исследований (Дубна), Европейской организацией ядерных исследований (ЦЕРН) (Женева) и Институтом ядерных исследований и ядерной энергетики Болгарской академии наук (София). Он был посвящен проблемам детекторной и ядерной электроники, применению вычислительной техники для измерений и контроля в научных исследованиях, системам сбора данных, системам автоматизации экспериментальных установок, методам анализа экспериментальных установок, вычислительным и информационным системам, проблемам локальных и глобальных коммуникаций и GRID-технологиям.

**УДК [539.12+539.14] : [621.38+004.7+004.6] (063)**
**ББК 22.381я431+22.381.9я431+32.973.2–018я431**

**ISBN 978-5-9530-0242-4**

# General Information

The XXII International Symposium on Nuclear Electronics and Computing (NEC'2009) was held on 7–14 September 2009 in Varna, Bulgaria. The symposium was organized by the Joint Institute for Nuclear Research (JINR) (Dubna, Russia), European Organization for Nuclear Research (CERN) (Geneva, Switzerland) and the Institute for Nuclear Research and Nuclear Energy of the Bulgarian Academy of Sciences (INRNE) (Sofia, Bulgaria). About 100 scientists from 13 countries (Russia, Bulgaria, Switzerland, Czech Republic, Poland, Belarus, Serbia, Slovakia, France, USA, Italy, Vietnam and Ukraine) have participated in NEC'2009. They have presented 56 oral reports and 26 posters.

**Organizing Committee**

**JINR (Dubna)**

V.V. Korenkov - co-chairman, E.A. Tikhonenko (scientific secretary), A. Chepigin, N.V. Gorbunov, R. Kalpakchieva, V.K. Novikova, Y.K. Potrebenikov, V.I. Prikhodko, T.A. Strizh, N.I. Zhuravlev

**CERN (Geneva)**

S. Citollin - co-chairman, T. Kurtyka, P. Hristov

**INRNE (Sofia)**

I.D. Vankov - co-chairman, A. Anguelov (secretary), L.P. Dimitrov, H. Shukov

**International Program Committee**

O. Abdinov (IoP, Baku), F. Adilova (IM&IT, AS, Tashkent), I. Bird (CERN, Geneva), F.D. Buzatu (IFA, Magurele-Bucharest), J. Elias (FNAL, Chicago), I. Golutvin (JINR, Dubna), H.F. Hoffmann (ETH, Zurich), V. Ilyin (SINP MSU, Moscow), V. Ivanov (JINR, Dubna), B. Jones (CERN, Geneva), D. Fursaev (Dubna University), G. Kryuchkyan (YSU, Yerevan), M. Lokajicek (IP ASCR, Prague), L. Mapelli (CERN, Geneva), G. Mitselmakher (UF, Gainesville), V.A. Petukhov (IHEP, Protvino), V. Shirikov (JINR, Dubna), A.N. Sissakian (JINR, Dubna), N. Shumeiko (NSECPHEP, Minsk), I. Stamenov (INRNE, Sofia), M. Turala (IFJ PAN, Krakow), A. Vaniachine (ANL, Argonne), G. Zinovjev (ITP, Kiev).

**MAIN TOPICS**

- Detector & Nuclear Electronics;
- Computer Applications for Measurement and Control in Scientific Research;
- Triggering and Data Acquisition;
- Accelerator and Experiment Automation Control Systems;
- Methods of Experimental Data Analysis;
- Information & Data Base Systems;
- Computer Networks for Scientific Research;
- Data & Storage Management;
- GRID computing.

# CONTENTS

# Prague Tier2 Computing Centre evolution

D. Adamova[1], L. Fiala, J. Horky, J. Chudoba, T. Kouba, J. Kundrat,
M. Lokajicek, J. Svec
*Institute of Physics AS CR and CESNET*
[1] *Nuclear Physics Institute, AS CR*

Czech Tier2 WLCG centre is located in the Regional Computing Centre for Particle Physics in the Institute of Physics of the Academy of Sciences of the Czech Republic in Prague. The centre evolved from D0 experiment simulation activity using a couple of personal computers to participation on the international GRID projects EDG, EGEE and WLCG. The centre computing and storage capacity slowly grew together with highly qualified and dedicated team of specialists. After a few years of regular investments into the centre computing hardware new electrical and cooling problems must be solved. The evolution of the centre capacities, monitoring, management and networking will be shown as well as its contribution to the collaborating experiments.

## 1. Introduction

Basic information, time development and contributions to experiments of the Prague Tier2 centre will be given in paragraph 2. Next paragraph will describe current computing and networking infrastructure of the centre. In the fourth paragraph, basic software infrastructure is described and conclusions are brought in the fifth paragraph.

## 2. Basic information and the time evolution

The Tier2 centre in Prague is located in the Regional Computing Centre for Particle Physics in the Institute of Physics of the Academy of Sciences of the Czech Republic. Main activities of the Institute of Physics are in the basic research in particle and solid state physics and optics. The Regional Computing Centre for Particle Physics is contributing in the framework of collaborations on the particle and nuclear physics and astro-particle physics international experiments to their high throughput computing needs. It also supports computing needs of solid state physics groups in the institute. The users of the centre are the mentioned big experiments and their collaborators both foreign and Czech.

We would like to acknowledge long term support of CESNET, Czech Research Network Provider that also supports novel computing services. CESNET provides special network infrastructure and computing resources described lower.

The successful delivery of simulation computing for the D0 experiment at TEVATRON in FNAL in 1998 was the stimulus to build bigger capacity for the simulation. The first results of the MONARC (Models of Networked Analysis at Regional Centres, http://monarc.web.cern.ch/MONARC/) project for the tiered structure for LHC computing and the first discussions of the grid computing in 2000 were further incentives showing that building smaller computing centre is reasonable target for contribution to the current and future experiments.

Table 1. Time evolution of the computing centre. Details are described in the text

| Year | # Cores | Storage TB | Network | Experiment |
|---|---|---|---|---|
| 1998 | Unix, Win PCs | 0,3 | TEN34>TEN155 | D0 simulation |
| 1999 | | | TEN155 | D0 |
| 2000 | 8 FZU | 1 | GEANT, Gb | D0, EDG prep. |
| 2001 | 8, 32 CESNET | 1 | | EDG |
| 2002 | 64, 32+32 | 1 | 2.5 Gb backbone in CZ | LCG |
| 2003 | | 10 | | |
| 2004 | 160, 64 | 40 | 10 Gb bb/ 2.5 Gb to Prg Tier3 | EGEE, CESNET as partner |
| 2005 | 200, 32 | | | |
| 2006 | 250, 32 | | Gb links FNAL, ASGC, FZK | |
| 2007 | 460, 32 | 60 | Gb link to BNL | |
| 2008 | 1300, 32 | 200 + 24 in Tier3 | | WLCG signed |

Together with CESNET we joined the preparation of the European DatagGrid EU project and took part in it as well as in the following grid projects EGEEx. In 2002 we joined the CERN LCG (LHC Computing Grid) project as 11$^{th}$ certified Tier2 centre, the WLCG (Worldwide LHC Computing Grid) MoU we signed only in 2008.

The time evolution is shown in Table 1. We started using few Unix computers for D0 simulations and slowly increased their number. In the year 2000 we used 8 cores and from 2001 CESNET contributed other 32 SGI cores (the second number in the # cores column is CESNET contribution). Important milestone was the construction of the new computing room by the Institute of Physics in 2004 with needed infrastructure for 180 kW electric power. The computing and storage capacity could irregularly grow from that time.

Outer networking infrastructure has been regularly upgraded by CESNET, including point-to-point optical links to other both local Prague Tier3 sites and international collaborating centres (see further).

Further evolution of the Tier2 centre comes to its electric power and cooling limits. We plan to install computing capacities in our collaborating institutions and investigate possibilities to run the Tier2 centre as distributed centre interconnected with high capacity optical network provided by CESNET.

Graph 1. Computing resources delivered by the centre for the experiments, shown in percentage of experiments total performance

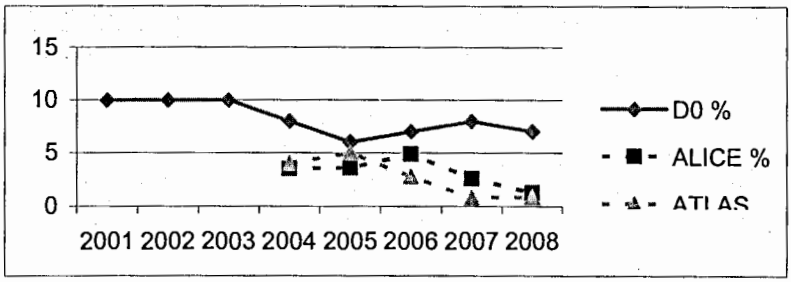


The Tier2 centre computing capacity usage is shown in the Graph 1. The early computing capacity has been delivered for the D0 simulation. We started early with substantial 10% contribution (in the number of simulated events) to the experiment. With build up of the new capacities for LHC in collaborating laboratories (used also for other purposes) our relative contribution diminished, later it stabilized on the level 6 - 7 %. Simulations for the ALICE and ATLAS experiments started again early in 2004 on the level of 4%. The relative contributions went down towards 1% in 2007 until we managed to get regular financing for the LHC computing from 2008 when we see some stabilization.

Similar behaviour is seen on the Graph 2 that shows our Tier2 contribution to the LHC experiments. The top graph shows the time evolution of the absolute contribution in thousands of computed jobs and in thousands of normalised CPUs hours delivered for the ALICE and ATLAS experiments. These numbers grow with the exceptions of the ALICE job count. Despite the absolute numbers growth, the relative contributions to the whole EGEE project dropped until 2008 when it stabilized as seen on the lower graph.

Graph 2. Upper graph: Absolute and relative contributions to the LHC experiments computing in thousands of jobs and thousands of normalized CPU hours. Lower Graph: Relative contribution to the LCG computing. Both graphs data for 2009 are for period January-August.

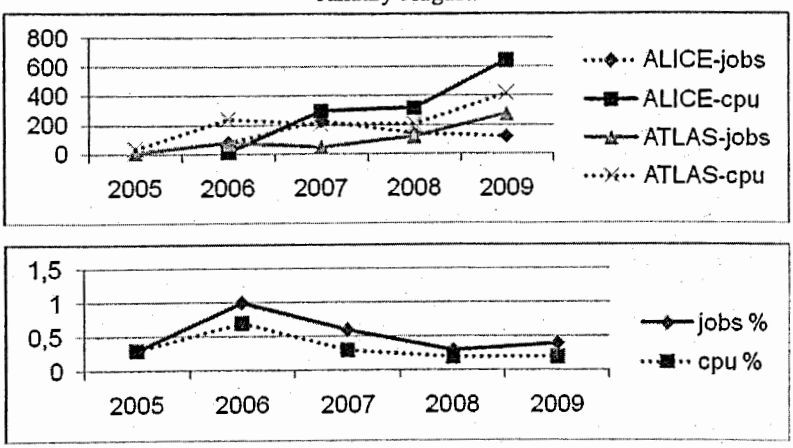

## 3. Current Computing and Networking infrastructure

The new computer room was built in 2004 with 65 $m^2$, 18 racks, electric power 180 kW, cooling capacity 110 kW, diesel 360 kW. The computing capacity in the middle of 2009 is described in Table 2 and storage capacity in Table 3. The total capacity was 17 kHepSpec with 2100 cores with 1500 cores from it for the WLCG activities. Total storage of 280 TB of the raw disk space and 100 TB of uncompressed tape space (extensible by addition of cartridges to 400 TB) is mainly for the LCG usage.

Fig. 1. The new computer room from 2004

Table 2. Computing capacity in middle 2009

| Vendor | Description |
|---|---|
| HP | Blades: BL35p (36x), BL20p (6x), BL460c (9x), BL465c (12x), HP BL 460C (10x8cores)<br><br>U1: DL140 (67x), DL145 (3x), DL360 (2x), LP1000r (34x)<br><br>Together 800 kSI2K, 3 200 HepSpec |
| SGI | Altix ICE 8200, infiniband<br>64 x 8 cores, E5420 2.5GHz, 512 GB RAM, for solid state physics<br>22.4 kW, 4 320 Spec06<br><br>Altix XE 310 (NPI)<br>40x8 cores, E5420 2.5GHz, 640 GB RAM |
| IBM | iDataPlex dx340<br>84 x 8 cores, E5440 2.83GHz,<br>1344 GB RAM, 23 kW, 6120 Spec06 |
| Total | **67 000 kSI2k, 16.8 kHepSpec, 2 100 cores from which 1500 cores for LCG** |

Table 3. Storage capacity in middle 2009

| |
|---|
| Tape Library Overland Neo 8000, LTO4, 100 TB (max non compression capacity 400 TB) with disk cache Overland , Ultamus 1200 |
| Disk array HP EVA 6000-A 2C4D Array, 80 TB |
| Disk array *EasySTOR*, 40 TB |
| Disk array VTrak M610p (CESNET), 16 TB |
| Disk Array Overland Ultamus 4800, 144 TB |
| **Together 100 TB tape space**<br>**280 TB raw disk space** |

### Electric power and cooling

Deployment of the computer equipment bought in 2008 brought us beyond the limit of available cooling capacity and close to the limit of available electric power. The computing room is equipped with the

- UPS Newave Maxi 200kVA,
- diesel F.G.Wilson 380 kVA,
- air conditioning Liebert-Hiross 2x56 kW.
- water chillers STULZ CLO 781A 2x 88 kW

The last item – water cooling was installed during 2009.The chilled water is accessible on more places in the computer room and a new water cooled equipment can be simply connected in future. Today complete cooling power is 290 kW. We can follow thus the so called N+1 rule - i.e. if one of the units stops working we should have sufficient cooling capacity. Further computing HW will be delivered in water cooled racks.

**Networking**

The production experience shows that both the internal and external network structure must have appropriate capacity to enable smooth data production.

The internal farm network has 1 Gbps infrastructure. Data servers are already connected with up to 4 gigabit links. That is why we change the internal network infrastructure to 10 Gbps in 2009. We plan to put all data servers on the local 10 Gb backbone.

CESNET has delivered a special infrastructure of external lines for the Tier2 centre. We collaborate with 5 particle physics groups in Prague. All 4 are connected via 1 Gbps link to CESNET. The link between CESNET and Institute of Physics is 10 Gbps and integrates the traffic both from the international and domestic lines. The details are visible on the Fig. 2. The Tier 2 farm is further connected to the scientific commodity internet 10 Gbps infrastructure.

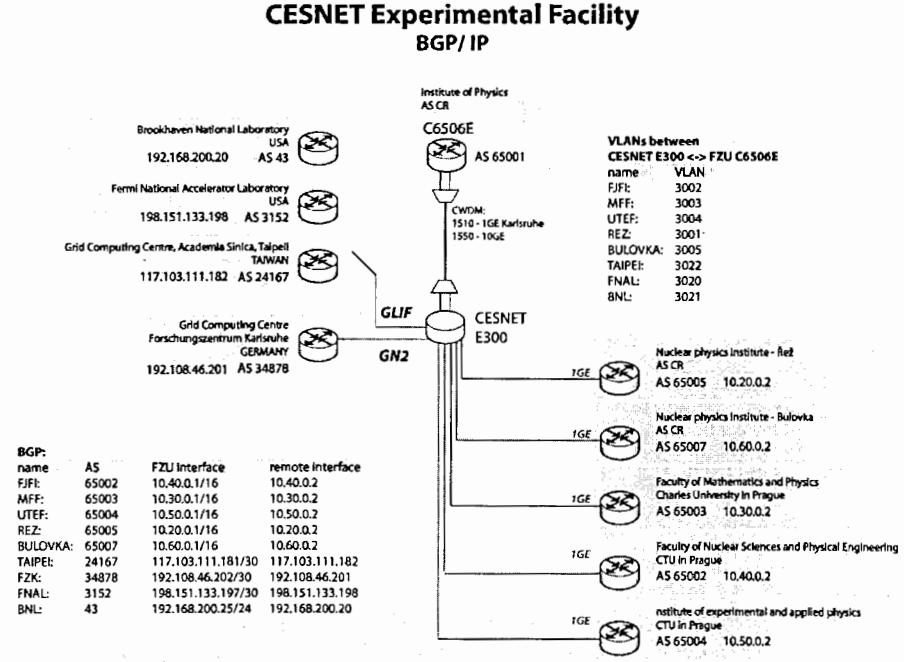


Fig. 2. External network structure of the Tier2 centre. Five gigabit links connect collaborating Tier3 groups in Prague and four international optical links connect Tier1 in FZK, Taipei, BNL and FNAL. The BNL and FNAL links are used also for STAR and D0 experiments computing.

CESNET also provides Link Monitoring System for all delivered links. It is graphical web interface that directly shows the load on all the links in both directions and gives access to big numbers of prepared graphs showing detailed lines status. The monitoring portal is accessible on the address http://www.ces.net/netreport/hep-cesnet-experimental-facility/ and shown on Fig. 3.

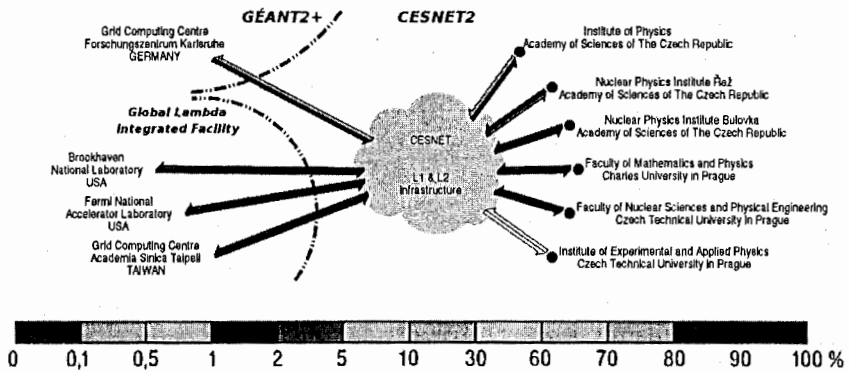


Fig. 3. CESNET monitoring system of the local and international links for Tier2

## 4. Basic software equipment, management and status monitoring

The Tier2 farm serves as WLCG centre supporting ALICE and ATLAS experiments and is further used for more other experiments. Basic operation system is Scientific Linux with current version 4.8 and 5.3 The SGI ALTIX ICE 8200 uses Scientific Linux Enterprise v. 10 delivered by SGI. We run two versions of queuing systems PBSPro server 9.2 with 480 licenses and Torque, Maui with free licences,1000 slots (free).The reason to change for Torque, Maui was the relatively high cost of the PBSPro licences per core and quick increase of number of cores with usage of new multi-core processors.

The EGEE software gLite 3.1 is available with its basic services as Computing Elements, Storage Element, sBDII, Vobox, UI. We support Virtual Organizations ATLAS, ALICE, AUGER, D0, CALICE and HONE. All users share same computing resources. The exception is SGI ALTIX ICE 8200 devoted to solid state physics computing and reserved for parallel tasks.

With higher number of computing nodes we try to automate the management and automatically run broad monitoring. We use network installation with support of the cfengine for automatic installation and configuration of individual nodes. Tools like ILO (HP), IPMI (for IBM and SGI) are used to enable both local and remote management of the computing nodes. Big number of functions and HW or SW states are permanently monitored with tools like Nagios, Ganglia, Munin, MRTG, RRD (graphs), as well as grid functions are tested with the help of the so called SAM tests. Few examples are shown in Table 4.

Table 4. Examples of monitored quantities on Tier2

| | |
|---|---|
| disk | filesystem usage (in %), IOstat |
| network | eth0 traffic, eth1 traffic, netstat, weather map |
| processes | number of processes, VMstat |
| system | CPU usage, load average, memory usage |
| sensors | HDD temperature |
| UPS, diesel, cooling, temperatures, ... | |

If a warning appears it is sent-out in condensed form and non-repeatedly to responsible staff. Long term graphs of all quantities are available. As an example a memory usage of one computing node is shown on the Graph 3.

Graph 3. Example of the memory status of one computing node

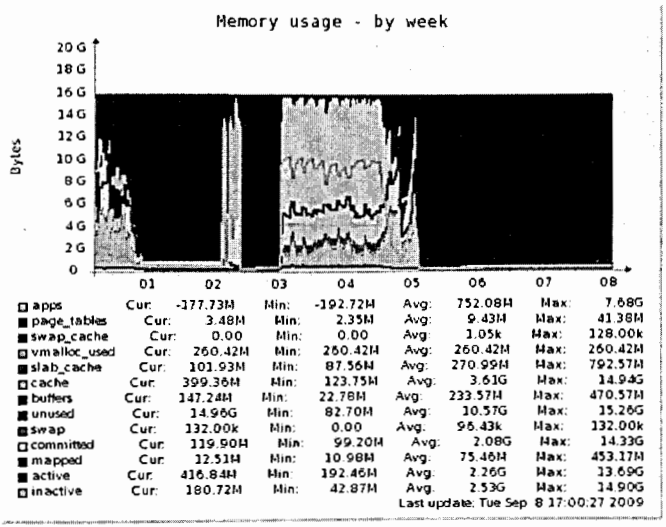


**Services failover**

The important topic of the service stability and sustainability is service failover. Generally, we try to run more instances of any service, if possible – like DNS, LDAP, computing element (CE), User Interface (UI) or DHCP servers. For storage we use dual connections over fibre channel. Services that can't be run in parallel are deployed on virtual machines, allowing us to migrate them if needed. For a special hardware (e.g. special interfaces) we keep a hardware copy that can be quickly deployed.

**Conclusion**

Prague Tier2 centre has been certified very early as 11$^{th}$ LCG centre. It quickly delivered services to D0, ALICE and ATLAS experiments. With later quick growth of other international centres its contribution of computing services to experiments decreased (except of D0). Only in 2008 we managed to assure financial resources for centre development for the WLCG for 5 years and its contribution quickly stabilized and we hope it will grow.

With new financial resources we immediately encountered problems with cooling and electric power that were solved with tripling the cooling capacity via addition of the liquid cooling system for rack cooling. For the UPS capacity, we will test using the working nodes without the UPS for future HW additions. In longer term we will investigate possibility to run the computing HW in Tier3 sites as distributed Tier2.

Prague Tier2 centre is a reliable higher capacity centre delivering stable services to number of international particle physics, astro-particle physics as well as parallel computing capacity for solid state physics groups.

# Grid development in Uzbekistan: current status and planned tasks

F.T. Adilova, R.K. Bazarov, A.D. Akhmedov, R.Sh. Ibragimov
*Institute of Mathematics and Information Technologies, NAS, Tashkent, Uzbekistan*

DREAMS_ASIA project funding by NATO is the first and, so far, the only grid project in Uzbekistan. At present we have deployed an independent educational grid site using gLite middleware with own Certificate Authority and other information services.

There are two tasks that planned to be completed in nearest future on the grid site. The first one is to deploy local bioinformatics platforms to process and store biological sequences for solving problems of structural genomics. At the same time the work is going on creation of a prototype of telemedicine system for providing second opinion with assistance of intellectual agents based on JADE multi agent system. Periodical machine relearning of intellectual agent depending on data and method requires substantial computational as well as storage resources for storing medical record. Therefore grid infrastructure seems to be appropriate solution for this. These two above mentioned problems are the themes for discussion of the present article.

The development of a GRID based genomic computing environment implemented in the GRID will introduce a common infrastructure for biomedical research institutions for mining and analyzing available data sources. As a result, efficient cross-site genomic studies and clinical trials can be performed and in most cases a seamless integration of multi-level data (from the molecular to the organ, individual and population levels) will be facilitated. The aim of this activity is to use computational Grids to analyze molecular biological data at a genomic scale. This necessitates adapting and the GRID technology proved to be an up-to-date tool necessary in genomics to support and enable the collaboration of people using resources through highly capable computation and data management systems. Our aim in this field just now is to select and deploy the bioinformatics platform useful for our needs. So we will discuss here the recommendations from [1] suitable to local capabilities and potential studies in bioinformatics.

Firstly, we shortly review actual problem in structural genomics, then describe our grid-infrastructure in comparing with existing bioinformatics platforms and then conclude what directions for local bioinformatics development are optimal.

The main task of proteomics is to understand protein functionality, both identifying the key role residues and describing how interactions take place. A typical approach to accomplish the identification of functional residues in proteins is to use methods which consist in finding similarities between well annotated proteins and the one under examination. A number of bioinformatics tools can be used to analyze sequences, in particular, if correspondences can be established with well characterized proteins. Typically an in silico application for the analysis of protein function begins with sequence based similarity search against specific reference databases. A more specific approach relies on performing a functional domain analysis of the protein sequences in order to search for the protein domain. A typical analysis on protein domain can be performed by using a set of databases and the related searching tools. To assign a specific function to a certain protein analyzing the structural methods can also be used to compare three-dimensional conformations, which usually are highly conserved for specific active site. Structural approach can be divided into two classes: methods relying on library of complex structural domains and methods that consider local characteristic of proteins. Working on local features of the macromolecular is

quite complex, but through the construction of templates of the protein local topology the analysis can be very sensible in recognizing the geometry of a functional site. These approaches can be very time consuming, due to the high number of configuration to explore while verifying similarities. For this reason a Grid based approach can be extremely useful to address these new challenges, providing a scalable solution for algorithms that imply a high computational load.

Most popular in bioinformatics is BLAST software. NCBI BLAST (Basic Local Alignment Search Tool) [2] suite of applications are used to compare biological sequences, either genomic or amino-acidic, against a set of known sequences database. BLAST is a variation and approximation of the exhaustive dynamic-programming Smith-Waterman [3] algorithm for local sequence alignment, resulting in a speed increase of 10-100x, at the expense of some sensitivity [4]. The various BLAST variants use two classes of reference databases: nucleotide databases and protein databases.

- *Blastp* compares a protein query (input) sequence against a protein database. As an example a user would employ *blastp* to search an unknown protein sequence to identify similar or homologous proteins from a protein database. *Blastn* compares a nucleotide query sequence against a nucleotide database. As an example a user would employ *blastn* to search an unknown nucleotide sequence to identify known genes.
- *Blastx* compares a nucleotide query sequence against a protein database, after translating the input sequence into all the six possible reading frames. As an example a user could use *blastx* to find potential translation products of an unknown nucleotide sequence or to identify which protein might be coded for by an unknown nucleotide sequence. *Tblastn* compares a protein query sequence against a nucleotide database translated in all six reading frames. As an example a user could use *tblastn* to identify which region of a genome coded for a given protein. More interesting for us *PHI-BLAST* (Pattern-Hit Initiated BLAST) which expects as input a protein query sequence and a pattern contained in that sequence. PHI-BLAST searches the specified database for other protein sequences that also contain the input pattern and have significant similarity to the query sequence in the vicinity of the pattern occurrences. PHI-BLAST uses protein databases. *PSI-BLAST* (Position-Specific Iterated Blast) can do an iterative search in which sequences found in one round of searching are used to build a score model for the next round of searching.
- *Mega BLAST* uses the greedy algorithm of Zhang et al. [5] for nucleotide sequence alignment search and concatenates many queries to save time spent scanning the database. This program is optimized for aligning sequences that differ slightly as a result of sequencing or other similar "errors". It is up to 10 times faster than more common sequence similarity programs and therefore can be used to swiftly compare two large sets of sequences against each other.

Traditionally developed in our institute methods of pattern recognition and cluster analysis, we plan to test for the tasks described above.

Even if the great majority of bioinformatics data comes in flat file format, it is becoming every day more common to find data available as relational database. The GRelC DAS, is a service providing a uniform access interface to relational and non-relational (i.e., textual databases) data sources. The aim of this data Grid service is to efficiently, securely and transparently manage databases on the Grid, across virtual organizations, with regard to modern Grid standards and specifications. Security is provided by means of the Grid Security Infrastructure (GSI) and data transfer leverages the Grid FTP protocol in order to obtain high performance and reduced communication.

Different types of data resources, including relation XML and files can be accessed with OGSA-DAI via web services. A number of popular data resource products are supported. Data within each of these types of resource can be queried and updated. Data can be transformed (using XSLT), compressed and delivered (using ZIP and GZIP

compression), delivered to clients, other OGSA DAI web services, URLs, FTP servers, GridFTP servers, or files.

AMGA is designed to provide metadata access for Grid application. It allows the use of several back-ends: Oracle, MySQL, PostgreSQL, SQLite. It is oriented to files (metadata describes files on the Grid), but it is possible to use it in order to access DB using a dedicated Languages, which is not SQL standard, even if it allows an important subset of the functionalities provided by the standard SQL . It provides both Web Services and socket connection and gives the possibility to exploit advanced replication functionality, also between servers using different back-end. API is available in several languages: C++, Java, Python, Perl, Ruby.

There are following research challenges in bioinformatics, that we must considered One of the major tasks of genomic analysis is the identification of genes and regulatory elements of gene expression. Among the different methods used to solve this task, comparative analyses have shown their strength and reliability. A critical problem – after the identification of conserved tracts - is the assessment of their coding potential (i.e. to determine if they are coding or non-coding sequences). CSTminer, an application, addresses this problem with a simple yet reliable two step procedure: first it compares two sequences in order to identify conserved regions (CSTs), than it assigns to each of them a coding potential score (CPS) based on their conformation to the expected evolutionary dynamics of coding sequences at both nucleotide and amino acid levels.

The challenge has been use to show the possibility analyzing the human Expressed Sequence Tags (EST), which are pieces of expressed genes, against the database of protein sequences, UNIPROT. This analysis it allows to identity the function of genomic sequences that will be translated into effective proteins completely annotated in UNIPROT.

In protein domain analysis the functional domain prediction in protein sequences have been performed with a set of software rely on a pattern search in a database, which range from the 1.18 GB of Panther to the 6.59 MB of PROSITE for an average dimension of 342 MB. These applications rely on different pattern recognitions system, working on specific designed database.

We expect that our potential users would like to avoid working directly on the grid middleware when porting an application to the grid; so a grid portal should be considered. A number of teams around Europe have developed grid portals which hide the grid complexity. In the case of using grid portals like Genius or P-Grade, it is necessary to have appropriate training to use the portal itself. Workflow engines such as TAVERNA or MOTEUR can be useful to implement more complex biological analysis.

Thus, a crucial aspect in life sciences nowadays is that biological technologies must be coupled with powerful computational resources like Grid computing. Personalized medicine when supported by the appropriate computation resources such as the Grid, can become an effective business solution.

In laboratory of medical informatics it is established grid-site with use gLite versions 3.1, including the following services: UI (user interface), CA (certificate authority), VOMS (virtual organization management system), WMS (workload management), LB (Logging and Bookkeeping service), top-BDII and BDII-sites, WN (work nodes)

All of them are realized by virtual machines OpenVZ: uica.imit.uz, voms.imit.uz, wmslb.imit.uz, topbdii.imit.uz, ce01-02bdii.imit.uz, wn001-003.imit.uz. Apparently from names, some services (not all) can work in common by one virtual machine. The principle of work with these services will consist in the following.

The user under the local account on uica.imit.uz addresses to voms.imit.uz with the request to give out to him the temporary certificate (usually for day). After reception of the certificate the user can send the tasks which have been made out as a jdl-file, or, obviously having specified a computing element (for example: ce01bdii.imit.uz), or having assigned

search of a suitable resource on wmslb.imit.uz which receives data on available computing resources (CE) from topbdii.imit.uz. In turn ce01bdii.imit.uz carries out transfer of the task and the control of performance of the task over one or several working sites: wn001.imit.uz, wn002.imit.uz wn003.imit.uz.

On physical machines with support of parallel computing are established (architecture i386):

* wn005.imit.uz, wn006.imit.uz - working sites (192.168.1.105, 192.168.1.106)

On virtual machines with support of parallel computing are established:

a. Work nodes wn003.imit.uz, wn004.imit.uz (192.168.1.103, 192.168.1.104);
b. Service lcg-CE, BDII_site - with a common catalog (/home) - for increasing in productivity of a cluster. (architecture i386);
c. Service topbdii - on the virtual machine topbdii.imit.uz (83.69.132.53);
d. Services wms (workload management) and lb (logging and bookeeping) on the virtual machine wmslb.imit.uz (83.69.132.51) are established;

With the colleagues on adjustment of mutual certification and inclusion of the local grid-site to virtual organization EDU teamwork is carried out (JINR, Dubna, Russia).Through remote access (from Dubna) successful start of test parallel tasks on IMIT grid-site is carried out.

An interest to multiagent systems and application is natural, because modern software system have reached such complexity that it is difficult and inefficient to develop manage them as monolithic systems. Required decomposition of the system is performed in various ways, - by objects, packages, libraries. But it is agents that are such kind of elements of decomposition that have a set of advantages – reusability, flexibility, maintainability, and autonomy.

The term 'agent', or software agent, at first was introduced in series of technologies and are widely used, e.g. in artificial intelligence, data bases, computer network, human computer interaction. An agent, it is a special piece of software that autonomous, that provides interoperable interface, and behaves like a human agent, working for its customers, carrying out their tasks. A set of agent forms multiagent system, using which it is possible build and model complex systems. Agents of such system interact with each other by passing messages, negotiations, or through their environment, changing it. Besides main feature of an agent – autonomy, some other ones are marked out: sociality – ability to cooperate with a human or another agents for achieving its purposes, reactivity – ability to perceive the environment and react on its changes, proactivity – ability to take upon it an initiative and act in goal-oriented way. Moreover, an agent can be learnable or mobile, i.e. possible to move among nodes of computer network. Mentioned above features of agent could be implemented in particular agent in different degree depending on its goals and objectives.

The GRID and MAS (Multi-Agent Systems) communities believe in the potential of GRID and MAS to enhance each other because they have developed significant complementarities. Thus, both communities agree on the"what" to do: promote an integration of GRID and MAS models. However, even if the "why" to do it has been stated and assessed, the "how" to do it is still a research problem.

Emerging telemedicine applications require the ability to exploit diverse and geographically distributed resources. High-speed networks are used to integrate advanced visualization devices, sophisticated instruments, large databases, archival storage devices, PC's, workstations, and supercomputers. This form of telemedical environment is similar to networked virtual supercomputers also known as metacomputing. Multiagent approach is seemed to be ideal here. That explains observed growth of applications of MAS in this area. Agent in telemedicine find a use for scheduling, monitoring of patients [6], medical knowledge retrieval from the Internet [7], research and diagnosing [8, 9].

The developed system has as purpose to automate the process of selection of required specialist for second opinion, and also to improve the quality of diagnosis with various methods of classification. The system consists of five types of agents: agent-specialist, agent-broker of specialists, classifier-agent, agent-broker of classifiers, data base agent (DB-agent). The number of launched agents of different types depends on structure of particular system to deploy.

Agent-broker of specialists manages agent-specialists of one its own type, and service requests for providing of required specialist for teleconsultations. Agent specialist presents an interface between the system and a physician, giving teleconsultation. By this agent a doctor speaks to requested specialist. Agent-specialist also communicates with the data base agent for patient data retrieval. This information is of common type (personal data, results of common analysis) and specific – collected for the particular domain of diagnostics. DB-agent decides itself, what kind of information is need for particular doctor. Each specialist agent registers its service in the system. After service has been found by corresponding broker-agent, linkage of the found specialist agent with the broker occurs, and the specialist agent switches to the dedicated state. The classifier-agent carries a knowledge model for recognition diseases on certain data. If it is necessary, the classifier-agent performs relearning, for example, as number of errors exceeds certain value or regularly. Data for learning are retrieved on corresponding request to the DB-agent. These requests are defined before ahead for every data extraction variant. In the system, for recognition on one data set several classifier-agents, which embody different knowledge models, can function. Thus classifier-agents represent an intellectual component of the system. Depending on data available and algorithm, learning process can take a lot of time and memory resources. To accelerate learning, it is desirable for a classifier-agent to move on free and more powerful computational resource and perform learning there. After that, the agent must move back and continue functioning, supporting decision making. Increasing volumes of medical data, their distribution, and associated computational costs, lead to that it is seems natural to deploy similar telemedical systems in grid environment [10,11], and namely employing multiagent approach [12].

Agent-broker of classifier is responsible for finding and sending task for diagnosing to the all classifier agents of certain its type. It also analyses results of the diagnosing and passes them to the requesting specialist broker-agent, which in its turn send them to the specialist agent. For launching and control of agents in the system special panel is used, which displays data on the possible type of agents, read from the data base, data on launched agents and other.

For implementation of prototype of the described system following software components were used:

- WEKA 3.6 –library of the up-to-date machine learning and data preprocessing algorithms, written on Java. Types of the classification algorithms, implemented in WEKA, include Bayesian classifiers, decision trees, decision rules, mathematical functions, and other. It is possible to use various schemes of learning. These methods can be embedded in your own code, as well as implementation of new, own learning method with common interface is possible. So, each classifier agent uses particular learning and classification method that passed as parameter.
- JADE 3.6 – is an open software platform, fully developed on Java. It simplifies implementation of multiagent systems, thanks to middleware, that complies with FIPA (Foundation for Intelligent Physical Agents. http://www.fipa.org), and set of graphical tools supporting debugging and deployment. This agent platform can be deployed on heterogeneous computational nodes and dynamically reconfigurable.

As data base server DBMS MySQL Server 5.1.30 is used. The offered system tested on small data set, and fully proved its operability, have shown main advantages of MAS.

Thus, considering the common experience in bioinformatics we present the some platforms and grid-services which we plan to implement in our grid node. It's clear that our final selection will be defined by biologists dealt with the problems of molecular biology, biotechnology have been developed in the country. But our aim is to create advanced Grid environment for the advanced studies in bioinformatics and potential collaboration with the world scientific community. Starting implementation of MAS in telemedicine, we hope to use these lessons in MAS applications in bioinformatics.

This work is executed at support of grant NATO Grant NIG EAP 952986

**References:**

[1] BioinfoGRID White Paper http://www.bioinfogird.eu

[2] C. Richard van der Wath, Elizabeth van der Wath, Antonio Carapelli, Francesco Nardi, Francesco Frati, Pietro Lio',Luciano Milanesi: Testing Bayesian phylogeny inference in a distributed computing system. EvoBIO'08 (submitted).

[3] GridICE: a Monitoring Tool for Grid System. Recent Evolution, Use Cases and Interoperability - HPDC (High Performance Distributed Computing) 2007 Monterey Bay California, June 27-29, 2007.

[4] Monitoring the user/application activities on the grid - CHEP 07 - Victoria, British Columbia, Canada from September 2-7, 2007.

[5] Comparative evaluation of tools providing access to different types of data resources exposed on the Grid / Maggi Giorgio ; Ghiselli Antonia ; Donvito Giacinto ; Carota Luciana; et al presented at EGEE User Forum, Manchester, United Kingdom, May 9-11, 2007.

[6] G.B. Laleci, A. Dogac, M. Olduz, I. Tasyurt, M. Yuksel, A. Okcan, SAPHIRE: A Multi-Agent System for Remote Healthcare Monitoring through Computerized Clinical Guidelines, Whitestein Series in Software Agent Technologies and Autonomic Computing Special Issue on Agent Technology and e-Health, 2008.

[7] L. Lhotská, L. Prieto, Intelligent Agents in Medicine //In International Special Topics Conference on Information Technology in Biomedicine, Piscataway: IEEE, 2006.

[8] V. Alves, J. Neves, J. Machado, A. Abelha, Agent based decision support systems in medicine, "WSEAS Transactions on Biology and Biomedicine", 2005.

[9] F.T. Adilova, R.Sh. Ibragimov, New Paradigm for Telemedical Collaboration: Design of Intelligent Agent Functions, Global Telemedicine and eHealth Updates: Knowledge Resources, Proceedings of Med-E-Tel Conference, Luxembourg. Vol. 1, pp.96-102. 2008.

[10] J. Foster, C. Kesselman, S. Tuecke, Brain Meets Brawn: Why Grid and Agents Need Each Other AAMAS'04, New York, USA, July 19-23, 2004.

[11] F.T. Adilova, D.D. Akhmedov, R.Sh. Ibragimov, R.K. Bazarov, Grid computing and multiagent systems: new direction of telemedicine development, Distributed Computing and Grid-Technologies in Science and Education: Proceedings of the 3rd International Conference, Dubna, Russia, pp. 81-85, June 30-July 4, 2008.

[12] C. Jonquet, P. Dugenie, S.A. Cerri, Service-based integration of grid and multi-agent systems models. R. Kowalczyk (ed.) et al., Service-oriented computing: Agents, semantics, and engineering, AAMAS 2008 international workshop, SOCASE 2008, Estoril, Portugal, May 12, 2008, Proceedings. Berlin: Springer, Lecture Notes in Computer Science 5006, pp. 56-68, 2008.

# Methods of $e/\pi$ identification with the Transition Radiation Detector in the CBM experiment

E.P. Akishina, T.P. Akishina, O.Yu. Derenovskaya, V.V. Ivanov
*Joint Institute for Nuclear Research, Dubna, Russia*

A problem of $e/\pi$ identification using $n$-layered transition radiation detector (TRD) in the CBM experiment is considered. With this aim, we elaborated algorithms and implemented various approaches. We discuss the characteristic properties of the energy losses by electrons and pions in the TRD layers and special features of applying artificial neural networks (ANN) and statistical methods to the problem under consideration. A comparative analysis is performed on the power of the statistical criteria and ANN.

**Keywords:** general statistical methods, multivariate analysis, pattern recognition, CBM experiment, transition radiation detector TRD.

## 1. Introduction

The CBM Collaboration [1, 2] builds a dedicated heavy-ion experiment to investigate the properties of highly compressed baryon matter as it is produced in nucleus-nucleus collisions at the Facility for Antiproton and Ion Research (FAIR) in Darmstadt, Germany. Figure 1 depicts a general layout of the CBM experiment. There is a Silicon Tracking System (STS) inside the dipole magnet. Ring Imaging Cherenkov (RICH) is designed to detect electrons. TRD arrays identify electrons with momentum above 1 GeV/c. TOF provides time-of-flight measurements needed for hadrons identification. ECAL measures electrons, photons and muons.

The measurement of charmonium is one of the key goals of the CBM experiment. For detecting $J/\psi$ meson in its dielectron decay channel the main task is the $e/\pi$ separation. One of the most effective detectors for solving this problem is the Transition Radiation Detector.

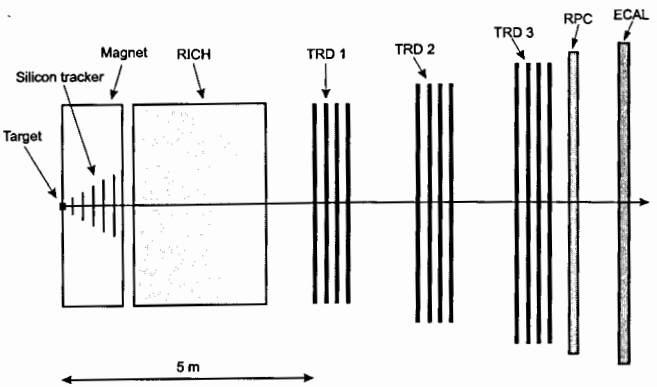


Fig. 1. Schematic view of the CBM experimental setup

The problem of particle identification (PID) using $n$-layered TRD consists in the following: having a set of energy losses measured in $n$ layers of the TRD, one has to estimate to which particle, $e$ or $\pi$, this set is relative. To estimate the efficiency of particle identification, we used different approaches.

## 2. Traditional statistical criteria: MV and LFR methods

In the mean value (MV) method the PID is based on a variable $\overline{\Delta E} = \frac{1}{n}\sum_{i=1}^{n} \Delta E_i$ (where $\Delta E_i$ is a particle energy loss in the $i$-th TRD layer and $n$ is the number of layers in the TRD). Fig. 2 shows distributions of variable $\overline{\Delta E}$ for $e$ (left top plot), $\pi$ (right top plot), and a summary distribution for $e$ and $\pi$ (bottom plot).

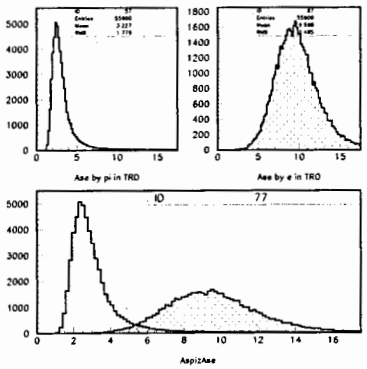


Fig. 2. Distributions of variable $\overline{\Delta E}$

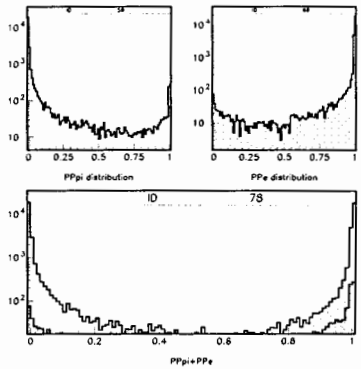


Fig.3. Distributions of variable $L$

While applying the likelihood functions ratio (LFR) test [3] to the PID problem, the value

$$L = \frac{P_e}{P_\pi}, \quad P_e = \prod_{i=1}^{n} p_e(\Delta E_i), \quad P_\pi = \prod_{i=1}^{n} p_\pi(\Delta E_i), \tag{1}$$

is calculated for each event (see Fig. 3), where $p_\pi(\Delta E_i)$ is the value of the density function $p_\pi$ in the case when the pion loses energy $\Delta E_i$ in the $i$-th absorber, and $p_e(\Delta E_i)$ is a similar value for electron.

We have found that the distribution of ionization losses of pions in the TRD is well approximated by a log-normal density function

$$f_1(x) = \frac{A}{\sqrt{2\pi}\sigma x} \exp^{-\frac{1}{2\sigma^2}(\ln x - \mu)^2}, \tag{2}$$

where $\sigma$ is the dispersion, $\mu$ is the mean value, and $A$ is a normalizing factor (see Fig. 4). The distribution of energy losses by electrons in the TRD is approximated with a good accuracy by the density function of a weighted sum of two log-normal distributions (see Fig. 5).

$$f_2(x) = B\left(\frac{\alpha}{\sqrt{2\pi}\sigma_1 x} \exp^{-\frac{1}{2\sigma_1^2}(\ln x - \mu_1)^2} + \frac{\beta}{\sqrt{2\pi}\sigma_2 x} \exp^{-\frac{1}{2\sigma_2^2}(\ln x - \mu_2)^2}\right), \tag{3}$$

where $\sigma_1$ and $\sigma_2$ are dispersions, $\mu_1$ and $\mu 2$ are mean values, $\alpha$ and $\beta$ are contributions of the first and second log-normal distributions, correspondingly, and $B$ is a normalizing factor.

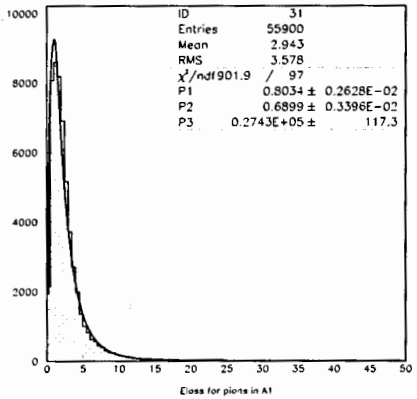


Fig. 4. Distribution of pion energy losses in one layer of the TRD and its approximation by a log-normal function (2)

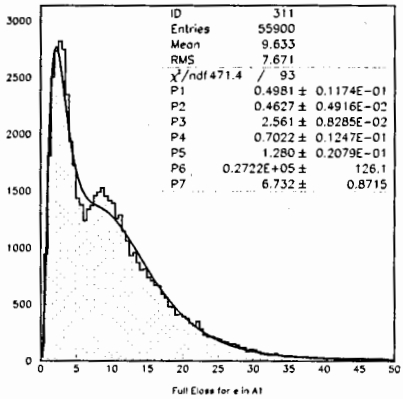


Fig. 5. Distribution of electron energy losses in one layer of the TRD and its approximation by a weighted sum of two log-normal functions (3)

### 3. Nonparametric goodness-of-fit $\omega_n^k$ -criterion [4, 5]

This test is based on the comparison of the distribution function $F(x)$ corresponding to the preassigned hypothesis ($H_0$) with empirical distribution function $S_n(x)$:

$$S_n(x) = \begin{cases} 0, & if \quad x < x_1; \\ i/n, & if \quad x_i \le x \le x_{i+1}, \quad i=1,\ldots,n\text{-}1. \\ 1 & if \quad x_n \le x, \end{cases} \tag{4}$$

Here $x_1 \le x_2 \le \ldots \le x_n$ is the ordered sample (*variational series*) of size $n$ constructed on the basis of observations of variable $x$.

The test statistics measures the "distance" between $F(x)$ and $S_n(x)$. Such statistics are known as *non-parametric*. We suggested a new class of non-parametric statistics (with $k \ge 3$):

$$\omega_n^k = -\frac{n^{\frac{k}{2}}}{k+1} \sum_{i=1}^{n} \left\{ \left[ \frac{i-1}{n} - F(x_i) \right]^{k+1} - \left[ \frac{i}{n} - F(x_i) \right]^{k+1} \right\}. \tag{5}$$

The goodness-of-fit criteria constructed on the basis of these statistics are usually applied for testing the correspondence of each sample to the distribution known *apriori*.

Energy losses for $\pi$ have a form of Landau distribution. We use it as $H_0$ to transform the initial measurements to a set of a new variable $\lambda$:

$$\lambda_i = \frac{\Delta E_i - \Delta E_{mp}^i}{\xi_i} - 0.225, \qquad i = 1,2,\ldots,n, \tag{6}$$

$\Delta E_i$ – the energy loss in the $i$-th absorber, $\Delta E_{mp}^i$ – the value of most probable energy loss, $\xi_i = \frac{1}{4.02}$ FWHM of distribution of energy losses for $\pi$.

In order to determine $\Delta E^i_{mip}$ and FWHM of the distribution of pion energy losses in the $i$-th absorber, the indicated distribution was approximated by the density function of a log-normal distribution (see Fig. 4).

The obtained $\lambda_i$, $i = 1, ..., n$ are ordered due to their values ($\lambda_j$, $j = 1, ..., n$) and used for calculation of $\omega_n^k$:

$$\omega_n^k = -\frac{n^{\frac{k}{2}}}{k+1}\sum_{i=1}^{n}\left\{\left[\frac{j-1}{n}-\phi(\lambda_j)\right]^{k+1}-\left[\frac{j}{n}-\phi(\lambda_j)\right]^{k+1}\right\}. \qquad (7)$$

Here the values of Landau distribution function $\phi(\lambda)$ are calculated using the DSTLAN function (from the CERNLIB library). Figure 10 shows the distributions of $\omega_{12}^6$ values for $\pi$ (top left plot) and $e$ (top right plot); the summary distribution is shown in the bottom plot.

## 4. Combined method

This approach is based on a successive application of two statistical criteria: 1) the mean value method, and 2) the $\omega_n^k$ test.

The main idea of this scheme consists in the following:

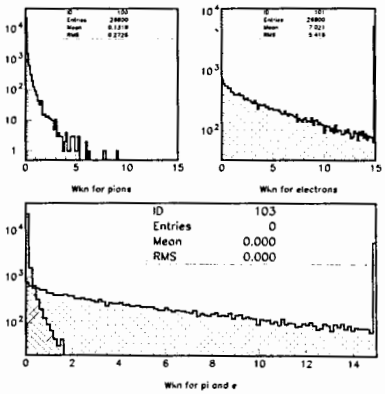


Fig. 6. Distributions of $\omega_{12}^6$ values for $\pi$ (top left plot) and for $e$ (top right plot) events; the summary distribution for $\pi$ and $e$ events (bottom plot)

- using the mean value method, we collect in the admissible region the main part of electrons together with a small admixture of pions,
- then we apply the $\omega_n^k$ test to the events selected in the admissible region; this way, we loose a small part of electrons together with additional suppression of pions.

## 5. Modified $\omega_n^k$ test

Fig. 7 shows the dE/dx distribution of $e$, and Fig. 8 presents the distribution of electron energy losses on the transition radiation (TR). Fig. 9 shows the probability of events with a

different number of TR counts. We see that the most probable value of TR counts in the TRD with 12 layers is 6, and we almost do not have the events with TR counts in all 12 layers.

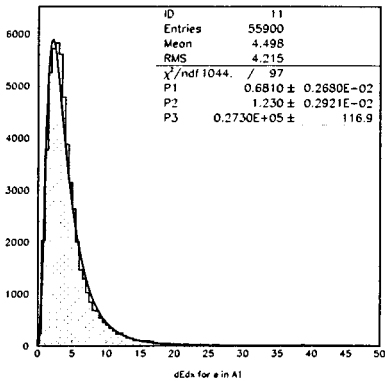


Fig. 7. Distribution of electron energy losses on the ionization and its approximation by a log-normal function

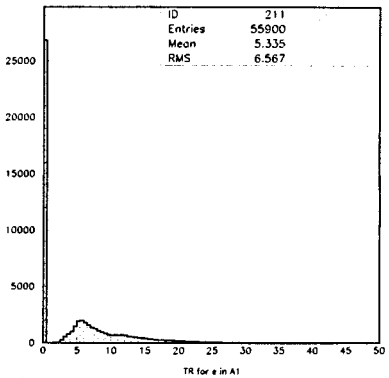


Fig. 8. Distribution of electron energy losses on the transition radiation

Let us turn back to the distribution of electron energy losses on the transition radiation (see Fig. 8). Fig. 8 shows that when $e$ passes the i-th layer with TR=0, then its energy loss follows the distribution of dE/dx losses (Fig. 7). In this case, it is practically impossible to distinguish electrons from pions on the basis of their energy losses. In the opposite case, when we have the TR count in the i-th layer, the electron energy loss will correspond to the sum of dE/dx + TR (right distribution in Fig. 8). Only such counts in TRD layers may permit us to distinguish electrons from pions.

When calculating $\omega_n^k$, in Eq. 7, one uses a sample of $\lambda_i$ values (see Eq. 6), which are ordered due to their values. The $\lambda_i$ value is directly proportional to the energy loss by a particle registered in the $i$-th layer of the TRD. In this connection and taking into account that the most probable value of TR counts in the TRD with 12 layers is 6 (Fig. 9), we may use in the $\omega_n^k$ test only that part of $\{\lambda_i\}$ sample which corresponds to indexes $i > 6$, i.e. to large values of particle energy losses.

Fig. 10 shows the distributions of $\omega_n^k$ values for GEANT samples: $i = 7$, $n = N_{layers} - i + 1$, $k = 6$.

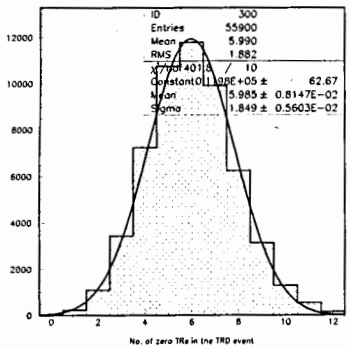


Fig. 9. Distribution of events with different number of TR counts and its approximation by Gaussian distribution

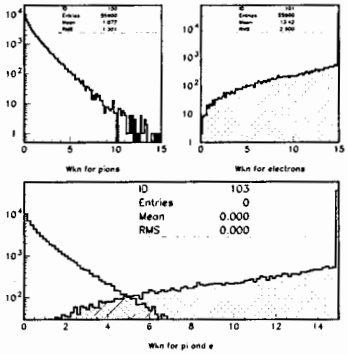


Fig. 10. Distributions of $\omega_n^k$ values calculated for $\pi$ (top left plot) and for $e$ (top right plot) events; the summary distribution (bottom plot)

## 6. Method based on artificial neural network (ANN)

To estimate the efficiency of PID, we applied a three-layered perceptron from the packages JETNET3.0 and ROOT [6]. Initially the training patterns were formed using the set of energy losses $\Delta E_i$, $i = 1, ..., n$ corresponding to the passage through the TRD pions or electrons.

In spite of the fact that the distribution of the energy losses by electrons significantly differs from the character of the distribution of the energy losses by pions, for such a choice of input data the training process was going on very slow (see bottom curve in 11), there were large fluctuations (against the trend) of the efficiency of events identification by the network. Moreover, one cannot reach the needed level of pions suppression.

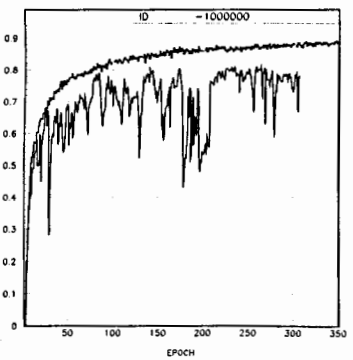


Fig. 11. The efficiency of pion/electron identification by the MLP for original (bottom curve) and transformed (top curve) samples

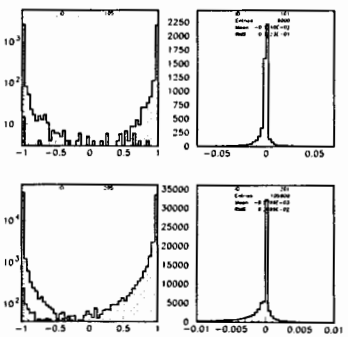

Fig. 12. Distributions of the MLP output signals (left plots); the right plots show the distributions of errors

Aiming to improve the situation, we decided to apply as input sets the sets of variable $\lambda$ (6): see top curve in Fig. 11. Fig. 12 shows distributions of the MLP output signals obtained at the training (top left plot) and testing (bottom left plot) stages; the right plots show the distributions of errors between the target value and the MLP output signal at the training (top plot) and testing (bottom plot) stages.

## Conclusion

Table 1 shows the results of comparison of the given methods for different particle (pion and electron) momenta.

This table demonstrates that the MV method and the $\omega_n^k$ criterion do not provide a required level of the pion suppression (~ 100-150). The main cause is that the electron energy losses are not described by a single distribution, but bear a character of a composite hypothesis.

The criteria simple from a practical viewpoint (the modified $\omega_n^k$ criterion and the composite criteria based on MV + $\omega_n^k$ criterion) provide high levels of the pion suppression.

Table 1. Comparison of the given methods: pion suppression factor for different momenta

| *p,GeV/c* | 1 | 2 | 3 | 4 | 5 | 7 | 9 | 11 |
|---|---|---|---|---|---|---|---|---|
| MV | 15 | 17 | 17 | 16 | 16 | 16 | 16 | 16 |
| $\omega_n^k$ | 104 | 96 | 73 | 55 | 44 | 35 | 29 | 25 |
| MV+$\omega_n^k$ | 284 | 271 | 249 | 242 | 203 | 198 | 157 | 159 |
| mod $\omega_n^k$ | 296 | 621 | 628 | 776 | 650 | 745 | 588 | 537 |
| LFR | 1273 | 1315 | 1581 | 1480 | 936 | 861 | 800 | 749 |
| root | 1219 | 1400 | 1112 | 1446 | 730 | 1054 | 610 | 882 |
| jetnet | 1857 | 1837 | 1378 | 1713 | 1446 | 1317 | 1045 | 1089 |

One succeeds in reaching the best pion suppression level using: a) ANN when transmitting from the initial energy losses in the TRD layers to a new variable typical for the $\omega_n^k$ criterion, and b) LFR method with the energy losses approximated by a lognormal distribution for pions and by a weighted sum of two lognormal distributions for electrons.

## References


[1] Letter of Intent for the Compressed Baryonic Matter experiment, http://www.gsi.de/documents/DOC-2004-Jan-116-2.pdf

[2] Compressed Baryonic Matter Experiment. *Technical Status Report*, GSI, Darmstadt, 2005, http://www.gsi.de/onTEAM/dokumente/public/DOC-2005-Feb-447e.html.

[3] W.T. Eadie, D. Dryard, F.E. James, M. Roos and B. Sadoulet, Statistical Methods in Experimental Physics, North-Holland Pub.Comp., Amsterdam-London, 1971.

[4] P.V. Zrelov and V.V. Ivanov, The Relativistic Charged Particles Identification Method Based on the Goodness-of-Fit $\omega_n^3$ -Criterion, Nucl. Instr. and Meth. In Phys. Res., A310 (1991) 623-630.

[5] E.P. Akishina, T.P. Akishina, V.V. Ivanov, A.I. Maevskaya and O.Yu. Denisova, Electron/pion identification in the CBM TRD applying a $\omega_n^k$ goodness-of-fit criterion, Particles & Nuclei, Letters, 2008, Volume 5, No. 2(144), pp. 202-218.

[6] E.P. Akishina, T.P. Akishina, V.V. Ivanov, M.I. Maevskaya, O.A. Afanas'ev, On electron and pion identification using a multilayer perceptron in the transition radiation detector of the CBM experiment, JINR Communication, P10-2009-61, JINR, Dubna, 2009, 15 p.

# Web monitoring of physical facilities at the Flerov Laboratory of Nuclear Reactions

V. Aleynikov, A. Krylov, V. Zager
*Joint Institute for Nuclear Research, Dubna, Russia*

There are many accelerator facilities at the Flerov Laboratory of Nuclear Reactions: U-400, MC-400, IC-100, MT-25, U-200 and the beam transport system DRIBs. A global system for collecting information from control systems of the accelerators and archiving it in the database has been created. It is based on the Internet technology and uses MySQL, PHP and Apache as a web server. The data exchange server uses TCP/IP and QNX SCADA FlexControl. The Client programme is written using LabVIEW. Historical trends can be viewed in any Internet browser with the of flash technology.

## Introduction

Since 1999 we have been using the Supervisory Control and Data Acquisition (SCADA) software named FlexCtrl 4 (BitCtrl Systems Ltd., Germany) [1]. It runs under a UNIX-style commercial real-time operating system QNX (QNX Software Systems Ltd., Canada). FlexCtrl is a process control system for the automation of technological processes. It is modular and extremely scalable [2]. The interface to the system is open and the user has a possibility of adding a custom device driver to the system. A cross-platform set of software to collect and display parameters of the physical installations over the Laboratory has been created. It consists of three main parts:

1. Server program. It runs on the accelerator's control system computer;
2. Client program. It reads and puts data to the MySQL database;
3. Web interface software interacts with the user.

The server is written for RTOS QNX. The client program and web interface can be run under MS Windows or Linux OS.

## General description

To ensure communication between the real-time database of SCADA FlexCtrl and MS Windows a server program was written. It is connected to FlexCtrl database as a general device driver [3]. To run the program it needs some parameters, such as:

- name of the FlexCtrl project (database name),
- TCP port for incoming connections,
- the right to access a remote client program. One can access the recording, which allows one to remotely control the accelerator,
- mask of client's IP addresses allowed for server access,
- node number in the QNX operating system in which the server is running,
- password to access the server,
- enable output debugging information.

Here is an example of the server parameter string:

./fcsrvr -p ic100 -P 8080 -w 1 -n 22 -m 159.93 –v,

where:
-p name is the FlexCtrl project name,
-P port is the TCP/IP port,

-w mode is the access mode: 0 for read, 1 for read/write,
-m mask is the net mask for the access program: 159.93.xx.xx,
-n node is the QNX node number,
-v is the verbose error logging to console.

The program starts to listen to all incoming connections to the port. In the event of connecting the client begins the exchange of data.

The client's portion of the program is written using LabVIEW. It reads the configuration file, in which all required parameters are specified:

- IP address of the MySQL server machine,
- TCP/IP port number of the MySQL server machine,
- user name and password to access MySQL,
- name of the table in the MySQL database for the collected data,
- IP address of the QNX computer in which the server software runs,
- TCP/IP port of the QNX computer,
- update time in milliseconds,
- name of the project (FlexCtrl database name),
- password to access the server,
- numbers of process variables of the FlexCtrl project,
- types of variables ( integer, floating-point, with a mantissa),
- commentary on each variable.

After starting the client program, it provides a connection to the server which runs on the QNX machine with control system software (see fig. 1). If the connection is successful, it sends configuration parameters to the server.

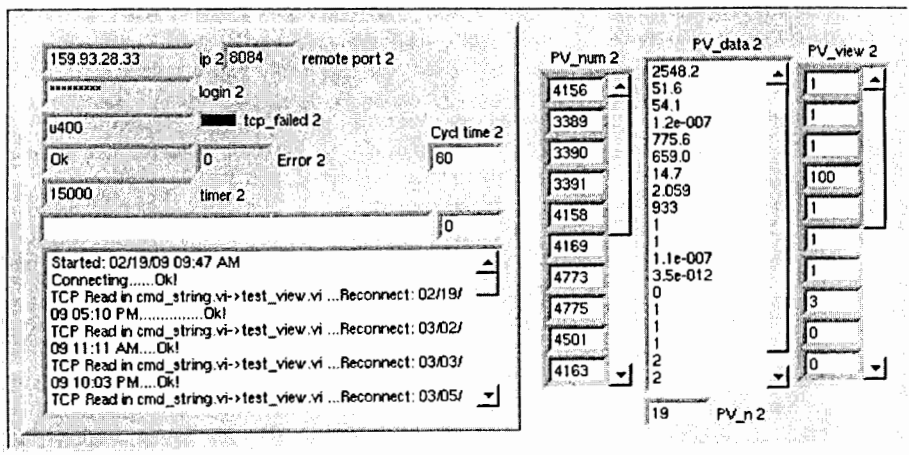


Fig. 1. Client program (LabVIEW)

It sends to the server the list of variables from the configuration file. Such pre-configuration allows one to reduce the traffic on the network and facilitates future work. Then the program starts with a cyclic server polling. The time interval is specified in the configuration file. The server program sends a command to read the data and the server

returns a set of data which was pre-defined after establishing connection. If any changes occur, the client program writes new values to the MySQL database.

The structure of the database table (fig. 2) looks as follows:

- unique MySQL number,
- type of variable,
- value,
- number of variable (PV),
- date of recording.

| id | type | value | pvnumber | date |
|---|---|---|---|---|
| 10947048 | 0 | 1 | 4174 | 2009-04-13 09:45:12 |
| 10947047 | 0 | 1 | 4163 | 2009-04-13 09:45:11 |
| 10947046 | 0 | 132472 | 4501 | 2009-04-13 09:45:10 |
| 10947045 | 0 | 1.980 | 4775 | 2009-04-13 09:45:10 |
| 10947044 | 0 | 14.7 | 4773 | 2009-04-13 09:45:09 |
| 10947043 | 0 | 622.8 | 4169 | 2009-04-13 09:45:09 |
| 10947042 | 0 | 601.8 | 4158 | 2009-04-13 09:45:09 |
| 10947041 | 0 | 1.3e-007 | 3391 | 2009-04-13 09:45:09 |
| 10947040 | 0 | 54.9 | 3390 | 2009-04-13 09:45:09 |
| 10947039 | 0 | 2547.1 | 4156 | 2009-04-13 09:45:09 |
| 10947038 | 0 | 52.4 | 3389 | 2009-04-13 09:45:09 |

Fig. 2. The contents of the database

The amount of data in the MC-400 and U-400 accelerators databases is shown in Fig. 3.

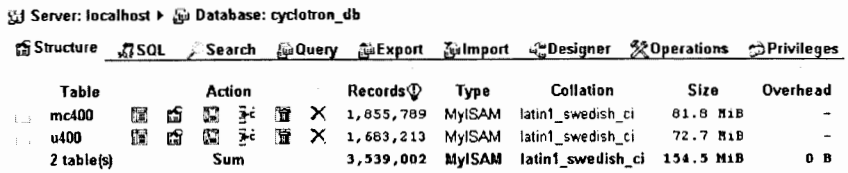


Fig. 3. Number of records in the database

The Custom Web interface is written using PHP, JavaScript and Adobe Flash. A bundle of Apache + PHP + MySQL is used as a Web server. The database administration is performed using phpMyAdmin.

To view a current status or historical data of the accelerator a user types into a browser the address http://nri128.jinr.ru/trend/. After loading the page the user will be prompted to select values to read. See Fig. 4.

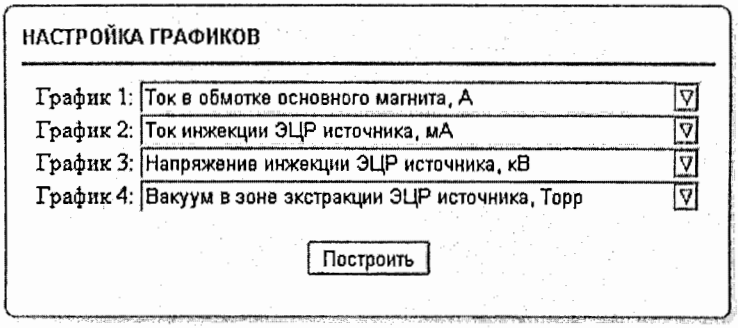


Fig. 4. Setting up the graphs

After the user made the selection, the data is loaded to the table (see Fig. 5). The construction of the drawing is based on Flash technology, and allows one to slide over the drawing, zoom in and out. The user can search the exact time or period of time and analyse important events.

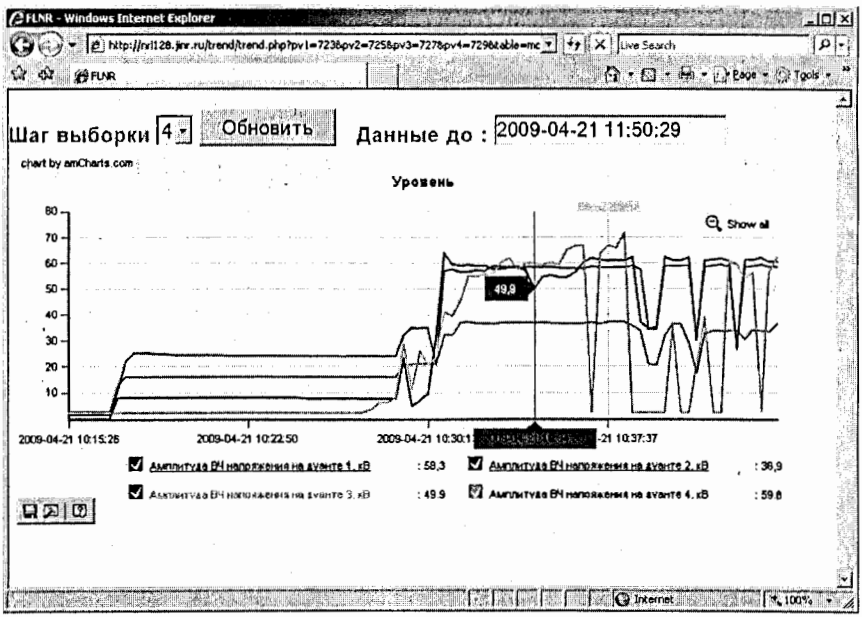


Fig. 5. Displaying data in a user's browser

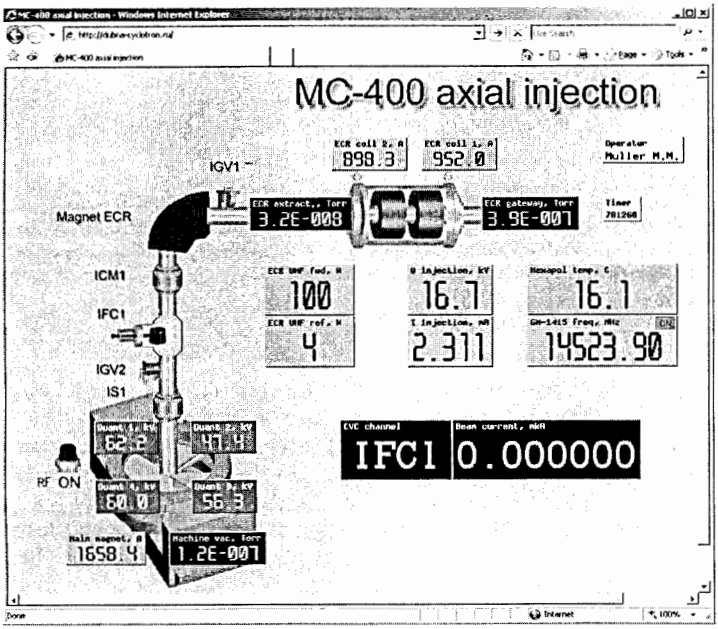


Fig. 6. Monitoring the parameters of the accelerator in the browser window

## Conclusions

The use of this package allowed us to identify and analyse several important problems in the operation of the accelerator MC-400 (Fig. 6). It helped us to fix the malfunctions in the RF system, caused by unstable work of power supplies. The special advantages of this program are:

- using the relational database MySQL which is freeware,
- programming language PHP is open and free for use,
- construction charts on the client's side remove additional workload from the server,
- ability to work with data from anywhere in the world,
- opportunity to work under any operating system with an internet browser.

There is a working version for the monitoring of main parameters of 4 accelerators in real time. Further development will allow the system to remotely control the accelerator. A graphical editor for designing visualization pictures in the browser window has been written. There is a set of libraries for the construction of dynamic pages for monitoring in browser. Ease of use and visibility of the display makes this software very attractive for use in any scientific research facilities.

## References

[1] V. Aleynikov, S. Paschenko, Using commercial SCADA in control system for ECR CyLab. PCaPAC 2000. Hamburg.

[2] FlexControl - System Architecture Manual. BitCtrl GmbH. October 1998.

[3] V. Aleinikov, A. Nikiforov, Integtrating custom software and commercial SCADA, NEC'2003.

# New Nuclotron Beam Intensity Monitoring Subsystem

V. Andreev, A. Butenko, A. Kirichenko, S. Romanov, G. Trubnikov, V. Volkov
*Joint Institute for Nuclear Research, Dubna, Russia*

A new Beam Intensity Monitoring Subsystem for the Nuclotron (BIMS) is based on a Parametric Current Transformer (manufacturer: BERGOZ instrumentation). It allows one to carry out monitoring of the Nuclotron beam current and intensity monitoring correlated with the main magnetic field signal (sampling rate is 100 kSamples/s). The common structure, electronic equipment, software and first results of the Subsystem, are described in this report

## Introduction

The superconducting synchrotron Nuclotron [1] is intended to accelerate nuclei and multicharged ions including the heaviest ones (uranium) up to the energy of 6 GeV/u for the charge to mass ratio Z/A = 1/2. Thirty-nine runs of the accelerator have been performed by the present time. The Nuclotron is also a key element of the currently designed accelerator complex NICA (Nuclotron-based Ion Collider fAcility) [2].

The Nuclotron Control System (NCS) [3] provided efficient support for the machine operation during all the runs. One of the NCS most significant tasks is internal beam intensity monitoring. The Nuclotron operators have successfully used the developed BIMS for monitoring of the beam current and intensity correlated with the main magnetic field.

## NBIMS structure

A general structure of the NBIMS is shown in Fig.1.

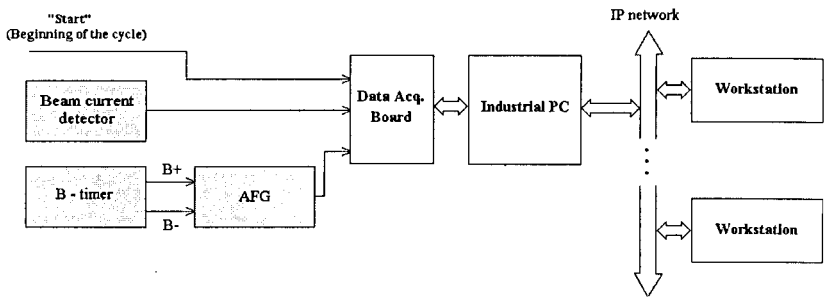


Fig. 1

The Analogue Function Generator (AFG) processes pulses from the Nuclotron B-timer to reproduce an analogue signal of the main magnetic field. DAQ board collects this signal and the one from the beam current detector. Industrial PC organizes the measuring cycle, processes the data and represents them for remote monitoring via network.

**Beam current detector**

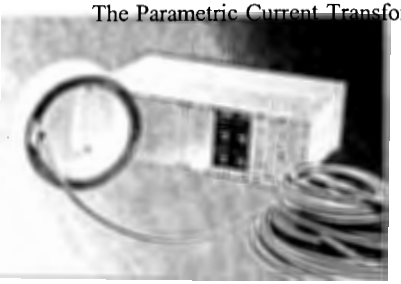

The Parametric Current Transformer (PCT) manufactured by Bergoz Instrumentation [4] is used as a beam current detector for the BIMS. The PCT, the latest evolution of the Unser Transformer, operates on most particle accelerators in the world to measure the average beam current. Its working range is from ±20mA to ±20A. The frequency response is up to 10 kHz. The PCT is a noise-immune device that is very important for the accelerator conditions. The Bergoz PCT with its sensor head is presented in Fig. 2.

Fig. 2

**NBIMS electronics**

Main blocks of the AFG (developed at VBLHEP) are the Counter and the DAC (see Fig. 3). The 2-channels Counter (based on Altera EPM7128) processes the B+ and B- pulse trains from the machine B-timer. The 14-bits DAC (based on AD 760) converts the digital output value of the Counter to the analogue one, which reproduces the main magnetic field waveform. These two blocks are galvanically isolated. The AFG works in the range from 0 till 10V. 1 bit of AFG corresponds to the magnetic field value of 0.1Gs.

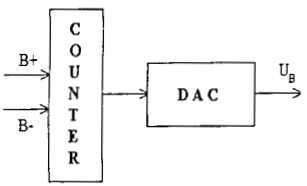


Fig. 3

The CyberResearch CMF 1622HRDA multifunction analog I/O board is used as data acquisition device for the BIMS. Some features of this board are:

- 16/8 inputs (Single Ended/Differential Mode),
- Up to 250 kHz sampling rate,
- 16 bits resolution,
- 8 MSamples Local Acquisition Memory,
- Possibility of external triggering,
- PCI plug-and-play.

2 channels of the board are used in a differential mode to acquire the beam current and the main magnetic field signal (sampling rate is 100 kHz).

The host industrial PC manages the BIMS working cycle as it is shown in Fig. 4. The measurement starts by the external signal "Beginning of the accelerator cycle".

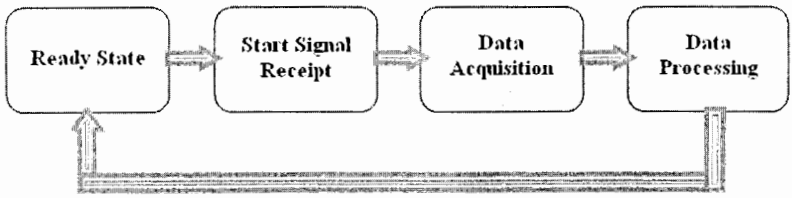


Fig. 4

**Reproduction of beam intensity**

At the first stage of testing the BIMS operated as the beam current monitor only. But the internal intensity is a more important parameter for the accelerator tuning and commissioning. The PCT detects only the average beam current. But there is the relation which allows one to get the intensity by means of the beam current and main magnetic field values:

$$I(t) = kU(t)\frac{f(0)}{f(t)} = kU(t)\frac{f(B(0))}{f(B(t))},$$

where U is a voltage signal from the PCT, f – beam revolution frequency, B – main magnetic field, $B(0) = B_{inj}$, k – constant of proportionality.

Now the BIMS successfully reproduces the beam intensity by processing the beam current and magnetic field waveforms. The Subsystem properly works in the $10^8 \ldots 10^{12}$ intensity range for the proton and deuteron beams.

**NBIMS software**

The BIMS software complex (developed for .NET Framework) consists of three parts:

- Server – equipment management, data acquisition and processing, data for the client,
- Client – remote viewing of the data from the Server,
- Administrator – remote management of client connections to the Server.

The Client as well as the Server display the beam current (voltage signal from the PCT), intensity and main magnetic field signals (see Fig. 5). Scaling and smoothing of the waveforms, browser shift, graphics or archive binary files saving, printing of the chart, are provided.

Remote viewing of the data is carried out by means of sockets technology via IP-network. Data transmission from the Server to multiple Clients is realized on the "Publish-Subscribe" model. To the Server the Client sends a special request to subscribe to the BIMS information. The Server either includes this Client in the "mailing list" or rejects the client's request. After acquisition and processing the new data,the Server dispatches it to all "subscribers". Such parameters as the list of the resolved addresses and the maximum number of client connections are given on the Server side. It is possible to change these parameters remotely and manage the "mailing list" by using the Administrator tool.

There are two modes of the Client: Simple and Extended. In the Extended mode the data with the maximum time resolution (sampling interval is 10μs) are transferred from the Server. Due to large amount of the transmitted data (about 10Mbytes) the number of these connections is limited by one. This mode is used for the machine precise tuning and investigations. In the Simple mode only 30 Kbytes of the data are transferred. It is sufficient for representation of the overall chart of the accelerator cycle. Time scaling is not provided in this mode.

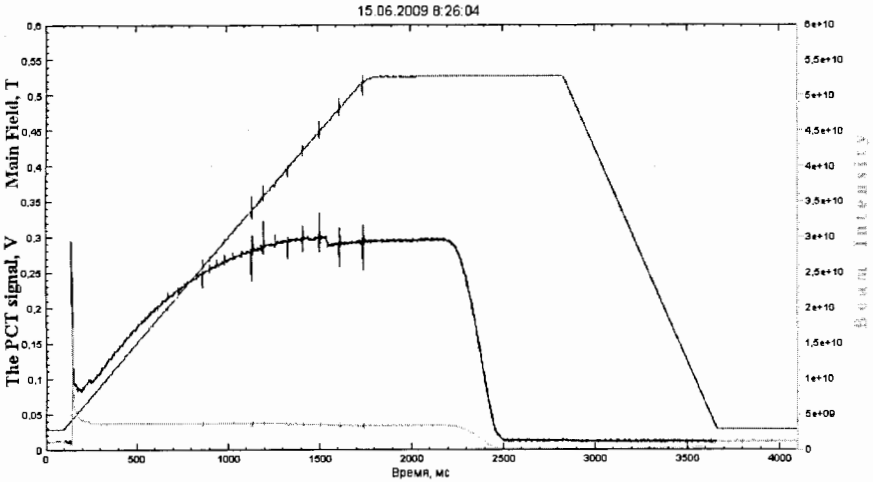


Fig. 5

**First results**

The BIMS was successfully used during two last runs of the Nuclotron [5]. The subsystem has proved to be a powerful tool for accelerator tuning. Also some important machine investigations, such as a two-step acceleration mode experiment, testing of the adiabatic capture equipment and energy evacuation system, were carried out by means of the BIMS [6].

**Future plans**

Future plans of the BIMS development are to carry out the following:

- Interface improvement: separate signals scaling on amplitude,
- Optimal increasing of the signals time resolution for the Client in the Simple mode,
- Web-support for external users.

**References**

[1] A.D. Kovalenko et al., Nuclotron-M project, JINR, Dubna, 2007.
[2] http://nucloserv.jinr.ru/nica_webpage/index1.htm
[3] V. Andreev et al., The Nuclotron Control System, NEC'2007, Proceedings of the Symposium, Dubna: JINR, 2008, pp. 59-65.
[4] http://www.bergoz.com/products/NPCT/NPCT.html
[5] N.N. Agapov et al., Status of the Nuclotron-M Project (Overall Results of Runs 37 and 38), Communications of the JINR, 2009, P9-2009-38.
[6] A.S. Averichev et al., Results of the 39th Nuclotron Run, Communications of the JINR, 2009, P9-2009-131.

# Telecommunication and network infrastructure of JINR Install 10G/sec external channel

K. Angelov, A. Dolbilov, I. Emelin, A. Gushin, V. Ivanov,
V. Korenkov, L. Popov
*Joint Institute for Nuclear Research, Dubna, Russia*

We present here development of external channels of Joint Institute for Nuclear Research. The first channel started from 64K/sec and finished up to 10G/sec. We discuss the channel organization, equipment choice, and perspectives of its development. We describe problems with the channel organization, installation and the channel management. We try to offer optimum ways of the decision of the problems connected with such high-speed channels.

## Development of the external JINR communications

The crucial project of 10 Gbps fiber data communication channel between JINR and Moscow Internet Exchange (MSK-IX), proceeded by five partners: Joint Institute for Nuclear Research, Russian Satellite Communication company, RosNiiROS, Moscow Internet Exchange, Jet Infosystems, was launched in May 2009.

On the diagram [Fig.1] one can see three places where the devices of the photonic data communication equipment were installed: the central telecommunication node (JINR LIT), settlement Radishevo, and Moscow Internet Exchange (MSK-IX).

The total length of the fiber optic communication line is about 250 km. This is almost the maximum distance for the typical optical transport equipment for the regional applications. To prepare the data channel, the technical specialists have made preliminary measurements of the signal parameters along the optical communication line to be able to make the precise adjustments of the optical I/O equipment in all three telecommunication locations along the data link and put the new 20 Gbps data channel into operation.

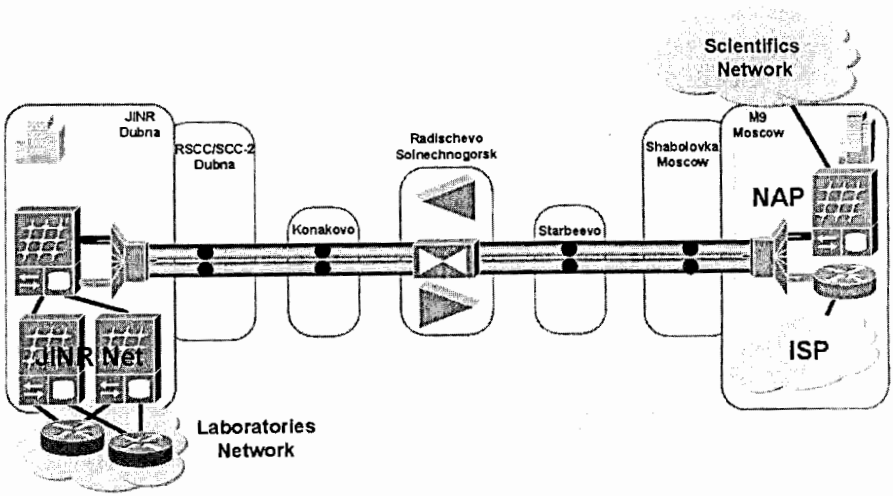


Fig. 1

The equipment for the data channel is manufactured by the Canadian vendor Nortel Networks, and installed, tested and tuned with assistance of the Jet Infosystems specialists (Moscow). The Nortel Optical Multiservice Edge 6500 terminals and Nortel Common Photonic Layer multiplexers are installed in LIT and in MSK-IX, and one Nortel Common Photonic Layer multiplexer is installed in Radishevo. The Nortel Company calls these pieces of equipment the "40G ready", what means that the data link capacity can be easily increased significantly.

This data communication channel use DWDM (Dense Wave Division Multiplexing) and 10 Gbps Ethernet technologies for the data transport. There are 2 optical light-paths (*lambda*) in use gaining 20 Gbps throughput. The throughput can be increased up to 800 Gbps by use 80 virtual lines through the implementation of the additional photonic modules.

- Currently the JINR network infrastructure has the following virtual lines:
  - direct communication line with CERN – 1 Gbps;
  - with RBnet – 10 Gbps;
  - with RASnet – 10 Gbps;
  - with RadioMSU – 10 Gbps;
  - with GEANT – 10 Gbps;
  - with GLORIAD – 1 Gbps;
  - with Moscow – 10 Gbps;
  - with Internet – 10 Mbps.

- The structure of the system for intra-Dubna network traffic exchange was optimized. It was done on the Cisco 7606 platform. Dubna Internet exchange use by the local internet providers, like Contact, LANPolis, Telecom-MPK, JINR.

**Network Security issues**

Security is gained with the implementations of the hardware and software products in the network infrastructure. To protect the computing and informational servers, users' workstations and the active routing and switching network equipment in JINR we use the industry–approved AAA approach – Authentication, Authorization, and Accounting. *Authentication* provides the method of identifying users, including login and password dialog, challenge and response, messaging support, encryption. *Authorization* provides for remote access control, including one-time authorization or authorization for each service, per-user account list and profile, user group support. *Accounting* provides the method for collecting and sending security server information used for reporting.

**Monitoring and control of the JINR network environment with IPDB**

During last two years this AAA system was successfully gradually integrated into NOC-developed product the IPDB – network data base with multiple features of monitoring and control on the basis of IP addresses. The IPDB became the main tool for the network and system administrators to maintain their everyday administrative tasks. This system was developed on the basis of My SQL software packet, was equipped with the web interface, written on ***php*** language, and incorporated the number of specialized front-end programs (written on ***perl*** and ***c*** programming languages) to deploy needed functions.

By this web interface NOC specialists and the network administrators in the Laboratories may have an access to the users' personal profiles, can monitor the IP addresses of the network elements, can change state of these elements when necessary, have an opportunity to verify the users' accounting records and the state of the different network services, the most important of which are DNS, VPN, AFS, electronic libraries, IP telephony.

The IPDB modular design principles allow to add a new feature when the need in such a service become evident, thus in 2007 the AFS system was adapted, in 2008 - the types of the network traffic, and in 2009 - IP telephony system (it is in a process of adaptation now).

The following is the summary of the various IPDB features invented last three years:

- It was developed the software control module for the AFS accounting records to be accessed from the IPDB directory;
- The support of the electronic libraries users is added into the IPDB inventory; a new user of an electronic library is also added through the IPDB interface;
- The method of the password encryption to protect users' email accounting records on the central email cluster ***mail.jinr.ru*** when connecting through the external networks was adapted;
- Due to legal SSL-encryption certificate ***Thawte*** it became possible to transfer the number of critical applications as email, network remote control, remote access to some internal sites to be used through the secured virtual channels;
- The server ***wsus.jinr.ru*** with the mirror of new Microsoft updates to increase the speed of updating and to limit incoming traffic is invented as the new service, the sever of NOD32 antivirus updates is invented also;
- The network statistics is enriched with module to calculate the traffic between JINR network and the networks of different research centers (Table 2); besides this the network traffic statistics can be presented by the traffic categories: scientific, local (Dubna), file exchange, etc., 700 grades;
- Invented the system to detect the computers infected with harmful content: viruses, trojans, mulware;
- The system to detect network intrusions and attacks ***snort*** was invented;
- The monitoring of the network state through the ICMP and SNMP protocols is put into deployment, serving more than 100 network elements;
- The new anti-spam packets help to filter about 1 million email spam-messages every 24 hours;
- There is a temperature monitoring proposal to be able to keep network and telecom room environment under permanent automatic control, as a part of the general monitoring system.

The following are some data on monitoring and control topic:

- This time NOC team supports 18 specialized servers which carry the main network services, which support JINR overall network environment: DNS, email, DHCP, statistics, data bases, remote access. If to add to that said quantity of servers the active routing and switching equipment we'll get around 70 units of the active network equipment,
- More than 50 users' requests are served during the working day,
- About 20 network incidents related to the security violation issues are investigated each month,
- The volume of the external traffic is about 20 Terabytes per month,
- There are 1700 active subscribers to the central email service.

In the table is the statistics of IPDB use by the specialists of the different profiles and different services.

Table 1

| IPDB Statistics | |
|---|---|
| Operator (Network and System administrators in the JINR divisions) | 43 |
| User | 3618 |
| Network Element | 6690 |
| IP address | 7772 |
| Remote Access (total in month) | 1275 / 15 |
| Electronic Library Access | 814 / 20 |
| AFS | 365 |
| Transaction per year | 160 000 |
| Scientific Networks | 270 |

Table 2

***The scientific data traffic exchange in 2009 (in Terabytes)***

| | Research center | Alias | To JINR | From JINR | % |
|---|---|---|---|---|---|
| 1 | Fermi National Accelerator Laboratory (US) | FNAL | 84 | 2 | 24 |
| 2 | Science Park Watergraafsmeer Amsterdam (NL) | SARA | 61,78 | 15,49 | 18.11 |
| 3 | Nationaal instituut voor subatomaire fysica (NL) | NIKHEF | 49,06 | 0,9 | 14,38 |
| 4 | European Organization for Nuclear Research (SE) | CERN | 40,6 | 27,73 | 5,24 |
| 5 | Institut National de Physique Nucleaire (FR) | IN2P3 | 17,89 | 15,9 | 5,24 |
| 6 | Rutherford Appleton Laboratory (GB) | RAL | 13,54 | 5,54 | 3,97 |
| 7 | National Grid Initiative (TR) | TR-GRID | 10,96 | 0,2 | 3,21 |
| 8 | Consorci Institut de Fisica Altes Energies (ES) | PIC | 10,35 | 0,6 | 3,03 |
| 9 | Deutsches Elektronen-Synchrotron (DE) | DESY | 7,42 | 3,19 | 2,17 |
| 10 | Forschungszentrum Karlsruhe (DE) | KFK-ULTRA | 6,71 | 2,25 | 1,97 |

As seen from the table CERN has only 4-th rank.

Table 3

**Dynamics of the JINR external channel, internet links and input traffic**

■ Evolution of the external channel

| Year | 1999 | 2001 | 2003 | 2006 | 2009 | 2010+ |
|---|---|---|---|---|---|---|
| Channel capacity Mbit/sec | 2 | 30 | 45 | 622 | 10 000 | K*10 000 |

Table 4

■ Evolution of the local network

| Year | 1986 | 1994 | 1998 | 2002 | 2004 | 2010+ |
|---|---|---|---|---|---|---|
| Channel capacity Mbit/sec | 0.512 | 10 | 155 | 100 | 1 000 | 10 000 |

Table 5

■ Input traffic in JINR

| Year | 2005 | 2006 | 2007 | 2008 | 2009 | 2010+ |
|---|---|---|---|---|---|---|
| Input traffic Tbyte | 46 | 83 | 242 | 376 | 536 | |

Table 6

**Traffic presentation by category**

| | |
|---|---|
| Scientific & educational networks | 87,00% |
| File exchange (torrent, ftp) | 5,9 % |
| Web-resourses | 1,50% |

**New projects and services**

• The JINR 10 Gigabit Backbone. With the invention of the 20-Gbps external data channel the time to make a transition to the 10 Gigabit Back-bone of the JINR LAN has come. This proposal was declared before the JINR Technical Council last fall. We have made two versions of the project: one for all JINR divisions with roughly estimated cost in 500 000$ (Fig. 3), and partial solution, which relates only to 3 or 4 divisions, and has the lower cost accordingly (Fig. 2).

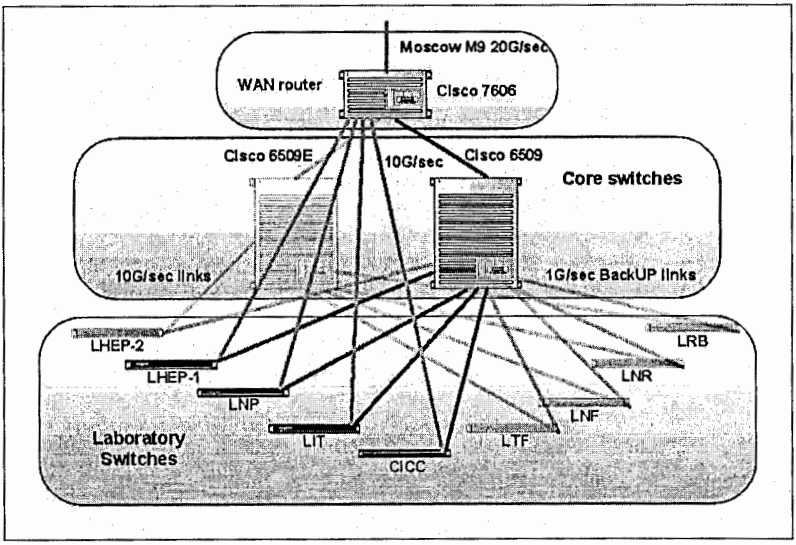


Fig. 2

• Offers on local network modernization. In connection with increase in capacity of external channel JINR to 20 Gb/s, there was a necessity for increase in throughput of local communication channels both to Central Information-computer complex, and to institute laboratories. On the basis of it were the variant of transition Backbone JINR on 10 G bit/sec a highway, as continuation of development of a network infrastructure of institute is considered (Fig. 3). It included acquisition two 16 ports 10Gb/s the Ethernet-module into two Cisco 6509 and 9 Cisco 3560E-12D in each laboratory.

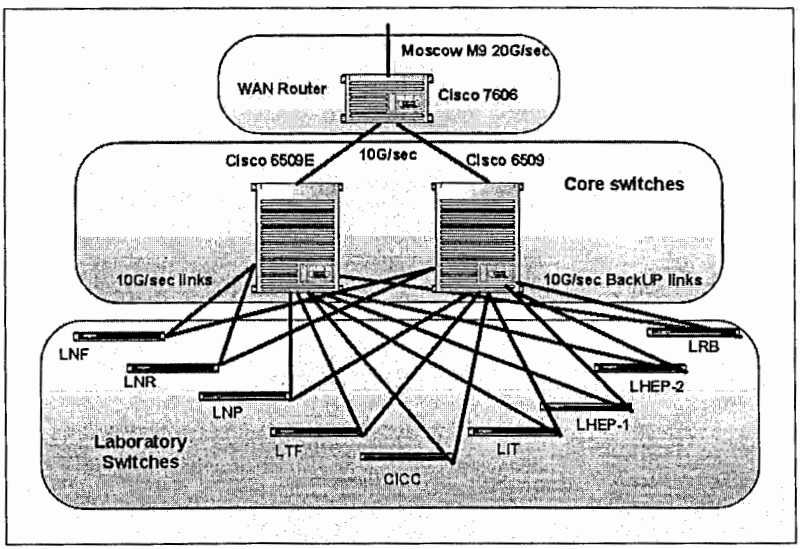


Fig. 3

• On-demand bandwidth. The capacity of the external data channel equipment allows providing the necessary bandwidth to the different organizations in Dubna-city, including so-called, resident-companies in the special economic zones in Dubna.

• New fiber optics cabling. To have the possibilities on-demand capacity provision the JINR fiber-optics infrastructure has to be essentially modified and terminated in some points of presence of Dubna-city network transport providers.

• Real-time services.

These types of services include IP-telephony, Video Conferencing, and IPTV. Below is the diagram (Fig.4) of IP-telephony solution. Implementation of the IP-telephony will allow cut down the expenses for the in-country and international phone calls, will provide possibilities to use Dubna phone numbers being around the scientific world from airports, etc. Invention of the IPTV will give the quality of the last to the video-conferencing.

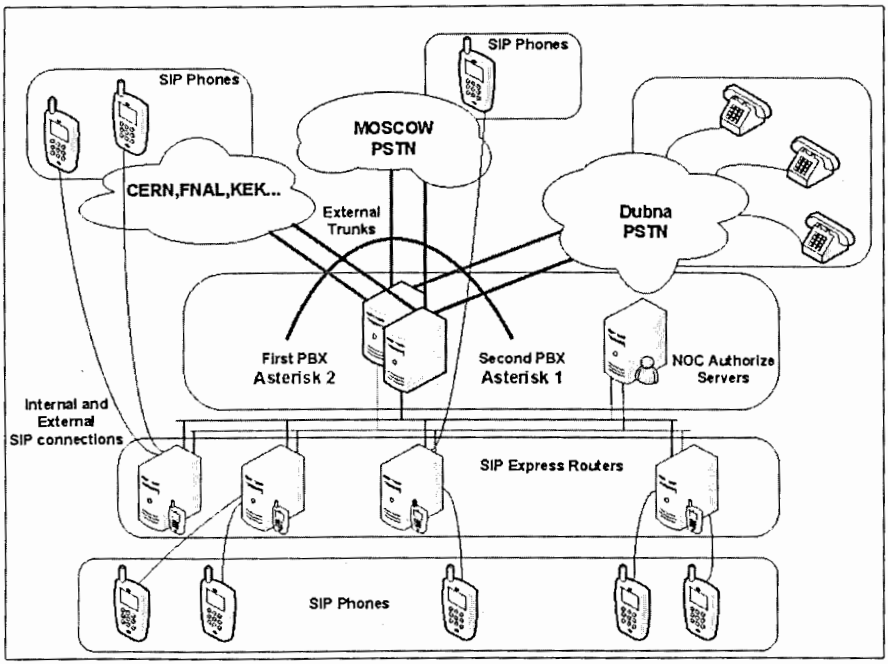


Fig. 4

# ATLAS Distributed Computing

A. Anisyonkov[1], A. Klimentov[2], D. Krivashin[1], M. Titov[3]
[1] *Budker Institute of Nuclear Physic,*
[2] *Brookhaven National Laboratory*
[3] *Moscow Engineering and Physics Institute*

The needs of large-scale simulation, reconstruction and analysis of ATLAS data required the development of distributed computing system, which allows efficient data access and makes use of all available computing resources.

The idea of distributed computing, and later of the computing grid, became fashionable at the turn of the century and looked promising when applied to HEP experiments' computing needs.

## Introduction

The ATLAS experiment produces petabytes of data annually through simulation production and will produce tens of petabytes of data per year from the detector itself when LHC starts up in production. This data will be distributed globally according to the ATLAS computing model [1]. After a first pass reconstruction at CERN, raw data from the detector and reconstructed data products are replicated to 10 Tier-1 centres according to the data type and the amount of data the centre has agreed to store. In addition to the data from the detector, simulated data is produced on Grid resources worldwide, and this data must also be replicated.

## Computing model

The ATLAS computing model embraces the Grid paradigm and a high degree of decentralization and sharing of computing resources. It has been developed over more than ten years to meet the challenges of the LHC era [2].

These challenges are many:

- Very many petabytes of raw and processed data per year,
- Diverse data formats, with both large and small files,
- A world-wide analysis community.

The primary event processing occurs at CERN in a Tier-0 Facility. The RAW data is archived at CERN and copied (along with the primary processed data) to the Tier-1 facilities around the world. These facilities archive the RAW data, provide the reprocessing capacity, provide access to the various processed versions and allow scheduled analysis of the processed data by physics analysis groups. Derived datasets produced by the physics groups are copied to the Tier-2 facilities for further analysis. The Tier-2 facilities also provide the simulation capacity for the experiment, with the simulated data housed at Tier-1s. In addition, Tier-2 centres will provide analysis facilities and some will provide the capacity to produce calibrations based on processing some raw data. A CERN Analysis Facility provides an additional analysis capacity, with an important role in the calibration and algorithmic development work.

The computing model gives rise to estimates of required resources that may be used to design the various facilities. It is not assumed that all Tier-1s or Tier-2s will be of the same size. However, the ratio of disk, tape and CPU resources required is implied in each case.

**Distributed Computing Components**

The ATLAS Grid architecture is based on:

- Distributed Data Management (DDM),
- Distributed Production System (ProdSys, PanDA),
- Distributed Analysis (DA), GANGA, PanDA [3],
- Monitoring,
- Grid Information System,
- Accounting,
- Networking,
- Databases.

**Distributed Data Management**

The ATLAS Distributed Data Management (DDM) [4] project was established to develop a scalable and reliable system for data organization and placement, on top of the WLCG Grid infrastructure. The DDM system based on Grid technologies provide tools for data transfer, monitoring and access to the physics community. The DDM software stack is called DQ2 [5], designed to implement the ATLAS computing model, and by interacting with the underlying Grid middleware, provides a single entry point for users requiring access to data.

DQ2 has three main components:

- Central Catalogues (Global services), responsible for book-keeping information,
- Site Services (Local services), responsible for fulfilling data movement requests (subscriptions),
- End-user tools to interact with Central Catalogues and Site Services.

Individual users and physics groups can subscribe for reasonable amount of data and request data transfer between grid sites.

DQ2 uses dataset based approach, where a dataset is a mutable or an immutable collection of files. Datasets are the unit of data replication and data organization: aggregating file in datasets allows to scale down the number of entities for data transfer, deletion and discovery, beside offering a simple way to share and aggregate data in a convenient way across the collaboration.

User tools for data replication: DQ2 client API, DQ2 command line utilities, DQ2 enduser tools, DQ2-based Data transfer request interface.

**Data Transfer Request Interface (DaTRI)**

DaTRI is a web-based application to handle user data transfer requests. It makes bulk subscriptions of chosen datasets to defined site and converts requests into appropriate DQ2-bulk subscriptions under a policy defined by the DDM management. DQ2 API(s) are used to subscribe and to control data replication. Also DaTRI provides possibility to transfer fraction of dataset.

**Distributed Production System**

The Distibuted Production System manages ATLAS simulation and jobs reprocessing on the Grid. Several services are involved into this system: DDM/DQ2 for data management,

PanDA (Production and Distributed Analysis System) for task request interface and job supervising, ATLAS Dashboard and PanDA Monitor for monitoring.

System workflow can be described in terms of tasks and jobs. Tasks are created through task request interface which PanDA gives. Afterwards they are splitted into groups of related jobs. Jobs defenition and it's state are stored in Production Database. DQ2 datasets are used as input and output for job.

**Distributed Analysis**

The distributed data analysis using Grid resources is one of the fundamental applications in high energy physics that has been addressed and realized for the start of LHC data taking. The needs to manage the resources are very high. Two front-end tools are available to users, namely Ganga and the PanDA Client (i.e. pathena, prun, etc.).

The Ganga job management system has been developed as a common project between the ATLAS and LHCb experiments. Ganga provides a simple and consistent way of preparing, organizing and executing analysis tasks within the experiment analysis framework Athena, implemented through a plug-in system. It allows trivial switching between running test jobs on a local batch system and running large-scale analyzes on the Grid, hiding Grid technicalities from the users.

PanDA system is a workload management system developed to meet the needs of ATLAS distributed computing. As pilot-based system it allows analysis to leverage production operations support, thereby minimizing overall operations workload.

**Monitoring**

The ATLAS Distributed Computing provides a consistent set of monitoring tools covering the Production System, Function Tests, Distributed Data Management, User Analysis, Central Services and Grid Infrastructure.

The Production System, DDM and Central Services dashboards are targeted mainly at shifters, and their interfaces reflect this by providing a quick overview of the overall status of the system, and promoting an easy navigation down to the detailed errors reports. Experimental support for automatic problem detection and report generation is available and is a main focus for continued development. Historical information is also available, less important for shifters but essential for longer term system performance analysis.

Functional Tests monitoring in addition with PanDA and Dashboard monitoring pages provide users with access to overview information how data is exported from CERN and replicated between ATLAS sites. This system is to be designed for monitoring replications of ATLAS detector data, reprocessed and simulation data. It also shows data replications during various ranges of tests and runs like Functional Tests, STEP09, etc.

**Grid Information System**

The overall purpose of ATLAS Grid Information System is to store and expose static, dynamic and configuration parameters needed by ATLAS Distributed Computing applications. AGIS architecture model and its relationship with other modules are shown on Picture 1.

AGIS is ORACLE based information system. AGIS stores as read-only data extracted 3 from the external databases (f.e, OIM, GOCDB, BDII) and ADC configuration information which can be modified.

The synchronization of AGIS content with the external sources is performed by agents (data providers), agents access databases via standard interfaces.

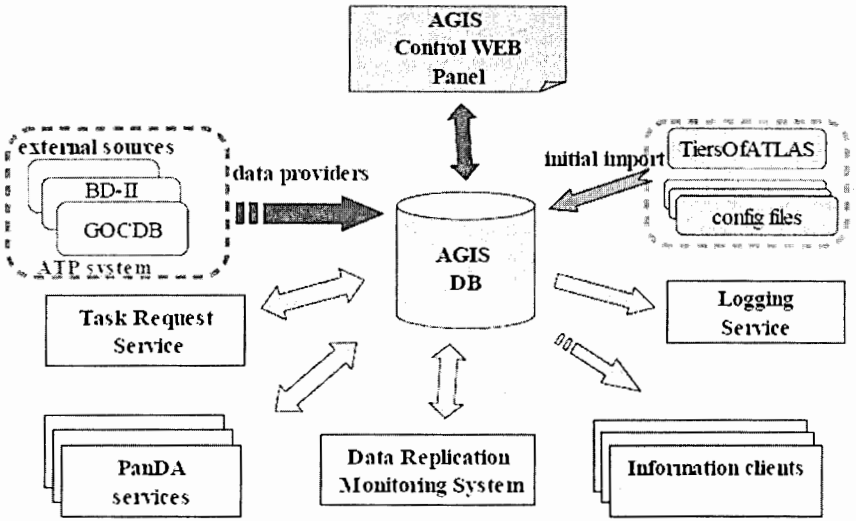


Fig. 1. AGIS Architecture overview

## Conclusion

The ATLAS Collaboration has developed a set of software and middleware tools that enable access to data for physics analysis purposes to all members of the collaboration. The ATLAS Distributed Computing model foresees the distribution of RAW and processed data to Tier centers, so as to able to exploit fully the computing resources that are also made available to the Collaboration members, independently of their geographical location.

Various components of ATLAS Distributed Computing system help user and shifters to manage, to monitor and to control data flow.

## References

[1] D. Adams et al. - ATLAS Collaboration. The ATLAS Computing Model, ATL-SOFT-2004-007; CERN-LHCC-2004-037/G-085.- Geneva: CERN, 2005.

[2] The ATLAS Computing Technical Design Report. ATLAS-TDR-017; CERN-LHCC-2005-022, June 2005.

[3] T. Wenaus, T. Maeno, Panda/DDM Integration. BNL DDM Workshop, BNL, September, 2006.

[4] D. Barberis et al., ATLAS Distributed Data Management Operations. G/ ATL-SOFTPUB-2006-006; CERN-ATL-SOFT-PUB-2006-006; ATL-COM-SOFT-2006-008- Geneva: CERN, 2006.

[5] M. Lassnig et al., Managing ATLAS data on a petabyte-scale with DQ2. CHEP-07, Journal of Physics: Conference Series, 2008.

# Teaching methodological complex 'Physics – Spheres' as the component of modern interdisciplinary information educational environment

D.A. Artemenkov[1], V.V. Belaga[1,2], I.A. Lomachenkov[1], Yu.A. Panebratsev[1], P.I.Semchukov[1], N.E. Sidorov[1], A.V. Shoshin[1,2], M.S. Stetsenko[1,2], N.I. Vorontsova[1]

[1] *Joint Institute for Nuclear Research, Dubna, Russia*
[2] *Dubna University, Russia*

Teaching methodological complex "Physics – Spheres" is a result of work of a big team of authors headed by prof. Yuri Panebrattsev. Several years ago, when our project was supported by the Russian National Foundation of Personnel Training, we started to develop educational materials on Physics for a secondary school course. Some time ago separate electronic educational resources were obtained by our group and then together with publishing house "Prosveshcheniye" began to develop a unitary teaching methodological complex named "Physics – Spheres".

What does it mean – the project "Spheres" of the publishing house "Prosveshcheniye"? It is a multiobjective interdisciplinary project aimed at creating a unitary system of the modern school informational educational environments which provides new approaches to the educational standard at a secondary school [1]. The publishing house "Prosveshcheniye" formulated a task to develop a unitary informational educational environment in the form of an interrelated system of educational resources presented in the written and digital forms. Methodological principles of the project "Spheres" provide the unitary educational technology and effective realization of interdisciplinary and supradisciplinary relationships. They also include wide implementation of information and communication technologies into the educational process [2]. Teaching methodological complexes (TMC) "Spheres" are published in the series of "Academic school textbook" which was developed in the framework of a wide-scale project "Russian Academy of Sciences, Russian Educational Academy, the publishing house "Prosveshcheniye" — for Russian School".

TMC "Spheres" includes a full set of educational materials in the written and digital forms for all grades of the middle and high schools which are required for rational organization of the educational process according to modern trends in physics teaching and educational methodology at the secondary school. Distinctive characteristics of the subject-informational educational environment are as follows:

- Recognizability,
- Unity of a navigation system of quick orientation which supports the unitary educational technology and easy acquisition of skills of selection, analysis and synthesis of information by school students,
- Presentation of educational materials on the basis of various types of informational resources.

The structure of informational educational environment "Spheres" (Fig. 1) can be divided into three levels. The central part belongs to the teaching methodological complex which consists of a text-book, class notebooks, etc. The next level includes subsidiary informational resources which are necessary for learning the subject. And, finally, the third level opens an access to additional resources for advanced study of separate themes.

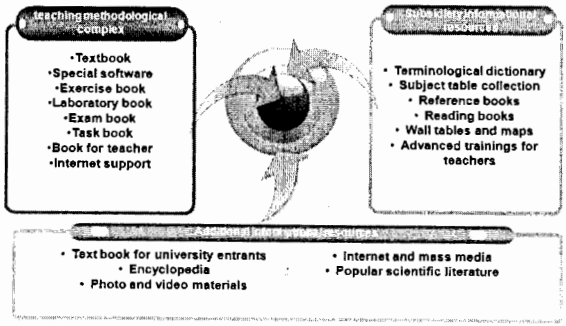


Fig. 1. Structure of informational educational environment 'Spheres'

At present the TMC on 7 school subjects: Physics, Math, Biology, Geography, History, History of Russia and Social science have already been developed and are in progress.

This year we have published the educational complex on Physics for the 7th grade which includes:

- Textbook,
- Additional software,
- Exercise notebook,
- Laboratory notebook,
- Exam notebook,
- Task book,
- Teacher's book.

The similar complex for the 8th grade is being prepared for publishing. The complex for the 9th grade is also being developed at the moment.

The central part of the complex belongs to the textbook which has a fixed format. This provides its navigational function in the system of the whole TMC. While developing this textbook we implemented a double-page spread principle in its construction. This, together with the same uniform construction of the basic divisions and every double-page spread, considerably simplifies the work with the textbook both for the teacher and school children.

Every chapter of the textbook includes the following obligatory elements:

- Short introduction,
- Main content,
- Conclusions and generalizations,
- Problems for discussion,
- Generalizing scheme.

As a rule every lesson is shown in one double-page spread and it has a fixed structure:

- Introductory rubrics of a lesson,
- Body text,
- "In focus" — main idea of lesson,
- "Attention" — highlighted basic formulas and definitions,
- Persons in Physics,
- Physics kaleidoscope,
- My physical research,
- Final test.

Fig. 2 shows one of the above double-page spreads.

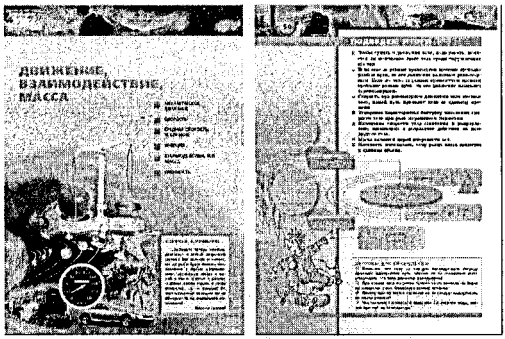


Fig. 2. Appearance of the chapter double-page spread

The chapter which needs the explanation of the tasks can include the additional double-page spread dedicated to the solution of the tasks. It is important that every structure unit has got its universal easy recognizable image. It considerably simplifies the work with the textbook.

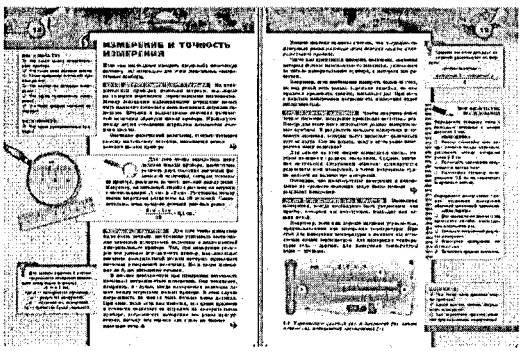


Fig. 3. Appearance of the double-page spread of the textbook

Additional software has also a multilevel structure. It includes the following basic insets:

- Textbook,
- Task book,
- Reference book,
- Laboratory works,
- Search,
- Control,
- Private folder,
- Help.

In the digital version of the textbook every double-page spread is presented as an active screen area. It includes references highlighted in the text that enable one to select media objects for the topic of the given lesson. The media objects (image and video collections, animations, interactive models and experiments, glossary, background materials, biography materials and interesting facts) are thematically related with the educational material represented on the double-page spread/screen. There are more than 1000 media objects, which

help to solve various types of educational tasks. For example, animations and interactive models help to understand quite complicated physical phenomena and processes.

Thereby every double-page spread fulfils the role of a navigator to search for informational resources (Fig. 4).

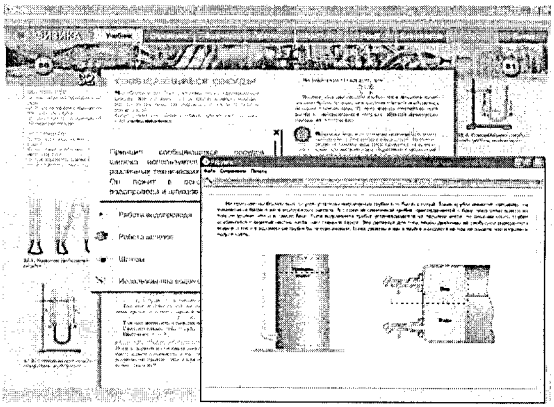

Fig. 4. Digital version of the textbook in special software after clicking into reference and selecting one of media object

The electronic application includes a set of virtual laboratory works, which can be used in various stages of the educational process. Some of them include video demonstration.

The task book of the special software can be used as a training system both for polish the skills of solving the tasks and self-testing. It has two modes of solving the tasks: with intermediate calculations and without them. For solving the task one should enter the necessary data and mark all points at the diagram. At the same time one could watch the animation which visually demonstrates the statement of some problem. The application checks the entered data and shows mistakes. Then one could try to solve the task once again.

The inset named 'Reference book' includes all necessary reference materials which can be sorted by different features that simplifies the work with information. Reference materials include basic formulas, basic tables, basic physical constants, etc., which could be selected for any lesson or chapter or separately.

In the application there are 2 modes of testing: the training mode and the mode of control. The first mode provides a repeatable system of testing. In the second mode results go into the database. You can improve your results only at the next session of the application. When you have passed the tests you can also see the detailed analysis of your mistakes. Tests contain questions which involve a selection of correct answers from the list and questions which involve an arrangement of scheme details in the right order. The results of test are shown in the inset 'My results'.

The inset named 'Search' (Fig. 5) gets an opportunity to work with separate media objects. Selected resources could be saved into 'Private folder' for the further work with them both in the shell of the software and independently. For example, separate resources of the application could be used in your own presentations or reports.

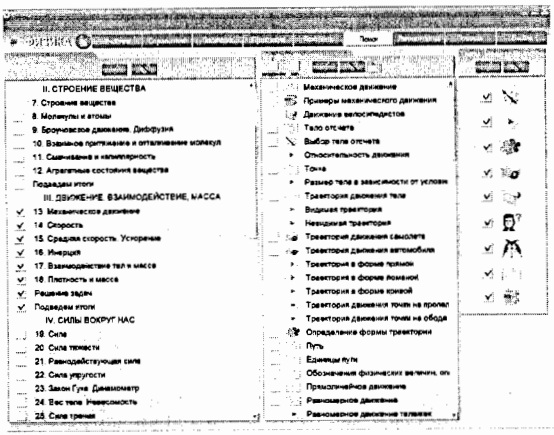


Fig. 5. Appearance of the inset named 'Search', when some lessons and all types of media objects are selected

Using the textbook as a navigator it gives opportunities to involve simultaneously to the educational process various informational resources (that is practically unrealizable in the frame of traditional education), choose a trajectory of the educational process in accordance with the specificity of the whole class or separate students and effectively organize independent work. Thereby the materials of the additional software can be a useful tool for lesson modeling.

Thus all the materials of the course, which vary in complexity and volume of the informational support, are organized in the unitary methodological scope which reflects a new concept of educational writings creation. All these distinguishes the present TMC and its 'core' (textbook) from previously published materials and allows us to tell about the realization of a qualitatively new level of the school textbook development as the fundamental unit of the information educational environment. We hope that TMC 'Physics – Spheres' will help to solve of the following tasks:

- Realization of the activity approach in the Physics education by using various components of the complex,
- Formation of the unified scientific picture of the World,
- Extension of the technical horizons of the school students,
- Presentation of the materials on Physics in their historical progress and as a result to improve the attitude towards Physics among school students.

**References:**

[1] Center 'Spheres' of the publishing house 'Prosveshcheniye', http://www.spheres.ru

[2] V.P. Dronov, Interview for the magazine «Open Education», http://www.vestnik.edu.ru/dronov.html

# Optimization of a CSA IC for silicon microstrip detectors

E. Atkin, I. Ilyushchenko, D. Semenov, A. Silaev, A. Voronin[1]
*National research nuclear university «MEPhI» , Russia*
*[1]Skobeltsyn Institute of Nuclear Physics , Russia*

The results of developing a CSA integrated circuit, intended for application with the microstrip detectors of the Silicon Tracking Station of the CBM experiment are presented.
The analysis of both the schematics and layout was carried out in accordance with the design kits of the 0.18u CMOS process of UMC.

## Introduction

The results of works on simulating the CSA IC are described. Further there follow a brief general information on the manufactured samples and the PCB, designed for testing the IC in lab conditions, and the results of characterization tests of the manufactured ICs for their compliance with the requirements of specifications.

## CSA circuit and its simulations

The schematic circuit of the studied CSA is presented in Fig. 1 (A,B). It consists of the following basic units:

1. CSA core (Fig. 1A),
2. Preamp core (Fig. 1B).

The charge-sensitive preamplifier schematics is based on a classical folded cascade architecture with an additional nonlinear feedback network. This solution allows to combine the well-known advantages of the charge preamplifier configuration in terms of gain stability with the possibility of detector leakage current compensation.

The CSA circuit of Fig. 1 was simulated in frames of Cadence IC 5.1.41 package. The noise properties of the circuit were evaluated by such a widely used parameter, as the equivalent noise charge (ENC), defined as [1].

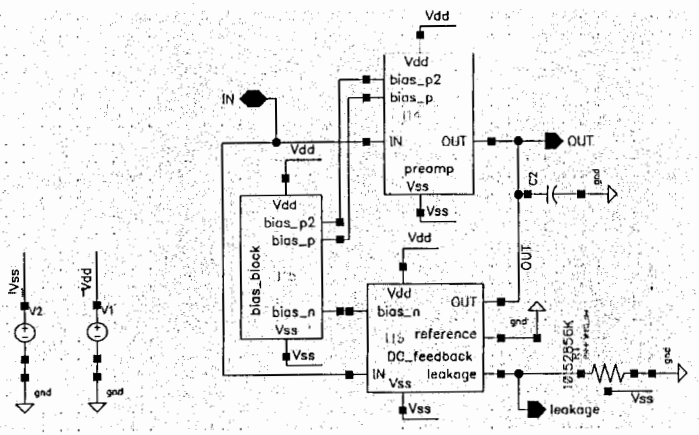


Fig. 1A. CSA structure

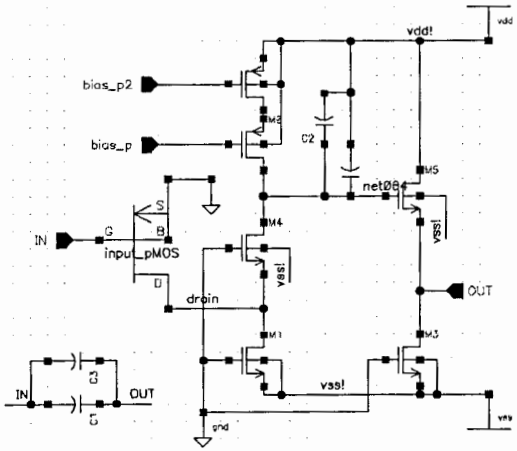


Fig. 1B. Preamp core

The circuit of Fig.1 was simulated by Cadence at the "transient" and "noise" kinds of analysis chosen. Those kinds of analysis result in the plots of Uout(t), (see Fig. 2). The circuit was extracted by Cadence's tool Assura, results of this extraction was simulated. Comparison between schematic and extracted (Uout) evaluated and plotted (see Fig. 3).

**Chip manufacture and packaging**

The 0.18 μm CMOS process of UMC, Taiwan (6 metals, 1 poly) with MMC and RF options, provided via Europractice foundation was used for the chip manufacture [2,3,4].

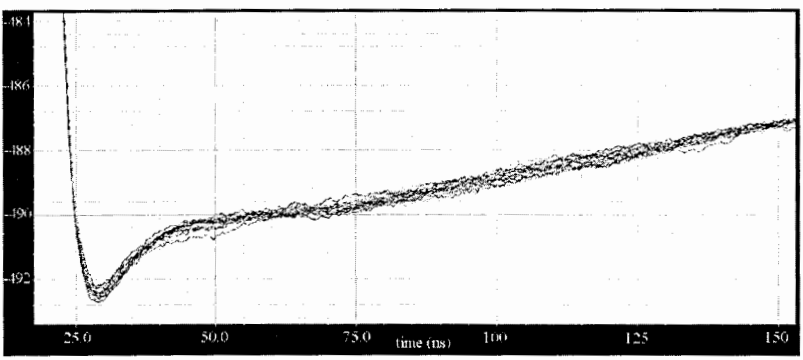


Fig. 2. Transient noise analysis

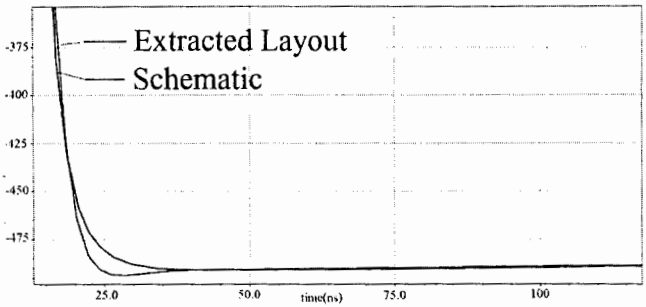


Fig. 3. Comparison between schematic and extracted view

**Conclusions and outlooks**

In the frames of the R&D work there has been developed and successfully tested a CSA IC, which is a critical block of front-end electronics, responsible for accurate matching of strip sensors of quite different geometry (range of capacitances is up to 100pF) with read-out chain.

First prototype chips have been manufactured according to the 0.18 μm CMOS process design rules of UMC company (Taiwan) in 2005. The results of the first measurements on a set of 5 CSA chips have shown the feasibility of the used solution.

**References**

[1] L. Gorn, B. Hazanov, Units of radiometric equpment built with ICs, M: Atomizdat, 1973.

[2] E. Atkin, Yu. Volkov, A. Voronin, A. Silaev, A. Smirnov, V. Tolochko, 0.18um CSA ASIC for Microstrip Detectors, NEC'2005, pp.67-70.

[3] E. Atkin, Charge sensative amplifier with extended dynamic range, NEC 2007, pp. 93-95.

[4] E. Atkin, M. Trubetskoy, A. Kluev, A. Voronin, Design of data-driven architecture for multichannel detectors, NEC'2007, pp. 102-105.

# Analog 128 to 16 de-randomizer ASIC

E. Atkin, A. Klyuev
*Moscow Engineering Physics Institute (State University)*

Reduction of transistor dimensions in today microelectronics makes it possible to increase significantly the degree of integration of the readout ASICs for the detectors in large experimental physical facilities [1]. One of the major experiments is the experiment on the study of compressed baryonic matter (CBM), the planned installation of the accelerator FAIR in GSI (Darmstadt, Germany) [2]. As an example, it should be noted, that the CBM experiment has a silicon tracking system with more than a million channels of further electronic processing. To ensure readout of such an amount of information there are necessary thousands of multi-channel chips (about 12 thousand for the CBM experiment). For such chip quantities the readout electronics is facing serious problems in optimizing overall dimensions and power consumption. One of the solutions is to use specialized analog-digital highly integrated chips for collecting and processing information.

Typically, the primary information data streams have an essential non-informational part, which is desirable to be reduced at the early stages of processing in near-real time scale. It is important not to lose useful information and reduce the dead time, which is often necessary to analyze the data.

This problem can be solved by using digital signal processing, but the area occupied on-chip by the high-speed ADC, as well as their power consumption is still a technical challenge, when they are used for each channel. The second major problem is the random nature of the input information, while digital systems are preferably designed to perform clocked, that is, the changes of digital inputs should be ongoing, what significantly reduces malfunctions in digital processing.

Taking into account that the system does not have 100% load on the total number of channels, but in fact the load is distributed in a certain way on the coordinates of the planes of the tracking system [3] (see Fig. 1), one can connect the chip so that the maximum number of the loaded readout channels (M) will not exceed the predeterminated number of processing channels (N).

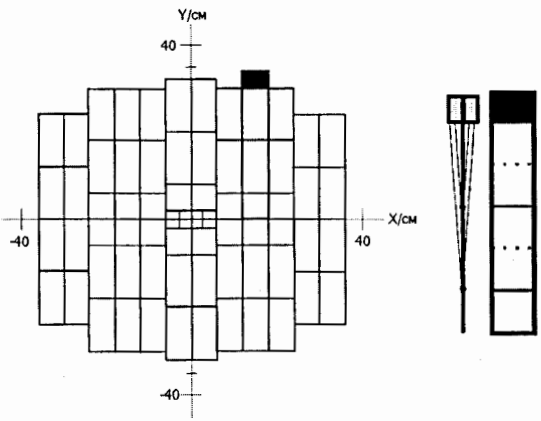


Fig. 1. Geometry of silicon detectors at FAIR

The ratio of M / N is a de-randomization factor [4], it has practical sense when M > N. In architectural terms, this supposes the system with M readout channels and N processing channels (analog and digital).

In an ASIC with analog de-randomization the readout channel consists of a charge-sensitive amplifier, shaper and comparator. The data processing channel may include a peak detector, sample and hold, a block such as the «time over threshold» one (a special case of Wilkinson transformation [5]), ADC. The block diagram has been presented in [4].

The function of de-randomizing analog signals is provided by an analog key matrix, managed by a logical unit that can analyze the chaotic appearance of the input signals in the readout channels and the possibility of their transfer to the free processing channels.

The logic of the de-randomizer is based on the fact that the pulse shape is known, and the fact that the full, but not excessive, load on the system is possible only in the case of simultaneous events in N channels, the number of occupied readout channels being not greater than the number of processing channels (provided that they are ready), and the repetition period of the event exceeding the signal processing time in the corresponding channel (see Fig. 2).

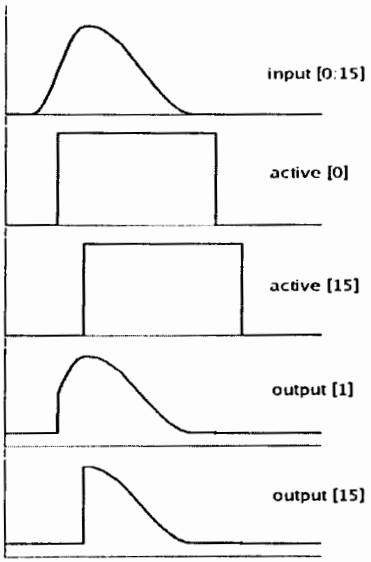


Fig. 2. Switching time diagrams

To avoid distortion of the amplitude information it is necessary to switch all channels in a time, not exceeding a certain peaking time of the signal.

Given that every act of switching the readout channel to processing channel occurs at the front of the clocking signal, it is sufficient to establish its frequency so, that the duration of N cycles will be less than the peaking time of the input signals. This case was simulated using AMS simulator (see Fig. 3).

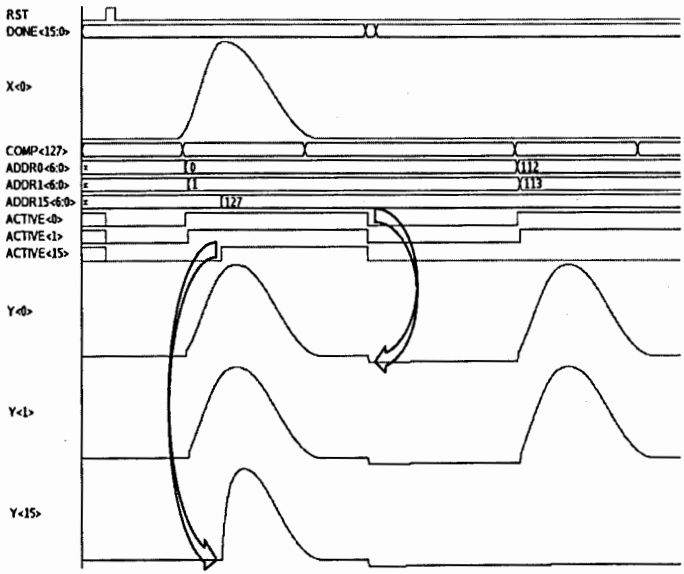


Fig. 3. The results of an AMS simulation

Schematic cell views were used in the matrix of analog keys, while logic was presented as verilog blocks. Mixed signal devices such as comparators were described using verilog-AMS language. The simulation shows results, matching the expected ones: logic functioning correct, but analog part needing some optimization. The ASIC is being floor planned now, while the analog parts are being optimized. Last version of the ASIC tentative floorplan is given in Fig. 4.

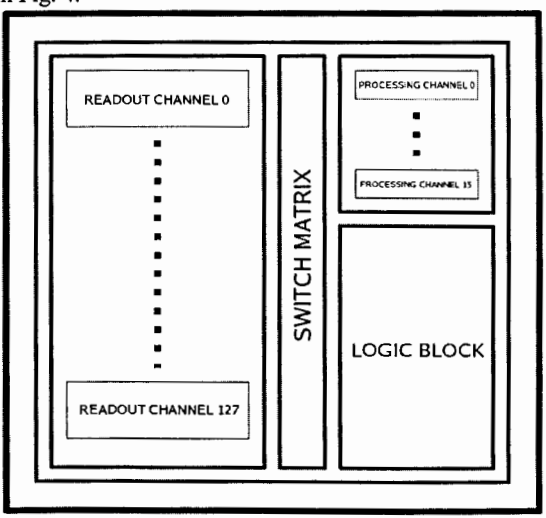


Fig. 4. ASIC tentative floorplan

**References**


[1] G.E. Moore. Cramming more components onto integrated circuits, http://download.intel.com/museum/Moores_Law/Articles-Press_Releases/Gordon_Moore_1965_Article.pdf

[2] A. Kiseleva The compressed baryonic matter experiment, //http://www.gsi.de/fair/ experiments/CBM/

[3] A. Kotynia. Silicon tracking system and micro-vertex detector, http://cbm-wiki.gsi.de/cgi-bin/view/Public/PublicSts

[4] E. Atkin, A. Klyuev, M. Trubetskoy, A. Voronin, Design of data-driven architecture for multichannel detectors. XXII International Symposium on Nuclear Electronics & Computing (NEC'2007) (Varna, Bulgaria, September 10-17, 2007), Proceedings of the Symposium, Dubna, JINR, 2008.

[5] D. Kollar Pulse processing and analyses, http://www.dnp.fmph.uniba.sk/~kollar/je_w/el3.htm

# Readout module for multichannel alpha detector

K.A. Balygin, V.P. Bolotsky[1], M.D. Karetnikov, A.I. Klimov, K.N. Kozlov, E.A. Meleshko, V.V. Shahovskoy[1]

*Russian Research Center "Kurchatov Institute"*

*[1] Central Research and Development Institute of Chemistry and Mechanics*

The architecture and ways of operation of the readout module of multichannel alpha detector are considered. The module is a part of DAQ system designed for tagged neutron technology. A number of channels (64) is defined by a number of anode pixels of PMT H8500D. A parallel two-coordinate addressing provides high performance and efficiency. A counting rate in each channel is measured by FPGA, a time of alpha particle detection is recorded by the signal from the last PMT dynode common for all PMT anode pixels. The results of preliminary testing of the module with isotope ($^{241}$Am) alpha source are presented.

## 1. Introduction

Interest to experiments with tagged neutrons is due to ability to use this technology in problems involving elemental analysis of organic materials—in particular, for recording of explosives. Tagged-neutron technology based on T(d,n)He reaction. Neutron accompanies alpha-particle. The neutron generator with build-in position sensitive alpha-detector, nanosecond electronics and fast gamma-detectors are key elements of this technology. At the present time neutron generators with sealed off tube are used for apparatus based on the tagged neutrons technology. The alpha-detector build-in the neutron generator is difficult and important element. This detector is exposed high temperature, irradiation by neutrons, charged particles and photons on-stream. Electromagnetic radiation, inducted in alpha-detectors signal output section is considerable factor. A special specifications are claim to radiation resistance and reliability of alpha-deterctor. Therefore the scintillation alpha-detector with multichannel PMT H8500D (Hamamatsu), placed outside useful capacity of the neutron generator, is perspective. Angle resolution and aperture tagged neutron beam for unauthorized laying detection apparatus can be improved using such detector. The module for readout and front-end processing data from multichannel PMT are considered in report. The module contain unit of alpha-signals shaper, placed nearby PMT, and logic unit placed in crate with other apparatus.

PMT H8500D (Hamamatsu) has 64 anode sections and one common dynode. Pulses from the anode section uses for fixing number of went off pixel of the alpha-detector. Provisional data about pulse width (~2ns), amplitude (~4mA) and maximum count rate ($2 \cdot 10^6 s^{-1}$ for common dynode and $5 \cdot 10^4$ $s^{-1}$ for each anode) was used for designing the readout module for this detector.

## 2. Readout information from H8500D PMT

Readout of information from multisection systems can be realized by parallel and serial method or combination. First method use amplifying elements with two outputs. One outputs connected to the "X" electrode, and other – to the orthogonal "Y" electrode (Fig.1).

The serial method of readout information is based on determining the registration point by charge propagation time. Performance of the detector define by number of elements and their response time (0,1 – 1 ns).

The parallel method of readout information was selected. Two-emitter transistors or OR-schemes with high-resistance inputs is necessary to use, because "X" and "Y" buses should not connected by amplifying elements. OR-schemes were used in design of the readout unit (Fig. 2). This method allows using simplest scheme with one transistor in the capacity of

the amplifying element of each pixel (Fig 3). A collector of this transistor has potential equal low ECL level. When a pulse is applied to the transistor base, the collector current is switched close to saturation. A positive pulse is shaped at the collector output, and it can be delivered to the OR circuit. Independent inputs of OR-schemes are used each "X" and "Y" buses. Two high resistance inputs of ECL schemes connected to the collector of each transistor.

16 mixers with 8 inputs should be used for 64 sections of the H8500D PMT (8 "X" buses and 8 "Y" buses). Thereby the number of the activated pixel encoded in two 8 bit position codes.

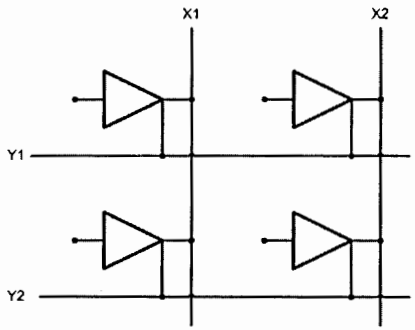


Fig. 1. Parallel method of readout information

Mixer outputs are connected to univibrators, which shape width pulses. Univibrators based on D-triggers. All logic elements based on the integrated circuit 10H series. Mixers with 8 inputs contain two 4-input OR-schemes. Pixel amplifiers based on high-performance transistors BFT92.

The amplifier of the dynode signal contains 3 wideband operation amplifiers AD8009.

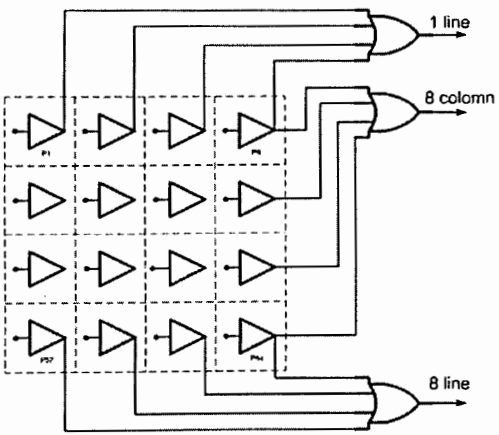


Fig. 2. Scheme of readout position information

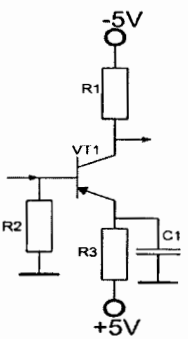


Fig. 3. Pixel amplifier

### 3. Purpose and architecture of logic unit

The logic unit has three tasks: generating time mark and time window for α-γ coincidence schemes; encoding the number of the activated pixel of PMT; and counting pulses from all section of the PMT. Constant fraction discriminator (CFD) fix time of recording pulse from the dynode PMT (Fig. 4). It also contains computer-controlled integral discriminator. Width of the output pulse from CFD shaped on UV1 and delayed constant (UV2) and variable (computer-controlled) delays (MC100EP195). Than this pulse trig univibrator UV3. This univibrator shapes the time window for α-γ coincidence schemes. Information about number of the activated pixel received from the alpha-shaper unit on 16 differential inputs of the logic unit by 16 twisted pairs. Each pair terminated in the logic unit on 100Ω. Then these signals receive through the ECL-TTL translators (D5, D6, D7) on the digital part of scheme. This part of the scheme based on a FPGA EP3C10E144C8N and process logic operation (encoding number of activated pixel into binary code for coincidence schemes, counting pulses from each pixel, control threshold of CFD and variable delay). Data communication with the personal computer is provided by the microcontroller (C8051F314QFP-32D22) using USB.

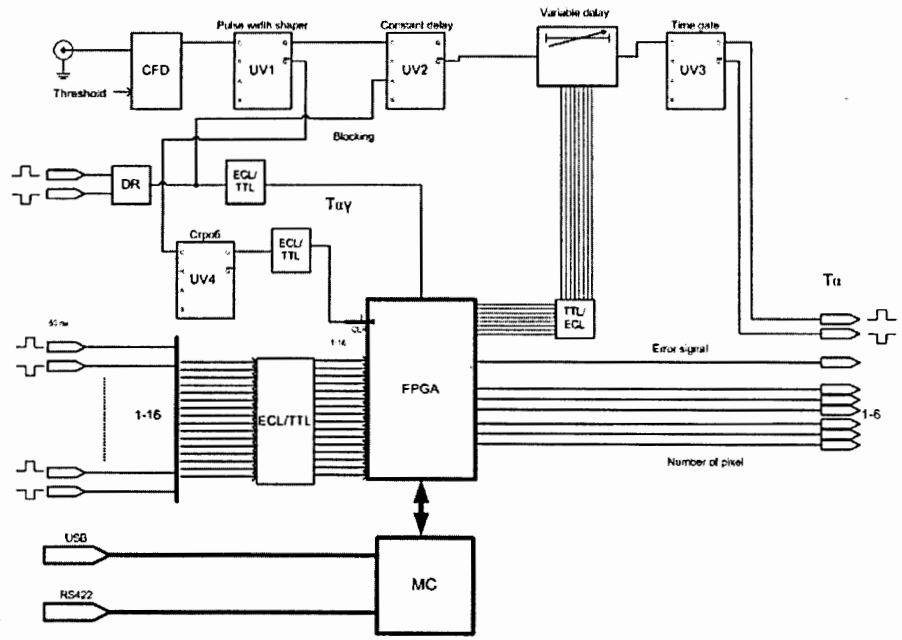


Fig. 4. Diagram of logic unit

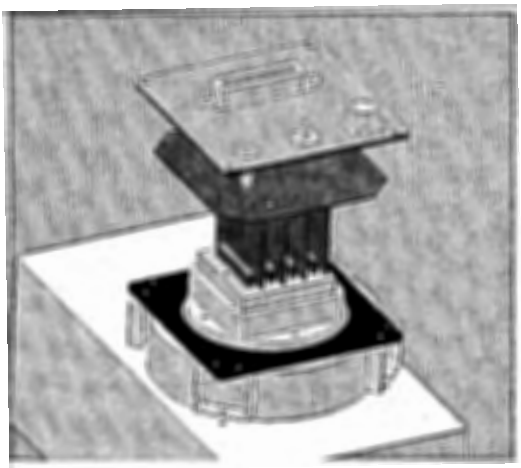

Fig. 5. Form of alpha signals shaper

| | 1 | 2 | 3 | 4 | 5 | 6 | 7 | 8 |
|---|---|---|---|---|---|---|---|---|
| 1 | 1 | 2 | 2 | 10 | 5 | 4 | 16 | 233 |
| 2 | 3 | 0 | 1 | 0 | 0 | 0 | 1 | 0 |
| 3 | 4 | 0 | 0 | 0 | 0 | 0 | 0 | 1 |
| 4 | 0 | 0 | 0 | [illegible] | 0 | 0 | 0 | 3 |
| 5 | 6 | 0 | 0 | 0 | 0 | 0 | 0 | 8 |
| 6 | 4 | 0 | 0 | 0 | 1 | 0 | 0 | 0 |
| 7 | 0 | 0 | 0 | 0 | 0 | 0 | 0 | 0 |
| 8 | 0 | 0 | 0 | 0 | 0 | 0 | 0 | 0 |

Fig. 6. Trigging in pixels

Software development for this module allows displaying spatial distribution alpha-event registered by the detector. Alpha-radioactive isotope ($^{241}$Am) was used for testing module. Configuration of this allows irradiating one pixel of the alpha-detector. Module precisely marks out irradiated pixel (Fig. 6). Trigging in the neighboring pixels is caused by their parasitic illumination.

# Charge and energy measurement systems for the NUCLEON experiment

N.V. Baranova[1], V.F. Boreiko[2], V.L. Bulatov[3], V.S. Dorokhov[3], N.N. Egorov[4], S.B. Filippov[3], S.A. Golubkov[4], N.V. Gorbunov[2], V.M. Grebenyuk[2], A.I. Kalinin[2], D.E. Karmanov[1], Z.V. Krumshtein[2], M.M. Merkin[1], A.Yu. Pakhomov[1], D.M. Podorozhnyi[1], A.B. Sadovskii[2], L.G. Sveshnikova[1], L.G. Tkachev[2], A.V. Tkachenko[2], A.N. Turundaevskii[1], A.V. Vlasov[3], A.G. Voronin[1]

[1] *Skobel'tsyn Institute of Nuclear Physics, Moscow State University, Russia*
[2] *Joint Institute for Nuclear Research, Dubna, Russia*
[3] *Gorizont, Ltd., Yekatirinburg, Russia*
[4] *Research Institute of Materials Science, Zelenograd (Moscow), Russia*

Arrays of silicon detectors are used as detecting elements of the charge measuring system (CMS) and energy measuring system (EMS) for satellite-based research of cosmic rays in the NUCLEON experiment. In this paper the structural design and electronics of the CMS and EMS are presented and the main requirements on the detectors and readout electronics of these systems are considered.

## 1. Purpose and main components of the NUCLEON silicon systems

The NUCLEON research equipment is a "layered" structure with the active part of the spectrometer as large as ~500×500×360 mm$^3$ in overall size. The research equipment incorporates, apart from other things, 688 silicon detectors combined into the following systems:

- Four layers of pad silicon detectors making up the charge measuring system (CMS) designed for precision measurement of the primary-particle charge;
- Six layers of microstrip silicon detectors which together with the carbon target (depth ~20 g/cm$^2$) and six layers of the tungsten converter (depth ~0.5 radiation unit $X_0$ each) make up the energy measuring system (EMS) and are designed for determining the primary-particle energy, localizing the place of the first inelastic interaction, an determining the primary-particle trajectory of arrival at the facility.

CMS planes are a duralumin structure. Silicon detectors are arranged on boards ("ladders"), eight detectors in each layer. Each CMS ladder comprises eight detectors with the overall dimensions 62×62 mm$^2$, each detector is divided into 15 pads, and each pad has an individual detection channel. The active part of the detectors covers ~92% of the facility's solid angle by one plane and ~100% by four layers.

The EMS structurally consists of a carbon target layer and six tungsten converter layers, each accommodating EMS ladders in two levels for complete coverage of the facility's solid angle by the active part of the detectors, nine per layer. Each EMS ladder comprises eight detectors with the overall dimensions 62×62 mm$^2$, and each detector is divided into 128 strips. Detectors of one ladder are connected in series, so that strips of one detector are continuations of strips of another detector. Each of 128 long strips of the ladder has an individual detection channel.

## 2. Electronics of CSM and ESM ladders

In the NUCLEON project, ladders are intended for detecting signals from ionizing particles (cosmic rays of accelerator beam). A charged produced by particles in the silicon

detectors is detected, and the electronics of the ladders carries out conversion of this charge to an analogue voltage pulse, analogue filtration of noise, conversion of voltage to the code, and intermediate storage of the digitized data on one event. The collected information is transferred on request to the data readout systems of the NUCLEON equipment. In addition, ladders ensure execution of some service functions, including calibration of the amplification channel (using built-in DAC and generator) and self-diagnostics (measurement of consumption currents and voltages by additional slow ADC).

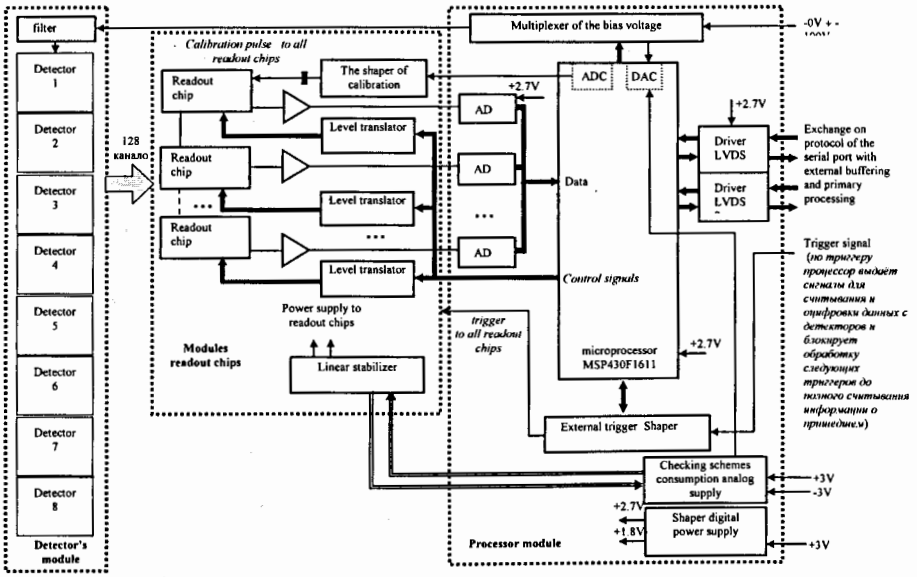


Fig. 1. Simplified block diagram of CMS/EMS ladder electronics. For the CMS, the 8-channel readout microcircuit CR1 serves one pad detector. For the EMS, the 32-channel microcircuit VA32HDR14.2 serves 32 "long" strips of eight detectors connected in series.

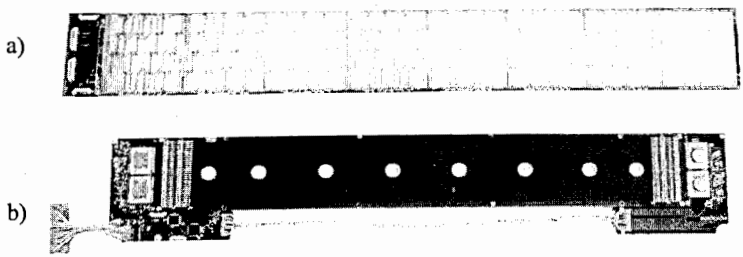


Fig. 2. General view of the ladders. The CMS ladder (a) is viewed from the pad detectors; its electronics is installed on the other side. The EMS ladder (b) is viewed from the electronics: four unpackaged readout microcircuits VA32HDR14.2 and part of the processor unit are seen.

A ladder consists of a base board accommodating eight pad (for CMS) or strip (for EMS) detectors, readout microcircuits, 16-bit ADCs (AD7687), a microcontroller, a linear power supply stabilizer for digital electronics, an analogue electronics supply voltage switching circuit, a detector bias circuit, consumption current and bias measurement circuits, signal (including trigger signal) level matching circuits, and two transceivers of the code communication line (LVDS). The simplified block diagram of the ladders is shown in Fig. 1, and their general view is shown in Fig. 2. The total number of channels in the detectors of one CMS/EMS ladder is 128. To read out information from the CMS ladder detectors, there are eight CR-1 microcircuits, including a 16-channel section of the charge-sensitive amplifiers (CSA) with analogue filtration of output signals and a sample-and-hold amplifier, and an analogue output multiplexer. In the EMS, readout is performed by functionally similar 32-channel VA32HDR14.2 microcircuits (four microcircuits per ladder). The ladder is controlled by the MSP430F1611 microcontroller (16-bit architecture, operation time 170 ns, 48-kbyte ROM, 256-byte electrically programmable memory, 10-kbyte RAM). The supply voltage for the analogue part of the ladder is $-3\ {}_{-0,3}^{+0,2}$ V; some of the analogue circuits and the digital electronics of the ladder use the supply voltage $+3\ {}_{-0,2}^{+0,3}$ V. The total power consumption of the ladder power supply circuits should not be larger than 0.95 W. One CMS/EMS ladder weighs no larger than 225 g.

In the NUCLEON project, the detector–amplifier–ADC channel for the charge measuring system should ensure reliable detection of both signals from relativistic singly charged particles (mip) and signals from nuclei up to the iron group (Z = 26). A channel of the energy measuring system should detect many particles from development of a cascade in the target. However, detection of small signals from several mips is also important because the count of the number of secondary particles at the periphery of the cascade allows the primary-particle energy to be refined by the method for kinematic determination of energy [1].

### 3. CMS and EMS detectors: design and manufacture

Detectors of the charge measuring system are pad detectors with the $p^+$-n-$n^+$ structure and galvanic readout (DC detectors). Structurally, the detector is a 4×4 array of pads 15×15 мм$^2$ in size surrounded by a system of $p^+$-type protective rings (PRs) with a floating potential. The detector is 450 μm thick. Detectors of the energy measuring system are strip DC detectors with the $p^+$-n-$n^+$ structure as well. The 60×60 mm$^2$ active area of the detector is divided into 128 strips at a step of ~470 μm. The strip array is surrounded by protective rings similar to those for the pad detectors. The EMS detectors are 450 μm thick in the "upper" four planes with respect to the carbon target and 300 μm in the "low" two planes. From the point of view of the physics problems to be solved by the CMS and EMS, size of the pads and the step of the strips should be decreased, but this will results in an increasing number of readout electronics channels, which is undesirable from the point of view of both the cost of the electronics and its power consumption. The thickness of the CMS detectors was dictated by the requirement of reliable separation of mip signals against the background of electronics noise. The signal from the ionizing particle in the silicon detector is proportional to its thickness, and at the same time the noise of the readout electronics based on the charge-sensitive amplifier is usually proportional to the capacitance of the detector or inversely proportional to its thickness. Thus, an increase in the thickness of the CMS detector, which detects single primary particles, by a factor ~1.4 (in comparison with the "lower" EMS detectors) improves the ratio $S_{mip}/N$ by a factor $\sim 1.4^2 \approx 2$, which allows having the ratio $S_{mip}/N \approx 4$ for the readout electronics based on the VA32HDR14.2 microcircuits. It is enough to reliably separate signals from singly charged particles at four-fold coincidences in four

layers of the CMS. Considerable noise of the readout electronics is due to a large area of the CMS detector pads: the capacitance of a CMS detector pad is 80 pF. To use CMS detectors >500 μm thick is undesirable because the full p-n junction depletion voltage of the silicon detector $V_{fd}$ is proportional to its thickness d squared, $d \approx 0.53(\rho_n \times V_{fd})^{1/2}$, and the operating voltage for the accessible range of specific resistances of the initial n-silicon ($\rho_n \sim 5$ kΩ cm) becomes >200 V, which considerably complicates the design of the CMS electronics through the necessity of using high-voltage components and special circuitry. Detectors of the "lower" EMS planes are located in the region where the cascade of secondary particles develops and some strips are hit by several particles (up to thousands at the center of the cascade). Under these conditions it is more important to maintain linearity of the gain for the signal from thousands of mips even at the expense of a decrease in the amplitude of the signal from one mip, which dictated a decrease in the thickness of the detectors in the "lower" EMS planes as compared with the other detectors.

Detectors are made of highly pure single-crystal n-silicon with the orientation <111> (specific resistance 6 $\pm$ 2 kΩ cm, lifetime of minority carrier >1 ms) produced by crucibleless melting. Silicon was produced and cut into plates at the Wacker company (Germany). Standard MOS and TTL technologies were used to make detectors. However, there are some specific features arising from the large area of the detector, use of high-resistance silicon unusual in microelectronics, and effect of the backside of the plate on the operation of the detector in the full depletion mode. This all imposes strict requirements on the purity, perfection, and uniformity of initial silicon; no mechanical defects are allowed on the face and back sides of silicon plates at all production process stages. Because of the large detector area, contact photolithography with a gap about 5 μm is used to form the structure of the detector. Detectors must have the smallest possible number of defect channels (0% for CMS and <5% for EMS), and since one plate accommodates one detector, defects on masks must be entirely excluded to secure the yield ~70–80% yield of good plates.

Strict requirements on the number of defect channels make it necessary to carry out quality control of the detectors before their installation in the ladders with electronics. In DC detectors there are two main causes why the channel becomes inoperative: high noise in the channel or short circuit with the neighboring channels. High noise in the channel is usually due to increased leakage current of the p-n junction. Classical shot noise of the p-n junction (leakage current fluctuations) becomes comparable with the electronics noise for currents >1 μA, which is a gross defect because the standard level of leakage currents stemming from the quality of the silicon plates and the production process is <2 nA/cm$^2$ (for detector ~300 μm thick). On the other hand, pulsed noise that appears to result from development of microavalanches in the region of silicon structure defects and at boundaries of $p^+n$ junctions shows up as an insignificant increase in the current (several-fold as compared with neighbouring structures), but it may also make the channel inoperative. In this connection, the quality control of EMS detectors implies measurement of leakage currents in each strip at the operating voltage, and the measured result should be no higher than 10 nA for a strip at the average current level <1 nA/strip. For CMS detectors it is required that the total current of detector pads at the operating voltage should be below 400 nA, or ~10 nA/cm$^2$. The other cause for defects of the detector channel, short circuit between structures, is usually due to microparticles of dust that become trapped between neighboring structures at the stage of aluminum etching or due to scratches on the surface of the plate (making their effect at the stages of implantation and spread of admixtures in $p^+$ regions). For CMS pad detectors, short circuit of pads is unlikely because of a large gap between them (60 μm). Here it is only necessary to check the quality of the aluminium photolithography mask to avid any scratches on it. For EMS strip detectors, this may be not enough because the gap between the strips is

only 20 μm. Therefore, absence of contact between strips of EMS detectors is directly checked by the leakage current between two probes fixed to the neighboring strips (test voltage 0.5 V). The operating voltage of each detector is determined from the C(V) characteristics of special test structures and should be within the range 20-100 V. Techniques of these and other measurements of mass testing of silicon strip detectors are described at length in [2].

## Conclusions

Ladders of the charge and energy measurement systems are developed and built for the technological specimen of the NUCLEON research equipment. In the summer of 2008 the technological specimen was tested in the SPS beam (CERN). At the end of 2009 it is planned to complete the ground test of the NUCLEON equipment and start making ladders for the airborne specimen. The assembly and adjustment of the airborne specimen is planned to be accomplished in 2010.

## References


[1] N.A. Korotkova, D.M. Podorozhnyi, E.B. Postnikov, T.M. Roganova, L.G. Sveshnikova, and A.N. Turundaevskii, New Method for Determining the Energy of Nuclei of the Primary Cosmic Radiation, Yad. Fiz. 2002, Vol. 65 (5), pp. 884–892.

[2] P.F. Ermolov, A.G. Voronin, D.E. Karmanov et al., Techniques for Mass Testing of One-Sided Microstrip Detectors, Prib. Tekh. Eksp. 2002, No. 2, p. 54.

# The collective modeling environment as the instrument for teamwork in classroom

V.V. Belaga[1,2], K.V. Klygina[1], Yu.A. Panebratsev[1], T.I. Rufanova[2], M.S. Stetsenko[1,2], M. Yu. Ushankova[2]

[1] *Joint Institute for Nuclear Research, Dubna, Russia*

[2] *Dubna University, Russia*

There are a lot of complicated systems (technical, social, ecological, etc.) that can be carefully studied by means of modeling. At the same time, if we divide modeling subtasks between students, we will have a possibility to organize the teamwork. Depending on the audience and training purposes, it can take various forms beginning from network games and up to educational simulators. Such kind of activity favors the development of cognitive, creative and communicative personal qualities. Nowadays these qualities are very important and reflected in a new educational standard.

The collective modeling environment (CME) is a distributed multimedia software and a methodical complex, made within the limits of client-server architecture, which provides the organization and support of teamwork in the classroom.

From the technical point of view, CME consists of several computing knots connected by local network. One of these knots (connected to a projector or a smart board) displays the general state of the described system. Besides, this node allows the teacher to handle an educational course, changing parameters of the subject model and choosing an educational trajectory. Other computing knots are intended for input commands from students.

We have used personal computers connected to a plasma panel and touch screens as computing knots. This decision provides functionality of commands input and high quality visualization. The knots are connected by using economical technology Ethernet 100.

The exhibit should be bright and attractive, so we use Adobe Flash Platform. Its integrated set of technologies provides everything you need to create engaging interactive interfaces and also programming tools. Unfortunately, Adobe Flash software is not enough to realize data transfer between the knots and we decided to use socket-technology and Borland Delphi environment (Fig. 1). The technology was chosen to transfer data by long-haul network (for future possibilities), and the programming environment is unimportant for users, so we use what we like.

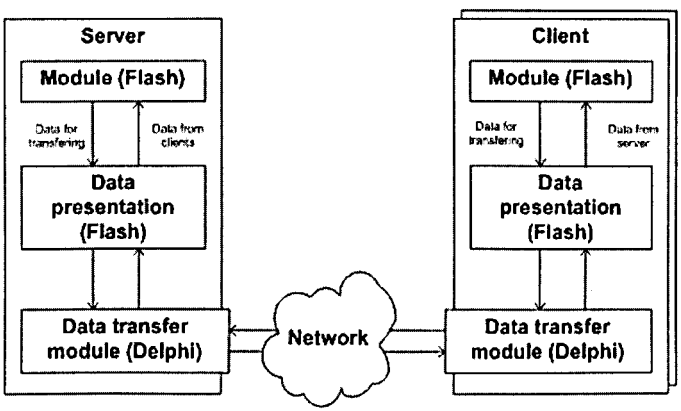


Fig. 1. Data transfer structure

This idea has been realized under support of Dynasty Foundation within the project «Scientific museum of the XXI-st century». 4 educational network modules were prepared for this project (Fig. 2).


Fig. 2. Menu of module choice

One of them represents a simple model of a collider. In this model students should choose a type of an elementary particle and orientation of collider magnets. After that the experiment starts. Fig. 3 shows the server and client screens. The right-handed side user selects the particle and magnets and starts the experiment. The particle passes through the properly placed magnets and sticks in the first incorrectly located magnet. Then the user is waiting for the collider to be repaired. At this time the left-handed side user reads the rules.


Fig. 3. Wrong experiment parameters

When the both users launch their particles through the correctly located magnets, they will see schematic animation of the collision as it shown in Fig. 4.

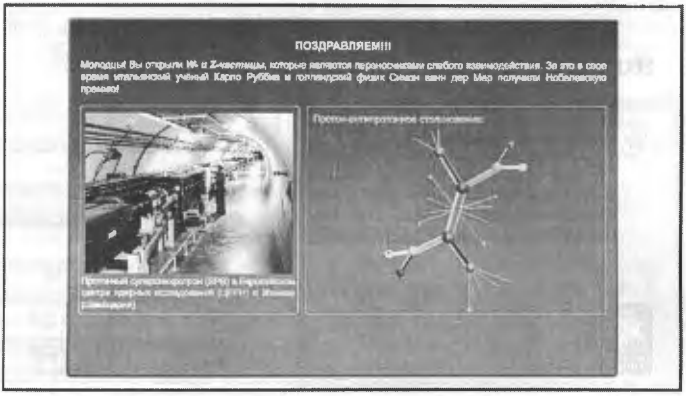


Fig. 4. Information about collision

The network module «Balloon voyage» gives basic knowledge in the field of aerostatics which could be used by students while aviating a balloon.

The exhibition based on these modules was supported by Dynasty Foundation and exposed in the JINR Museum of Science in Dubna and the Polytechnic Museum in Moscow (Fig. 5).

Fig. 5. The exhibition in the Polytechnic Museum in Moscow

. This system was upgraded by connecting a smart board to a server. This extension allows the teacher to handle the educational process by changing parameters of the model and choosing an educational trajectory.

The teacher in this environment is the organizer of the educational process. He sets a problem for pupils and supervises the process of solving the problem. The problem is

formulated on a smart board by means of all variety of its functions, including demonstrations of interactive images, painting, making notes and etc. Materials for the problem formulation are software components, thus, the teacher can alter tasks by writing a necessary text, selecting necessary zones graphically and etc. School students carry out the task individually or in micro-groups. The quantity of working groups depends on the quantity of computers in the class. The tasks can have different goals: examination, to study a problem by students or compete between themselves. Results of the groups' work (or individual work of students) are displayed on a smart board, and the teacher can perform comparative analysis of the results with explanation of errors and conclusions.

The module «Epoch of Dinosaurs» allows the junior schoolchildren to arrange a skeleton of a dinosaur simultaneously in a competitive way. When the task is fulfilled, students can see the educational animation about the dinosaur.

In the network educational module «Constellations» students should find all the stars of the chosen constellation in the night sky (Fig. 6). The properly selected stars are shown on all the screens and you can also see the number of the stars, which have been selected by each user.

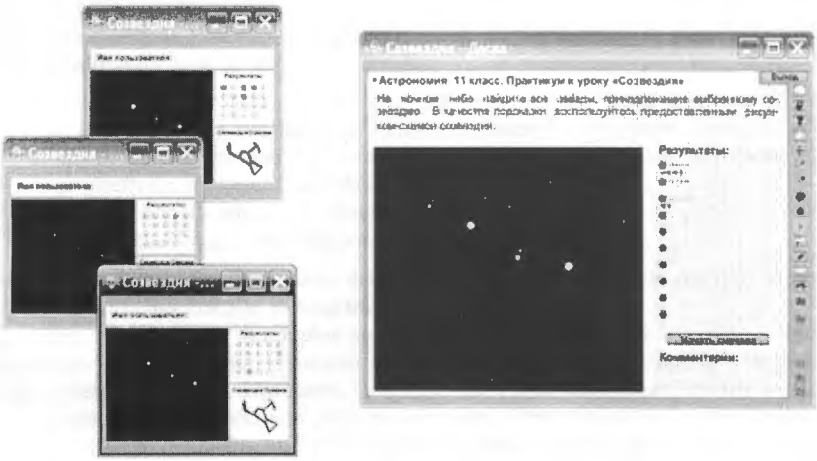

Fig. 6. Server and clients screens, model 'Constellations'

When the task is completed, the educational animation about the constellation is played.

Unfortunately, such modeling systems have a problem: the quantity of knots for the user. The common task of the collective modeling consists of several separate subtasks. Each subtask is related with its separate knot. So, we need to formulate a separate subtask for each knot and this is an additional problem, because it requires to take into account many parameters while being formulated. Technically, a large number of knots results in a well-known «bottleneck» problem.

Now we work at the system with symmetric architecture (Fig. 7) which would allow modeling complicated social and biological phenomena and processes.

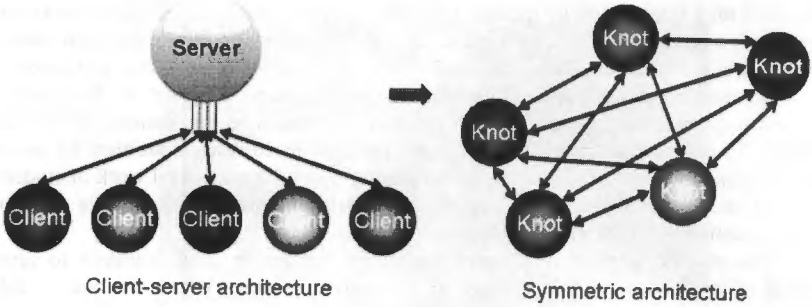


Fig. 7. Future CME development

In this system with the symmetric architecture the increase of the number of knots will become an advantage but not a problem.

# Experience in development of Grid monitoring and accounting systems in Russia

S.D. Belov, V.V. Korenkov
*Joint Institute for Nuclear Research, Dubna, Russia*

## 1. Introduction

Various monitoring systems are now extensively used to keep an eye on real time state of each service of distributed grid infrastructures and jobs running in the Grid. Tracking current services' state as well as the history of state changes allow rapid error fixing, planning future massive productions, revealing regularities of Grid operation, etc. We participate in different Grid projects, where monitoring and accounting is an important feature.

Along with monitoring, accounting also is a tool which shows how the Grid is used. The data considered are statistics on Grid sites' resources utilization by whole virtual organizations and single users.

## 2. Grid monitoring systems

The monitoring is rather general concept. Most common tasks we deal with while participating in different projects are:

- Continuous watching for the state of Grid services both common for all infrastructure and in a particular Resource Center;
- Obtaining information on resources amount (CPU number and total site productivity, disc space) and their utilization;
- Execution monitoring, e. g. data transfer, job submission;
- Quality checking of network links between Resource Centers.

For effective control, planning and faults detection it's important to know not only current state of Grid infrastructure but also to keep track of state history.

Last five years we keep developing and supporting monitoring and accounting system for Russian Data Intensive Grid consortium (RDIG)[1]. It was made in addition to global monitoring systems like GStat, SAM tests, GridView and ARDA Dashboard mainly because of specific needs of regional VO and site's management. Other points were advantages of having an independent monitoring and accounting for regional grid infrastructure, allowing to customize a set of parameters to gather and provide a possibility to display all essential information about regional Grid infrastructure on a single web-site in the most convenient form.

RDIG monitoring system is partially based on MonALISA package [2]. This is a tool for building distributes customizable monitoring solutions. MonALISA has modular structure and allows to use both standard modules and specially designed ones. Other important features of the package are scalability and presence of flexible visualization tools. Scalability of the system is based on using of mutlithreading and self-described dynamic services, and also on the possibility of each service to register itself and be used by other services and clients which are asking for such information.

The following parameters were chosen as the main ones for Russian Data Intensive Grid (RDIG) [1, 3]:

- Number of busy, free and down CPUs;
- Total CPU productivity (in kSpecInt2000 [11]) of each Resource Center;

- Amount of running and waiting jobs for each virtual organization (VO);
- Used and available disc space for each VO (integral and per-site);
- Main servers load (e.g. for Computing Element);
- Available bandwidth in networks between Resource Centers.

Now let's describe monitoring architecture. Monitoring services should be installed in each Resource Center (RC). This service is responsible for the collection of all necessary information from WLCG/gLite site. Information system (GIIS) is running in each RC and can be accessed via LDAP protocol. To collect data special module was developed which asks GIIS, gets the response and then stores received values in the local database. Among these parameters are running and waiting jobs count, used and available disc space for each VO. Such service operation mode is called *pull mode* because the service works as an active side examining corresponding components. Another operation way is so called *push mode*. In this case MonALISA service works in a passive mode listening predefined port and just storing incoming information in the local database. For sending such data there's a standard library ApMon realized for five programming languages. We've used the Java and Perl versions. A special module was developed to get needed information from a local resource management system PBS (number of working/down and busy/free CPUs, and also the number of jobs – running and waiting for resources). This module should be installed on Computing Element and then sends UDP packets with collected values to the MonALISA service. Data transfer from all RC to common repository is organized using Web-services technology. Each service registers itself in a Lookup and Discovery Service (LUS). The repository uses LUS to make a search, based on predefined filters and predicates, for services providing appropriate data. Then the gathered data are saved in the repository own database (see Fig. 1).

For the representation of collected information repository has a web-interface based on Apache Tomcat web server using Java Servlets and Java Server Pages technologies. It makes possible to display data in the most suitable view for each case – as tables, plots, diagrams, on geographical maps, etc. User can select information by different criteria such as time period, Resource Centers, Virtual Organizations (see screenshots on Fig. 2).

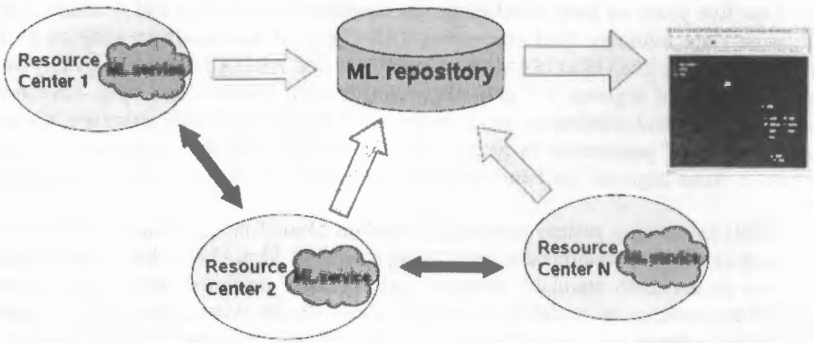


Fig. 1. Monitoring information gathering among Resource Centers

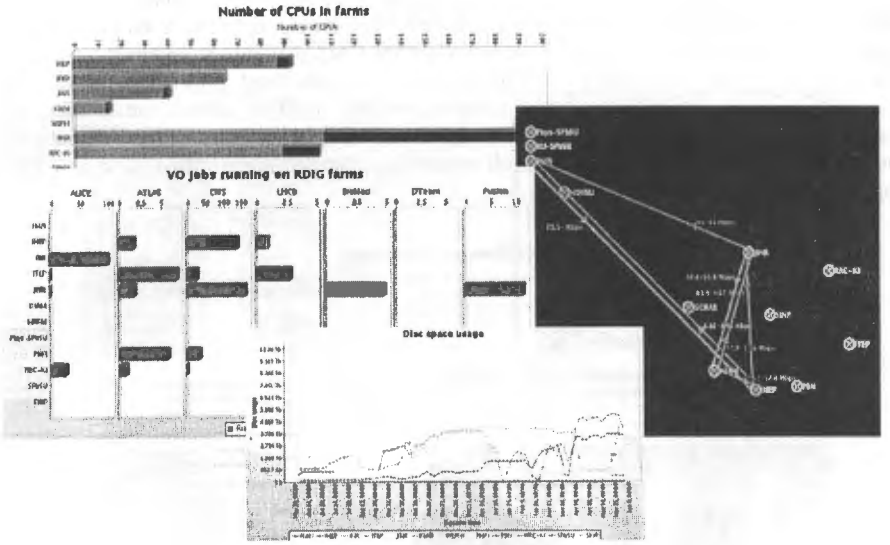


*Fig. 2. Screenshots of RDIG monitoring website*

By now we've prepared a monitoring service distribution for Russian Resource Centers. It has already been installed in all Resource Centers. Developed system properly operates giving required functionality [4]. System architecture allows adopting monitoring system to Grid middleware changes and easily varying the set of collected parameters. Experience of making monitoring for LCG/gLite-based infrastructure was also exploited in creation of monitoring system for Romanian Tier2 Federation.

The second project where we use MonALISA-based solution is monitoring for SKIF-GRID (supercomputer program of Union State of Russia and Belarus, [5]). There was accomplished almost the same monitoring structure as for RDIG. Differs are in information sources: base Grid middleware UNICORE [6] and local batch system Cleo [7]. So, special monitoring information collectors packages were prepared. Monitoring system for SKIF-GRID is in production mode now [8].

The next project we participate in is GridNNN, Grid support for national nanotechnology network of Russia. The main goal of the project is to provide an effective access to the distributed computational, informational and networking facilities for nanotechnology science and industry. The base middleware of particular GridNNN services (like MDS, GRAM) is Globus Toolkit 4, some services are developing by the project team (e.g. job handling tool Pilot). Operation of GridNNN, unlike RDIG, is more centralized: there are about 15-30 resource centers (supercomputers) controlled from two operation centers (one is main and one is backup). The infrastructure has one central information index where all information providers have to publish their data. At the moment, monitoring of resources and services is based on gathering all necessary data, published by modified information providers, from the central information index. Job's monitoring information and accounting data are taken from Pilot (job handling tool).

There is also an experience in different areas: monitoring of file transfers and jobs in the Grid using log files of corresponding software. We participate in two such projects. The first one is a monitoring of PhEDEx file transfers for CMS experiment within Russian Data Intensive Grid. Each file transfer event in log flies to be considered, files transfer statistics is available on dedicated Web page (example is on Fig. 3). The second one is user jobs monitoring for Open Science Grid (OSG) for Dashboard project in CERN. User jobs are submitted there via Condor-G system, job events data come to monitoring system also from log files processing.

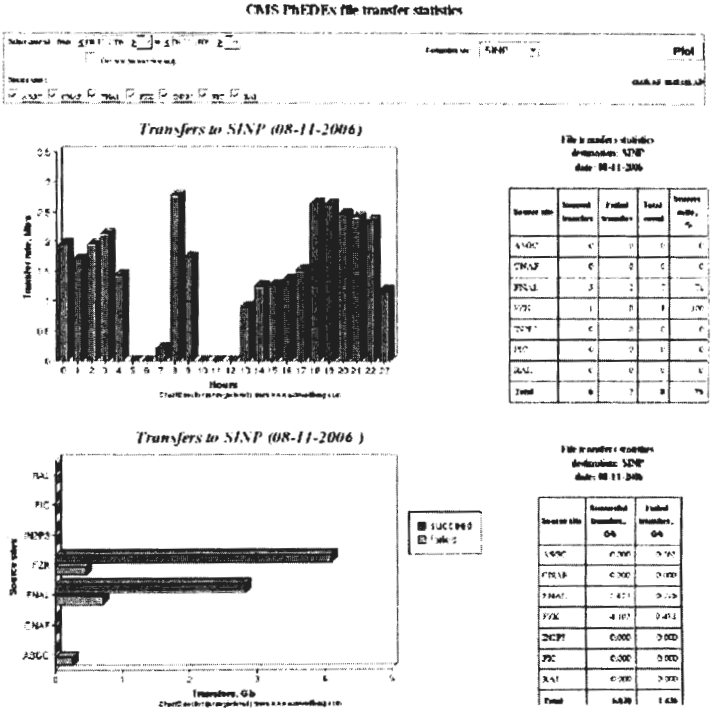


Fig. 3. PhEDEx file transfer monitoring page for RDIG

## Grid accounting

The main goal of accounting in the Grid is to collect statistics of resource usage (particularly utilization of processors) by single users and the whole Virtual Organizations. Statistic should be available for each Resource Center.

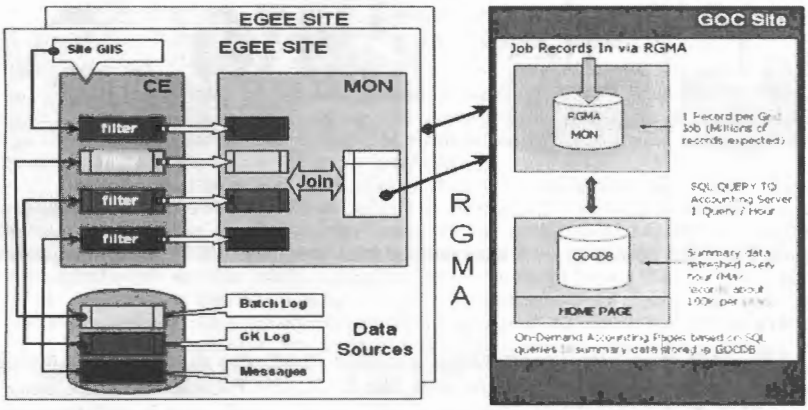


Fig. 4. Job accounting information aggregation in EGEE

Concerning EGEE project, job accounting information gathering works as following: APEL log processor [9] handles log files of Gatekeeper and local batch system on grid site and extracts from there detailed finished jobs information like a job's unique identifier, user certificate DN, job start and finish time, used CPU time. Then accounting information from different sites is to be aggregated and published by means of R-GMA [10] as it depicted on Fig.4. It is worth to notice that to unify CPU usage metrics, consumed processor time normalization is applied (CPU productivity is measured in kSpecInt2000 [11]).

Then job data is collected from R-GMA by special collector tool and after pre-processing is placed to relational database (see Fig. 5). Relying on this information, accounting statistics for RDIG sites is provided on the web interface (sample charts are on Fig. 5).

Partial function duplication with EGEE accounting is required for more detailed analysis of processes in the Grid. Having data on each job in RDIG, it's possible to catch errors, discover unusual infrastructure behavior and so on. Own independent accounting facility was very helpful in studying of two cases of seriously spoiled accounting information. The first one was related to unofficial changes in the way of forming unique grid job identifier for accounting (this caused double-counting for about 200'000 jobs only for Russian sites). The second one concerned with the way how site's productivity (in kSI200) and therefore normalized CPU time for each job is announced – only site administrator is responsible for correctness of all published CPU parameters. So, when one of the sites in region starts to give out a hundred times more normalized CPU time than it was before, the reason should be investigated.

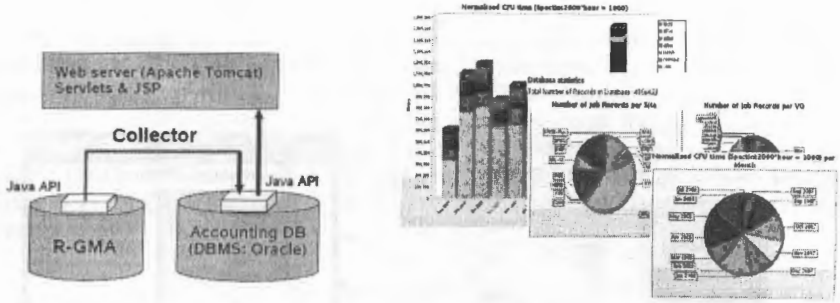


*Fig. 5. RDIG job accounting collector and sample charts from RDIG accounting website*

## Summary

LIT JINR team have longstanding successful experience in making monitoring and accounting systems for various Grid projects like RDIG, SKIF-GRID and some other local projects. Also there is good experience in developments in this area in collaboration with different Russian and foreign institutes. The main point is to develop scalable, reliable and interoperable solutions for Grid monitoring and accounting, which will be extensively used in real Grid projects. Main parts of work results are available as a finished software packages.

## Acknowledgments

The authors wish to express thanks to Igor Tkachev for many years of collaboration in development of Grid monitoring and accounting tools. Also we are very grateful for all our colleagues who are collaborating with us in different grid projects: Elena Tikhonenko, Tatiana Strizh, Irina Nekrasova, Maxim Matveev, Elena Matveeva, Ignat Lenskiy (all from JINR), Slava Ilyin (SINP MSU), Andrey Kiryanov (PNPI) and many others.

## References

[1] Official website of Russian Data Intensive Grid, http://egee-rdig.ru
[2] H.B. Newman et al., MonALISA: A Distributed Monitoring Service Architecture, CHEP 2003, La Jola, California.
[3] S.D. Belov, I.M. Tkachev, Monitoring system for Russian EGEE/LCG sites, Scientific report 2004-2005 years, LIT JINR, Dubna, pp. 46-47 (2005-179), ISBN: 5-9530-0099-5.
[4] Russian Data Intensive Grid monitoring and accounting website, http://rocmon.jinr.ru:8080
[5] Official website of SKIF-GRID project, http://skif-grid.botik.ru
[6] UNICORE project, http://www.unicore.eu/
[7] Cleo batch system, http://parallel.ru/cluster/batch-system.html
[8] SKIF-GRID monitoring website, http://skifmon.jinr.ru
[9] R. Byrom et al., APEL: An implementation of Grid accounting using R-GMA, UK e-Science All Hands Conference, Nottingham, 19-22 September, 2005.
[10] A.W. Cooke et al., The Relational Grid Monitoring Architecture: Mediating Information about the Grid, Journal of Grid Computing, Vol. 2, No. 4, 2004.
[11] Standard Performance Evaluation Corporation benchmark of Kilo Specmarks Integer year 2000, http://www.spec.org/cpu2000

# Educational grid infrastructure: status and plans

S.D. Belov[1,2], V.V. Korenkov[1,2], N.A. Kutovskiy[1]
[1] *Joint Institute for Nuclear Research, Dubna, Russia*
[2] *University "Dubna", Dubna, Russia*

The grid technologies are ones of the crucial and rapidly raising area of information technologies. The increasing significance and extensive usage of Grid causes a demand for people who can deal with it: users, trainers, administrators and developers. Also it is worth to introduce such critical technologies for future IT specialists who are present-day students for the time being.

Having in mind these vital needs, several years ago a full-featured autonomous educational Grid environment was created in LIT JINR. It has become distributed and currently it integrates the resources of several organizations from the JINR Member States with core services located at JINR. It is used for training students and system administrators, grid applications development and grid middleware testing purposes. Based on this infrastructure, semester courses in Grid are provided at the University Centre of JINR and University "Dubna". Users and administrators from the JINR Member States are trained as well. Apart from that it is used for performing obligations in different Grid related activities of local and international projects.

A specific implementation, status, applications of this autonomous distributed educational, training and testing grid infrastructure as well as future plans are described.

The successful use of t-infrastructure (it is a short term for referring to the autonomous distributed educational, training and testing grid infrastructure) in its initial configuration described e.g. in [1] allows one to build on that base a more complex system in order to satisfy the growing demands in such activities and to raise efficiency of its utilization extending a set of its potential applications. The current components of the JINR part of the t-infrastructure configuration and services distribution over physical hosts are shown on Fig.1.

One can see the following parts:

- three gLite grid sites (RU-JINR, RU-JINR-2, RU-JINR-MPI) which are the core part of distributed educational and training grid infrastructure (see Fig.2);
- Globus Toolkit 4 testbed;
- testbed for EGEE SA3 activity;
- java application server for running custom grid services;
- web- and monitoring server.

By that time this t-infrastructure has been used and is been used for the purposes listed below:

1. Semestral educational course at the University "Dubna":
   - 3 years of successful experience, more than 200 students;
   - Grid basics;
   - gLite middleware;
   - practical work within the Grid;
   - scientific research activities of students and post-graduate students.
2. Semestral educational course at the JINR University Centre:
   - focus on research activities;
   - train physicists for their practical work within the Grid.
3. Grid administrators training courses (on demand from organisations of the JINR Member States).
4. Research and development projects:
   a) Grid-oriented applications development on the basis of SOA:
      - grid-oriented application for data quality processing (parsing, cleansing, standardization, enrichment etc.) on a large volumes of data;
      - grid service for minimum spanning tree computation;

b) Grid service for storage and processing of stream video;
c) Molecular dynamics simulation on parallel Grid clusters using MPI technology.

5. gLite services testing within EGEE SA3 activity (MPI enabled gLite clusters).

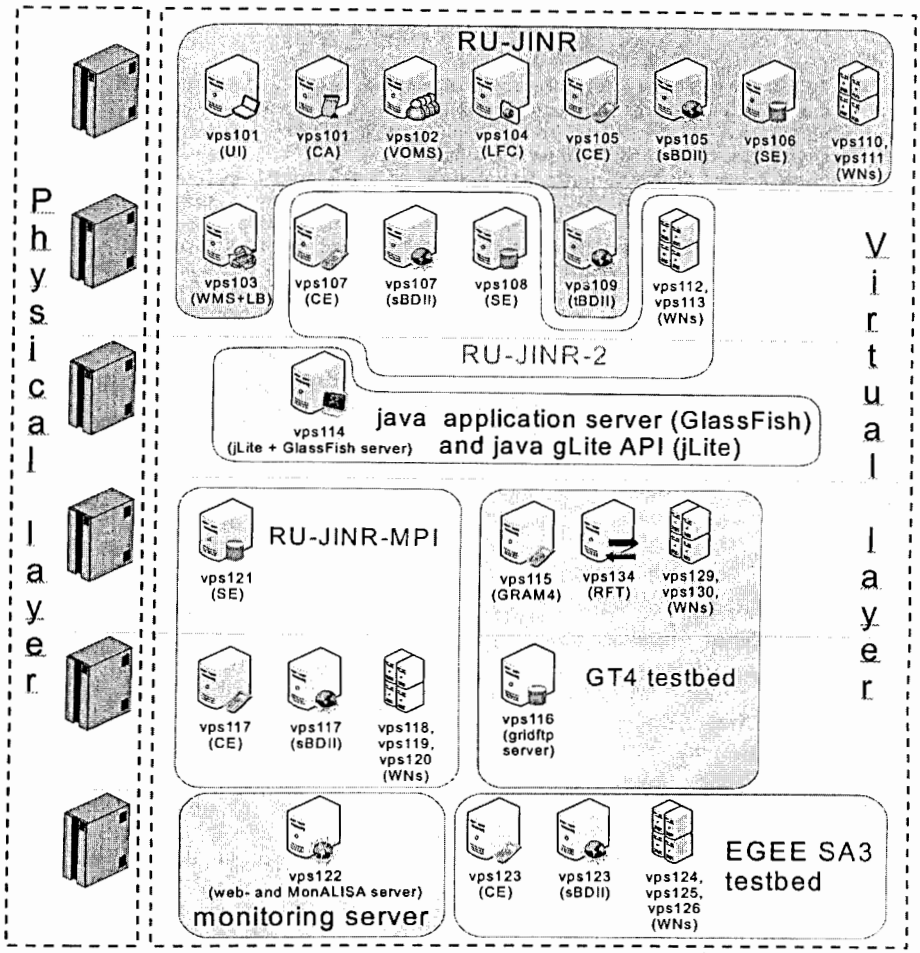


Fig. 1. Components of JINR part of the t-infrastructure and services distribution over hosts

There is a web-portal (https://gridedu.jinr.ru) containing information about the t-infrastructure, guide for admins on setting up gLite on OpenVZ, instructions how to integrate grid site into the education gLite environment, shell access to gLite user interface via web. Apart from that there is an ongoing work on the educational web-portal which aims to provide a possibility for distance learning grid technologies. It includes a detailed user guide for work with educational grid infrastructure, lectures, methodical materials, interactive tests for each topic, full-featured web access to the Grid infrastructure.

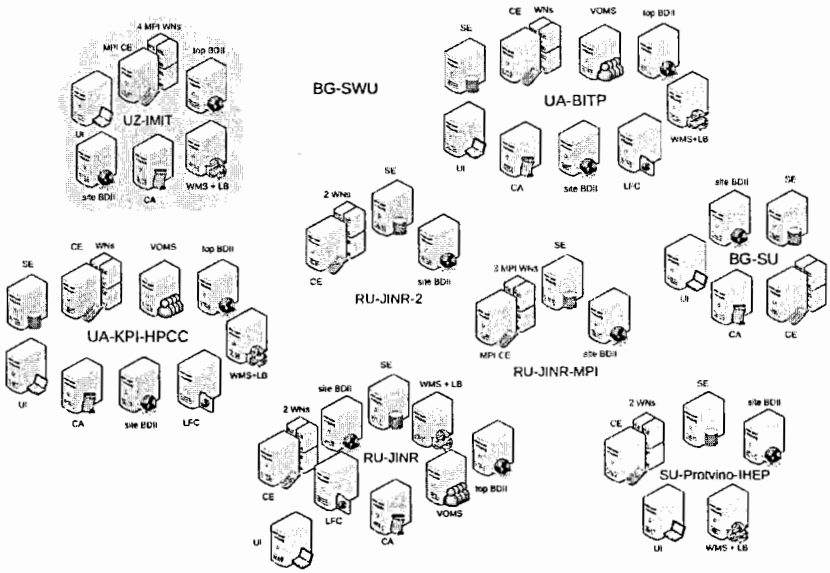


Fig. 2. Distributed educational infrastructure based on gLite middleware

The future plans comprise evaluation of modern virtualization technologies and migration the JINR t-infrastructure to them; integration of new sites to the infrastructure; making courses on Globus Toolkit 4 and grid applications and services development; innovative grid projects support.

## Conclusion

The educational, training and testing grid infrastructure is intensively used for a wide range of tasks related to training different groups in grid-technologies as well as research and development activities in this field. More and more organizations from Russia and the JINR Member States show interest in this t-infrastructure and would like to set up and integrate their own grid sites into common distributed testbed in order to join the grid technologies and popularize them.

## References

[1] S.D. Belov, V.V. Korenkov, N.A. Kutovskiy, Educational Grid infrastructure at JINR, Distributed Computing and Grid Technologies in Science and Education, Proceedings of the 3rd International conference, Dubna, 2008, pp. 341-342.

[2] V.V. Korenkov, N.A. Kutovskiy, I.M. Tkachev, The experience in trainings grid technologies, Proceedings of XII Scientific Conference of JINR young scientists and specialists, 4 - 8 February, 2008, Dubna, Russia, pp. 80 - 83 (in Russian).

[3] https://gridedu.jinr.ru

# VITESS software package: simulations of neutron instruments

A. Belushkin, A. Ioffe[1], S. Kulikov, S. Manoshin, V. Zhuravlev
*Joint Institute of Nuclear Research, Dubna, Russia*
[1] *Jülich Centre for Neutron Science, München, Germany*

## 1. VITESS software package: general description

The role of Monte Carlo simulations is particularly important in the context of complex instrument and facility design and optimization. An accurate carefully benchmarked computational model of the instrument can provide information similar to that of the standard sample over the whole parameter space of the experiments not restricted by the availability of good standard samples.

Both of these basic sides of application – to underpin the design of new facilities and to enhance the efficiency of using existing and future facilities – make the development of powerful Monte Carlo instrument simulations codes to be the most important part of progress in neutron scattering research.

In FLNP (Dubna, Russia) and JCNS (Munich, Germany) VITESS (Virtual Instrument Tool for European Spallation Source) software package has been successfully used to perform Monte Carlo simulations. The realized projects and the projects under development are:

1) Instrumentation for the European Spallation Source and IBR-2M reactor,
2) Neutron transport: conventional, convergent, parabolic and elliptic neutron guides,
3) High Resolution Crystal Spectrometers (incl. Backscattering),
4) Small Angle Neutron Scattering Diffractometers,
5) Neutron Spin Echo (incl. NRSE – resonance spin echo),
6) TOF Spectrometers,
7) Powder Diffractometers,
8) Reflectometers,
9) Neutron Spin Echo spectrometers with rotating or gradient magnetic fields,
10) Neutron refraction lenses and focusing SANS diffractometers,
11) Drabkin resonator.

VITESS is a virtual instrumentation tool for neutron scattering at pulsed and continuous sources developed for the operating systems Unix (SunOS V5.6, OSF1 V4.0), Linux (from version 2.0.3.5) and Windows/DOS. The software package, which has been downloaded by more than 200 users can be obtained from: http://www.hmi.de/projects/ess/vitess/. As shown below, the program is supported by a graphical user interface (GUI), which generates and controls command lines according to a given input. A complicated instrument (spectrometer) can be easily built by the user as well as a simple instrument for testing purposes and checking new ideas. The screenshot of the GUI is presented in Fig. 1.

VITESS has simple modular structure consisting of independently executable components that describe the instrument components. Each module refers to the coordinate system provided by the preceding module, changing the neutron beam input. On the other hand, the output is a function related only to the parameters of the respective module.

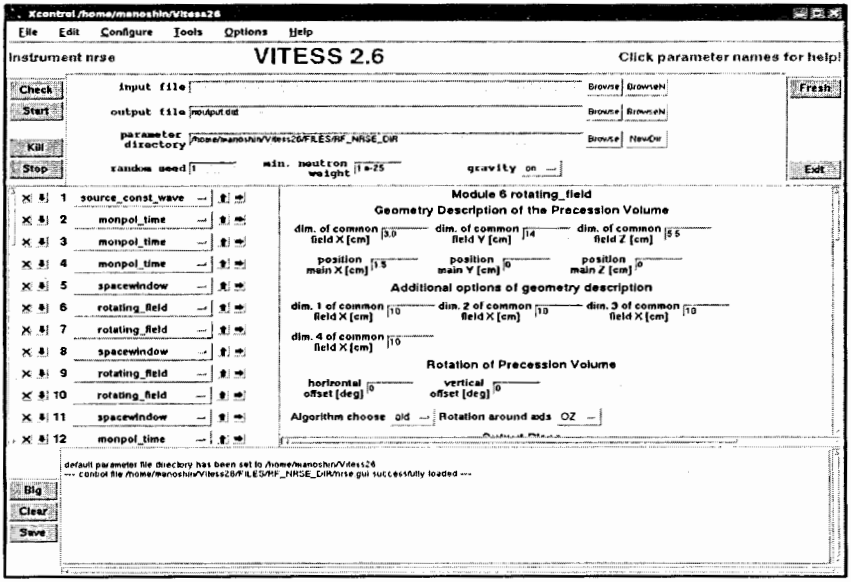


Fig. 1. The Graphical user interface (GUI) of the VITESS software package

The neutron beam input and output represent an optionally large number of neutron trajectories each of which is described by 12 coordinates in the following order: *time of flight, wavelength, probability weight, coordinates (x, y, z), flight directions (cos(α), cos(β), cos(γ)), S1, S2, S3.* The latter is the 3-component representation of the neutron spin. Every neutron trajectory is generated by the module source, see Fig. 2. As the 12 coordinates per neutron trajectory are consecutively written to (or read in), the user can check the changes of the neutron coordinates anywhere in the instrument and generate the statistics of the trajectories.

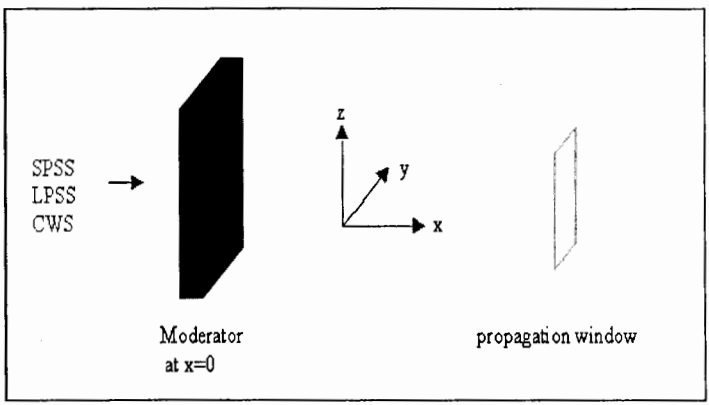


Fig. 2. VITESS module "source of neutrons": a moderator and a propagation window with a coordinate system

# VITESS software package: simulations of neutron instruments

A. Belushkin, A. Ioffe[1], S. Kulikov, S. Manoshin, V. Zhuravlev
*Joint Institute of Nuclear Research, Dubna, Russia*
[1] *Jülich Centre for Neutron Science, München, Germany*

## 1. VITESS software package: general description

The role of Monte Carlo simulations is particularly important in the context of complex instrument and facility design and optimization. An accurate carefully benchmarked computational model of the instrument can provide information similar to that of the standard sample over the whole parameter space of the experiments not restricted by the availability of good standard samples.

Both of these basic sides of application – to underpin the design of new facilities and to enhance the efficiency of using existing and future facilities – make the development of powerful Monte Carlo instrument simulations codes to be the most important part of progress in neutron scattering research.

In FLNP (Dubna, Russia) and JCNS (Munich, Germany) VITESS (Virtual Instrument Tool for European Spallation Source) software package has been successfully used to perform Monte Carlo simulations. The realized projects and the projects under development are:

1) Instrumentation for the European Spallation Source and IBR-2M reactor,
2) Neutron transport: conventional, convergent, parabolic and elliptic neutron guides,
3) High Resolution Crystal Spectrometers (incl. Backscattering),
4) Small Angle Neutron Scattering Diffractometers,
5) Neutron Spin Echo (incl. NRSE – resonance spin echo),
6) TOF Spectrometers,
7) Powder Diffractometers,
8) Reflectometers,
9) Neutron Spin Echo spectrometers with rotating or gradient magnetic fields,
10) Neutron refraction lenses and focusing SANS diffractometers,
11) Drabkin resonator.

VITESS is a virtual instrumentation tool for neutron scattering at pulsed and continuous sources developed for the operating systems Unix (SunOS V5.6, OSF1 V4.0), Linux (from version 2.0.3.5) and Windows/DOS. The software package, which has been downloaded by more than 200 users can be obtained from: http://www.hmi.de/projects/ess/vitess/. As shown below, the program is supported by a graphical user interface (GUI), which generates and controls command lines according to a given input. A complicated instrument (spectrometer) can be easily built by the user as well as a simple instrument for testing purposes and checking new ideas. The screenshot of the GUI is presented in Fig. 1.

VITESS has simple modular structure consisting of independently executable components that describe the instrument components. Each module refers to the coordinate system provided by the preceding module, changing the neutron beam input. On the other hand, the output is a function related only to the parameters of the respective module.

In VITESS the modules that belong to the hardware have characteristic input parameters allowing an accurate description of the instrument components.

- **Source**: initializes neutrons with randomly distributed parameters (such as wavelength λ, flight direction and spin state) starting over a moderator surface. Source modules for HMI, ISS, ILL, IPNS, SNS and ESS are available in the program but can also be personalized by the use of a binary input file.

- **Monitors:** intermediate information can be obtained without disturbing the program sequence, by placing the modules monitor and/or write-out anywhere on the sequence.

- **Sample:** VITESS provides 7 different modules to describe various samples:

  1) Elastic Isotropic Sample,
  2) Inelastic sample,
  3) Powder sample,
  4) Reflectometer sample,
  5) SANS samples,
  6) Single crystal sample,
  7) S(Q) sample.

Considering that neutron optics is one of the most important techniques to control neutron beam quality and to extract physical quantities, in this project we also aim to systematically develop modules that lead to the best description of neutron optical devices. The goal is to open new possibilities of neutron scattering experiments. For this reason we have developed the following modules:

- **Neutron Guides**

- **Polarization:** a series of modules that allows polarization analysis has been developed, such as polariser-He3, polariser_SM, super mirror ensemble, resonator Drabkin, gradient flipper, rotating field.

More information on the VITESS modules is available by clicking on "Help" at the menu bar of the VITESS program.

## 2. VITESS module lenses

One of the recently developed important VITESS component is the module *"lenses"*, which simulates stack (or one of them) of neutron refraction lenses. Two kinds of lens are included in the simulations: with spherical geometry (as usual well known geometry) and parabolic geometry. The geometry has to chosen at the first step. (See radio button "Lenses surface geometry"). The second step is to describe the geometry of a lens numerically. Four parameters are included in the module "Cur_radius1", "Cur_radius2", "RadiusMain" and "Thickness": see VITESS GUI.

For spherical geometry it is shown in Figure 3 (at the left). For parabolic geometry it is shown in Figure 3 (at the right).

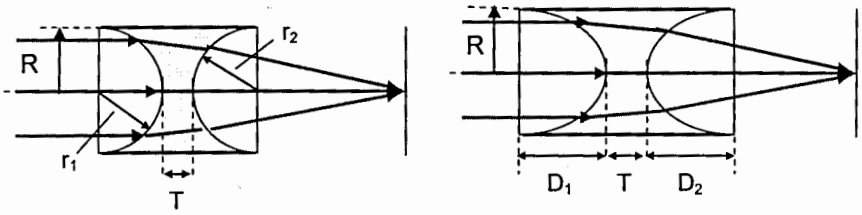


Fig. 3. Left: spherical geometry of a lens – concave shapes, the parameters r1 and r2 are positive. Right: parabolic geometry of a lens – concave shapes, the parameters D1 and D2 are positive.

The main features of the module lenses are:

- Set of identical lenses can be used for simulations,
- Gravity is taken into account,
- 15 materials are incorporated ($SiO_2$, $MgF_2$, Al, ....),
- Refraction coefficient can also be given by the user,
- Attenuation of neutron fluxes inside the lens can be taken into account,
- Visualization of trajectories (under Linux - PGPLOT),
- Parabolic and spherical geometries of lenses are included.

The first option of the list is "Number of lenses". This option is very important due to a very small refractive coefficient for most materials for neutron waves and to have an appropriate focal distance (10-20 m), you have to use a stack of 5-20 lenses usually. If this module simulates only one lens, you have to create a long pipe with a lot of modules "lenses", it is very uncomfortable and can use more memory on PC and be quite slow due to the transportations of neutrons between the modules, which requires additional time for calculations. To avoid these problems, you can simply specify the number of the lens that you want and lenses will be situated one after another.

The gravity effect can be activated or disabled. The gravity simulated in the module lenses as well as in other modules can be useful for long distances and large wavelengths to explore gravitational aberrations: especially important for SANS instruments with lenses.

The examples of simulations of spherical and parabolic lenses are presented in Fig. 4 and 5.

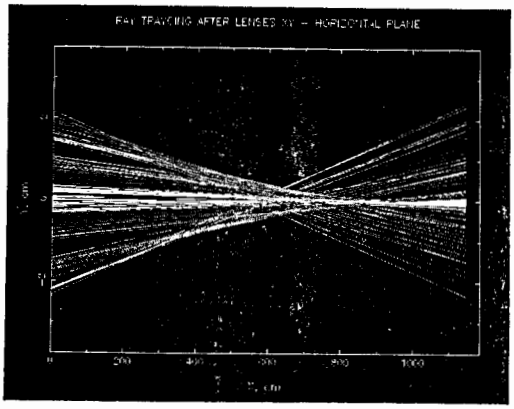

Fig. 4. Simulations of neutron trajectories after a stack of 10 spherical lenses. The spherical form is not ideal for focusing parallel beams: the focal length depends on the distance from the lens axis – the spherical aberration.

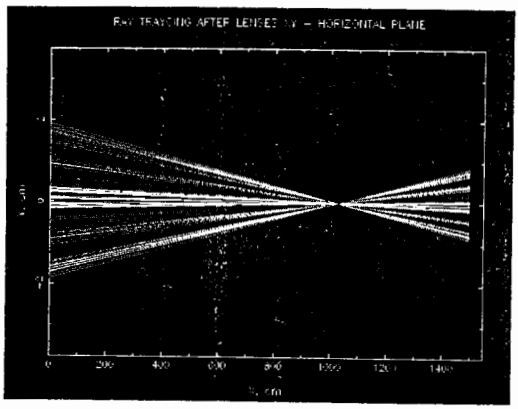

Fig. 5. Simulations of neutron trajectories after a stack of 3 parabolic lenses: no spherical aberrations, significantly reduced attenuation of the neutron beam. However, chtromatic aberrations take place.

# Xen hypervisor for building of non-production Grid sites

A.Ya. Berezhnaya, E.V. Popova
*Institute of High Energy Physics, Protvino, Russia*

Xen is a virtual machine monitor (VMM) or hypervisor. It allows several guest operating systems with different architectures to be executed on the same computer hardware concurrently. Xen helps to use computer resources more efficiently. It is a free software licensed under GPL2.

Non-production cluster with t-infrastructure has been realized under Xen at IHEP to serve training purposes at the Russian Data Intensive Grid consortium (RDIG). CE, SE (dCache), WMS/LB, BDII-top, WNs and UI grid services have been installed at the same server. The experience of cluster construction and usage is discussed.

## Introduction

System installation and adjustment with Xen hypervisor is a solution for many industrial problems such as optimum congestion of computation park, testing new software taking into account various computing platforms and architectures. In the frame of one server we can receive some virtual servers, comparable on productivity with the real one.

## Description of non-production training cluster structure

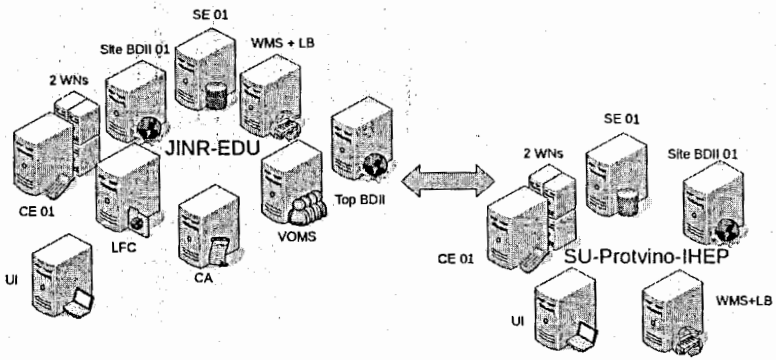


Fig. 1. Cluster structure

In EGEE Project training grid infrastructure (t-infrastructure) intends for spreading knowledge about Grid Technology. It gives an opportunity for users and system administrators to gain experience in working with Grid.

For t-infrastructure in IHEP CE, SE (dcache), WMS/LB, WNs, UI, Site BDII were constructed (Picture 1).

**User Interface (UI)** is a server providing access to Grid resources. Users can start jobs and get results by way of UI. They are able to obtain information about job status, find necessary resources for execution of the specific task.

**Computing element (CE)** (Computing Element) is a grid resource node for jobs management (start, submit, execute etc.) It also gives information about resource states.

**Working Nodes WNs** are cluster computing nodes in GRID infrastructure.

**Storage Element SE** (Storage Element) provides uniform access to storage resources. It could be simply a disk servers, large disk arrays or Mass Storage System such as dCache or Castor.

**Workload Manager System WMS** examines Requirements and Rank expressions (and also any data requirements) in the JDL. All CE are filtered against the Requirements, and the Rank is calculated for all the CEs which match and on the basis of Rank determines which CE to submit the job to. For that purpose, the WMS must retrieve information from the IS and the File Catalog

**Logging and Bookkeeping LB** is a Grid service that keeps a short-term trace of Grid jobs as they are processed by individual Grid components.

**Site BDII (Information Index)** is a database server for site resource information.

**Main system**

Some virtual machines can be installed on Xen server. In our case: 5 DomUs and Dom0. Suggested arrangement is shown on Fig. 2.

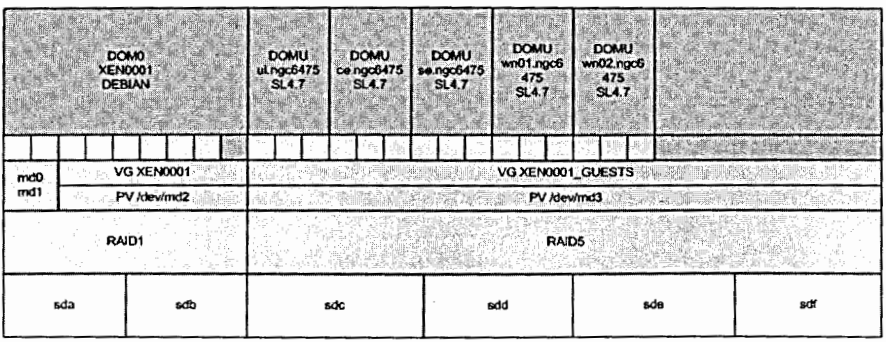


Fig. 2. System schema

For task realization we got server with such characteristics: dual-core processor Intel(R) Xeon(TM) CPU 2.80GHz, ROM 4 Gb, 6 iSCSI disks on 73,5 Gb each. Two disks for software RAID1 (mirror) were used under main domain (Dom0). Other disks became base for software RAID5.

**Dom0 installation and maintenance**

For main domain (Dom0) we decided to choose Debian 4.0r3 etch i386 as an operating system. Dom0 was setup on two disks joined by RAID1. We had to use two additional disks because of system couldn't be loaded from RAID5. Two partitions (/ and /boot) were mounted to raid devices /dev/md0 and /dev/md1 accordingly as Grub loader prevented booting from LVM partitions. /dev/md2 became physical volume (PV) for logical volume (LV) XEN0001. With the framework of XEN0001 VG logical volumes were created (for example xen0001-xen0001_home).

For xen we installed two main packages: hypervisor itself (xen-hypervisor-3.0.3-1) and kernel modified for working under xen environment (2.6.18-6-xen-686). During installation all necessary modifications were made in /boot/grub/menu.lst automatically.

We faced with problem in pygrub. Pygrub is a Python tool which can look inside a disk image or a filesystem to find a GRUB menu.lst. Then it emulates the GRUB menu and returns the kernel, initrd, boot arguments etc. that GRUB would normally have selected. It's a way to keep all the kernel stuff inside the guest filesystem so it can be managed as usual by the admin of the guest. Pygrub comes as part of Xen, and on Etch it can be found at /usr/lib/xen-3.0.3-1/bin/pygrub. In xen on Debian Etch in pygrub there were no some files in /usr/lib/xen-3.0.3-1/lib/python/grub/fsys/ext2/. That's why we downloaded xen sources and copied files from build/lib.linux-i686-2.4/grub/fsys/ext2/*.

**Setup of DomU's sample**

Primarily we decided to create prototype for DomUs. This sample became base for other DomUs. It was created logical volume SL4.7_001 by 12 Gb in logical group xen0001_guests.

lvcreate -L12G -n SL4.7_001 xen0001_guests

For DomU SL4.7_001 we edited configuration file /etc/xen/SL4.7_001:

```
name = "SL4.7_001"
memory = 256
selinux = 0
disk = [ 'phy:xen0001_guests/SL4.7_001,xvda,w' ]
vif = [ 'ip=10.165.1.10' ]
on_poweroff = 'destroy'
on_reboot   = 'restart'
on_crash    = 'restart'
```

It was downloaded installation kernel and ramdisk from http://linuxsoft.cern.ch/cern/slc4X/i386/images/SL/xen/.

The last command was:

```
/usr/sbin/xm create SL4.7_001 -c \
        kernel=vmlinuz \
        ramdisk=initrd.img \
        extra="method=http://linuxsoft.cern.ch/cern/slc4X/i386/"
```

After installation we corrected configuration file adding string for pygrub as a loader.

**DomUs creation under sample**

For sample designing it was necessary to use kpartx for block device creation of every image parition. Before using kpartx we had to stop DomU.

xm shutdown SL4.7_001

We made some block devices:

kpartx -v -a /dev/xen0001_guests/SL4.7_001

ls –lah /dev/mapper/xen0001_guests-SL4.7_001p1

ls –lah /dev/mapper/xen0001_guests-SL4.7_001p2.

Later we temporally mounted file systems for full dump

mount /dev/mapper/xen0001_guests-SL4.7_001p1 /mnt/SL4.7_001/boot/

mount /dev/mapper/xen0001_guests-SL4.7_001p2 /mnt/SL4.7_001/root/

and dumps created themselves.

/sbin/dump 0 -L FULL_boot -f /BACKUP-XEN/SL4.7_001_boot.colddump /mnt/SL4.7_001/boot/

/sbin/dump 0 -L FULL_root -f /BACKUP-XEN/SL4.7_001_root.colddump /mnt/SL4.7_001/root/

File systems unmounted.
umount /mnt/SL4.7_001/boot/
umount /mnt/SL4.7_001/root/.
Bloch devices removed.
kpartx -d /dev/mapper/xen0001_guests-SL4.7_001p1
kpartx -d /dev/mapper/xen0001_guests-SL4.7_001p2.
These dumps let setup similar DomUs saving time noticeably.
Stages:

1) Logical volume allocation for DomU, file system forming.
   lvcreate -L10G -n pps11.root xen0001_guests
   lvcreate -L500M -n pps11.boot xen0001_guests
   lvcreate -L500M -n pps11.swap xen0001_guests
   mkfs -t ext3 /dev/xen0001_guests/pps11.root
   mkfs -t ext3 /dev/xen0001_guests/pps11.boot
   mkswap /dev/xen0001_guests/pps11.swap
2) Dump unwrapping
   mount -t ext3 /dev/xen0001_guests/pps11.root /mnt/tmp/
   cd /mnt/tmp/
   restore -rf /root/BACKUP-XEN/SL4.7_001_root.colddump
   cd ~
   umount /mnt/tmp/
   mount -t ext3 /dev/xen0001_guests/pps11.boot /mnt/tmp/
   cd /mnt/tmp/
   restore -rf /root/BACKUP-XEN/SL4.7_001_boot.colddump
   cd ~
3) Xen conf file preparation
   cp /etc/xen/SL4.7_001 /etc/xen/pps11
   vim /etc/xen/pps11
4) DomU tuning before starting
   mount -t ext3 /dev/xen0001_guests/pps11.root /mnt/tmp/
   vim /mnt/tmp/etc/fstab
   vim /mnt/tmp/etc/sysconfig/network
   vim /mnt/tmp/etc/sysconfig/network-scripts/ifcfg-eth0
   vim /mnt/tmp/etc/hosts
   umount /mnt/tmp/
5) DomU creation
   xm create pps11 –c

We built DomUs for IHEP non-production training cluster in that way.

| Name | ID | Mem(MiB) | VCPUs | State | Time(s) |
|---|---|---|---|---|---|
| Domain-0 | 0 | 129 | 2 | r----- | 102173.7 |
| ce.ngc6475 | 52 | 640 | 2 | -b---- | 219665.7 |
| se.ngc6475 | 47 | 512 | 2 | -b---- | 265444.8 |
| ui.ngc6475 | 50 | 256 | 1 | -b---- | 9835.4 |
| wn01.ngc6475 | 34 | 128 | 1 | -b---- | 19582.8 |
| wn02.ngc6475 | 31 | 128 | 1 | -b---- | 19743.5 |

## Conclusions

At present Xen hypervisor is widely spread on many enterprises. It may be setup on different hardware and architectures. Xen allows to ensure high productivity for virtual machines. Under Xen it's possible to create a "sandbox" in which testing of software may be executed.

Described system adjusts successfully at IHEP for realization of non-production cluster with t-infrastructure.

## References


[1] William von Hagen Professional Xen®Virtualization Published by Wiley Publishing, Inc. 10475 Crosspoint Boulevard Indianapolis, IN 46256.

[2] TEST Xen guest domain installation for SLC 4.X / i386 or SLC 4.X / x86_64, http://twiki.cern.ch/twiki/bin/view/LinuxSupport/InstallingXenParaVirtualizedSLC4

[3] Re: Subject: Re: [Fedora-xen] How to backup a Domu filesystem (on LVM) from Dom0 on Fedora 8? http://www.redhat.com/archives/fedora-xen/2008-June/msg00011.html

[4] http://linuxforum.ru/index.php?showtopic=89090&pid=830273&mode =threaded&start=#entry830273

[5] Xen and the Art of Virtualization By Paul Barham, Boris Dragovic, Stevan Hand, Tim Harris, Alex Ho, Rolf Neugebauer, Ian Pratt, and Andrew Warfield, Presented by Diana Carroll.

[6] http://strugglers.net/~andy/blog/2008/01/20/red-hat-based-linux-under-xen-from-debian-etch/

[7] EGEE – Logging and bookkeeping, http://egee.cesnet.cz/cs/JRA1/LB/

[8] GRID Glossary, http://www-numi.fnal.gov/offline_software/srt_public_context/ GridTools/docs/glossary.html#wms

# Preparation of KIPT (Kharkov) computing facility for CMS data analysis

O.O. Bunetsky, L.G. Levchuk, S.T. Lukyanenko, A.S. Pristavka, D.V. Soroka, P.V. Sorokin, S.S. Zub

*NSC Kharkov Institute of Physics and Technology, Ukraine*

## 1. Introduction

Development of an effective procedure to distribute experimental information from the Large Hadron Collider (LHC) for subsequent remote processing turned out to be a serious challenge for the LHC experiments. The data stream from the four major LHC detectors, ATLAS, CMS, ALICE and LHCb drastically exceeds the flow typical of previous-generation experimental installations in the high-energy physics.

The LHC nominal luminosity of $\sim 10^{34}$ $cm^{-2}s^{-1}$ corresponds to $\sim 10^9$ proton-proton collisions at the record (for laboratory conditions) total energy, 14 TeV. The CMS detector [1] is located at one of the four LHC beam-crossing points and is expected to provide data capable of fulfilling the impressive physics program of this experiment (see Ref. [2]). The CMS trigger system selects only $10^{-7}$ of the total amount of collision events for offline processing which occurs remotely. In other words, the rate of event transfer to regional centers possessing proper mass storage systems is ~100 Hz. Since the CMS raw event size is assumed to be ~1 – 3 MB, this means that the transfer rate is ~100 – 300 MB/s (more than ~1 PB/year). So, one has to process at CMS (as well as in case of other large LHC experiments) a huge amount of information at a very high rate.

On the other hand, samples of, typically, $10^8 - 10^9$ events ($\sim 10^{15}$ bytes of information) have to be processed and analyzed in order to select events that manifest "new physics", according to estimates based on computing simulations which involve contemporary theoretical models to describe high-energy proton-proton collisions.

This sets extremely hard requirements upon the performance of computing facilities (mass-storage and CPU capacity, WAN bandwidth, etc.) which provide their resources for remote data processing. The solution of the problem lies in splitting the total flow of experimental information into several streams and directing them to several regional centers, with the latter providing an effective and reliable access to the data in distributed computations. An adequate framework to implement such a scheme has been given by the Grid technology, and the global Grid infrastructure, Worldwide LHC Grid (WLCG) [3] has been built.

## 2. CMS Computing Model

The CMS computing model [4] rests on the WLCG and follows the MONARC [5] hierarchical scheme. At present, CMS has 8 Tier-1 (T1) centers which have to take CMS real data from the Tier-0 located at CERN, provide event reconstruction and storing datasets of all types, *viz.*, raw (RAW), reconstructed (RECO) and 'analysis object' (AOD) data including skimming datasets and simulated data (see details in Refs. [4,6]).

The selected subsets of data (in particular, the AOD) are also transferred to Tier-2 (T2) sites which bear full responsibility for CMS data analysis and Monte Carlo (MC) production.

According to the computing model [4], a "nominal" CMS T2 center has to have ~4 kHEPspec06 (~1000 kSI2k) of the total worker-node (WN) CPU capacity and ~200 TB of disk space on the storage element (SE). The WAN connectivity of ~1 Gb/s is also assumed. Currently, there are ~50 CMS T2 sites.

There are no special requirements to resources of CMS Tier-3 (T3) centers which are not involved in the data-distribution model of the experiment and are not expected to provide any resource pledges. At present, the CMS computing infrastructure includes ~50 T3 sites.

An important issue within preparation of the CMS computing infrastructure for distributed data processing is site commissioning (see Ref. [7]). To estimate the quality of operation of, *e.g.*, a T2 center, several sources of information are taken into account. The first one comes from the CMS Site Availability Monitor (SAM) which adds several CMS-specific critical tests to the "routine" WLCG SAM monitoring of the site. If the overall daily SAM availability of the facility does not exceed 80%, the site cannot be marked as 'ready'.

Another source is the fraction of successful jobs submitted by the 'JobRobot' (JR) which is automatic submission "fake" CMS analysis jobs via WLCG (typically, several hundreds jobs per day). Again, the daily JR efficiency must be not worse than 80%.

At last, a T2 center must have a certain number of operational network channels connecting it with T1 sites. There should be such links *to* at least two T1 centers (to commission the link, a load-test traffic of 5 MB/s has to be sustained during 24 hours) and *from* at least four T1 centers (traffic of not less than 20 MB/s must be sustained during 24 hours for link commissioning).

The operability of the T1 and T2 centers is a subject of permanent monitoring (see Ref. [7]). If the site is commissioned (*i.e.*, marked as 'ready') and this daily readiness is stable (does not fall below 80% during several weeks), then it is moved to the list of 'production' sites.

We present here the status of the KIPT computing facility within the CMS computing infrastructure with an emphasis on its reliability and quality of its operation on the eve of the LHC restart in the fall of 2009.

## 3. KIPT CMS T2 Center

The first stage of the KIPT computing facility to host computations within the CMS research program was built in 2001 representing then a Linux cluster of several Pentium III CPU's (see Ref. [8]). Currently, the facility combines more than 30 dual nodes with x86-64 processors in total. There are also 2 dual AMD64 nodes which are used for interactive work (in particular, with WLCG external resources through the Grid user interface (UI) installed on these machines). All the computers run the Scientific Linux CERN (SLC) operating system (versions 4 and 5). Batch jobs are processed by the OpenPBS/Torque-Maui configured in the system.

At present, ~70 CPU cores at WN's of the system are allocated to CMS jobs. The facility has two types of WN's which are running the SLC5. For these nodes, the HEPSPEC06 benchmark tests have been carried out following the procedure described in Ref. [9]. The results are presented in Table 1.

Table 1. Results of HEPSPEC06 benchmark tests for WN's of KIPT CMS computing facility

| System | OS | Kernel | Mem | gcc | Benchmark | Total | Per core |
|---|---|---|---|---|---|---|---|
| Dual Intel Xeon EM64T 3.4 GHz | SLC5 | 2.6.18-128.7.1.el5 | 4 GB | 4.1.2 | S2k6 all_cpp 64bit | 13.8 | 6.9 |
| Dual CPU, Quad Core, Intel Xeon E5420 2.5GHz | SLC5 | 2.6.18-128.7.1.el5 | 16 GB | 4.1.2 | S2k6 all_cpp 64bit | 63.8 | 8.0 |

The facility also includes a distributed SE of the DPM [10] type, which consists of 12 nodes supplied with RAID5 and RAID6 disk arrays. The current total SE disk space is 50 TB. The upgrade of this storage system is underway in order to have on it more than 120 TB allocated to CMS data-processing and computation activities by the LHC restart in the end of 2009.

The KIPT CMS computing system has been registered in the WLCG/EGEE structures as 'Kharkov-KIPT-LCG2' (see Ref. [11]) since 2005. After configuration of the current-generation CMS software (CMSSW and PhEDEx), it has been also registered in the CMS SiteDB [12] as 'T2_UA_KIPT'.

In June 2009, the T2_UA_KIPT center successfully passed through all the CMS commissioning tests, and, since then, has been marked as 'ready' for participation in the distributed CMS analysis at the Tier-2 level. The information about the first 6 commissioning PhEDEx LoadTest data transfers to the site from T1 centers (T1_CERN_Buffer, T1_ES_PIC, T1_DE_FZK, T1_IT_CNAF, T1_US_FNAL and T1_FR_CCIN2P3) is displayed in Fig. 1. As follows from the plot on the top of this figure, the connectivity of T2_UA_KIPT with these T1 sites turned out to be fairly good, and the commissioning threshold of 20 MB/s for the daily (24 hour) traffic was exceeded at least 12 times. The 6 commissioning LoadTests occurred during more than 1 month, with transferring more than 30 TB in total to the T2_UA_KIPT SE for the period (see the plot in the bottom of Fig. 1). At present (September 2009), the T2_UA_KIPT site has 8 'from' and 3 'to' commissioned links with the CMS T1 sites.

After commissioning, the site continued to provide regularly a successful fulfillment of the CMS monitoring of readiness [7], and T2_UA_KIPT was moved to the list of CMS 'production' T2 centers by August 2009. At present, this site is among the most stable CMS T2 sites. In particular, the T2_UA_KIPT center was on the top of the T2 quality-ranking list by September 2009 (see Fig. 2).

Of course, the CMS monitoring activity does not exploit considerable computing or storage resources on the system. As an example, we present here the T2_UA_KIPT workload diagram for August 2009 (see Fig. 3). It is seen that typically ~50 jobslots were occupied by CMS MC production and analysis jobs, while resources taken by the SAM and JR jobs are negligible.

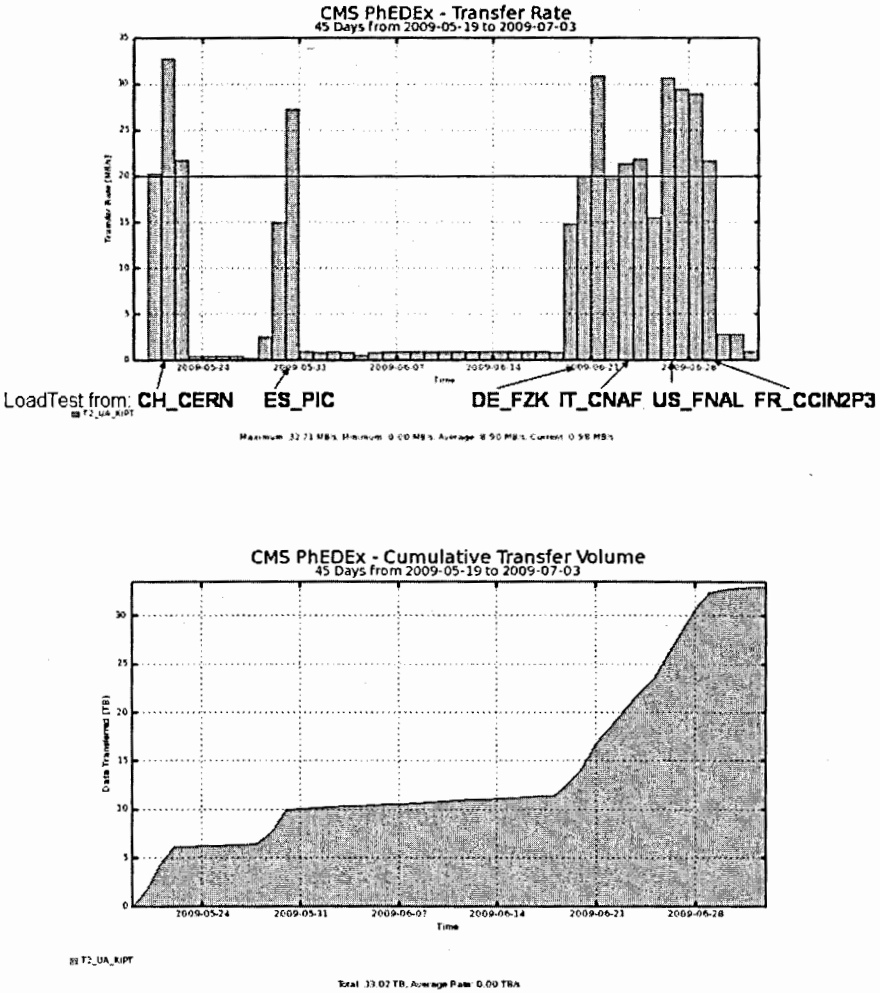


Fig. 1. Commissioning of the first 6 links to T2_KIPT_UA from CMS T1 centers

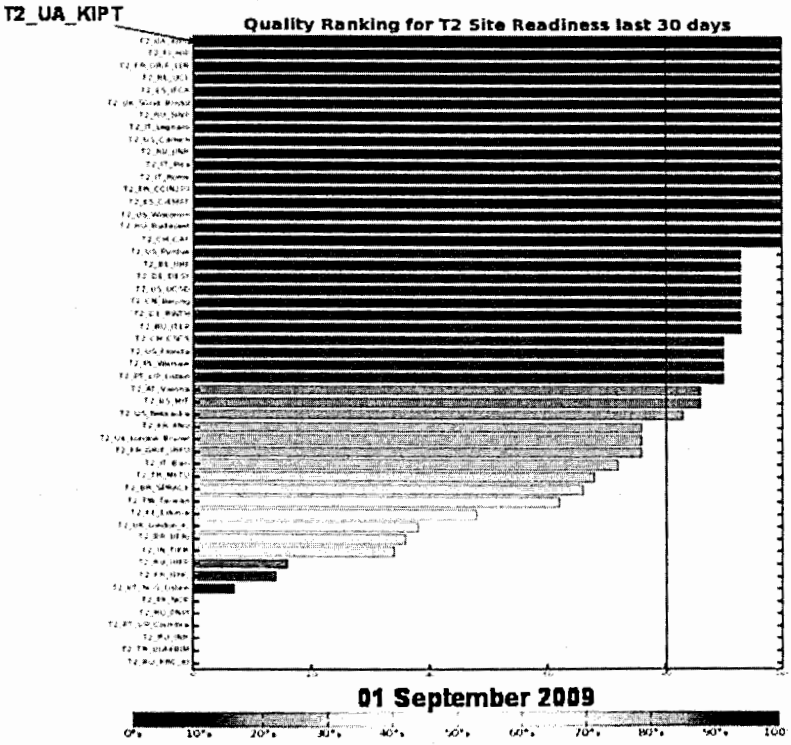


Fig. 2. Quality ranking for CMS T2 centers in August 2009

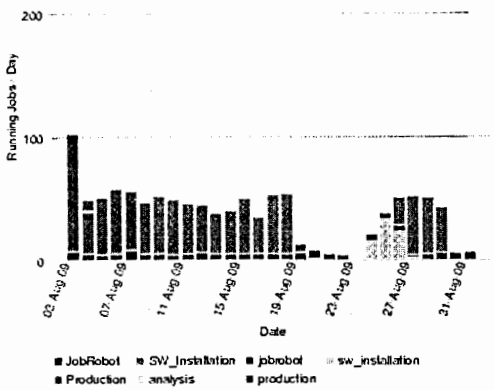


Fig. 3. Load of KIPT T2 center with CMS jobs in August 2009

## 4. Conclusion

The KIPT CMS computing facility, T2_UA_KIPT is commissioned and ready to take part in the WLCG-based CMS distributed data analysis at the Tier-2 level. The site stably satisfies the CMS 'readiness' condition based on the SAM and JR daily results and provides in this sense a fairly good quality of operation. Work on increase of the system resources is currently underway to meet the requirements of the CMS computing model [4] for a "nominal" T2 center.

The work has been supported by a grant of the Russian Foundation for Basic Research (RFBR) and the National Academy of Sciences of Ukraine (NASU) awarded within the cooperative RFBR – NASU scientific project for 2008 – 2009 years to the joint (JINR LIT (Dubna, Russia) – NSC KIPT (Kharkov, Ukraine)) research team.

## References

[1] G. Bayatian et al. (The CMS collaboration), The Compact Muon Solenoid Technical Proposal, CERN/LHCC 94-38, 1994.

[2] G. Bayatian et al. (The CMS collaboration), J. Phys. G: Nucl. Part. Phys., 34 (2007) 995; ibid. 34 (2007) 2307.

[3] LHC Computing Grid Project, http://lcg.web.cern.ch .

[4] G. Bayatian et al. (The CMS collaboration), CMS: The Computing Project; Technical Design Report, CERN-LHCC-2005-023, CMS TDR 7, 2005.

[5] M. Aderholz et al., Models of Networked Analysis at Regional Centers for LHC Experiments (MONARC) – Phase 2 Report, CERN/LCB-2000-001, 2000.

[6] D. Bonacorsi (The CMS collaboration), Nucl. Phys. B (Proc. Supl.), 172 (2007) 53.

[7] PADA Site Readiness, https://twiki.cern.ch/twiki/bin/view/CMS/PADASiteCommissioning

[8] L.G. Levchuk, P.V. Sorokin, D.V. Soroka, and V.S. Trubnikov, Probl. of At. Science and Techn., Ser. "Nucl. Phys. Investigations" 2(40) (2002) 49.

[9] Running HEP-SPEC, https://twiki.cern.ch/twiki/bin/view/FIOgroup/TsiBenchHEPSPEC

[10] LCG Disk Pool Manager (DPM) Administrators Guide, https://twiki.cern.ch/twiki/bin/view/LCG/DpmAdminGuide

[11] S. Zub, L. Levchuk, P. Sorokin, and D. Soroka, Nucl. Instr. and Meth. A, 559 (2006) 35.

[12] CMS SiteDB: Site Directory, https://cmsweb.cern.ch/sitedb

# A system for the registration of experimental information from the separator VASSILISSA

M. Chelnokov, V. Chepigin, A. Isaev, A. Kuznetsov[1], E. Kuznetsov[1],
O. Malishev, A. Svirikhin, A. Yeremin
[1] *"Tekhinvest" Ltd., Moscow, Russia*
*Joint Institute for Nuclear Research, Dubna, Russia*

## Introduction

In the recent experiments (February-March, 2009) on alpha -, beta- and gamma spectrometry using a beam of heavy ions (FLNR) new detectors and registration electronic system described in this work were used. In particular, new multichannel preamplifiers, spectrometer amplifiers and analogue-digital converters, schemes of selection of events and the «global clock» system have been applied.

## 1. Separator VASSILISSA

The kinematic separator VASSILISSA (Fig. 1) has been used at the FLNR JINR /1, 2/ since 1987.

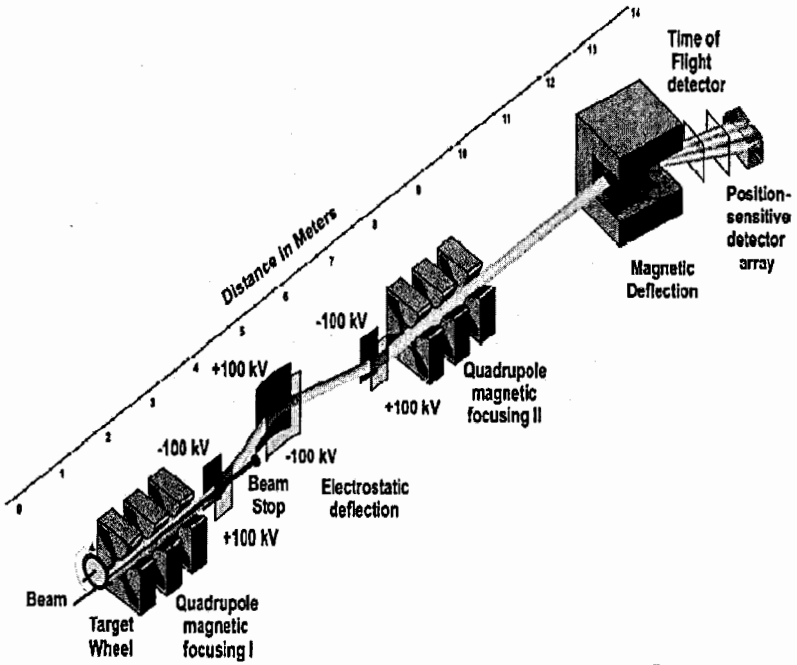


Fig. 1. Separator VASSILISSA

## 2. Detecting system of the separator

The detecting system of the VASSILISSA setup /3/ was modernized in 2007-2008. It is located in the focal plane of the separator and in any experiment includes:

- 2 foils – electron emitters;
- 4 microchannel plates (MCP);
- position sensitive detector array.

A general scheme of the module with MCP is shown in Fig. 2. The flight base between the foils is 40 cm. The time resolution for recoils with energies (10 – 30) MeV and mass number of about 200 is 0,5 ns. The recoil registration efficiency using such detectors is 99,95 %.

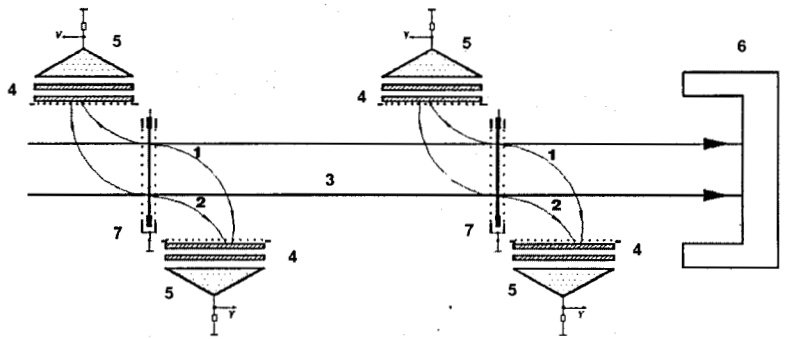


Fig. 2. Time-of-flight system
(1, 2 – electron trajectories, 3 – recoil trajectories, 4 – MCP, 5 – anode,
6 – focal plane detector, 7 – emitter (plastic foil, diameter 80 mm))

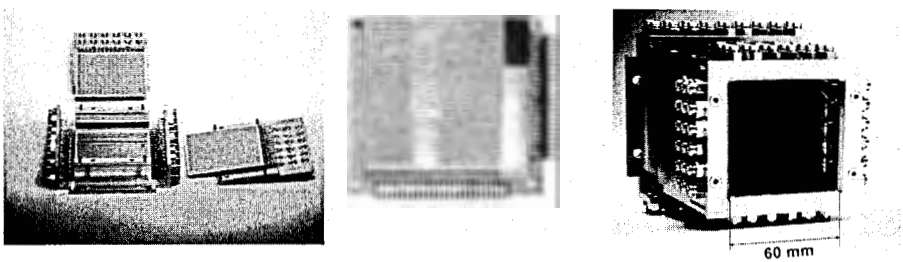


Fig. 3. Disassembled "Well", 48 x 48 double side detector, assembled "Well"

A semiconductor detector (SCD) array in a form of a "well" consists of the double side 48x48 focal plane detector and four lateral 32 x strip detectors (Fig. 3).

In the recent experiments (February-March, 2009) at the FLNR heavy ion beam seven Ge detectors and six BGO detectors were also used. A detecting system named GABRIELA (Gamma Alpha Beta Recoil Investigation with the Electromagnetic Analyzer) is shown in Fig. 4.

For additional clearing from the background of light high-energy particles behind the focal detector veto-detectors of the same size are used. Background gamma rays are cleaned by a system of anticoincidence in which the signals of BGO – detectors are also included.

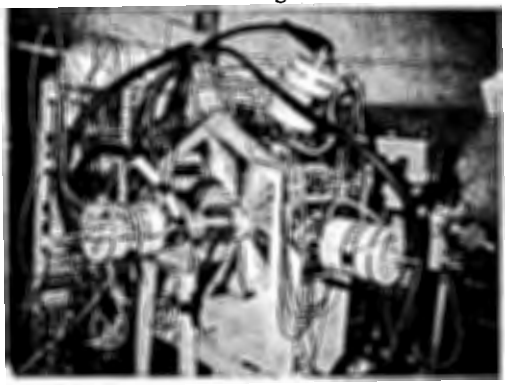

Fig. 4. Detecting system GABRIELA
FWHM Gamma (600 keV) ~ 2.5 keV, Beta (200 keV) ~ 8 keV,
Alpha (5500 keV) ~ 20 keV

### 3. Electronic system of registration

In Fig. 5, a block-scheme for 16 spectrometer channels is shown. 16-channel preamplifiers (PA) are made in the form of a standard charge sensitive scheme with a low noise field effect transistor at the input. Spectrometer amplifiers (SA) have fast outputs and passive base line restorers of the consecutive type. For each channel there are 2 outputs with the signal amplitudes differing from one another precisely by 11 times. It is made to increase the accuracy of registration of low energy particle amplitudes when a wide dynamic range of registered amplitudes is available.

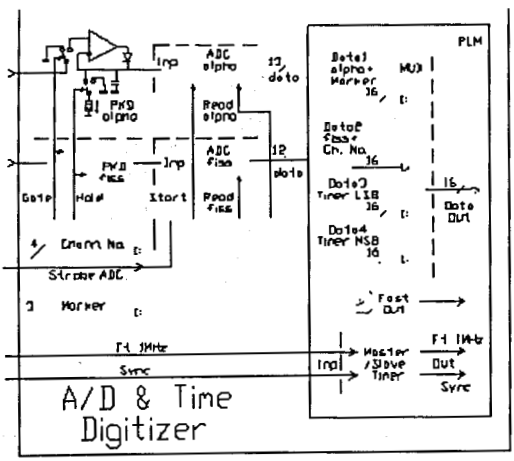


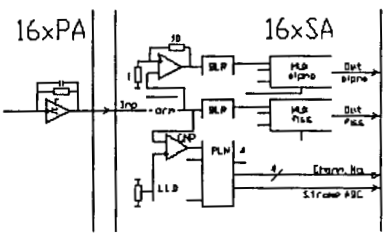


Fig. 5. Block-scheme for 16 spectrometer channels

At the first fast signal the logic scheme of the SA connects the given channel with the built-in multiplexers on the outputs, named "alpha" and "fission", and also forms a binary code of the channel number and a "strobe" for further processing.

For the registration of signals from the double side 48 x 48 detector we used a new device named A/D and Time Digitizer. When a "strobe" signal linear gate is open, peak detectors are transferred into a storage mode, the signal of a total fast output for the event selection system is generated. The code of channel number, markers of the event and current time of the counter-timer are written in the memory of programmed logic scheme. At the end of the "strobe" there is a start of analogue-digital converters (ADC). Target data of each event are four 16-bit words of the data:

- code of ADC "alpha" (13 bit) and data from the register of event "markers" (3 bit);
- code of ADC "fission" (12 bit) and data from the register of the channel number (4 bit);
- low bits of the time counter (16 bit);
- main bits of the time counter (16 bit).

All spectrometer devices for processing the signals of 64 channels are shown in Fig. 6. For the double side 48 x 48 detector we used two identical A/D and Time Digitizer modules.

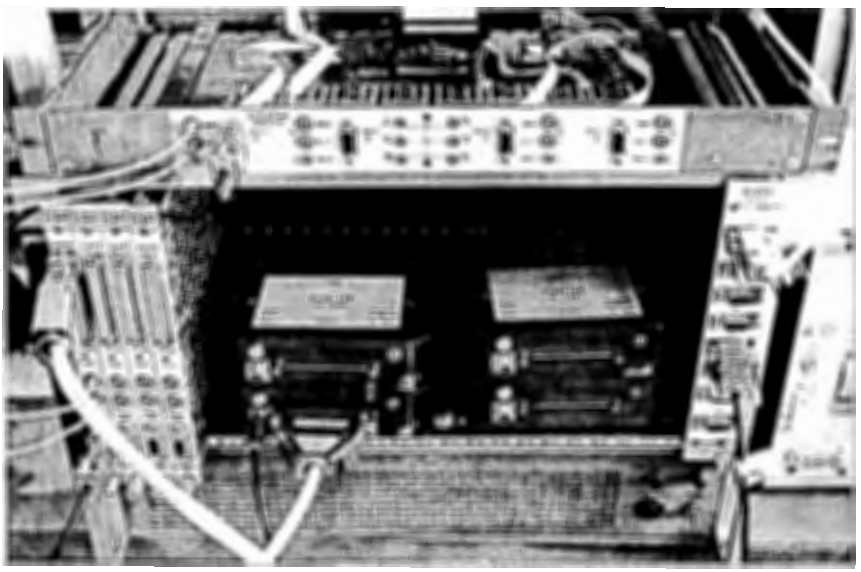

Fig. 6. Electronic devices for 64 spectrometer channels

During the experiment spectrometer paths have shown high enough stability of the parameters. So, displacement of the alpha peak positions at the duration of measurements of more than a month and temperature fluctuations of $\pm 5^0$C was less than 0.05 %.

## 4. "Global clock" system

We used a new approach in making the "global clock" within the common registration system. One of A/D & Time Digitizers (Fig. 7) was the "master" for all the system, including CAMAC crates. It generates a clock frequency of 1 MHz and, using the second wire, a special code message allowing the synchronization of all "slave" counters - both LSB and MSB on all "slave" subsystems. The period of code messages was 32 ms, and a counter cycle – more than an hour. At each message the current time was also registered by an internal clock of the data acquisition system computer. Thus the "global clock" system has been related with the astronomical time.

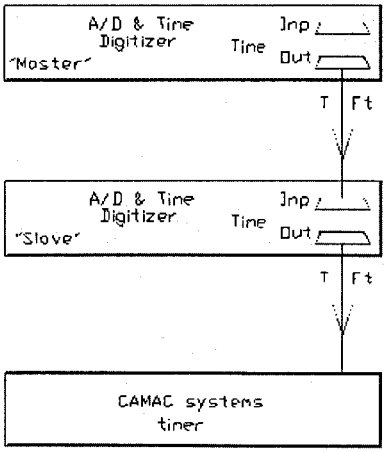


Fig. 7. "Global clock" the system

## 5. Events selection system

The particles transited through the separator have an energy of (1 – 15) MeV. They create a background at recording the alpha-particles and ions implanted in SCD in the separator focal plane. Part of the diffused beam particles, recoils, their alpha-particles and fission fragments is suppressed by anticoincidence MCP and SCD signals.

The block-scheme of the events selection system is shown in Fig. 8.

From the signal of first pair MCP the univibrator UV_coin shapes the time of coincidence and if the signal of the second pair MCP at this time arrives, the marker "time of flight" and signals Start, Stop for TAC are formed. The logic "OR" of MCP signals starts the shaper of the "suspicion" interval of the recoil.

When the fast signal SCD gets into a "suspicion" interval, the recoil marker, or, in the other case – an alpha-particle marker, is formed. At the left-hand side of Fig. 7 the front panel of the events selection block is shown.

## 6. The summary

A new multichannel system for the registration of experimental information was created and checked in experiment. The system includes:

- 16-channels preamplifiers,
- 16-channels CAMAC spectrometer amplifiers,
- 64-channels module A/D & Time Digitizer,
- "global clock" system,

CAMAC module of selection of events.

During the experiment the spectrometer channels showed high resolution and stability of parameters. The displacement of the alpha peak positions at the duration of measurements of more than a month and temperature fluctuations within $\pm$ 5$^0$C was less than 0.05 %.

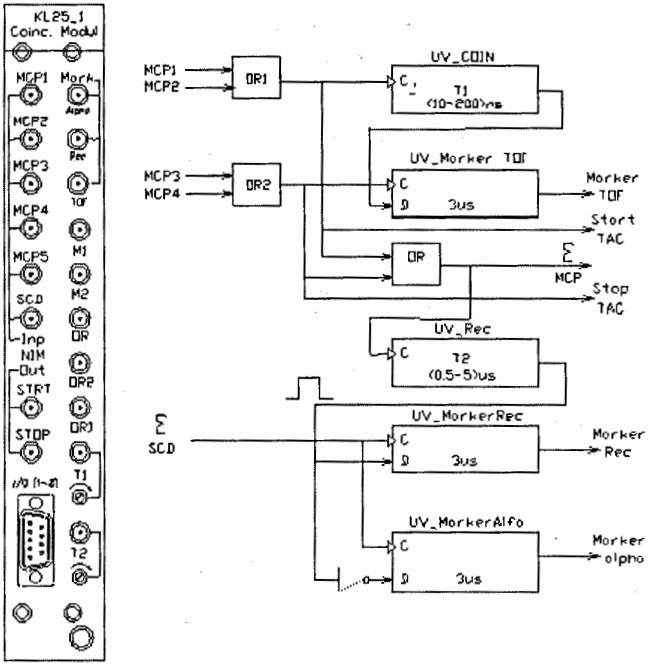


Fig. 8. Events selection system
(MCP – signals of the microchannel plates after PA and CFD;
SCD sum – the logic "OR" of all fast SCD signals)

The compact A/D & Time Digitizer module serves 64 spectrometer channels. It has a resolution of 13 bits for the alpha-spectra, that of 12 bits for the fission-spectra, and a conversion time of 2 us. A step of time digitizing is 1 us, the full cycle of the timer is more than an hour. The module organizes the "global clock" for the whole data acquisition system.

A module for the selection of events is a reprogrammable CAMAC block. It can be used in the future systems having various configurations for the selection of events.

**Acknowledgements**

The authors express their thanks to V. Popov for the high-quality installation of equipment for the presented system.

**References**

[1] A.V. Yeremin et al., The VASSILISSA facility for electrostatic separations and study of complete fusion reaction products, Nucl. Instr. Meth. A, 1989, Vol. 274, pp. 528-532.

[2] A.V. Yeremin et al., The kinematic separator VASSILISSA performance and experimental results, Nucl. Instr. Meth. A, 1994, Vol. 350, pp. 608-617.

[3] O.N. Malyshev et al, Modernization of the detector system at the recoil separator Vassilissa, Nucl. Instr. Meth. A, 2000, Vol. 440, pp. 86-94.

# A centralized administration of the grid infrastructure using cfengine

J. Chudoba [1,2], J. Horký[1,2], T. Kouba[1,2], J. Kundrát[1,2], J. Švec[1,2]
[1] *Institute of Physics, Academy of sciences of the Czech Republic*
[2] *CESNET*

## 1. Introduction

Computational grids these days are organized in "tiers" according to their size and tasks. Tier 2 sites used to be small sites with only tens of computers and a few services offered to users. As the grid grows even the tier 2 sites become big sites with hundreds or thousands of computers and dozens of services provided. This growth brings new challenges and one of the biggest one is how to manage the services and machines in a systematic way, how to keep track of configuration changes and how to make sure the requested services are running with proper configuration.

This set of problems is usually solved by several shell scripts programmed by administrators of the given site. After some time these administrators find out that such concept is no longer sustainable, because the scripts are too complex or not generic enough. Such scripts usually contain a lot of conditions to find out if the given feature is already switched on and if not the script does its work. Another problem of these "in-house" shell scripts is that the administrator has to take care of executing them on all appropriate machines. It becomes a real problem when the number of computers gets high and so it is very probable that some machine is off-line, waiting for maintenance.

The next logical step in managing the site is to use some software for configuration description and execution. Such systems are for example: Cfengine, Puppet, Quattor.

In this article we describe why we have chosen cfengine, how we are satisfied with it and several wins and loses we encountered during the last 15 months of using cfengine.

## 2. Cfengine advantages

Cfengine supports various UNIX platforms as clients and there is also a limited Windows support (with help of cygwin software). It is a very generic configuration tool. It has tools and is designed to be able to configure any aspect of UNIX-like operating system. Cfengine has a long development and usage tradition. Its first production version was released in 1993. It means that the code base is solid and not error prone.

Another big advantage of cfengine is broad user community that is willing to help (usually via user mailing lists) and many sites involved in grid computing use cfengine for a long time and have a good practice and documentation about their experience. We can name scotgrid as an example with their blog [1].

Last but not least advantage that should be mentioned is an optional commercial support available at http://www.cfengine.com/

## 3. Cfengine basics

When a site administrator wants to use cfengine there is one big obstacle in the way: the philosophy of cfengine. It is quite different from shell scripts that one usually uses to install and maintain a grid site.

The main difference is that you describe a state not steps to be done. For example it means that you tell cfengine that you want *httpd* process to be running and let it do anything

cfengine wants to ensure that the process is actually running. This different approach is similar to the difference between procedural and non-procedural programming languages (C vs. Prolog). It also means that one line in cfengine language can result in many actions that are taken to satisfy the request expressed in the line. This different thinking can be difficult at the beginning but it results in a very effective way how to describe configuration of services and hosts.

### 3.1. Classes

The main word that is used throughout the whole cfengine documentation is class. Class is basically any property belonging to a host. So it can be hostname, operating system version, list of services that should run on a host etc.

The classes can be divided into two categories: implicit classes and explicit ones.

Implicit class is something that cfengine defines automatically according to its internal mechanisms for host description. An example of classes defined on worker node running SL5 in private network 172.16.0.0/24 (obtained from cfagent command with -v option):

```
Defined Classes = ( 172_16_2 172_16_2_1 64_bit Day1 GMT_Hr11 Hr13 Hr13_Q3 Min35_40 Min38 October Q3
Thursday Yr2009 any cfengine_2 cfengine_2_2 cfengine_2_2_10 compiled_on_linux_gnu cpu0_high_normal
cpu1_high_normal cpu2_high_normal cpu3_high_normal cpu_high_normal cz domain_golias
entropy_cfengine_in_low entropy_dns_in_low entropy_dns_out_low entropy_ftp_in_low entropy_ftp_out_low
entropy_icmp_in_low entropy_icmp_out_low entropy_irc_in_low entropy_irc_out_low entropy_misc_in_low
entropy_misc_out_low entropy_netbiosdgm_in_low entropy_netbiosdgm_out_low entropy_netbiosns_in_low
entropy_netbiosns_out_low entropy_netbiosssn_in_low entropy_netbiosssn_out_low entropy_nfsd_in_low
entropy_nfsd_out_high entropy_smtp_in_low entropy_smtp_out_low entropy_ssh_in_low entropy_ssh_out_low
entropy_tcpack_in_low entropy_tcpack_out_low entropy_tcpfin_in_low entropy_tcpfin_out_low
entropy_tcpsyn_in_low entropy_tcpsyn_out_low entropy_udp_in_low entropy_udp_out_low entropy_www_in_low
entropy_www_out_low entropy_wwws_in_low entropy_wwws_out_low farm_particle_cz fe80__21f_c6ff_fed9_468a
ipv4_172 ipv4_172_16 ipv4_172_16_2 ipv4_172_16_2_1 linux linux_2_6_18_128_7_1_el5 linux_x86_64
linux_x86_64_2_6_18_128_7_1_el5 linux_x86_64_2_6_18_128_7_1_el5__1_SMP_Mon_Aug_24_08_12_52_EDT_2009
loadavg_high_normal lsb_compliant messages_low_normal net_iface_eth0 net_iface_lo
otherprocs_high_normal particle_cz redhat scientific scientific_sl scientific_sl_5 scientific_sl_5_2
scientificsl scientificsl_5 scientificsl_5_2 scientificsl_boron verbose_mode )
```

These classes are simply obtained from running system by cfengine client and they contain things like IP address (several parts of the address in several formats), MAC address, kernel version, OS version in various formats (n.b. scientific_sl and scientific_sl_5_2). There are also classes describing current state of the machine like load, time etc.

Explicit classes are defined in configuration files by the administrator. These classes can be defined directly for the host in *group:* section of the configuration file (it is a good common practice to have this section just once in a file called *groups.conf*). An example line can be:

```
groups:
        storage = ( storage3 storage5 storage6 )
```

We can understand this line like this: define a group called *storage* that contains three hosts *storage3, storage5* and *storage6*. But in fact we define class *storage* and we define it for these three hosts. Another source for explicit classes are conditional definitions in cfengine configuration. Let's say we want to install an apache daemon and after the installation we want it to be started automatically. Of course if the apache is already installed, we do not want it to be started (again). So in the cfengine language we say something like this: "install apache package, if it wasn't already installed define a class" and in another part of the configuration we say: "if certain class is defined, start the httpd daemon". The actual configuration will look like this:

```
packages:
        httpd
                version=2.2.3-22.sl5.2
                cmp=ge
                action=install
                define=start_httpd
shellcommands:
        start_httpd::
                "/sbin/service httpd start" umask=022
```

### 3.2. Cfengine client

The program that actually reads the configuration and does the changes is cfengine client. The main tasks of the client are: authenticate with the cfengine server, download current configuration from the server, define implicit classes, read the configuration and define explicit classes, try to fulfill the required state.

The last step is the most important one and it means mainly installing packages, (re)starting daemons, automatic file editing etc.

There are various ways how to launch the cfengine client. It can be run periodically from a cron job (usually every hour). It can be run manually from command line (commands cfexecd). Or it can be run remotely from the server via cfrun command. The last mentioned option is useful when the administrator wants to ensure that the changes are in production as soon as possible.

## 4. Cfengine disadvantages

The first impression of cfengine can give an administrator a false feeling that the configuration with cfengine will alway be tidy and clean. But cfengine is powerful tool and it allows a user to write his configuration in a chaotic way.

A typical problem is separation and cross referencing. It is highly recommended to separate every single function into one file and use imports. This way an administrator does not have to repeat every configured feature for multiple hosts or types of hosts.

There is one obstacle with imports though. Cfengine does not import the content of files literally (e.g. like C preprocessor does). It means that if a variable is defined in an imported file, it is not visible in the importing file. Therefore it is a good practice [2] to use imports in one file only. It means to have one file (called imports.conf for example) that just puts things together and do not use *import* directive
in other files at all.

Another problem that is faced sooner or later by every cfengine user is dependency resolution. The cfengine defines (in *actionsequence* directive) the sequence of actions that will be taken by cfengine. For example *actionsequence = (copy processes tidy)* means that files are copied first, then running processes are checked and at the end files are tidied up (deleted).

This sequence is walked through only twice and it means that if the consequence of *processes* directive is a definition of a class that is then used in *copy* directive, everything will work. But if the dependency is even more complicated cfengine will not go through this "oriented graph of dependencies". If the configuration gets this complicated it is usually sign of bad concept and it should be redesigned. Or as a workaround administrator can make cfengine run several times to satisfy all requests and dependencies.

## 5. One bigger example

As an example how cfengine helped us to manage changes of our configuration we present this situation: Security team decides to forbid ssh connection using password authentication and allow ssh keys only.

Before cfengine it meant to make ssh connection to all machines, edit /etc/ssh/sshd_config and reload the ssh daemon. This editing can be done manually or with help of tools like sed or the configuration file can be copied from some central place. None of these option is very comfortable.

Another problem would be if some machines are powered off because of hardware problem or they are reinstalled after this change, so the administrator has to ensure somehow that this particular change is really in production.

The cfengine solution looks like this:

```
editfiles:
        prague_cesnet_lcg2::
                { /etc/ssh/sshd_config
                HashCommentLinesMatching "^PasswordAuthentication.*yes$"
                AppendIfNoSuchLine "PasswordAuthentication no"
                HashCommentLinesMatching "^PubkeyAuthentication.*no$"
                AppendIfNoSuchLine "PubkeyAuthentication yes"
                DefineClasses "proc_service_sshd"
        }
shellcommands:
        scientific.proc_service_sshd::
                "/sbin/service sshd restart" umask=022
                "/sbin/chkconfig --level 2345 sshd on" umask=022
```

These lines just ensure that the /etc/ssh/sshd_config file contains lines that forbid password authentication and allow public key authentication. And if these lines are not present the configuration file is edited accordingly and sshd daemon is restarted.

There are many advantages in this approach:

1. It is repeatable when any node is reinstalled.
2. It is descriptive enough so we do not need to have documentation describing what to do.
3. We store the cfengine files in SVN so we have history of all configuration changes.

## 6. Cfengine usefulness

In this section we present some problems that have occurred during last year. We also present solutions implemented in cfengine.

### 6.1. Old python logging package

There was a bug in gLite worker node configuration that caused atlas software to import old python logging package, which was part of gLite WN installation. This caused atlas production to stop. The suggested solution was to either reinstall the node with a new version of gLite or manually delete old python logging package and let the python to load the system version of this package.

We decided to take the second suggestion and instead of deleting the directory manually, we let
cfengine to do this:

```
tidy:
        # workaround for https://savannah.cern.ch/patch/?2842
        /opt/glite/lib/python/
                pattern=logging
                age=-1
                recurse=2
```

### 6.2. Security problem in recent kernels

At the beginning of September there was an important security problem in linux kernel. First there was no fix for the problem and RedHat only announced a workaround. The suggested workaround was to remove some kernel modules from running kernel and prevent them from loading. It meant editing /etc/ modprobe.conf on all machines.

This work was exactly the kind of problem to be solved by cfengine:

```
editfiles:
        { /etc/modprobe.conf
                AppendIfNoSuchLine "install pppox /bin/true"
                AppendIfNoSuchLine "install bluetooth /bin/true"
                AppendIfNoSuchLine "install appletalk /bin/true"
                AppendIfNoSuchLine "install ipx /bin/true"
                AppendIfNoSuchLine "install sctp /bin/true"
                DefineClasses "rmmod_vulnerable"
        }
shellcommands:
rmmod_vulnerable::
"/sbin/modprobe -r pppox; /sbin/modprobe -r bluetooth; /sbin/modprobe -r appletalk;
/sbin/modprobe -r ipx; /sbin/modprobe -r sctp" umask=022 useshell=true
```

### 6.3. Missing ldconfig entry

When gLite 3.2 on Scientific Linux 5 was launched, there were many problems with it. One of them was that lcg utilities were not capable of loading classad libraries. The problem was caused by the fact that the location of the libraries was not present in configuration file of the linux dynamic linker. So the solution was to add the directory (/opt/classads/lib64) to the configuration and rerun ldconfig:

```
editfiles:
        # workaround for https://gus.fzk.de/ws/ticket_info.php?ticket=47857
        64_bit.(scientific_sl_5|scientific_slc_5)::
                { /etc/ld.so.conf.d/classad_fix.conf
                        AutoCreate
                        BeginGroupIfNoSuchLine "/opt/classads/lib64/"
                                DeleteLinesStarting "/opt/classads/lib64/"
                                Append "/opt/classads/lib64/"
                        EndGroup

                        DefineClasses "run_ldconfig"
                }
shellcommands:
        run_ldconfig::
                "/sbin/ldconfig" umask=022
```

### 7. Conclusion

We have presented the basic philosophy of cfengine and basic ways how this tool is used at Prague tier 2 grid site. We have shown that it is a very valuable tool for managing configuration of many nodes.

We have also presented some usual problems and their solutions.

### References


[1] http://scotgrid.blogspot.com/

[2] http://euvethker.blogspot.com/2005/12/cfengine-best-practices.html

# Readiness of the JINR grid segment to process the first ATLAS data

M. Demichev, A. Dolbilov, N. Gromova, M. Shiyakova,
A. Zhemchugov, P. Zrelov
*Joint Institute for Nuclear Research, Dubna, Russia*

The ATLAS experiment on the Large Hadron Collider at CERN will start operation in 2009. The amount of experimental data is expected to be enormous, and will reach several petabytes per year. To process such an amount of data, the distributed computing system based on Grid has been constructed. Joint Institute for Nuclear Research participates this activity as part of Russian Tier-2 federation. Status of preparation work carried out at JINR is presented. Readiness of the JINR grid segment to process the first ATLAS data is reviewed.

The main goal of the ATLAS experiment is to investigate various aspects of elementary particle properties in high-energy interactions of protons at the Large Hadron Collider (LHC), which is being constructed at the European Laboratory for Particle Physics (CERN). The experiment is expected to start operation in November 2009.

Data flow from the detector is estimated to reach 3.5 Pb/year. The experiment's data processing includes event reconstruction, simulation and physics analysis.

Due to large amount of data to be processed, the ATLAS Computing Model assumes that computing resources are distributed across multiple locations. The tier structure is implemented to combine distributed resources, with distinct roles of the various tiers. Joint Institute for Nuclear Research (JINR) participates Russian ATLAS Tier-2, in scope of the EGEE-RDIG consortium. According to the Tier-2 role, JINR computing facilities should provide analysis capacity for physics working groups to process 20% of the full sample of data (AOD) and computing resources for the Monte-Carlo simulation.

Currently, resources of JINR grid segment are represented by two computing elements (CE) of 314 CPUs (984 cores of 2.2 MSi2K computing power) in total, and by the storage element (SE) with total capacity 400 Tb of disk space. Storage element is operated by dCache storage system. Access via SRM service is also provided. Monitoring and proxy nodes are available. The grid segment is running SL4 operation system and gLite-3.1 middleware. Transition to SL5 is under way. Internal connectivity is provided by 1 Gbps network.

JINR site is integrated into the ATLAS Distributed Data Management System (DDM) since 2007. Currently, it allows to subscribe to the datasets, available at the relevant Tier-1 centre (SARA), exactly in the same way as it should be done for experimental data, when LHC starts operation. Recent production versions of the ATLAS software are installed centrally and available at the CE. Distributed analysis tools Ganga and Pathena are available for the ATLAS users at JINR. A dedicated queue ANALY_JINR has been created to run analysis jobs at the CE more effectively.

To assure the robustness of the computing system, JINR has participated a number of tests, carried out in scope of the ATLAS distributed computing project. These tests included replication of M4 and M5 cosmic data, various functional tests of the data transfer system, stress-tests of the ATLAS analysis structure and, most recently, the combined tests of the LHC computing system (STEP09). Participation in these tests helped a lot to improve an integration of JINR into the ATLAS computing system, and examined readiness of the JINR site for the LHC start-up.

Since grid tools are rather new for the most of the physicists, an intensive work is ongoing among JINR participants of ATLAS experiment, to train and practice with the distributed analysis tools. Starting from 2007, several tutorials and practice lessons have been organized in Dubna.

**References**


[1] ATLAS Collaboration (1994) ATLAS: Technical proposal for a general-purpose p p experiment at the Large Hadron Collider at CERN (CERN-LHCC-94-43).

[2] LHC Study Group (1995) The LHC conceptual design report, CERN/AC/95-05.

[3] ATLAS Collaboration (2005) Computing Tech. Design Rep. TDR (CERN-LHCC-2005-022).

[4] http://www.egee-rdig.ru

[5] LHC Computing Grid -- Technical Design Report (CERN-LHCC-2005-024).

# Novel current mirrors application in high side current sensing in multichannel power supplies

L.P. Dimitrov, G.M. Mitev
*Institute for Nuclear Research and Nuclear Energy, Bulgarian Academy of Sciences*

In the multichannel power supply systems with common power return for all channels, the measurement of the load currents has to be carried out on the high voltage side. Many manufacturers provide specialized ICs for high side current sensing, for voltages around 100V. Working with small values of the electric current (up to 10 μA) the efficiency of these circuits steeply decreases, and it might fall down to values under 0.1%.

Our goal is to develop electronic circuits with improved characteristics for applications with semiconductor detectors. Several schematics, based on electric current mirrors with a work range of up to 400V and improved efficiency, are proposed. Comparative results from simulations and experimental measurements are presented.

**Keywords**: Widlar current mirror, Wilson current mirror, BJT, current sensing, DC power supply, semiconductor detector.

## 1. Introduction

The application of different types of semiconductor detectors is increasing in modern large detector systems for research in high energy physics, astrophysics and astronomy. The recently developed SiPM (silicon photomultiplier) detectors [1] are considered as replacement of the nowadays widely used vacuum devices - PMT (Photo- Multiplier Tubes) and HPD (Hybrid Photo Diodes), in many industrial and research applications.

The main advantages of semiconductor detectors are: the high energy and position resolution, the fast response, the possibility of high level of segmentation - strips, microstrips, pixels, etc., the room temperature operation ability; they do not need high voltage power supplies, connectors and cables; they are insensitive to magnetic fields, can be exposed to ambient light and do not include manual processes in the production.

A major disadvantage is the insufficient radiation hardness - the intense particle flux will cause radiation damage to the detectors thus increasing their "dark current" and requiring changes in the bias voltages during the operation period. This states as requirement to the used power supplies to provide reliable, precise and stable current monitoring in wide dynamic range.

The working voltage of most semiconductor detectors does not exceed 400 V. That allows for the examination of simpler and cheaper approaches for current monitoring, different than the measurement circuits commonly used in high voltage power supplies. That kind of research will be especially useful for the development of future multichannel power-supply systems (voltage distributors) with common power return. In such systems, where the current can be sensed only on the high-side, the possibility to monitor currents trough floating power supplies is a great benefit.

There is a variety of specialized integrated circuits, designed for current sensing in multiple low voltage industrial applications (telecommunications, motor control, portable devices power supplies, chargers etc.) [3]. The high-voltage manufacturing process used to produce such ICs allows them to handle common-mode voltages of 80 V and higher, even when operating from supply voltages as low as 2.8V. Using one or two high-voltage transistors the sensing range for some of these can be extended up to 500V. Obviously, such a modification increases the final price and, as a rule, increases the quiescent current consumed from the measured voltage line, thus reducing power efficiency. These ICs normally have low power efficiency at low current measurements.

## 2. Using "classic" Widlar BJT current mirrors as a current sensing circuit

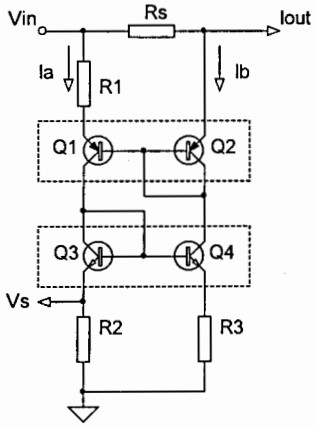


Fig. 1

Different types of current mirrors are known [4]. A single chip high-side current sensor including two complementary simple Widlar BJT current mirrors is commercially available (e.g. ZDS1009). The current measuring scheme of same configuration as ZDS1009 is shown on Fig. 1. The measuring and temperature characteristics of the circuit are strongly dependent on the good symmetry between its two legs. That is the reason $R_2$ and $R_3$ are usually chosen equal in such applications. Assuming that the base currents are negligible, from the schematic, it is evident that:

$$I_a = I_b \tag{1}$$

$$V_s = I_a.R_2 \tag{2}$$

$$I_a.R_1 = (I_b + I_{out})R_s = (I_a + I_{out})R_s \tag{3}$$

$$I_a = I_{out}\frac{R_s}{R_1 - R_s} \tag{4}$$

Therefore we can calculate the value of Vs:

$$V_s = I_{out}\frac{R_2 R_s}{R_1 - R_s} = k.I_{out}, \tag{5}$$

where $k = \dfrac{R_2 R_s}{R_1 - R_s}$.

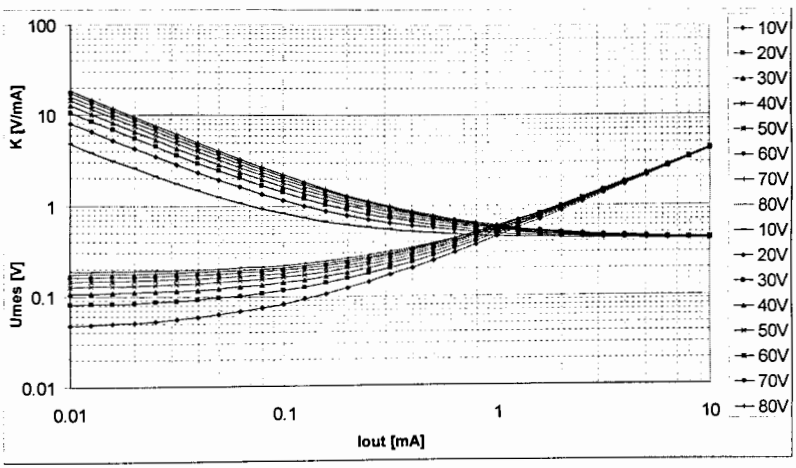


Fig. 2

The real I-V transfer characteristics are shown on Fig. 2. They are gained through a SPICE simulation of the schematic, using the following elements and values: $Q_1$, $Q_2$ – BC556, $Q_3$, $Q_4$ – BC546, $R_s$ = 100Ω, $R_1$ = 15kΩ, $R_2$ = 63kΩ, $R_3$ = 63kΩ and different $V_{in}$ values.

Due to our assumptions we received linear I-V transfer characteristic (5). Besides, we

completely neglected the so-called „Early effect" which causes the dependence of $V_s$ on the supply voltage and the transistors' leakage currents that limit the minimum measurable output current value. The Early effect explains the increase of the collector current of the BJT in response to an increase in the base - collector voltage:

$$i_c = I_s e^{\frac{V_{be}}{V_t}}\left(1+\frac{V_{bc}}{V_A}\right), \tag{6}$$

where:

- $i_c$ is the collector current
- $I_s$ is the reverse saturation current
- $V_{be}$ is the base-emitter voltage
- $V_t$=kT/q is the thermal voltage
- $V_{bc}$ is the base-collector voltage
- $V_A$ is the Early voltage

Obviously, at constant $I_{out}$, $V_s$ is dependent on $V_{BC}$ of $Q_1$, i.e. of the input voltage $V_{in}$.

### 3. Using BJT Wilson current mirrors as a current sensing circuit

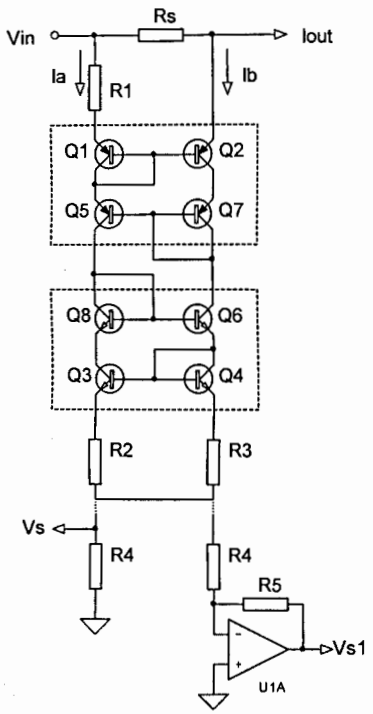


Fig. 3

The known different subsequent modifications of the current mirror offer a considerable improvement over the simple current mirror in terms of the output impedance, precision and temperature characteristics. Named after their inventor, the "basic Wilson current mirror" (3-transistors structure) and the "full Wilson current mirror" (4-transistors structure) are the most convenient for our purposes. The current sensing circuit, using two complementary full Wilson current mirrors, is shown on Fig. 3. By adding just one transistor ($Q_5$ for the upper stage), two main effects are obtained – the $Q_5$ transistor "sources" its base current to right leg, compensating the $Q_2$ base current sinking by the right leg of the current mirror; and second, $V_{BC}$ of $Q_2$ is always nearly equal to $V_{BC}$ of $Q_1$ and almost constant, i. e. the influence of the Early effect is reduced drastically. The same is true for the bottom current mirror. The proposed schematic features a small practical improvement – the common resistor $R_4$. It collects the currents of the two mirror legs, thus reducing the noise sensitivity at low currents, and facilitating the current sensing in power supplies with floating power return (the connection in that case is shown at the bottom right corner of Fig. 3). The schematic using basic current mirrors is the same just the $Q_7$ and $Q_8$ diode-connected transistors are omitted. This slightly worsens the temperature compensation and the Early effect compensation but simplifies the circuit. The SPICE simulation of the I-V transfer characteristics at different $V_{in}$ values is shown on Fig. 4. The component values are chosen as follows: $Q_1$, $Q_2$, $Q_5$ and $Q_7$ – BC556, $Q_3$, $Q_4$, $Q_6$ and $Q_8$ – BC546, $R_s$ = 100Ω, $R_1$ =

15kΩ, $R_2$ = 1kΩ, $R_3$ = 1kΩ, $R_4$ = 31kΩ.

The comparison to Fig. 1 shows that the Early effect is almost completely eliminated and the transfer function is mostly linear. When measuring small currents the leakage currents of the transistors are of a comparable magnitude, which makes measuring even smaller currents practically impossible.

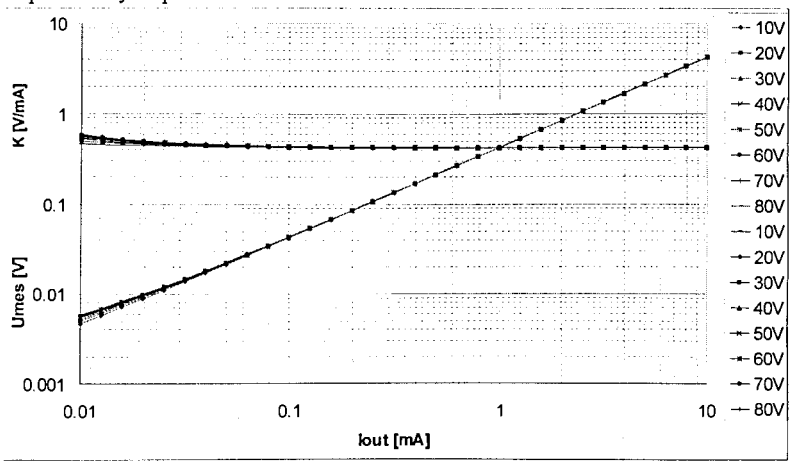


Fig. 4

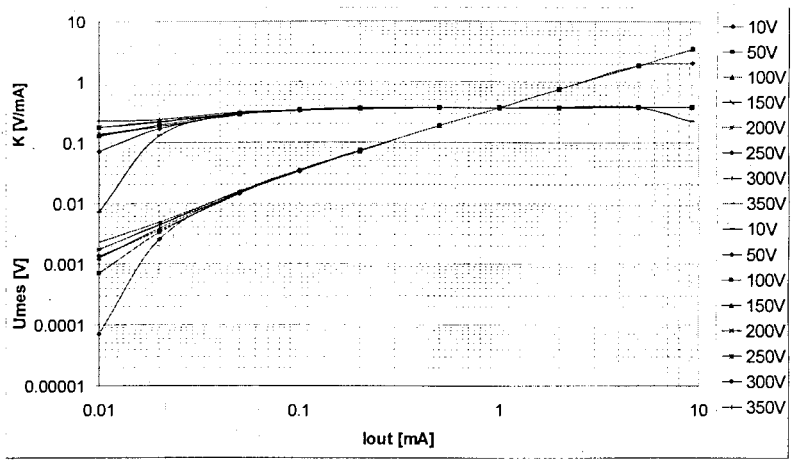


Fig. 5

The experimental measurements for the same circuit are presented on Fig. 5. The transistors have been exchanged for the high-voltage complementary pair FMMT548/FMMT558. There is a good correspondence between the simulation and the experimental results. At very low supply voltages and high output currents the transistors get saturated and the measured voltage is clamped at some maximal value.

## 4. Conclusion

Current mirrors are primarily used as IC building blocks. Their use in measurement circuits is well known but the existing solutions are aimed at industrial applications like motor control and battery charging devices. Typical DC power supplies can be grouped in three main categories - low-voltage low-power supplies, low-voltage high-power supplies and high-voltage high-power supplies. Detector supplies are unique compared to other power supplies as most of them can be classified as high-voltage low-power supplies. The current measurement circuit is usually required to maintain its characteristics in a wide dynamic range of both voltages and currents.

Simpler current mirrors that are used in typical power supplies are poorly suited for large changes in output voltage. This is addressed by using more sophisticated schematics like the Wilson current mirror. It allows for much better measurement characteristics while keeping component count to minimum and maintaining good power efficiency.

The proposed circuit has shown very good linearity in the range of 2.5 decades of change of the output current (50nA – 10mA) and output voltages from 10 to 400V. Its ability to measure smaller currents (under 50nA) is limited of the transistor leakage currents.

It is simpler and more power efficient than the currently used OP-amp measurement circuits.

## References


[1] B. Dolgoshein et al., Silicon photomultiplier and its possible applications, NIM A, 504 (2003), pp. 48–52.

[2] O. Ayranov, The accurate measurement of load currents provided by high-voltage DC power supplies, Meas. Sci. Technol. 10 (1999) N51-N54.

[3] T. Regan, Current Sense Circuit Collection. Linear technology application note (2005), http://www.linear.com/ad/current_sense.jsp

[4] Linden T. Harrison, Current Sources & Voltage References, Elsevier-Newnes (2005), ISBN: 0-7506-7752-X.

[5] A.S. Sedra, K.C. Smith, Microelectronic Circuits (5th ed.), New York: Oxford (2004), Eqs. 4.103–4.110, p. 305, ISBN 0-19-514251-9.

# Experience with gLite at university of Sofia

V. Dimitrov
*Faculty of Mathematics and Informatics, University of Sofia, Bulgaria*

Grid model is described by OGSA, but still it is not a mature technology. There are some standards specified now, but more are under development. After several years Grid will be common standardized technology available all over world like Internet now.

On the other hand, gLite – EGEE Grid middleware is near to be finished. In this paper is presented our experience with gLite at university of Sofia.

## Some History

The initial efforts for creation of national Grid segment in Bulgaria are dated in the period 2002-2003. Before that CERN has accepted as strategy to be created pan European Grid infrastructure for support of researches with LHC [1]. Naturally, this initiative came from the physics working in High Energy Physics from Faculty of Physics at University of Sofia and Institute for Nuclear Research and Nuclear Energy at Bulgarian Academy of Science (INRNE). These people had participated in building of LHC and creation of this infrastructure was of strategic importance for their future participation in research after LHC start.

Initial idea was to be created a big farm at INRNE where all the participants would collect their computers. There are several reasons to do that.

First, there was big free space at INRNE for establishing of big computer farm.

Second, in Bulgaria, traditionally science is funded very low and as result of that to collect the needed computer techniques for a computing farm requires big and concentrated efforts. The idea includes support of the farm to be done by the Faculty of Mathematics and Informatics at University of Sofia (FMI). It is not an interesting job for a physic – with Grid no Master or PhD thesis could be done.

Third, Internet connectivity of the country with the world was very bad. There were two main factors for that. First one was endless wars in former Yugoslavia, which closed the direct links to Central Europe. The second one was the "old lady" Bulgarian Telecommunication Company (BTC), which owned total monopoly on the telecommunications in the country. There was a project for establishment of fast communication channel through Yugoslavia funded by the project DANTE [2], but it failed because of wars. The other alternatives were Romania and Greece. At this time Romania was a blank spot on the telecommunications map, but meanwhile the situation changed there. Nowadays, the main communications are through Romania going round of Western Balkans. First connection fast that has been implemented was with Greece (1 MBit), but there is still a weak link from the border to Thessalonica. Many problems created BTC, at this time, all communication installations had to be property of the monopolist. If someone wanted to developed some new communications, he had to ask for permission BTC and when built it had to donated to BTC without any reward. This approach was unacceptable to the European Union – to fund infrastructure for scientific research and then to give it freely to a company for commercial use, even if the company is government own.

So, at the end of 2003 fifteen computers had been collected in INRNE and the start of the cluster had been announced. It was a local cluster, the software had to be installed and then the cluster to be certified as Grid farm. But this was the end of joint effort, INRNE

decided to develop its cluster only with its own efforts and we at the University of Sofia had to start from the beginning to create our own cluster. This happened in 2005, and at the beginning of 2006 the cluster was connected and certified to Grid. Currently, our cluster consists of:

- Computing Element (1): CPU: 2 x 2.2 GHz AMD Athlon 64 X2 Dual Core Processor 4200+, HDD: 250 GB, RAM: 4 GB,
- Storage Element (1): CPU: 2 x 2.8GHz Intel Xeon, HDD: 160 GB (RAID1), RAM: 1GB,
- Worker Nodes (5): CPU: 4 x 1.8GHz Dual Core AMD Opteron, HDD: 140 GB, RAM: 4GB,
- MON (1): CPU: 2 x 2.8GHz Intel Xeon, HDD: 160 GB, RAM: 1GB.

In 2004 a new Grid player in Bulgaria raised – the Institute for Parallel Processing at BAS (IPP). This institute is specialized on computing networks, has experience in development of scientific ones and has good international connections. So, IPP got the Grid initiative coordination. The local Grid initiative of physics SEE-GRID [3] and the coordination of EGEE [4] are under IPP control.

At this time an organization for Grid has been created only among BAS institutes, but this organization had no life. The problem is that BAS institutes chronically have no young researchers eager to move forward the new ideas.

This organization has been created as "Grid for all scientists". One very important thing that is still misunderstood is that the Grid has to have real users, but not potential ones. In Bulgaria, such real users are only researchers in High Energy Physics that participate in LHC collaboration. There are no other areas in Bulgaria that really need Grid. Funding structure of science in Bulgaria undoubtedly shows what is supported in really in the country. It cannot be expected that chemists, biologists, medics or astrophysics have any real need of Grid resources – in the best case a local cluster of ten computers is enough for them.

**Research Activities**

Till now we have talked about motivation of physicist in Grid – they are motivated to be supported in their research in LHC experiments, but what about motivation of people from Computer science? A scientist in Computer science does researches in new scientific concepts and the Grid undoubtedly is such one.

The next question is "Is it possible in EGEE framework?" to do some research in Computer science. The answer is no. this project is aimed to develop Grid infrastructure, but not to any research. The certified cluster is production one and it is impossible to do any experiments with its system software.

On the other hand, to collect computers for production farm is a problem, because funds have to be from internal or national sources, but not from above mentioned EU projects. In EGEE the funding is for support that is something than nothing. The Grid middleware development gLite [5] is done by 60-80 developers that are not enough even for the development of simple business office software. For young men it is not attractive to enter in new technologies that have no direct business applications, so it is impossible to have some expectations that this could use. Even when some students start to work Grid, after some time (usually when they finish their studies) they shift in some parallel business area. In this situation it is nonsense to create second big research farm.

So, the variants are to look for special niches. Two of them are investigated here.

In Grid blueprints, it is supposed that the Grid interface have to be virtual reality [9]. There is nothing sensible done till now in that direction – there are some demonstrative project, but nothing else. What can be done, without production farm, is to visualize the results from the calculations on the local workstations. It is impossible to do dynamic simulation of virtual reality – for this is needed direct access to the cluster and some changes in the middleware.

On the other hand, local workstation is with limited resources and something real could not be done. For example, visualization of drugs database would catch all the workstation resources independent of its power, even when on the demonstrations in pilot application with a few data the things look good.

The second niche is Service-Oriented Architecture (SOA) [6]. The OGF for Grid [7] is it development to be service-oriented – it is OGSA [8]. What can be done with gLite in that direction? This question we divide in two parts. An environment could be developed using SOA and could not be service-oriented and one environment could be service-oriented without being developed with SOA. What is gLite? Is it developed with SOA? The answer is no. Then the second question is, "Is it service-oriented?" and the answer again is no. There is declared intentions service-orientation of gLite, but there are no service specifications (in WSDL), no service registry, no orchestration and the other components needed service-oriented environment, at least till now. That is why research on SOA in Grid is, usually, done with Globus Toolkit [10], but not with gLite. More precisely, gLite is based on older versions of Globus Toolkit. Indeed, Globus Toolkit is developed mainly for research on Grid, but it still far way from OGSA.

Finally, this restrictions on the usage of the production farm leads to development of independent Grid middleware like GrOSD [11].

**Usability of Grid and the farm**

The usage of the farm is symptomatic one. As above is mentioned, funding for computers is mainly from the national budget. The success of the funding could be approved through the farm usage. If the farm computers have suitable parameters for the jobs in the Grid, then the farm would be preferable location for jobs execution. For it, it is needed the farm servers to have good performance and enough main memory. These characteristics are very dynamic one and they depend of the used software in the target virtual organizations. It is better to have smaller number of servers in the farm, but with better characteristics, than a big number of servers with worse characteristics. In the last case, the farm will stay unloaded most of the time with exploitation charges for nothing.

Now, the problem is: if the funding is from the national budget how much the farm is used by Bulgarian scientists? The answer is not good. Statics from the last three months shows that users with CERN certificates by virtual organizations are:

- atlas – 10,
- dteam – 392,
- lhcb – 4430,
- ops – 6034,

and only three users from the country! The truth is that most of the users prefer have CERN certificates to be "first class" users, and it is so we will see later.

The distribution of all users by projects is as follow:

- atlas – 2140,

- biomed – 3447,
- cms – 14,
- dteam – 439,
- lhcb – 825,
- meteo – 1,
- na48 – 84,
- ops – 2935,
- see – 464,
- seegrid – 2031,
- seismo – 5,
- atlas – 1,
- biomed – 142,
- seevo – 1.

Bulgaria participates only in CMS, NA48, SEE, SEEGRID, SEEVO and SEISMO. So, this statistic is not so bad for the farm usage. Only in CMS and NA48 is participating University of Sofia, but it is national university...

Let's now return back to the "first class" users. Let's you have Bulgarian certificate and try to use the EGEE Grid as it is promised: your job would be executed somewhere and it is not important exactly where – you would receive the results. Let's the job is simplest one the "Hello, world!" program. Even execution of such a simple program is a problem, if you have not explicitly directed to your local farm, and the job is directed somewhere in the region Turkey, Israel or Greece and usually there is someone merciless administrator, who will cancel your job directly from the queue. If you have a chance and your job is directed outside of the region and is directed to Holland or to Scandinavian countries after half an hour you would received desired results. The truth is that no one desires to execute somebody else jobs except to load its resources. Execution of jobs is still not payable and farm load is preferable to be with national jobs for reports. That is why it is so difficult to execute a job at somewhere else location that the local one.

On the other hand, no administrator will cancel a job batched with CERN certificate – he/she would have problems for "badly supported site". In such a way users with CERN certificates are "first class" users.

Another serious problem with gLite usage is the absence of standard libraries on the work nodes of the farms. gLite Grid is like a mega computer that is executing jobs in batch mode. When a job is started for execution, it is usually needed of some run-time libraries for its execution. If these libraries are dynamic ones and they are not available at the execution work node then the job is "successfully" canceled. That is why to be sure that this problem will not arise, simply link your executable code with the needed static libraries. This leads to very big execution code and increase the traffic. To resolve this problem it is needed to define what libraries have to be installed on the work nodes for supported virtual organizations.

But there are no such regulations. It is needed virtual organizations to put some requirements to the software available on the participating clusters or in the clusters' registry to be supported that information. This topic is well defined in Web services standards, but how we mentioned gLite still do not support them.

The software that could be executed in gLite has to be developed in C++ or FORTRAN for currently supported, by gLite, version of Scientific Linux. All other kinds of

software development, usually, fail. For example, if you try to develop some software in Java, you would be faced with numerous problems. The first one is that a Java program needs of a Java virtual machine, such a virtual machine is available at every gLite worker node, but the problem is its version. Sun does not support compatibility from version to version, and that is why the gLite developers use several Java virtual machines with different versions. On the other hand, the situation is not very different with the libraries for Java. That means that if you want to be sure that your Java application would be executed, you have to apply above mentioned approach: to create machine level executable code linked with all needed libraries and this code to directed to compatible hardware environment. This approach is far away from the Java concepts as language for development of distributed applications in heterogeneous environments. Initially, Java developers have attempted to use C for distributed application, but they have failed, so we can say that Java is C++ for distributed environment. The above mentioned approach is a total return to the Java roots – C++. The situation with the other available in gLite languages, like Perl and Python, is not different.

For resolving the problems with the run-time environment of the jobs, virtual machines are advertized as a final solution. The idea is that on the farm would be available installed and configured many virtual machines with different operating systems and including different libraries. When the job arrives, a suitable virtual machine would be started and the job would be executed in it. In such a way, the middleware remain homogenous one. This sounds very good, but there are three fundamental problems. The first one is that some regulation on what a kind of virtual machines have to be supported must be done – such a thing still have not been done. The second problem is that 3-4 virtual machines are enough to overload any computing farm. Virtual machines tend to be huge, and its diversity is enormously big, especially for Linux, where successfully to execute an application developed in one Linux on another Linux tends to be with zero probability. The third problem is that loading a server with several virtual machines one by one or one over one would be catastrophic for any server. Our experience shows that a computer like ThinkCentre M55 (64-bit architecture), running Windows/XP (32-bit operating system) with virtual Linux machine, running Java applications has dramatically bad performance. Why this happens? Initially, 32-bit machine instructions of Windows/XP are interpreted on 64-bit hardware architecture. Then the virtual Linux machine is interpreted in Windows/XP operating system. After that virtual Java machine is interpreted in Linux virtual machine. So, finally when some useful work has to be done, "all the locomotive steam has gone to the whistle."

The natural solution is OGSA – service-oriented Grid environment where there are no virtual machines and layers. One process is a set of interacting services that are accessed in standardized way in heterogeneous environment – that is Service-Oriented Architecture, where real resources are virtualized and there is no need of virtual machines, libraries etc.

**Conclusion**

The situation is not so bad. At first, calculations have to be payable how it is supposed for Grid. Then such tricks, like a higher priority to the local jobs and real participation only part of computing resources of the farm, will be forgotten.

At the second place, it has to be understood that gLite does not support OGSA and would not do that in the future – simply there are no more funds for that. It is better to move to Globus Toolkit. The software used for researches in HEP would not suffer – it is not linked with gLite.

At third place, it had to be understood that is not a mega computer running batch jobs, as it is in gLite. It is not a task of the physicists to write software, but to investigate the results of their experiments. For that they need of user friendly environment for composing SOA applications for Physics.

**Acknowledgments**

This work is funded under the contract FSCI 200/2009 of University of Sofia "Development of Grid Infrastructure for Teaching and Scientific Research".

**References**

[1] LHC - The Large Hadron Collider, http://lhc.web.cern.ch/lhc
[2] DANTE, http://www.dante.net
[3] SEE-GRID, http://www.see-grid.org
[4] EGEE, http://public.eu-egee.org
[5] gLite, http://glite.web.cern.ch.
[6] В. Димитров, Ориентирана към услуги архитектура, Технологика, 2009.
[7] Open Grid Forum, http://www.ogf.org
[8] Open Grid Services Architecture, http://en.wikipedia.org/wiki/Open_Grid_Services_Architecture
[9] Virtual Reality, http://en.wikipedia.org/wiki/Virtual_reality
[10] Globus, http://www.globus.org
[11] GrOSD, http://hdl.handle.net/10506/211

# Towards open access publishing at JINR

I.A. Filozova, V.V. Korenkov, G. Musulmanbekov
*Joint Institute for Nuclear Research, Dubna, Russia*

## Introduction

Traditional channels of distribution of scientific results by means of the publications in scientific journals undergo radical changes with the advent of the Internet and a broader access to digital resources. These changes are connected with transition from a paradigm of the traditional publication to creation of open archives (repositories) of scientific literature. This paradigm which has been put forward in Declarations of the Budapest and Berlin Initiatives, has received the name "Initiative of Open Access" (**OAI** – Open Access Initiative) [1]. Availability of any publication for reader means "open access" via the Internet to this publication which can be read, loaded, copied, extended or used for other lawful purposes in the absence of financial, legal and technical barriers. Now growing number of the academic institutes all over the world create own repositories, accumulating and arranging them in the form of open access for the world community. This tendency is a consequence of growing necessity of transition to open access to the scientific literature, defined by OAI principles: digital access, free for any user, decrease in restrictions on license access and copyrights. In the long term it is supposed, that this transition will develop in two directions: i) repositories with Open Access (**OA**), created by libraries of universities and scientific research institutes and ii) free, reviewed journals with OA.

In the field of high energy physics (HEP) and related areas the popular open access archive of electronic preprints **arXiv.org** is an efficient place for the free distribution of digital preprints of scientific papers [2]. However, **arXiv.org** gives the limited access to publications, namely, only to preprints and is not in full sense the repository of open access. "Orthogonal" to **arXiv.org** OA repositories, like CERN Document Server (CDS) [3], which additionally make available refereed post-print publications in agreement with the policy of scientific journals. OA repositories, joined in network, offer range of library management services such as a user-friendly interface, powerful search functions and collaborative features.

Thus, in JINR necessity of creation own archive (repository) and its inclusion in the international system of archives of open access within the OAI has ripened. Our aim is to build the Open Access repository on the basis of the JINR Document Server (JDS), analogical to CDS.

## Open Access (OA) to Research

Open Access to Research — a way to make scientific results available to all scientific community by the Internet, so that any person can get access to product from any place and at any time at an own choice. OA does not cancel the copyright and does not contradict it. The personal nonproperty author rights are not alienated and remain with him irrespective of a publication way. The decision about the OA publication representation is accepted by the author voluntary. OA is realized by two ways: publication in open access journals; depositing documents in public scientific archives and repositories (institutional and subject). The basic principles of OA are declared in documents of Budapest Declaration Open Access Initiative and Berlin Declaration on Open Access to Knowledge in the Sciences and Humanities.

Open Access is beneficial for researchers, institutions and society as a whole. For scientists and researchers it results in expansion readership and increasing readability, increasing publication citation, scientific impact, growth of the author popularity and fastening of a scientific priority.

For organization it leads to management their digital resources, increasing the scientific

prestige of the organizations. For society – to return on investment in research, removing barriers to information sharing, creation of additional information services for different users categories. Further trends in developing of the Open Access Initiative are conversion of the commercial journals into the open access ones and changing of the subscription policy, as proposed by SCOAP[3] consortium.

**Goals and Requirements JDS**

JINR repository is intended to be a place on network for collection, preservation and dissemination of digital scientific and research documents and located on the platform of JINR Document Server, JDS. It is implemented as an institutional repository in the framework OAI, the content of which will be composed of the following products: publications issued by JINR researchers and in co-authorship with scientists from other institutions; archive documents describing all essential stages of the JINR research activity; documents providing informational support for scientific and technological research performed in JINR. Building the institutional repository has as its objects to make accessible the scientific and research results of JINR employees for the international scientific community; to increase the efficiency of using information resources of JINR Publishing Department and Scientific and Technical Library; to increase the level of informational support of JINR employees by granting an access to other scientific OA archives; to estimate the efficiency of scientific activity of JINR employees.

To achieve these goals we should determine the requirements to the software for creation and management of the OA repository as follows: possibility to harvest and upload documents from other archives; subject classification; wide set of management services for authors and users; web-interface; access rights differentiation; integration with the international catalogues, registers; integration with JINR internal information resources; multilingual interface support; metadata support; support for OAIPMH [4] ; possibility of any format files loading; possibility of the open reviewing and discussions for all interested users even before article acceptance in reviewed journal.

**JDS Software – CDS Invenio**

There is a lot of digital library software packages on the market designed to build and manage OA repositories. Most popular among them are EPrints [5] and DSpace [6]. Several institutions collaborating with CERN implemented the package CDS Invenio [7, 8]. Since all three packages meet the above requirements, the CDS Invenio is of choice for building and managing the JINR repository. This choice is motivated by close partnership between JINR and CERN in theoretical and experimental researches in high energy physics and the existing tendency of consecutive unification of information resources of both institutes. CDS Invenio is the integrated digital library system, applications suit that provides the framework and tools for building and managing an autonomous digital library server. The software is free, licensed under the GNU General Public License (GPL). Now CDS Invenio is installed on JINR Document Server, JDS. Installation packages include OS Linux SL5, Webserver Apache 2.2.3, DBMS MySQL 5.0.45, Python 2.4.3, CDS Invenio 0.99.1. CDS Invenio covers all aspects of digital library management. It complies with the Open Archives Initiative metadata harvesting protocol (OAIPMH) and uses MARC 21 as bibliographic standard. Its flexibility and performance make it a comprehensive solution for the management of document repositories of moderate to large size. Data acquisition is performed from three different sources: direct author submission (using email or the web interface), OAI and non-OAI harvesting (Fig. 1). The metadata is immediately converted into a standard internal metadata representation (MARCXML) whereas full texts are converted into PDF and directly submitted into the document server. Upon upload into the biblio-

graphic server, metadata can be the subject of quality assessment procedures by library cataloguers. Metadata is additionally enriched with citation extraction from the relevant full-texts. The bibliographic server can then be queried to generate indexes, ranks, clusters and formats of bibliography, suitable for fast retrieval. The information is finally delivered, at the right, to users and OAI service providers, through OAIPMH requests, email alerts and the web search engine. In addition, the web interface offers access to personalized collections of the documents (reader baskets or bookshelf), documentation and statistics.

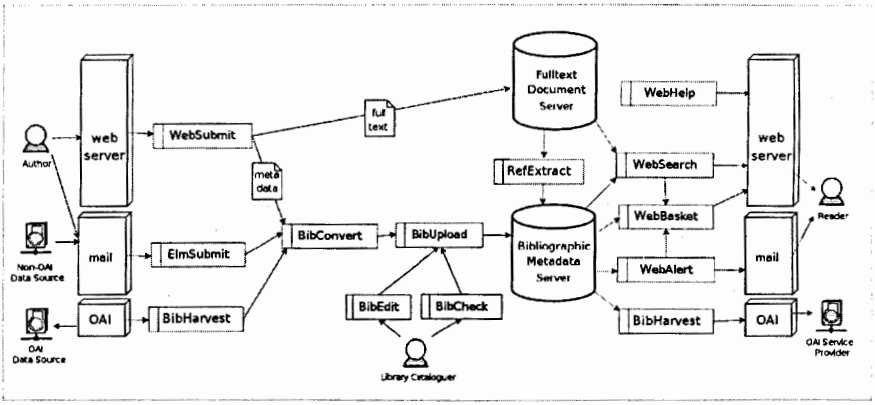


Fig. 1. CDS Invenio Architecture

## The Structure of JDS

As a document server JDS should represent well described and interoperable document collections. All harvestable and deposited documents will be structured in several ad-hoc collections covering articles and preprints, books and conference proceedings, dissertations and reports, presentations and talks, handbooks and manuals and various kinds of multimedia. These collections are arranged in a basic (regular) collection tree by classification principle corresponding to publication type (on the left):

***Basic Collection***

- ☐ **Articles & Preprints**
  - ✓ Articles
  - ✓ Preprints
- ☐ **Books & Conferences Proceedings**
  - ✓ Books
  - ✓ Proceedings
- ☐ **Theses & Reports**
  - ✓ Theses
  - ✓ Reports
    - o *JINR Annual Reports*
- ☐ **Presentations & Talks**
  - ✓ Presentations
  - ✓ Lectures
  - ✓ Conferences Announces
- ☐ **Handbooks & Manuals**

***Subject Collection***

- ☐ **Articles & Preprints**
  - Theoretical Physics
  - Experimental Physics
  - Accelerators
  - Condensed Matter
  - Information Technologies
  - Nanotechnologies
  - Computational Physics
- ☐ **Jinr Laboratories and Divisions**
- ☐ **Theses & Reports**
- ☐ **External Experiments**
- ☐ **Experiments in JINR**
- ☐ **Basic Facilities in JINR**

- ✓ Handbooks
- ✓ Manuals

☐ **Multimedia & Outreach**

- ✓ Photos
- ✓ Video
- ✓ Posters

The regular collection tree is enlarged by the subject collection tree (on the right) that allows one to perform selective search. It may be advantageous to present a different, orthogonal point of view on nodes of the regular tree, based on the other attributes. The subject tree involves the following sections: Theoretical Physics, Experimental Physics, Accelerators, Condensed Matter, Informational Technologies, Nanotechnologies, Computational Physics, JINR Laboratories and Divisions, Experiments with JINR participation, Experiments in JINR, Basic Facilities in JINR. As an OAI document provider, JDS can provide for collections arranged according to arXiv.org specifications.

The potential sources of bibliographic and factual information for uploading at JDS (Fig.2.) are others OAI-archives (for example, full-text archive of arXiv.org); bibliographic archive of JINR Science and Technology Library (STL JINR Bibliographic Archive); full-text archive of JINR Publishing Department (PD JINR Full-text Archive); INIS bibliographic archive (INIS Bibliographic Archive); full-text and bibliographic archives of the informational system PIN (PIN Full-text and Bibliographic Archive) ; submission of documents by authors in self archiving mode .

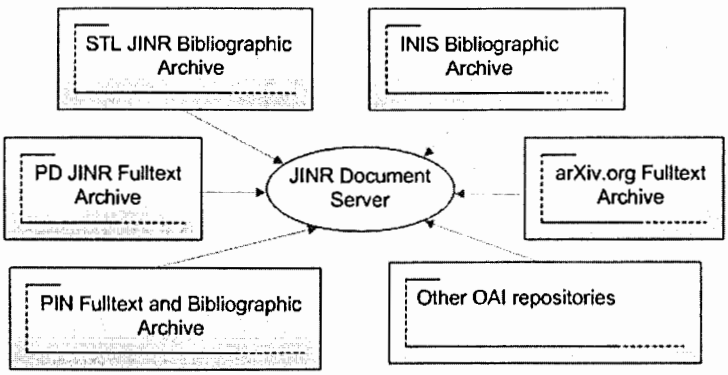


Fig. 2. JDS Data Sources

Delivery of documents into JDS from OAI-repositories is performed by metadata harvesting. The BibHarvest module handles metadata gathering and delivery between OAI-PMH compliant repositories. It enables to configure OAI-metadata harvester for eventual periodical batch upload of data – data sources definition to harvest, periodicity, data transformation type before uploading them into CDS Invenio. Receiving documents from nonOAI data sources is performed by consecutive usage of the modules BibConvert and Bibupload. BibConvert utility enables one to convert metadata records from various metadata formats into another metadata format supported by the CDS Invenio. It is designed to process XML harvested metadata records, converting them into MARC21 before they are uploaded into the database. However, BibConvert is flexible enough to deal also with other structured metadata according to your needs, and offers a

way to actually insert what you want into the database. After uploading documents a library cataloguer has possibility to manipulate bibliographic data directly, edit a single record, do global replacements, and other cataloguing tasks (modules BibEdit, BibCheck). Uploaded publications can be subjected to active discussion and reviewing that can be conventionally done online. The CDS Invenio provides a comprehensive tool for commenting, reviewing and messaging that will allow users and groups to discuss content and share knowledge privately and publicly. Usage and citation statistics of any publication can be derived from the repository.

**Conclusion**

Currently, JINR's institutional repository, JDS, being created as OAI-compliant, makes available on-the-fly the results of scientific research performed at JINR for physical community over the world. It is built on the base of elaborated by CERN the software package CDS Invenio that promotes further partnership with CERN. Additionally, JINR scientists get open access to a vast amount of documents in the field of particle physics and related areas and also a set of advanced user and library oriented services. Early availability of research results of JINR scientists for other world will make an impact of these results on the community and increase recognition and prestige of authors.

**References**


[1] Open Archives Initiative, http://www.openarchives.org
[2] arXiv.org, http://www. arXiv.org
[3] CERN Document Server, CDS, http://cdsweb.cern.ch/
[4] OAI Release of the Protocol for Metadata Harvesting, http://www.openarchives.org/news/oaiv2press020614.html
[5] Official Website EPrints, http://www.eprints.org
[6] Official Website DSpace, http://www.dspace.org
[7] CDSware Overview, http://cdsware.cern.ch/invenio/index.htm
[8] A. Pepe, J.-Y. Le Meur, T. Simko, Proc. CHEP06 conf., Mumbai, India, 13 – 17 Feb., 2006.

# RDMS CMS computing activities to satisfy LHC data processing and analysis

V. Gavrilov
*Institute of Theoretical and Experimental Physics, Moscow, Russia*

I. Golutvin, V. Korenkov, E. Tikhonenko, S. Shmatov
*Joint Institute for Nuclear Research, Dubna, Russia*

V. Ilyin, O. Kodolova
*Skobeltsyn Institute of Nuclear Physics, Moscow State University, Moscow, Russia*

## 1. Introduction

Russia and Dubna Member States (RDMS) CMS collaboration [1], founded in the 1994 year and now involving more than twenty institutes from Russia and Joint Institute for Nuclear Research (JINR) member states, takes an active part in the CMS (Compact Muon Solenoid) collaboration [2] at the Large Hadron Collider (LHC) [3] at CERN [4]. RDMS CMS scientists, engineers and technicians were actively participating in design, construction and commissioning of all CMS sub-detectors in forward regions. RDMS CMS physics program has been adopted taking into account the essential role of these sub-detectors for the corresponding physical channels. RDMS scientists made large contribution for preparation of study QCD, Electroweak, Exotics, Heavy Ion and other physics at CMS. The overview of RDMS CMS physics tasks and RDMS CMS computing activities are presented in [5-10]. RDMS CMS computing support should satisfy the LHC data processing and analysis requirements at the running phase of the CMS experiment [11].

## 2. Current RDMS CMS Activities

During the last few years, a proper grid-infrastructure for CMS tasks has been created at the RDMS CMS institutes, in particular, at Institute for High Energy Physics (IHEP), Protvino, Joint Institute for Nuclear Research (JINR), Dubna, Institute for Theoretical and Experimental Physics (ITEP), Moscow, Institute for Nuclear Research (INR) of the Russian Academy of Sciences (RAS), Moscow, Skobetsyn Institute for Nuclear Physics (SINP), Moscow, Petersburg Nuclear Physics Institute (PNPI) of RAS, St. Petersburg, P.N. Lebedev Physical Institute (LPI), Moscow and National Scientific Center, Kharkov Institute of Physics and Technology, Kharkov, Ukraine (NSC KIPT). In the CMS global grid-infrastructure these RDMS CMS sites operate as CMS centres of Tier 2 level with the following names: T2_RU_IHEP, T2_RU_JINR, T2_RU_ITEP, T2_RU_INR, T2_RU_SINP, T2_RU_PNPI, T2_UA_KIPT. The very solution that CERN will serve as T1 center for RDMS serves as a strong basement to provide the RDMS CMS computing model requirements.

The RDMS CMS computing model should provide a valuable participation of RDMS physicists in processing and analysis of CMS data. At the running phase of the experiment, the CMS basic requirements to the CMS Tier2 grid-sites for physics group hosting are:

- persons responsible for site operation at each CMS T2 site;
- site visibility in the WLCG global grid-infrastructure (BDII);
- availability of CMSSW actual version;
- satisfactory execution of regular file transfer tests;
- certified links with CMS T1- and T2 grid-sites;
- regular CMS Job Robot (JR) testing;

- disk space of 150-200 TB for: central space (~30 TB), analysis space (~60-90 TB), Monte Carlo space (~20 TB), local space (~30-60 TB) and local CMS users space (~1 TB per user);
- CPU resources ~ 3KSI2K per 1 TB disk space, 2GB memory per job.

During 2008-2009 years RDMS CMS took part in CMS computing testing, cosmic run data processing and analysis, large MC samples production. As example of successful participation in STEP'09 (Scale Testing for the Experimental Program in 2009) activities in June, 2009 is shown at the Fig. 1.

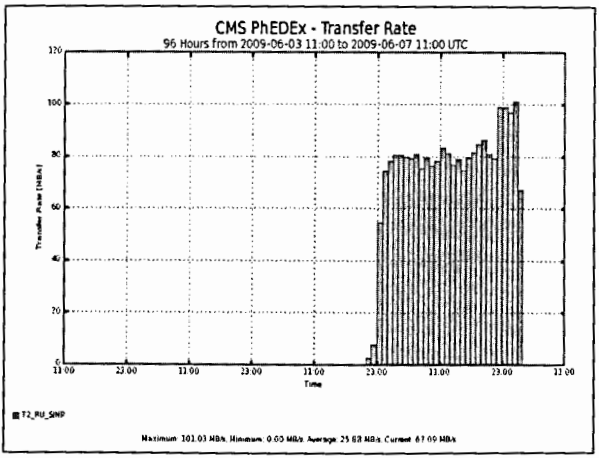


Fig. 1. Transfer rates (up to 100 MB/s) at the SINP T2-site during STEP'09

Network links testing and also massive CMS jobs submission gave a possibility to detect and avoid bottle-necks in the RDMS CMS grid-sites configuration. For example, at the JINR site, it lead to a necessity to reorganize the internal network and Storage Element configurations. In result of creation of dedicated sub-network for disk pools, computing farm and a number of NFS-servers it became possible to increase significantly the efficiency of CMS jobs execution at the JINR grid-site. Finally these works on the reconfiguration increased the JINR grid-site efficiency on the whole.

In 2009 year CMS T2 sites (computing centers) were considered in the context of the CMS computing requirements as "ready" for the running phase of the experiment in the case of:

- site visibility and CMS virtual organization (VO) support;
- availability of disk and CPU resources;
- daily SAM tests availability > 80%;
- daily JR efficiency > 80%;
- commissioned links TO Tier-1 sites ≥ 2;
- commissioned links FROM Tier-1 sites ≥ 4.

The state of RDMS CMS sites readiness (by September, 2009) is shown at the Fig. 2.

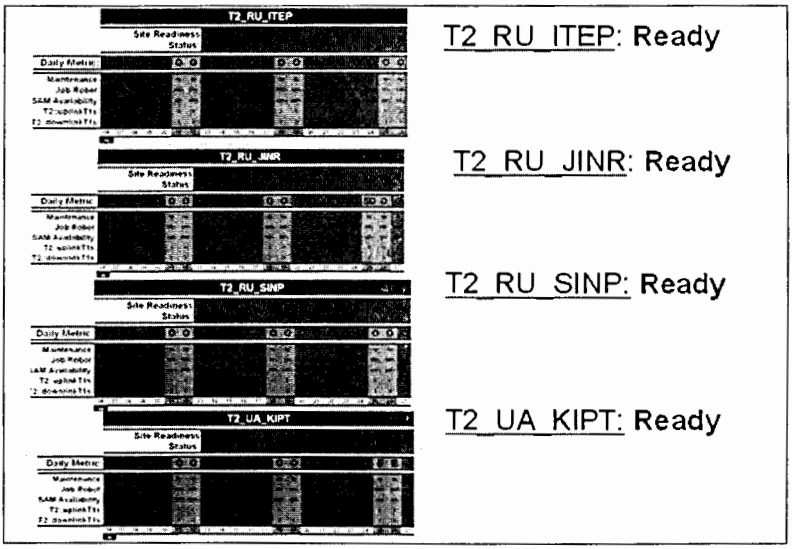


Fig.2. The state of RDMS CMS sites readiness by September, 2009 (for a current situation see *http://lhcweb.pic.es/cms/SiteReadinessReports/SiteReadinessReport.htm*)

In October 2009 the special global test of the CMS Computing and Data model ("October Exercise") was performed. All stages of data processing and physics analysis spreading at the Tier-0/Tier-1/Tier-2 were stressed. The goals were checking of the CMS readiness for the first data taking and analysis at the end of 2009. The RDMS took part in the test within two Physics Groups (Exotica and Muon) associated with JINR sites. During the Exercise accessibility and stability of data transfer links, disk resources, job slots, core and CMS software were tested again and again. To check the reconstruction and analysis procedures about 80 TB both MC data (RECO and AOD) and cosmic test data (RAW) were transferred. The final step was on-line processing of transferred data by RDMS physicists and publication of obtained results in the CMS Discovery Data Base.

In the context of the CMS computing requirements for the running phase of the experiment, now it is provided at RDMS CMS grid-sites:

- the computing and data storage resources in a full volume;
- centralized installation of actual versions of CMS specialized software (CMSSW);
- VOBOX grid-services for CMS with Phedex server installed to provide data transfers between the CMS grid-sites with the usage of the FTS grid-service;
- SQUID proxy-servers for the CMS conditions DB access;
- certification of network links at the proper data transfer rates between JINR and CMS Tier1 and Tier2 centers;
- daily massive submission of CMS typical jobs by the CMS Job Robot system;
- CMS data replication to the JINR data storage system in the accordance with RDMS CMS physicists' requests;

- participation in the CMS Monte-Carlo physical events mass production in the accordance with the RDMS CMS physicists' scientific program.

A group of RDMS CMS specialists takes an active part in the CMS Dashboard development (grid monitoring system for the CMS experiments) (/http://dashboard.cern.ch /cms) [12].

RDMS CMS physicists work in the WLCG environment, and now we are having about 30 members of CMS Virtual Organization (VO). To help them to work in the WLCG environment, a number of training courses for CMS users have been conducted [13].

Starting 2008 the RDMS Tier2 is associated with CMS Exotics Physics Analysis Group and CMS Muon Physics Object Group (both groups hosted at the JINR site), CMS Heavy Ion Physics Analysis Group (hosted at the MSU site) and JetMet/HCAL Physics Object Group (hosted at the ITEP). The special tests shown that the RDMS Tier2 is satisfied all requirements for such hosting including the additional requirements for certification of data transfer links between RDMS sites and other Tier-2 centers associated also with the same CMS Physics Groups. In general, RDMS CPU resources are sufficient for analysis of the first data expected after the LHC start and for simulation.

## 3. Summary

The RDMS CMS computing centers have been integrated into the WLCG global grid-infrastructure providing a proper functionality of grid services for CMS. During 2008-2009 years the significant modernization of the RDMS CMS grid-sites has been accomplished. As result, computing performance and reliability have been increased. In the frames of the WLCG global infrastructure the resources of the both computing centers are successfully used in a practical work of the CMS virtual organization. Regular testing of the RDMS CMS computing centers functionality as grid-sites is provided.

All the necessary conditions for CMS data distributed processing and analysis have been provided at the RDMS CMS computing centers (grid-sites). It makes possible for RDMS CMS physicists to take a full-fledged part in the CMS experiment at its running phase.

The RDMS CMS computing activities were partially supported by the 08-07-91000-CERN and 08-07-90410-Ukr_a RFBR grants.

## References

[1] V. Matveev, I. Golutvin, Project: Russia and Dubna Member States CMS Collaboration /Study of Fundamental Properties of the Matter in Super High Energy Proton-Proton and Nucleus-Nucleus Interactions at CERN LHC, 1996-085/CMS Document, 1996; http://rdms-cms.jinr.ru

[2] CMS Collaboration, Technical Proposal, CERN/LHCC, 94-38, 1994; http://cmsinfo.cern.ch

[3] http://public.web.cern.ch/Public/Content/Chapters/AboutCERN/CERNFuture/WhatLHC/WhatLHC-en.html

[4] http://www.cern.ch

[5] V. Gavrilov et al., RDMS CMS Computing Model, in Proc. of the Int. Conference "Distributed Computing and Grid-Technologies in Science and Education", Dubna, 2004, p. 240.

[6] V. Gavrilov et al., RDMS CMS Computing, in Proc. of the 2nd Int. Conference "Distributed Computing and Grid-Technologies in Science and Education", Dubna, 2006, p. 61.
[7] D.A. Oleinik et al., RDMS - CMS Data Bases: Current Status, Development and Plans, in Proc.of the XXth Int. Symposium on Nuclear Electronics and Computing, JINR, Dubna, 2006, p. 216.
[8] V. Gavrilov at al., Current Status of RDMS CMS Computing, in Proc. of the XXI Int. Symposium on Nuclear Electronics and Computing, Dubna, 2008, pp. 203-208.
[9] D.A. Oleinik at al., Development of the CMS Databases and interfaces for CMS experiment, in Proc. of XXI Int. Symp. on Nuclear Electronics & Computing (NEC'2007), ISBN 5-9530-0171-1, 2008, pp. 376-381.
[10] V. Gavrilov at al., RDMS CMS Computing activities before the LHC startup, in Proc. of 3rd Int.Conference "Distributed Computing and GRID-technologies in Science and Education, Dubna, 2008, pp. 156-159.
[11] CMS Collaboration, The Computing Project, Technical Design Report, CERN/LHCC-2005-023, CMS TDR 7, 2005.
[12] J. Andreeva et al. Dashboard for the LHC experiments, CERN-IT-NOTE-2007-048, presented at CHEP'2007 and published in J.Phys.Conf.Ser.119:062008, 2008.
[13] http://www.egee-rdig.ru/rdig/user.php

# Status of the facility for experiment on RF heating of the copper cavity –the imitator of the CLIC high-gradient accelerating structure

N.S. Ginzburg[1], I.I. Golubev, E.V. Gorbachev, A.K. Kaminsky, A.P. Kozlov, N.I. Lebedev, S.V. Kuzikov[1], E.A. Perelstein, N.Yu. Peskov[1], M.I. Petelin[1], N.V. Pilyar, T.V. Rukoyatkina, S.N. Sedykh, A.S. Sergeev[1], V.V. Tarasov, A.I. Vikharev[1], N.I. Zaitsev[1]

*Joint Institute for Nuclear Research, Dubna, Russia*

*[1] Institute of Applied Physics RAS, N. Novgorod, Russia*

The facility for joint experiments of JINR-IAP RAS has been commissioned to investigate the lifetime dependence of the CLIC high-gradient accelerating structure on the surface damage by repetitive high-power RF pulses[1]. The facility is based on the 30 GHz JINR free-electron maser, which uses an electron beam of the induction linear accelerator LIU-3000.

The distributed data acquisition system was constructed several years ago, and it demonstrated its versatility and reliability. Recently some new features have been added, such as a remote control of the magnetic lens power supplies and an active automatic start time control for the modulators of the induction linear accelerator.

The full-scale experiments have shown the damage of the copper surface observed after $3*10^4$ pulses with the pulse heating of 200°C - 240°C. After $6*10^4$ pulses the damage of the surface of the oxygen-free copper cavity became strong enough to cause regular breakdowns inside the test cavity.

## Introduction

The project of the compact electron-positron collider CLIC with a room-temperature accelerating structure is now developed by the international collaboration for CERN [1]. The damage of the wall of the accelerating structure caused by very intensive cyclic heating induced with short high-power RF pulses can be one of the most severe limits on the accelerating gradient or serve as a criterion to choose materials for structure manufacturing [2]. Several experimental groups around the world have started investigations of this effect using different methods. Collaboration of JINR and IAP RAS has developed an experimental facility to get the RF pulse heating with the temperature more than 200°C. The expected lifetime of the copper cavity at such high temperatures was not more than $2*10^5$ pulses.

## Experimental facility

The facility is based on the 30 GHz 20 MW free-electron maser (FEM), which uses an electron beam of the induction linear accelerator LIU-3000 [3]. The radiation spectrum width does not exceed 10 MHz at pulse duration of 180 ns, repetition rate is 0.5-1 pulse per second.

The Gaussian wave beam from the FEM output waveguide is passing through the thin diagnostic film to the symmetrical two-mirror quasi-optical transmission line. After the oversized waveguide with an input vacuum window the radiation is transformed by the input horn from the Gaussian distribution into the $TE_{11}$ mode and then – into $TE_{01}$ mode by a specialized mode converter. After the output horn the radiation is monitored by a detector with a dielectric waveguide and then it is fully accepted by the calorimeter (Fig. 1).

A specially designed test cavity operates at the mode $TE_{01}$ with zero electric field near the wall to prevent the inner discharge. It consists of two diaphragms and the inner ring with a rather thin edge. The most heated area is the inner edge of the ring. The quality factor of the

[1] This work is partially supported by RFBR grants: # 06-02-16418-a, # 07-02-00617-a, # 09-08-00743-a.

cavity is 1500. The precise frequency matching of the cavity with the FEM oscillator can be achieved by changing the distance between the diaphragms. The test cavity module has its own vacuum system.

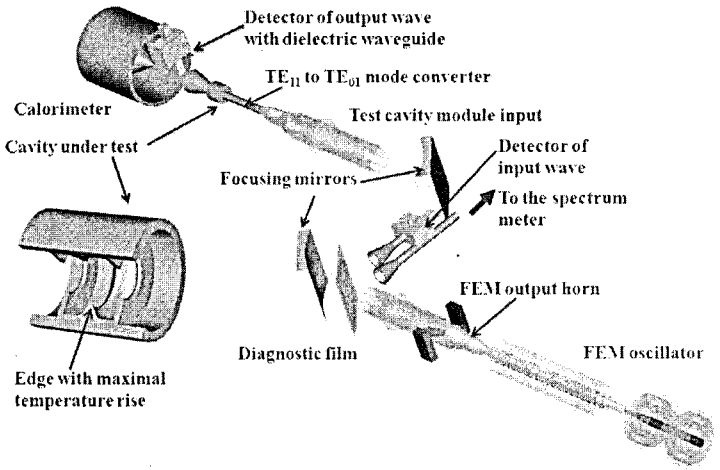


Fig. 1. The layout of the experiment on 30 GHz copper cavity heating

To measure the radiation power, we have applied silicon detectors and a solid-state calorimeter with a big aperture. The spectral diagnostics is based on the heterodyne facility with the on-line Fourier analyser.

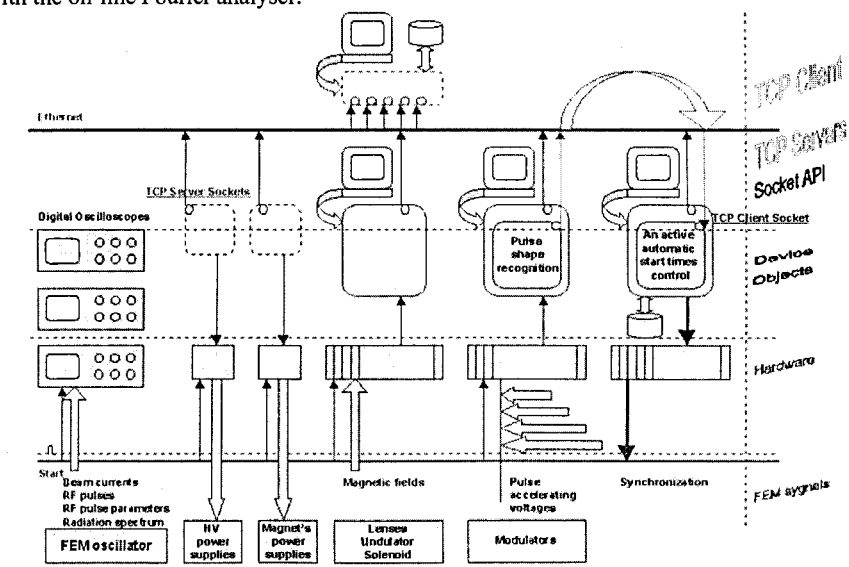


Fig. 2. Schematics of the modernized data acquisition and control system

**Data acquisition and control system**

The distributed data acquisition system was constructed several years ago [4, 5], and it demonstrated its versatility and reliability. Recently some new features have been added. The schematic of the modernized system is shown in Fig. 2.

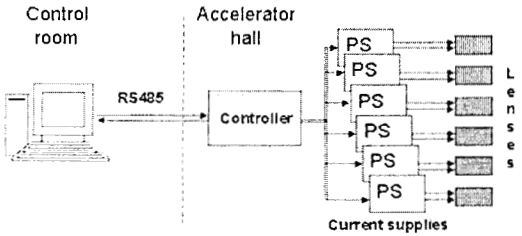


Fig. 3. Schematic of the distributed automatic stabilization sub-system for magnetic lenses (left) and photo of the rack with power supplies inside the accelerator hall (right)

The automatic stabilization sub-system [6] has been exploited in the test regime with local control during 1 year, now it is installed inside the accelerator hall and completely switched to the remote control (Fig. 3). The electron beam focusing system consists of 12 magnetic lenses along the accelerator and beam line. Each magnetic lens is fed with an individual stabilized current supply. The controller is connected to the PC and current supplies by means of RS-485 protocol, allowing controlling the individual lenses currents. The main parameters of the system are listed in Table 1.

Table 1. Parameters of the stabilization sub-system for magnetic lenses

| | |
|---|---|
| Conversion frequency | 40kHz |
| Maximum output current | 15 or 30A (two types) |
| Current regulation range | 60% |
| Accuracy | better than 0.1% |

The switching element is MOSFET IRFP264 with low channel impedance of 0.075Ohm and 38A of the maximum output current, the regulating element is PWM-controller TL494. The filter uses power ferrites Epcos, series ETD.
The main parts of the controller are:

- Atmel MEGA16 single-chip microcontroller;
- ADM2486 *i*Coupler® High Speed Isolated RS-485 tranceiver;
- Max3443 fault-protected RS-485 transceivers;
- MAX504 12-bit DACs with SPI interface;
- HCPL-2630 high speed optocouplers.

Another new feature of the control system is an active automatic start time control for the modulators of the induction linear accelerator. It means the local feedback between the synchronization sub-system (which was operating previously only in the human-controlled regime) and the modulator pulse control sub-system. The hardware core of the pulse control subsystem is a set of fast ADC with memory buffers and input multiplexors. The server

program is now completed with a module of pulse shape recognition, which calculates the time when a flat top of the pulse starts. TCP server module of this subsystem is ready to send these data to the client module in the synchronization subsystem. The synchronization program calculates the difference between the measured value and the desired one and then sends the correction to the synchronization channel connected with the corresponding modulator. The list of channels taking part in this regime can be corrected by the operator in the on-line regime. The screenshot (Fig. 4) shows a set of the data received from the pulse shape recognition module. The active automatic start time control for the modulators significantly improved the stability of the pulse shape of accelerating field.

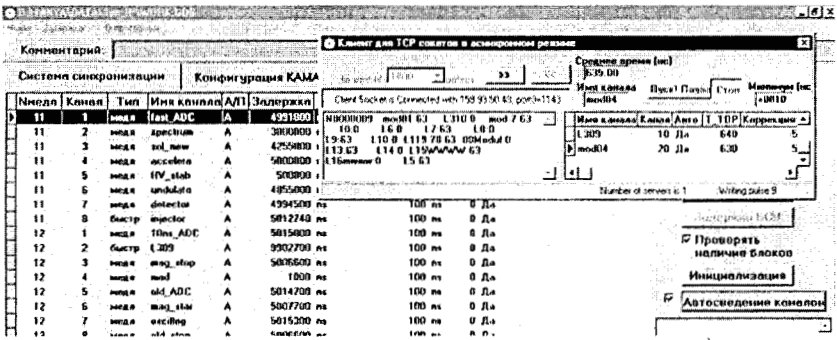


Fig. 4. A screenshot fragment of the code for the active automatic start time control of the modulators

The core of the synchronization sub-system has been also modernized. Now we use new crate controllers with TCP/IP and USB interfaces. DB platform of the synchronization program has been changed from Access to Interbase 6.0 under the Windows XP operating system. Upgrade of the control system and the achieved level of the facility regime stability reduced the time required for the experiment to 2 weeks.

**Experimental results**

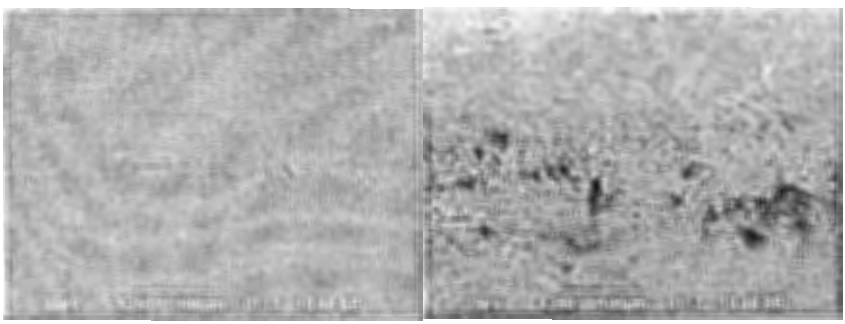

Fig. 5. Electron-microscopic images of the cavity surface before (left) and after $6*10^4$ RF pulses at pulse temperature rise of 220°C - 240°C (right)

Several full-scale experiments have been performed using the created facility. The inner ring of the test cavity, which imitates the CLIC accelerating structure, has been manufactured from oxygen-free copper by turning with a diamond tool. We have controlled

the heating regime in each pulse, the RF mode purity and absence of the vacuum breakdown inside the test cavity. The pulse temperature in different experiments was varied from 200°C up to 240°C. We controlled visually the surface of the inner ring after $1.6*10^4$, $3.2*10^4$, $4.8*10^4$ and $6*10^4$ pulses using an optical microscope. After the experiment each ring was cut into 6 sectors and investigated carefully by the electron microscope. The first damages of the copper surface were observed after $3*10^4$ pulses [7]. After $6*10^4$ pulses the damage of the surface of the oxygen-free copper cavity became strong enough to cause regular breakdowns inside the test cavity.

**Conclusion**

The experimental facility has been constructed, it consists of the linear induction accelerator LIU-3000, the 30 GHz free-electron maser with the output power 15-20 MW, the wave transmission line, the diagnostics of the electron beam and RF radiation, the modernized system of data acquisition and control. The goal of these experiments was to find the proper choice of the material for the accelerating structure of the future electron-positron collider CLIC.

The distributed data acquisition system was constructed several years ago and demonstrated its versatility and reliability. Recently some new features have been added: a remote control of the magnetic lens power supplies and an active automatic start time control for the modulators.

The series of experiments have been fulfilled to investigate copper cavity damages conditioned by the repetitive action of the high-power RF radiation. The damage of the copper surface was observed after $3*10^4$ pulses with the pulse heating of 200 °C -240°C. After $6*10^4$ pulses with a temperature rise of 240°C the surface of the oxygen-free copper cavity was damaged strong enough to cause the regular breakdowns inside the cavity.

The experimental results obtained using the facility can be applicable not only to find the proper choice of the material for the CLIC accelerating structure, but also for the development of high-power microwave generators of any types if the magnetic field near the wall causes high pulse heating.

**References**


[1] I. Wilson, The compact linear collider CLIC, CERN AB-2004-100, CLIC Note 617, Dec. 2004, pp. 12.

[2] D.P. Pritzkau, R.H. Siemann, Experimental study of rf pulsed heating on oxygen free electronic copper, Physical review special topics, accelerators and beams, 2002, Vol. 5, p. 112002.

[3] A.V. Elzhov, N.S. Ginzburg, A.K. Kaminsky et al., Test facility for investigation of heating of 30 GHz accelerating structure imitator for the CLIC project, Nuclear Instruments and Methods in Physical Research, A, Vol. A528, 2004, pp. 78-82.

[4] N.I. Lebedev, A.V. Pilyar, N.V. Pilyar et al., Data acquisition system for lifetime investigation of CLIC accelerating structure, Dubna, Proceedings of NEC'2005, Dubna, JINR, 2006, pp. 181-187.

[5] D.E. Donets, N.I. Lebedev, T.V. Rukoyatkina, S.N. Sedykh, Distributed control systems for modernization of JINR linear accelerators and HV power supplies of polarized deuteron source POLARIS, Proceedings of NEC'2007, Dubna: JINR, 2008, pp. 181-186.

[6] E.V. Gorbachev, V.V. Tarasov, A.A. Kaminsky, S.N. Sedykh, The Focusing Magnetic Field Stabilization System for LIU-3000 Accelerator, Proceedings of NEC'2007, Dubna, JINR, 2008, pp. 29-30.

[7] Yu.Yu. Danilov, N.S. Ginzburg, I.I. Golubev et al, First full-scale result in CLIC-JINR-IAP RAS experiment on 30 GHz copper cavity heating, Strong Microwaves: sources and applications, IAP RAS, Nizhny Novgorod, 2009, Vol.1, pp. 230-235.

# Implementing elements of digital transverse feedback system in Altera FPGA

E.V. Gorbachev, N.I. Lebedev, V.M. Zhabitsky
*Joint Institute for Nuclear Research, Dubna, Russia*

The transverse feedback system is intended to damp beam position errors after injection into an accelerator and cure beam instabilities during acceleration. The system consists of pick-ups, low level electronics making necessary signal processing and power electronics. Implementation of the low level electronics elements in Altera StratixII DSP development kit, is described. The realized digital signal processing allows one to hold an optimal phase between a pick-up and a kicker while changing the revolution frequency during the accelerating cycle.

## Introduction

The transverse feedback system is intended to damp beam position errors after injection into an accelerator and cure beam instabilities during acceleration. The system consists of pick-ups, low level electronics making the necessary signal processing and power electronics. The typical schematic diagram of the digital transverse feedback system is shown in Fig. 1.

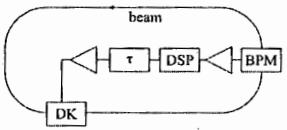


Fig. 1. Digital transverse feedback schematic diagram

The beam displacement signal measured by the beam position monitor (BPM) is amplified, converted to the digital form, processed by the digital signal processing (DSP) circuit, delayed to match the signal transition time from the BPM to the deflector (DK) with the beam flight time, converted back to the analog form, amplified and applied to the beam by the deflector. The digital signal processing circuit must hold an optimal phase between a pick-up and a kicker while changing the revolution frequency during the accelerating cycle.

As a minimum a notch filter to suppress all the revolution harmonics (DC included) is required in the feedback loop. After passing through the notch filter, the magnitude of the difference signal from the BPM electrodes is proportional to the bunch deviation from the closed orbit. The transfer function of the notch filter is $H(z) = 1 - z^{-1}$. The notch filter changes gain $g$ and phase $\varphi$ of the open loop transfer characteristics. The gain can be adjusted by DSP or the amplifier in the feedback. However, the damping rates for the TFS with the notch filter still change due to the phase shift $\varphi_{NF}$ resulting in the damping slower than for the case of the ideal TFS.

A cascade of two FIR (finite impulse response) filters can be used to provide damping rates close to the ideal TFS. The first FIR filter is a notch filter, and the second one is designed with the parameter $a_2$ to obtain optimal damping (see Fig. 2).

The transfer function for the cascade of two FIR filters is $H(z) = (1 - z^{-1})(1 + a_2 \cdot z^{-1})$.

The phase advance between BPM and DK has to be $\pi/2$ multiplied by an odd number for optimal damping. Two BPMs separated by a quarter of the betatron wave length can be used to implement the so called 'virtual pick-up', which has a correct betatron phase advance relative to the deflector position. The signals from pick-ups have to be mixed with coefficients

$b_1$ and $b_2$. The principle is described by means of the trigonometric expression: $\cos(\omega t \pm \varphi) = \cos\omega t \cdot \cos\varphi \mp \sin\omega t \cdot \sin\varphi$.

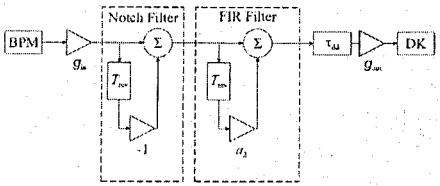


Fig. 2. Digital filters design details

**Hardware**

Altera Sratix II EP2S60 DSP development board was used for the digital processing and control unit implementation. The core of the board is Stratix II EP2S60F1020 device, which provides more than 60,000 equivalent logic elements (LEs), up to 2.5 Mbits of internal memory arranged in TriMatrix memory blocks, operating at up to 450 MHz. The device also contains 8 enhanced/fast phase-locked loops (PLLs) and 36 DSP blocks, giving 144 18x18 bit multipliers. Analog I/O of the board includes two 12-bit 125-MHz ADCs and two 14-bit 165-MHz DACs from Analog Devices. The digital I/O contains 10/100 Ethernet physical layer/media access control (PHY/MAC) and RS-232 serial port. The board contains 32 Mbytes of SDRAM, 1 MByte of SRAM, 16 Mbytes of flash memory which can be used by the FPGA.

The rich set of the development board and FPGA features allow one to implement both the digital processing and controlling program in order to realize the complete digital transverse feedback on a single board.

**DSP implementation**

The block diagram of the digital signal processing unit is shown in Fig. 3.

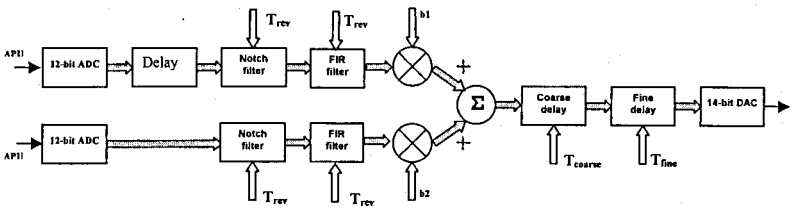


Fig. 3. Block diagram of the digital signal processing unit

The signals from the two pick-ups are digitized by 12-bit ADCs running at the fixed system clock of 100 MHz. The signal of the first pickup is delayed to compensate a particle flight time between the pick-ups. The closed orbit offset signals at the revolution harmonics are removed by notch filters. The FIR filters compensate phase shifts introduced by the notch filters. After that, the signals are mixed with coefficients $b_1$, $b_2$ to adjust the betatron phase advance. The coarse delay and fine delay units introduce an additional delay to match the

signal propagation on the path from the pick-up to the deflector to the time of flight of the particle. In case of variable revolution frequency it is necessary to make adjustments during the accelerating cycle. The necessary delay value can be either set digitally by the external control system or calculated from the external signal (revolution frequency).

The FPGA implementation of the digital processing elements is described below in detail.

The coarse delay unit functional diagram is shown in Fig. 4. It is implemented as a dual port memory clocked with the master clock frequency of the board allowing to adjust the coarse delay in 10 ns step. The size of the memory and clock frequency vaue define the maximum delay that can be achieved. The EP2S60F1020C3 device has more than 2.5 Mbits of internal memory allowing to implement up to 2 ms delay for the 12 bit data with a master clock frequency of 100 MHz.

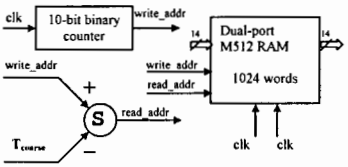


Fig. 4. Coarse delay implementation

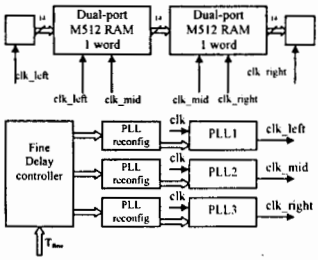


Fig. 5. Fine delay implementation

The fine delay is implemented by using internal FPGA resources such as PLL (phase locked loop). EP2S60F1020 device contains 8 PLLs to produce the phase shift of the clock allowing to delay data for a specified period of time. The minimum delay step depends on the frequency of the PLLs voltage controlled oscillator (VCO) and is equal to the $1/8^{th}$ of its period allowing to achieve 125 ps resolution. PLL can be reconfigured in the real time allowing to adjust the output clock phase on the fly (see Fig. 5). The clock domain transfer is organized by using two M512 dual-port memory blocks with individual clocks for writing and reading. The data are written and read out from the same RAM cell but with different clocks shifted on the phase.

The phase response of the board when switching between the delay from 0 to 25 ns (-9° phase shift at 1 MHz) is shown in Fig. 6. 20 ns of the delay are introduced by the coarse delay module and remaining 5 ns - by the fine delay module.

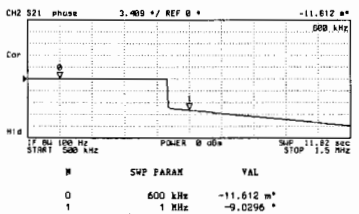


Fig. 6. Phase response with 25ns digital delay

The notch filter consists of one-turn delay and a synchronous adder (see Fig. 7). The one-turn delay is implemented the same way as the coarse delay described above.

FIR filter circuit is similar and contains an additional multiplier (see Fig. 8).

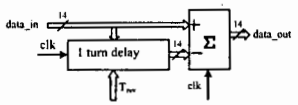


Fig. 7. Notch filter implementation

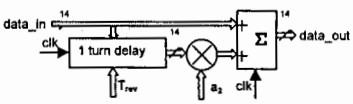


Fig. 8. FIR filter implementation

Fig. 9, 10 and 11 show the measured frequency responses of the notch filter, compensating FIR filter and resulting response of the both filters together. Parameters of the filters correspond to revolution frequency $f$=2 MHz and accelerator tune $Q$=6.73.

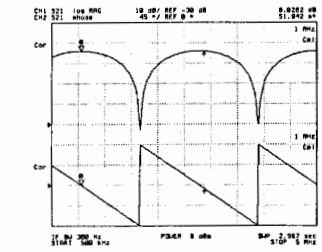

Fig. 9. Notch filter gain and phase response

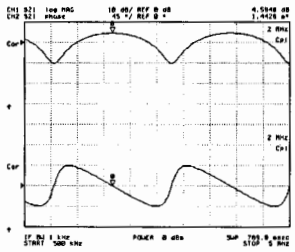

Fig. 10. FIR filter gain and phase response

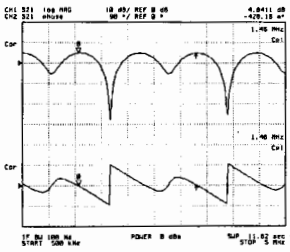

Fig. 11. Resulting frequency response

It can be seen that the notch filter blocks the signals with frequencies $f = f_{rev} \cdot n$, where $f_{rev}$ is the revolution frequency and $n$ is a positive integer, while the FIR filter blocks signals with frequencies $f = f_{rev} \cdot (n + 0{,}5)$. The resulting phase response shows that the phase shift is compensated at the frequencies $f = f_{rev} \cdot (1 \pm q)$, where $q$ is the fractional part of the accelerator tune $Q$.

**Control UNIT implementation**

The main task of the control unit is to communicate with the external control system, recalculate coefficients and delays according to the revolution frequency and update the DSP part of the system.

The embedded NIOSII processor was used to fulfil this task. The processor is implemented in the same FPGA by using some part of its resources as well as external board resources such as 1 Mbyte SRAM memory, 16 Mbytes flash memory and 10/100 PHY/MAC Ethernet controller (see Fig. 12).

The processor runs the real time operating system (RTOS) µC/OS-II, which executes two tasks: InterNiche TCP/IP stack and the control application which calculates the DSP coefficients using the information received from the external PC via network. The interface between the application and the DSP part of the FPGA is carried out by the memory mapped I/O ports.

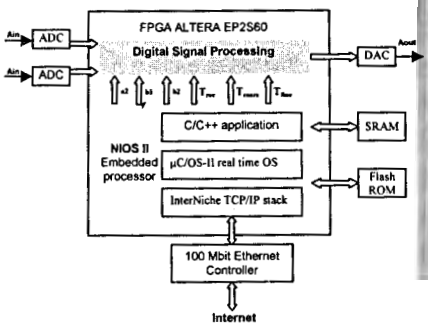


Fig. 12. System layout

Fig. 13. LabView control program

The external PC control program is written in LabView system (see Fig. 9). It allows communicating with the board via network, setting the revolution frequency and delay, enabling or disabling individual DSP elements.

**Conclusions**

The prototype of the digital part of a transverse feedback system for an accelerator with a variable revolution frequency was developed. It includes:

- DSP electronics with the automatically adjustable notch filter, the phase compensating FIR filter and the variable delay based on Altera StratixII development kit using Altera Quartus VHDL/Schematics;
- the control system developed and implemented on the same board by using an embedded processor NIOSII, µC/OS-II real-time operating system and a custom C/C++ application;
- LabView program on a PC to manage the board over the Internet.

The important feature of the system is realization of the DSP and control parts on a single FPGA. It allows organizing simulations of the feedback with calculated beam responses.

The authors thank W. Höfle (CERN) for the constructive assistance and fruitful discussions.

**References**

[1] E. Gorbatchev et al., Transverse Damping System at SIS100, EPAC 2006, Edinburgh, June 2006, p. 3014.

[2] V. Rossi, Digital Signal processing and implementation for accelerators, CERN-SL-2002-047.

[3] V. Rossi, Digital Signal Processing for 1-Turn Delay Feedback Systems of the CERN Accelerator Chain, CERN-BE-2009-009.

[4] V. Zhabitsky, Beam Stability in Synchrotrons with Digital Filters in the Feedback Loop of a Transverse Damper, JINR Communications, Dubna, E9-2009-82, 2009.

[5] V. Zhabitsky, Stability of an ion beam in synchrotrons with digital filters in the feedback loop of a transverse damper, Proceedings of VIII Scientific Seminar in Memory of V.P. Sarantsev, Alushta, 2009.

# The data acquisition subsystem for parameters of beam injection into the Nuclotron

E.V. Gorbachev, T.V. Rukoyatkina, G.S. Sedykh, V.I. Volkov
*Joint Institute for Nuclear Research, Dubna, Russia*

The distributed subsystem is intended to measure the beam spatial characteristics such as a profile, center-of-mass-position and sizes in two cross-sections of injection channel and in three cross-sections of first linear space. It is also intended to measure the absolute values of the inflector magnet (IM) current and the inflector plate (IP) voltage and to register the injection dynamic processes (the injected beam current, the circulation of the beam in the accelerator cavity).

The server part of the subsystem is located in the concentrator which is ~50 m away from the sensitive elements. It consists of an industrial computer and 4 data acquisition modules: the multi-function isolated USB module DT9836 from Data Translation and 3 modules from National Instruments - two 5½-digit multi-meters NI PCI-4060 and the oscilloscope module NI PCI-5105. The graphical client applications start on the local and/or central control panel.

The subsystem was made in LabVIEW 8.6 from National Instruments and was tested with a self-made module imitating a beam profile with a pre-setting distribution. The autumn session on the Nuclotron is expected to be the main severe test for the subsystem.

## The requirements to the data acquisition subsystem for parameters of the beam injection

The measurements of spatial beam parameters are carried out by means of multi-wire collector detectors (MWD) with control surfaces X and Y. The gilded tungsten wires with a diameter of 100 mkm form each of the above surfaces. The quantity of the signal wires and the step between them are selected on the basis of typical sizes of the beam at the detector location.

The block-diagram and the time-diagram are presented in Fig.1 and [1]. The charge-voltage converters (CVC), the sample-and-holds (S/H) and the multiplexers (MPX) are located in the boxes near the sensitive elements, but the analogue-digital converters (ADC) and the passive timer-synchronizator (T/S) are located in the data acquisition centre. The sample-and-holds (S/H) are in the hold regime when signals are reswitched. The signal levels from the sensitive elements are from 10 mV to 1..5 V.

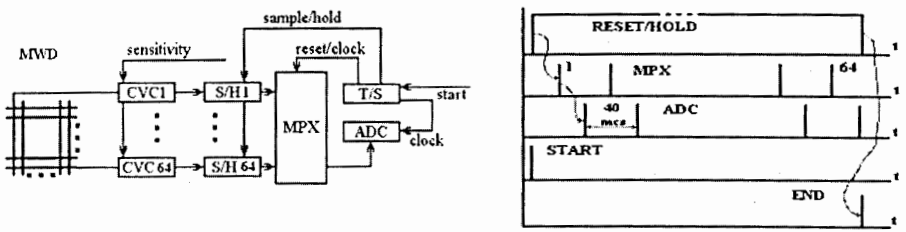


Fig.1. The block-diagram and the time-diagram

The registration of the signals from 5 beam profile-meters in every Nuclotron cycle is carried out by means of the multi-function isolated USB module DT9836 from Data Translation (16-Bit resolution, 6 or 12 SE analogue inputs at 225 kHz sampling speed per channel). The data acquisition cycle is launched by the synchronization signal START (the delayed pulse of injection beginning). The synchronization signal END is the sign that the cycle is finished.

To register the injection dynamic processes, the multifunctional DAQ oscilloscope module NI PCI-5105 is used (8 register channels, 12-Bit resolution, 60 MHz sampling rate, 16 MB RAM). Its analogue signal scope is from 10 mV to some volts. It starts on the injection synchronization signal START and sends the data when the buffer is full. Two 5½-digit multi-meters NI PCI-4060 measure the IM current and the IP voltage every 250ms.

The main features of the described DAQ subsystem are: the multi-level multi-channel client-server architecture based on TCP/IP asynchronous sockets, autonomous low level servers.

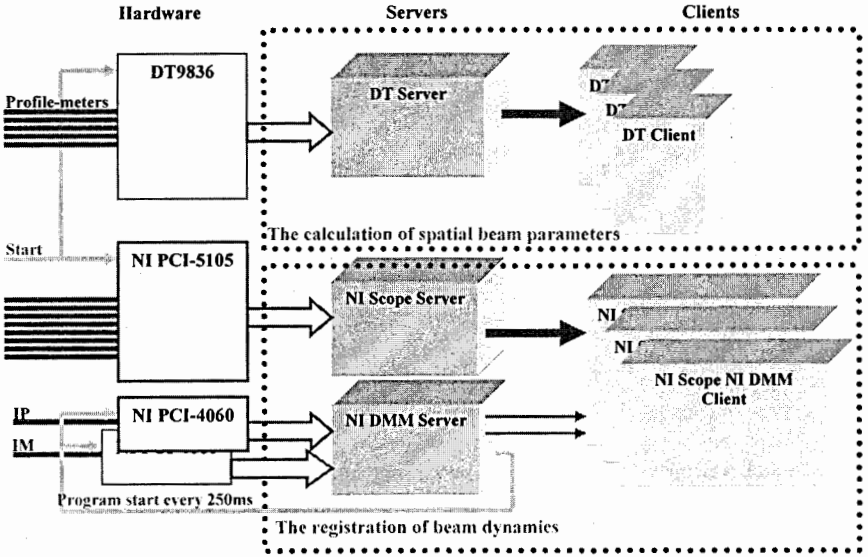


Fig. 2. The structure of the client-server DAQ subsystem for parameters of beam injection

**The client-server program for calculation of spatial beam parameters**

All the data acquisition subsystem for parameters of beam injection into the Nuclotron was made in LabVIEW 8.6 from National Instruments.

The task of the first server is to measure and compute the signals from 5 beam profile-meters received in every Nuclotron cycle by means of the multi-function isolated USB module DT9836 from Data Translation (16-Bit resolution, 6 or 12 SE analogue inputs at 225 kHz sampling speed per channel).

The program to calculate spatial beam parameters was tested with the self-made module imitating the beam profile with a pre-setting distribution. The interface program was also made in LabVIEW 8.6 and can determine the parameters of COM-port communication with a self-made module and parameters of the selected distribution:

- the type of the distribution: uniform, serrated, linear or Gaussian - with different sigma, amplitude and mathematical expectation;
- the maximum output voltage;
- the polarity.

The formed X, Y signals imitating the beam profile signals are sent to the EPIK-3 electronics and then - to the server, when the button Start is pushed.

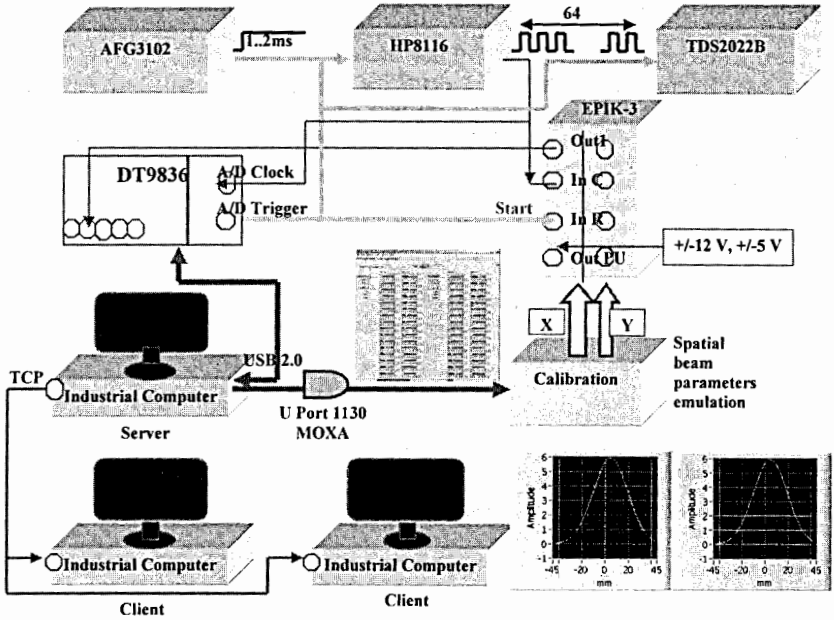


Fig. 3. The block-scheme of testing the client-server program to calculate spatial beam parameters

**The server program for calculation of spatial beam parameters**

The LV-LINK software from Data Translation is necessary to create the server for DT9836 in LabVIEW. LV-LINK is the program interface for LabView (from National Instruments) based on .NET Framework architecture and NI-DAQmx instrument driver. LV-LINK consists of a class library of polymorphic virtual instruments (.VI).

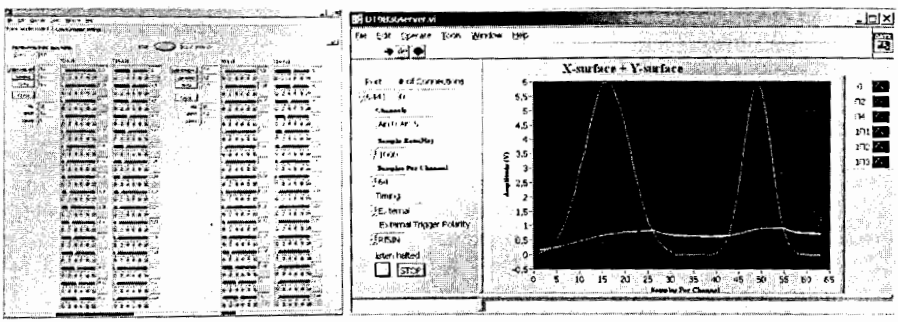


Fig. 4. The calibration program for the self-made module imitating the beam profile with a pre-setting distribution, and the server program for calculation of spatial beam parameters

The server must measure 5 input analogue signals from profile-meters on the external digital trigger and send them to the clients. The operator can select Channel Numbers (Ain0:Ain5), Sample Rate (1000 Hz), Sample per Channel (64), Timing (External), External Trigger Polarity (RISIN).

When the server begins to work, it creates a TCP socket, introduces measuring regime parameters to the DT9836 and begins to measure and draw the signals in 5 selected channels (32 points from X-wires plus 32 points from Y-wires in every channel for one profile-meter). This occurs in the first program loop. The second loop waits for the requirements from the client connections and puts their numbers into the queue for the maintenance. When the requirements are received then the data copies are sent for every active connection in the first program loop.

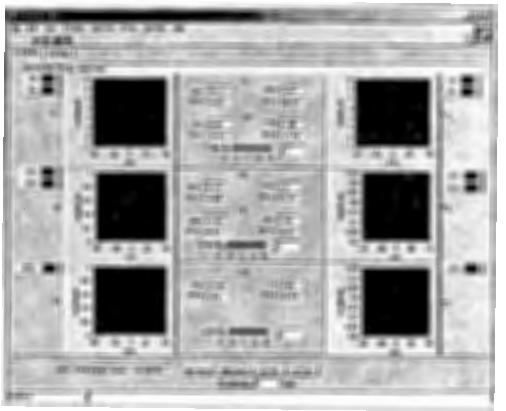

Fig. 5. The client program for calculation of spatial beam parameters

**The client program for calculation of spatial beam parameters**

When the client program starts working, it connects to the server and begins to operate. It is intended to calculate the spatial beam parameters from 5 profile-meters, located in two cross-sections of the injection channel and in three cross-sections of the first linear space. The client is able to Start/Pause on-line watching the measurement results and to Save/Save as/File Open (off-line) the interesting information.

The beam spatial characteristics such as the profile figure, the centers-of-mass-position Xo (Yo) and the sizes - the double middle square deviations Wx (Wy) - are measured, calculated and presented on the screen for every control surface (X and Y) and for every profile-meter. The figures with vertical stretching are grouped by two profile-meters, every profile-meter is reflected with its own colour. The 'instantaneous' values of profiles from the injection process are averaged by means of the least squares method on the basis of the wire coordinates, the distance among them (3..4 mm) and the signals from them. The subtraction of the ADC pedestals measured in electronics control session is carried out when the 'integral' profile is under formation.

**The client-server program to register the dynamic injection processes**

The second client-server program organizes the multi-client simultaneous operation of 3 modules from National Instruments:

- The multifunctional DAQ oscilloscope module NI PCI-5105 records the injection dynamic processes (8 registering channels, 12-Bit resolution, 60 MHz sampling rate, 16 MB RAM). Its analogue signal scope is from 10 mV to some volts. It starts on the injection synchronization signal and sends the data when the buffer is full.
- Two 5½-digit multi-meters NI PCI-4060 measure the IM current and the IP voltage every 250ms on the program start.

**The client-server program to register beam dynamics: NI DMM server**

Two 5½-digit multi-meters NI PCI-4060 measure the IM current and the IP voltage every 250ms on the program start. The operator can set Measurement Type (DC Volts), Range (25V), Resolution Digits (5½, 4½), Auto Zero (Off), Trigger Source (Immediate). When the server starts working, it creates a TCP socket, introduces measurement regime parameters to the both NI PCI-4060 and begins to measure and draw the both signals. This occurs in the first program loop. The second loop waits for the requirements from the client connections and puts their numbers into the queue for the maintenance. When the requirements are received then the data copies are sent for every active connection in the first program loop.

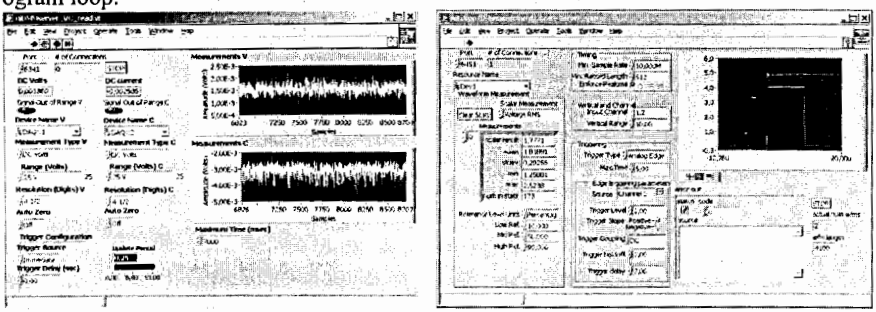

Fig. 6. NI DMM server and NI Scope Server to register beam dynamics

**The client-server program to register beam dynamics: NI Scope Server**

The oscilloscope module NI PCI-5105 records the injection dynamic processes (8 registering channels, 12-Bit resolution, 60 MHz sampling rate, 16 MB RAM). The operator can set Min Sample Rate (10,000M), Min Record Length (512), Input Channel (1, 2), Range (10), Triggering (Analog Edge, Digital Edge). When the server starts working, it creates a TCP socket, introduces measurement regime parameters to the NI PCI-5105 and begins to measure and draw the signals in the selected channels. This occurs in the first program loop. The second loop waits for the requirements from the client connections and puts their numbers into the queue for the maintenance. If the requirements are received then the data copies are sent for every active connection in the first program loop.

**The client program to register beam dynamics**

When the client starts working, it connects the NI DMM server and NI Scope server and begins to operate with the servers. It is intended to register the absolute values of the inflector magnet (IM) current and the inflector plate (IP) voltage every 250 ms, and to draw the registration of the injection dynamic processes in 8 channels (the injected beam current, the circulation of the beam in the accelerator cavity, and so on) in every Nuclotron cycle.

The client is able to Start/Pause on-line watching the measurement results and to Save/Save as/File Open (off-line) the interesting information. It reads out and saves the actual number of waveforms (<=8) with their attributes from NI Scope server (working with NI PCI-5105) in .HWS files (NI-HWS - Hierarchical Waveform Storage) and from NI DMM server (working with two NI PCI-4060) in binary files with the same names.

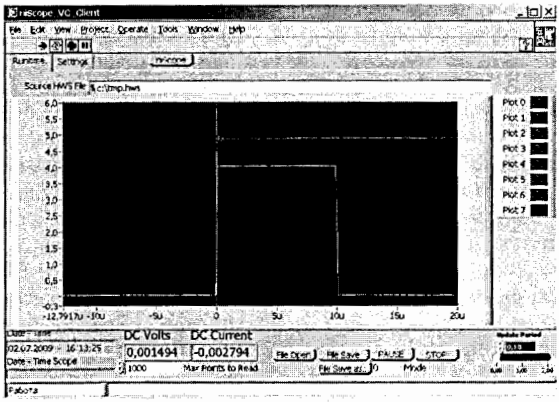


Fig. 7. The client program to register beam dynamics

## Conclusion

In the results of work and testing we have managed to develop the data acquisition subsystem for parameters of beam injection into the Nuclotron. The basic principles of this DAQ subsystem are as follows:

- Distributed client–server architecture based on asynchronous sockets using TCP transport protocol.
- Multilevel multichannel control - control task is divided vertically (between the client, server and module, if it is active) and horizontally (between independent low level subsystems, modules and channels).
- Each low level subsystem has an autonomous server capable to support independent action of the diverse subsystem equipment with different speed, and provides information enough for the operator.
- Object oriented programming - runtime creation and activation/inactivation of modules and channels objects.
- Parameters saving and system runtime configuring are performed from (.INI) files or the remote or local database (in future), depending on the system complexity

We have used these principles to develop a data acquisition subsystem for parameters of beam injection for the JINR NUCLOTRON-M (Veksler and Baldin Laboratory of High Energy Physics). The autumn session on the Nuclotron will be the main severe test for the subsystem.

## References


[1] A.N. Balandikov et al. , R10-89-365, Dubna, 1989.
[2] N.I. Lebedev et al., Dubna, E10, 11-2006, 45, p. 181.
[3] http://www.ni.com/
[4] http://zone.ni.com/devzone/
[5] http://www.datatranslation.eu/

# RDIG (Russian Data Intensive Grid) e-Infrastructure: status and plans

V.A. Ilyin[1], V.V. Korenkov[2], A.A. Soldatov[3]
[1] *SINP MSU, Moscow, Russia*
[2] *Joint Institute for Nuclear Research, Dubna, Russia*
[3] *RRC "Kurchatov Institute", Russia*

To create a global infrastructure for a scientific sphere, the EGEE project (*Enabling Grids for E-sciencE)* [1] was organized in the 2003 year. The aim of the EGEE project is to gather all current national, regional and application grid developments into a common grid-infrastructure for the scientific research [2]. The EGEE project infrastructure provides a 24-hour access to the most high-performance computing resources independently of their geographical location. The world-wide distributed scientific communities can use this infrastructure in the accordance with the common access rules. As the EGEE project started in fact at the WLCG global infrastructure, the EGEE and WLCG projects infrastructures are considered as a common WLCG/EGEE infrastructure. The monitoring map of the WLCG/EGEE infrastructure can be seen at the Fig. 1.

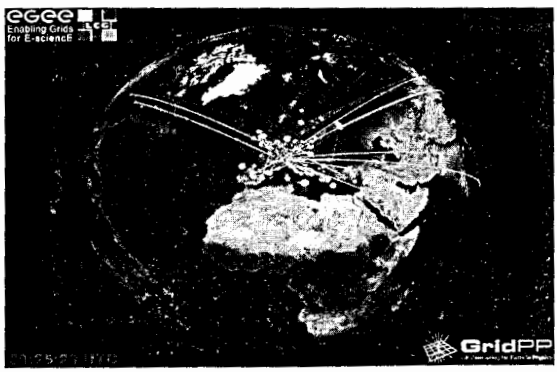


Fig. 1. 3D-monitoring map of the WLCG/EGEE infrastructure

By the 2009 year, the constructed global WLCG/EGEE grid-infrastructure comprised 350 sites in 55 countries with 120,000 CPUs and data storage of 26 PetaBytes. More than 15,000 users from 300 Virtual Organizations (VO) submit about 370,000 jobs daily.

The JINR and seven Russian institutes (IHEP - Institute of High Energy Physics, Protvino; IMPB RAS - Institute of Mathematical Problems in Biology , Pushchino; ITEP - Institute of Theoretical and Experimental Physics, Moscow; JINR - Joint Institute for Nuclear Research, Dubna; KIAM RAS - Keldysh Institute of Applied Mathematics, Moscow; PNPI-Petersburg Nuclear Physics Institute, Gatchina; RRC KI - Russian Research Center "Kurchatov Institute", Moscow; SINP-MSU - Skobeltsyn Institute of Nuclear Physics, Moscow) participating in the EGEE project founded the Russian Data Intensive Grid consortium (RDIG) as a national EGEE federation for to accomplish commonly the works in the EGEE project, develop the EGEE infrastructure in Russia and involve another Russian

organizations from different scientific, educational and industry spheres (see the RDIG consortium map at the Fig. 2).

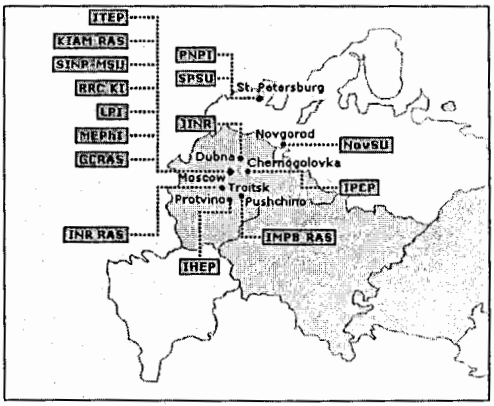


Fig. 2. Russian Data Intensive Grid Consortium

Now the RDIG EGEE is a part of the global LCG/EGEE infrastructure and its infrastructure comprises 15 Resource Centers with more 7000 CPU and more 1850 TeraBytes of disk storage.

The main directions in RDIG e-infrastructure development and maintenance are:

- support of basic grid-services;
- support of Regional Operations Center (ROC);
- support of Resource Centers (RC) in Russia;
- RDIG Certification Authority (CA);
- RDIG monitoring and accounting;
- participation in integration, testing, certification of grid-software;
- support of users, Virtual Organization (VO) and application;
- user & administrator training and education;
- dissemination, outreach and communication grid activities.

The RDIG institutes participating in the LHC experiments (ALICE, ATLAS, CMS and LHCb) take part in the WLCG (Worldwide LHC Computing) project [3-5] in the following directions of the activities:

- creation and support of the WLCG infrastructure;
- testing of gLite middleware;
- WLCG monitoring [6-8];
- development and support of the Monte-Carlo generator repository and data base (MCDB) [9-11].

The special server has been installed and supported to provide the RDIG EGEE/LCG sites monitoring based on the MonALISA system [12]. The RDIG monitoring and accounting system is accessible at the *http://rocmon.jinr.ru:8080*.

Current status of RDIG institutes connectivity to external links is: 20 Gbps for JINR, 10Gbps for RRC KI and SINP MSU, 1 Gbps for ITEP, IHEP, INR RAS, LPI , PNPI, MEPhI and SPbSU and 100 Mbps for BINP (Novosibirsk). The international connectivity for RDIG is the following: GEANT2 PoP - 2.5 Gbps (plans for 10 Gbps) and dedicated connectivity to CERN 1 Gbps (Moscow-Amsterdam-CERN).

Users support and training (courses, lectures, trainings, publication of user guides in Russian) stimulates user's active usage of the WLCG/EGEE resources. During last years the induction courses, courses for application developers and site administrators training have been conducted at PNPI, RRC KI, JINR, IHEP, ITEP and SINP MSU [13]. More than 200 physicists from different LHC centers in Russia have got a special training how to submit their analysis jobs and access physical data in the WLCG/EGEE environment. It is especially important just before the LHC start-up. During the 2009 year, a distributed training infrastructure (grid-sites in Dubna, Protvino, Tashkent and Sofia) has been constructed and is in a practical use [14].

The RDIG-EGEE informational web-portal has been developed and is supported (*http://www.egee-rdig.ru*). All EGEE Info sheets and EGEE news releases are regularly translated into Russian and they are accessible at the RDIG-EGEE portal. The 3rd International conference "Distributed computing and Grid technologies in science and education" (GRID-2008) was organized and hosted by JINR (*http://grid2008.jinr.ru*). GRID-2008 gathered more than 200 scientists from Russia and CIS countries. It is the only conference in Russia especially devoted to the modern grid technologies.

As a result of RDIG participation in the WLCG and EGEE project, the RDIG sites are fully integrated into the worldwide WLCG/EGEE grid infrastructure providing all the necessary resources, services and software. RDIG supports about twenty virtual organizations providing computing and data storage resources for scientists from various fields (physics, biology, chemistry, biomedicine, geophysics and some others). We shall continue our activities at the EGI project [15] starting this year. A special attention will be paid to the grid deployment of new applications from the fields of nanotechnology, industry, medicine and engineering.

The results of RDIG activities in the WLCG and EGEE projects have been presented at the international conferences ("Distributed Computing and GRID-technologies in Science and Education", Dubna, Russia, 2008; ACAT 2008, Eriche, Italy, 2008; CHEP'2009, Prague, Czech, 2009; NEC'2009, Varna, Bulgaria, 2009) and the EGEE conferences (Istanbul, 2008; Barcelona, 2009) [16].

**References**


[1] http://www.eu-egee.org

[2] A.P. Demichev, V.A. Ilyin, A.P. Kryukov, Introduction into grid technologies, preprint SINP MSU, 2007-11/832, 2007, 87 p. (in Russian), http://dbserv.sinp.msu.ru:8080/sinp/files/pp-832.pdf

[3] LHC Computing Grid Technical Design Report, LCG-TDR-00, CERN-LHC-2005-024, CERN, Geneva, 20 June 2005, available at http://cern.ch/lcg/tdr

[4] http://lcg.web.cern.ch/LCG/

[5] A.P. Demichev, V.A. Ilyin, A.P. Kryukov, L.V. Shamardin, Grid technologies on Large Hadron Collider's computing services, Informatization in science and education, 4, 2009, Moscow, p.158 (in Russian), http://www.informika.ru/about/informatization_pub/publications/2009/4/4-p158.pdf
[6] http://dashboard.cern.ch
[7] J. Andreeva et al., Dashboard for the LHC experiments, J. Phys. Conf. Ser., 119:062008, 2008.
[8] V.V. Korenkov, A.V. Uzhinski, Monitoring system of data transfer service (FTS) in the WLCG/EGEE projects (in Russian), JINR Communications, Dubna, 2008, P11-2008-80.
[9] http://mcdb.cern.ch
[10] S. Belov et al., LCG MCDB - a Knowledgebase of Monte Carlo Simulated Events, Computer Physics Communications, Volume 178, Issue 3, 2008, p. 222.
[11] S. Belov et al., LCG MCDB and HepML, next step to unified interfaces of Monte-Carlo simulation, PoS ACAT08:115, 2008.
[12] S.D. Belov, I.M. Tkachev, RDIG monitoring and accounting, in Proc.of the 2nd Int. Conference "Distributed Computing and Grid-technologies in Science and Education", Dubna, 2006, pp. 26-27.
[13] http://rus.egee-rdig.ru/rdig/user.php
[14] V. Korenkov, N. Kutovski, Infrastructure for education of grid-technologies, Opensystems, 11, 2009, pp. 48-51 (in Russian).
[15] http://web.eu-egi.eu/
[16] http://grid2008.jinr.ru;http://acat2008.cern.ch; http://nec2000.jinr.ru/program.as; http://www.particle.cz/conferences/chep2009

# Development of the remote control of the spectrometers on the IBR-2M reactor

A.S. Kirilov, S.M. Murashkevich, R.J. Okulov, T.B. Petukhova
*Joint Institute for Nuclear Research, Dubna, Russia*

The presentation is devoted to current development of the WebSonix [1,2]. The system allows one to reflect the actual statuses of some IBR-2M instruments, view measurements protocols, display acquired spectra, and control the course of the experiment on the spectrometers under control of the Sonix+ software package (Windows XP operational system). The system does not depend on the spectrometer characteristics and permits simple changes of their structure and easy adaptation to special features of spectrometric data representation.

The Sonix+ system is equipped with two additional *s_spectra* modules for reading current spectra and recording them into the file and *c_channel* modules for executing commands of the web server.

The GNU/Linux Debian operational system and Apache 2 web-server are installed on the website computer.

Websonix+ has been written with PHP 5. Also for our project we use AJAX. For documentation we use wiki engine called (dokuwiki). Mantis bug-tracking system was used.

## Intro

Remote instrument control is one of the urgent points of agenda. In our previous work we discussed various approaches to organize this control as well as first steps in WebSonix+ system design. First try was in 2008 as research for possibilities of modern web-platform. We choose PHP for our research because it very similar to C. Also HTML 4 was used for static pages.

## Initial requirements to WebSonix+ system

The system must satisfy the requirements of all potential users. It should accept not only supervision but control over the instrument as well. It should be expandable, i.e., the inclusion of new spectrometers should not require many and big changes in the system. Besides, the architecture of the system must be independent of specific features of spectrometers. Its architecture should avoid individual pages as mush as possible, but must be easily adapted to particular spectrometer. The system must be stable and protected from unauthorized access.

## First version

The system allowed one to reflect the actual statuses of some IBR-2M instruments, view measurements protocols, display acquired spectra, and control the course of the experiment on the spectrometers under control of the Sonix+ software package (Windows XP operational system). The system does not depend on the spectrometer characteristics and permits simple changes of their structure and easy adaptation to special features of spectrometer data representation. Because IBR2 was stopped we are testing WebSonix+ in real mode very similar to real operation.

We allocated a server which linked with control computers where Sonix+ installed. WebSonix+ is a set of PHP scripts which connect with Sonix+ software through sockets. Also the Sonix+ system is equipped with two additional module: *s_spectra* for reading current spectra and recording them as a the file and *c_channel* for executing commands of the web server.

Here is list of these pages: *Database, Log Viewer, Spectra Viewer, Control panel.*

Database page is used to show database itself in plain-mode and user have the possibility to select the most important parameters (favorites)into a separate trace list for example measurement time, motors axises, current user script and so on. User can add or delete these parameters in a simple way.

Log Viewer page is used to show log files measurement which contain the detailed information about the progress of the experiment.

Spectra Viewer
Visualization of current spectra from all detectors is also important. The generation of a picture on the control computer is much more reasonable than transfer of initial data massive, especially high-resolution position-sensitive detectors.

Testing shows us the following issues:

1. Slow page generation,
2. Big amount of traffic transmission,
3. No chance for intensive interactivity.

All these items are derived directly from the features of the PHP interpreter itself.

**Improved version**

In the second version we have tried to overcome disadvantages mentioned above. Also we reported on the work done within the laboratory and offered to our users to make their proposals and wishes, which was done.

Here is what we had got:

- Make error checking for script before execution,
- Show the current executable command,
- Show the current status as a colored line (red line — error, green line — all works fine).

Also we have updated our pages design, improve some parts of our system for better user experience like: "Favorite parameters", simpler navigation in log viewer and logarithmic spectra. We have been significantly improved the control panel for spectrometers.

Second, we need to separate some PHP code into different files for simple using AJAX technology, which consists of JavaScript and XML.

**What is AJAX**

Ajax stands for *Asynchronous Javascript And XML*. Is a group of interrelated web development techniques used on the client-side to create interactive web applications or rich Internet applications. With Ajax, web applications can retrieve data from the server asynchronously in the background without interfering with the display and behavior of the existing page. The use of Ajax has led to an increase in interactive animation on web pages and better quality of Web services due to the asynchronous mode. Data is retrieved using the XMLHttpRequest object. Despite the name, the use of JavaScript and XML is not actually required, nor do the requests need to be asynchronous.

Example:

```
ajax('getlog.php?curlog='+document.getElementById('log_2').value,'GET',null,getanswerlog
);
```

*ajax* is a function where the first parameter is a *curllog* that is passed to *getlog.php* script second is a type of transmission, *null* is a browser parameter and *getanswerlog* is a link to processor function.

**Second release features**

Now, when you click, for example, the database update button, then redrawn only field containing the text concludes the database, but not all of the window as before.

This approach significantly reduces traffic and increases the responsiveness of the interface. As I said before we reworked "Favorite parameters" for easier to use.

Also, at the time to develop version 2.0, we decided to radically improve the documentation to make it easier to change by other users.

**Documentation**

For documentation we use wiki engine called (dokuwiki). This engine was created specially for documentation. All data are stored in plain-text files. It has simple administrator panel which allows to add users, closed pages and give permissions to one to add pages by themselves.

**Some screenshots**

On the database viewer page Fig.1 you can add needed parameters from the drop-down list "Choose path" and update it's values with "Update database" button.

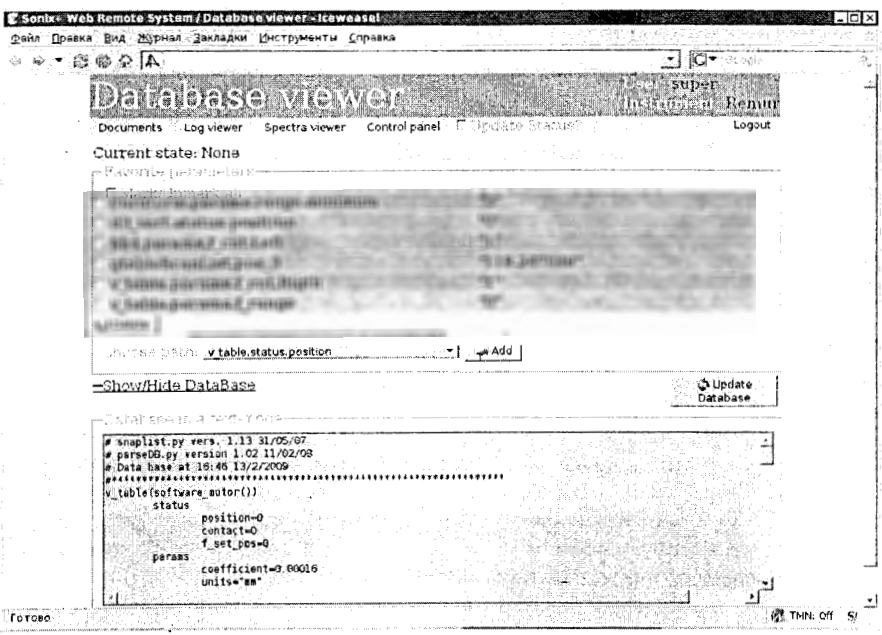


Fig. 1. Database viewer

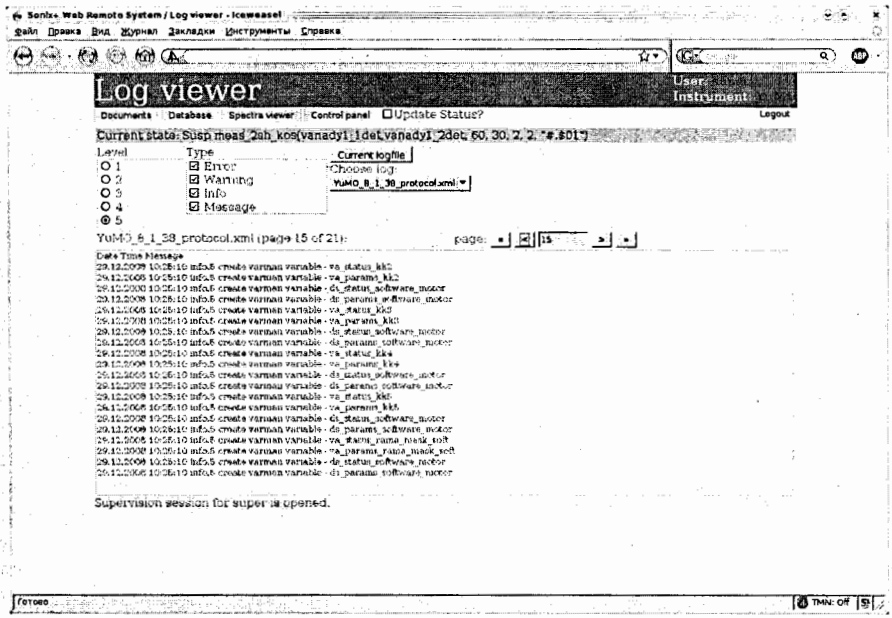


Fig. 2. Log viewer page

On the log viewer page Fig. 2 you can see current log, or some previous. Also you can choose type and level of messages. You can move forward or backward in pages.

## Conclusion

The server is allocated. The project is good enough for testing by users. We also hope that the project would benefit to all.

## References

[1] A.S. Kirilov, S.M. Murashkevich, R.J. Okulov, T.B. Petukhova, Remote instrument supervising and control for the IBR-2M reactor, [Nec2007].

[2] Instruments and Experimental Techniques, 2009, Vol. 52, No. 1, pp. 37–42.

# Using Chroot environments for large scale computing as an alternative to virtualization

V. Kolosov
*ITEP, Moscow, Russia*

Though virtualization technology can deliver many benefits for large scale computing including hardware abstraction, management simplification and operational flexibility the cost for these benefits is degradation in performance relative to the characteristics of the host system especially for I/O operations. Chroot environments allow to use the obsolete systems above the modern host system without performance losses. Recent linux kernel modifications can provide the transparent access to the host resources from the guest environments and dramatically simplify the management.

## 1. Introduction

During last years the technologies of hardware virtualization demonstrate a wide spread in various areas from implementations in BIOS [1] to using VM as a backend to cloud computing platform. "Overall, IDC views virtual machines as a foundational technology to the dynamic IT," said John Humphreys, program director with IDC's Enterprise Platform Group. "Virtualization, which decouples the application from the underlying hardware, allows the customer to create service oriented infrastructure whereby they can begin to manage services and employ policy-based automation to manage and deliver the underlying infrastructure" [2].

Virtual systems can be completely independent of physical resources, so IT groups will have more time to devote to solutions that increase business value. Virtualization also makes it possible to avoid application incompatibility problems by running them in separate, isolated virtual servers on the same physical server. Two years ago we studied the possibility to use the virtualization technology in large scale computing environments [3]. Though it was demonstrated that the hardware virtualization could provide some benefits for the such tasks we should pay for them by the degradation in a performance especially in I/O operations. The significant overhead in memory usage due to the requirements of the virtual machine itself should be taken into account as well.

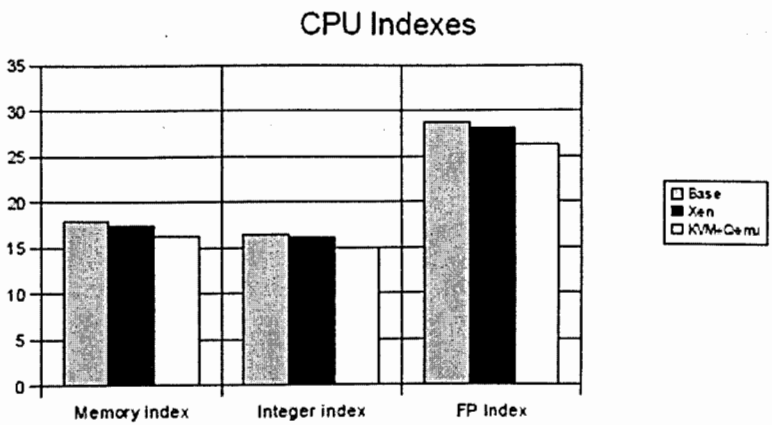

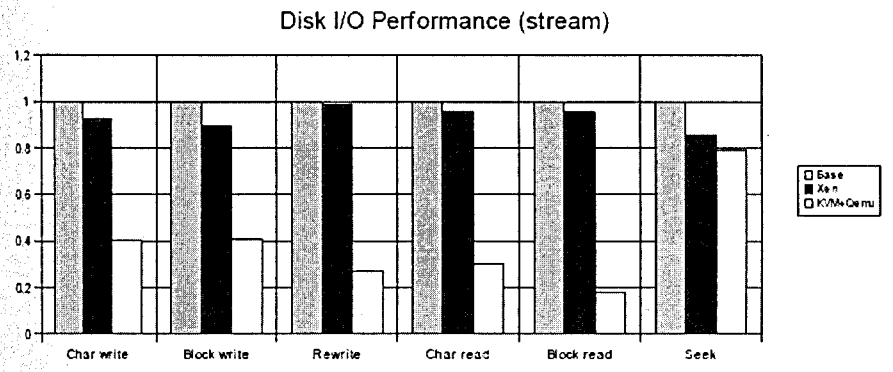


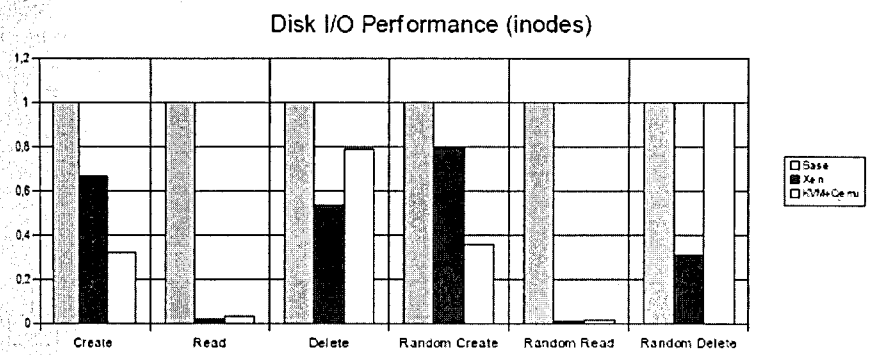


Seeking for other ways to provide the necessary level for the service virtualization we recalled the old UNIX approach which used the chroot based environments.

## 2. Using the Chroot Environments for Large Scale Computing

The key feature of the chroot environments is based on the property of any UNIX (Linux) process to use any directory in the mounted filesystem as the root directory for itself and for its children. Chroot environments traditionally are used to improve the security for various services, for example DNS, FTP, mail-servers (postfix) etc by placing them into chroot jail[4]. For the aims of the large scale computing the chroot environments can be used to create and host a separate virtualized copy of the operating system.

Historically the mechanism of chroot has serious limitations in access to the network filesystems and local filesystems which are mounted outside of the chroot jail. The such behavior can be a problem when you will try to maintain several chroot environments for one host. The problem increases in much degree because the modern Linux distributions use the pseudofilesystems `/dev`, `/dev/pts`, `/proc` and `/sys` which can not be simply copied to another location.

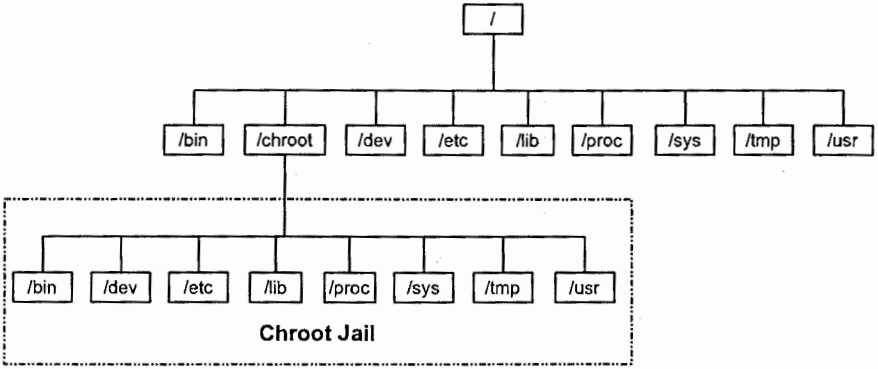


Fortunately the up-to-date Linux kernels have the mechanism for the binding of the filesystem objects which can simplify the chroot system building dramatically. For user it works in a way similar to directory hardlinking in UFS, though this implementation of the binding is independent to filesystem type and can act across different filesystems. This mechanism allows to mount filesystems or even its parts to several different places. For purposes of the virtualized chroot environments this means that processes in jail can have an access to kernel specific parts of filesystem.

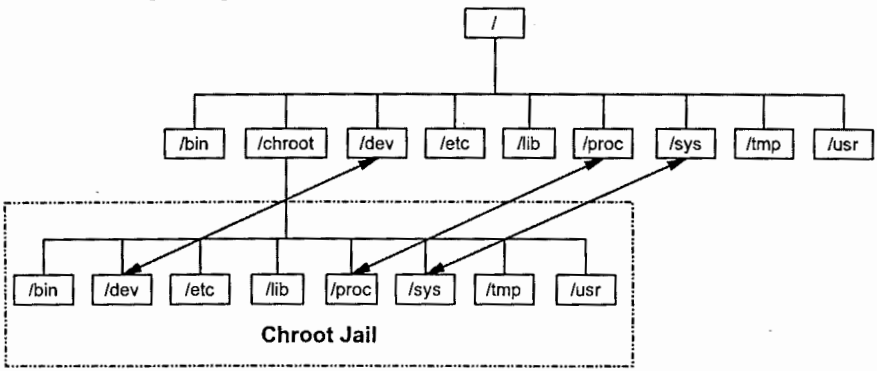


The preparation of the chroot environment is rather simple. You should choose the place for chroot jail, for example `/chroot` and prepare some parts its internal structure:

```
mkdir /chroot/dev
mkdir /chroot/proc
mkdir /chroot/sys

mount --rbind /dev /chroot/dev
mount --rbind /proc /chroot/proc
mount --rbind /sys /chroot/sys
```

If `automount` provide an access to the network filesystems its configuration (/etc/auto.master) can be modified to add mount points inside chroot jail:

```
...
/net -hosts
/chroot/net -hosts
...
```

When all necessary preparation were done the operating system can be install. There are at least two ways for this procedure: if you already have an installation somewhere else it can be simply copied to new place (by means of `rsync` for example), or it can be installed from scratch. For RedHat based distributions yum from host system can be used:

```
yum -y -c /chroot/etc/yum.conf --installroot=/chroot install
```

When the OS will be installed the necessary daemons should be configured. They require the following prefix to standard `init.d` scripts:

```
chroot /chroot script [options]
```

## 3. Conclusions

It was shown that it is possible to use chroot environments as an alternative to the virtual machine.

- The such environments have some advantages over VM approaches especially in performance which is equal to the performance of the host system.
- The memory overhead for chroot is much smaller then one for VM.
- Chroot approach does not require additional software because it is a part of any UNIX (Linux) system.
- The maintenance costs for chroot is similar to the costs for VM support.
- Some benefits which exist for VM like possibility to migrate virtual machine between hosts are hardly possible for chroot.
- Chroot environments allow to run guest systems of the same flavor as the host has that is Linux over Linux.

## Acknowledgments

I would like to thank my colleagues from ITEP in particular E. Lublev and M. Sokolov for support of this work and E. Korolko for many fruitful discussions. I am grateful to G. Davidenko for the equipment which were provided for testbed and for participation in the tests.

## References

[1] Phoenix Technologies Ltd, Phoenix Technologies Announces Major Milestone - First Customers for Phoenix FailSafe(TM) and HyperCore(TM), 2008, http://investor.phoenix.com/releasedetail.cfm?ReleaseID=319319

[2] IDC Report, Worldwide Virtual Machine Software 2005 Vendor Shares, 2006.

[3] V. Kolosov, Using Virtualization Techniques For Large Scale Computing, 2007.

[4] E.D. Larson, How to Secure Services by Running in a Chrooted Environment, 2001, http://www.sun.com/bigadmin/content/developer/howtos/chrooted.html

```
...
/net -hosts
/chroot/net -hosts
...
```

When all necessary preparation were done the operating system can be install. There are at least two ways for this procedure: if you already have an installation somewhere else it can be simply copied to new place (by means of `rsync` for example), or it can be installed from scratch. For RedHat based distributions yum from host system can be used:

```
yum -y -c /chroot/etc/yum.conf --installroot=/chroot install
```

When the OS will be installed the necessary daemons should be configured. They require the following prefix to standard `init.d` scripts:

```
chroot /chroot script [options]
```

### 3. Conclusions

It was shown that it is possible to use chroot environments as an alternative to the virtual machine.

- The such environments have some advantages over VM approaches especially in performance which is equal to the performance of the host system.
- The memory overhead for chroot is much smaller then one for VM.
- Chroot approach does not require additional software because it is a part of any UNIX (Linux) system.
- The maintenance costs for chroot is similar to the costs for VM support.
- Some benefits which exist for VM like possibility to migrate virtual machine between hosts are hardly possible for chroot.
- Chroot environments allow to run guest systems of the same flavor as the host has that is Linux over Linux.

### Acknowledgments

I would like to thank my colleagues from ITEP in particular E. Lublev and M. Sokolov for support of this work and E. Korolko for many fruitful discussions. I am grateful to G. Davidenko for the equipment which were provided for testbed and for participation in the tests.

### References

[1] Phoenix Technologies Ltd, Phoenix Technologies Announces Major Milestone - First Customers for Phoenix FailSafe(TM) and HyperCore(TM), 2008, http://investor.phoenix.com/releasedetail.cfm?ReleaseID=319319

[2] IDC Report, Worldwide Virtual Machine Software 2005 Vendor Shares, 2006.

[3] V. Kolosov, Using Virtualization Techniques For Large Scale Computing, 2007.

[4] E.D. Larson, How to Secure Services by Running in a Chrooted Environment, 2001, http://www.sun.com/bigadmin/content/developer/howtos/chrooted.html

# Development of the System remote access real time (SRART) at JINR for monitoring and quality assessment of data from the ATLAS LHC experiment (Concept and architecture of prototype SRART at JINR)*

V.M. Kotov, N.A. Rusakovich
*Joint Institute for Nuclear Research, Dubna, Russia*

## 1. Introduction

Current status of large international collaborations in high-energy physics has become essential that collaborators can participate in the operations of experimental facilities from remote locations.

To address the needs for remote operations and remote participation in the ATLAS experiment, in this report would be suggest the problem of the construction in System remote access real time (SRART) at JINR Dubna. The purpose of the SRART is to help scientists and engineers JINR working on ATLAS contribute their expertise to commissioning and operations activities at CERN.

SRART at JINR has primary functions:

- provide a physical location with access to information that is available in control rooms and the operations centers inside Point1 at CERN;
- communications conduit between CERN and members of the ATLAS community located in Russia and also allows experts from the participating institutes to be involved in the quality assessment of the data during their processing.

In accordance with the ATLAS object model, the distributed data quality assessment should be included in all processing levels from on-line data taking to off-line processing by Tier 0-2.

## 2. ATLAS Remote Operations

For the start of ATLAS operations all control of the ATLAS detector, trigger and data acquisition systems as well as real-time online monitoring of data quality will be the responsibility of a shift crew working in the ATLAS CONTROL ROOM (ACR).

### 2.1. Monitoring system

The remote operations centers, such as SRART at JINR, are expected to have the same kinds of monitoring as the ATLAS Point1. The ATLAS operations model is expected to evolve, and in the future more and more of the responsibilities may be transferred from the control room to the remote centers.

There are many monitoring applications that are being developed by ATLAS collaborators for use in the control room and remote sites [1]:

* This work was supported by Russian Federal Agency of Science and Innovation Contract № 02.514.11.4083.

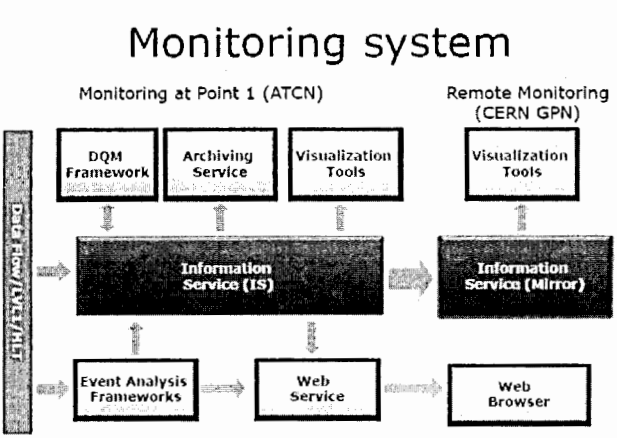


Fig. 1. Monitoring system

Table 1. Remote Monitoring

| RM User | RM Technology |
|---|---|
| **Public community** | Web Monitoring |
| **Remote experts** | Secure log-in by request of Run Coordinator |
| **Remote shifters** | Copy monitoring data in quasi real-time mode from P1 to dedicated machines in CERN GPN |

### 2.2. Web Monitoring Interface

Periodically generates HTML pages with monitoring information 2 plug-ins are currently used at P1:

- Run Status,
- Data Quality.

Referenced from the ATLAS Operation page:
• http://pcatdwww.cern.ch/atlas-point1/operation.php
New Trigger plug-in is being developed now.

### 2.3. Remote Monitoring Approach

TDAQ Monitoring Working Group proposed and evaluated the following solution :
• Run mirroring copy of the basic configuration and monitoring infrastructure services **outside** P1;
• Remote users can run the standard ATLAS Control Room X-sessions on some dedicated machines **outside** P1.

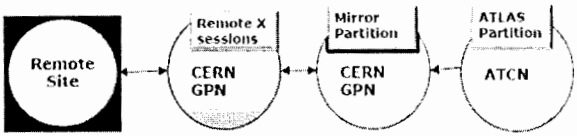


Fig. 2. Remote Monitoring

### 2.4. Remote Monitoring: Commissioning Status

- 5 PCs have been commissioned for remote monitoring:
  - 8 cores Intel Xeon 2.5 GHz, 16 GB
  - 3 PCs for running mirror partition infrastructure
  - 2 PCs for hosting remote sessions
- On the public remote monitoring nodes:
  - Monitoring SW is taken from AFS
  - Monitoring configurations are periodically copied from P1 (once per hour)
  - The main desktop is the same as at P1
  - All the monitoring displays are the same as being used at P1.
- System has been used by LAr during their slice week in April .

### 2.5. Concept for the SRART JINR

The concept, architecture, and service composition of the system under development comply with the architecture of the TDAQ ATLAS CERN and this system is a fragment of the entire ATLAS information infrastructure.

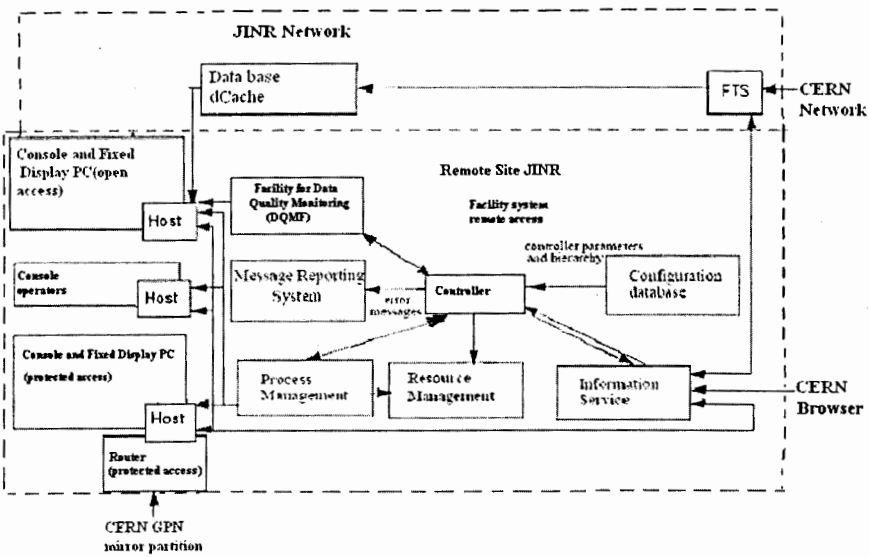


Fig. 3. SRART@JINR

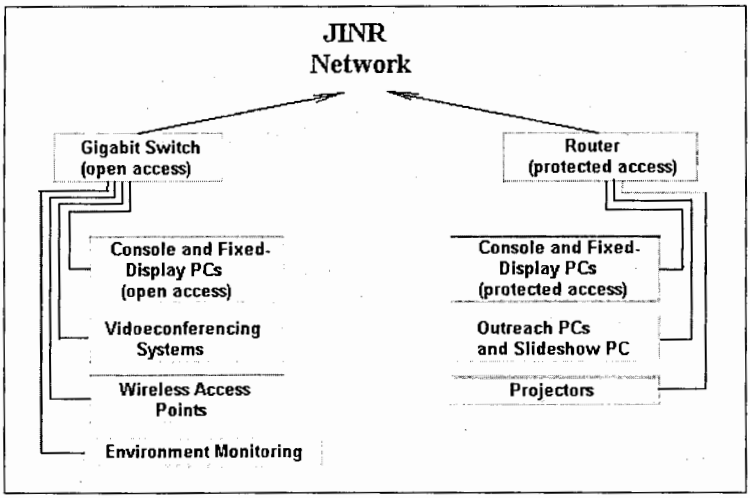


Fig. 4. SRART@JINR Computing Network

Development of the prototype SRART at JINR is based on the experience gained by JINR programmers, physicists, and engineers in design of the data acquisition and processing system TDAQ ATLAS at CERN, which allows a side range of TDAQ services to be used for the development of the SRART at JINR and its integration in the general distributed system for handling ATLAS LHC data.

Modern high-energy physics investigations require handling of large amounts of information beginning with on-line data collection and processing for input compression and further in off-line analysis using the GRID technology.

Management of multilevel geographically distributed computation systems which underlie the information GRID infrastructure of high-energy physics experiments requires a distributed control system with a developed system for quality monitoring and assessment of the data from experiments at CERN's LHC. Being geographically distributed, the processing system should allow remote access to the status of the detectors used in an experiment and remote data quality monitoring for all institutes participating in an experiment.

The SRART had always planned for remote data quality monitoring of ATLAS during operations and SRART was interested in providing support for training people before going to CERN, and remote participation in ATLAS studies. We saw an opportunity for JINR scientists and engineers to work together with detector experts to contribute their combined expertise to ATLAS commissioning.

### 2.6. Features

With construction the SRART @ JINR coming into complete operation the following features have been realized:

- CERN-style consoles with 6 workstations,
- Videoconferencing installed for one console which can be expanded to two,
- Webcams for remote viewing of SRART @ JINR,
- Secure network for console PCs,

- HD viewing of SRART @ JINR,
- Screen Snapshot Service (SSS) as like at Fermilab. [2] This work is in progress to develop the necessary tools.

SSS is an approach to provide a snapshot of a graphical interface to remote users. A "snapshot" is defined as an image copy of a graphical user interface at particular instance in time such as a DAQ system buffer display of operator control program. It is a view-only image, so there is no danger of accidental user input. SSS was initially implemented for desktops, but could be targeted to application GUIs.

**Console**

- Machine hardware:
  - Linux box (specs equivalent to those of ACR machine):
    - Dual or quad core CPU, 2.4 GHz,
    - 4 GB RAM and 2 x 500 GB HD,
    - Gigabit Ethernet card.
  - Displays:
    - 1 x 30" monitor @ 2560x1600,
    - 6 x 19" monitor @ 1280x1024.
- Software:
    - CERN Scientific Linux 4,
    - NX Client,
    - Athena,
    - ROOT,
    - Any monitoring software.

## 3. Acknowledgements

Successful completion of this work would not have been possible without the dedicated efforts of the following:

the JINR: A. Kazakov, M. Mineev, I. Aleksandrov, E. Aleksandrov, A. Yakovlev, V. Korenkov, S. Atanasov,

the TDAQ ATLAS Group at CERN: L. Mapelli, S. Kolos, G. Lehman-Miotto, I. Soloviev, M. Caprini.

## References

[1] S. Kolos, Monitoring, TDAQ Workshop, Rome, Italy, May 2009.

[2] Eric Gottschalk, Remote Operation for LHC and CMS, Fermilab, RTO7, May 2007.

# Data acquisition and control system for the DELTA spectrometer

V.A. Krasnov, S.N. Kuznetsov, A.N. Livanov, A.V. Pilyar
*Joint Institute for Nuclear Research, Dubna, Russia*

The data acquisition and control system for the DELTA spectrometer is described. The DELTA spectrometer has been designed and completely assembled to study neutral meson production with polarized nucleons at LHEP, JINR. It includes a 300 - channel γ, e-Cherenkov spectrometer for neutral meson detection consisting of two blocks each based on 150 lead-glass prisms, a 14 - layer scintillation telescope of detectors based on opto-fiber plates and used to identify charged particles and measure their energy by the method of repeated ionization loss measurements. The pulses from the photomultipliers pass through the analogue sum units to the charge-to-digital converters to measure and correct the high voltages by the multichannel digital-to-analog converters. The data readout is performed by the intelligent controller and the collected data are transmitted through the Ethernet to the main computer.

The system is used in the experiment on the JINR LHEP Nuclotron.

## Introduction

The study of neutral particles production processes is one of the most perspective directions in hadron-nuclei physics and nuclei-nuclei collisions. To study such processes, a dual arm spectrometer of neutral mesons DELTA was built at LHEP JINR, Dubna. The general layout of the detectors of the DELTA spectrometer is shown in Fig.1. It has the following main units: a 300- channel γ, e-Cherenkov spectrometer consisting of two blocks (CH1 and CH2) each based on 150 lead-glass prisms, a 14 - layer scintillation telescope of detectors (ST) based on opto-fiber plates that used to identify charged particles and measure their energy by the method of repeated ionization loss measurements [1].

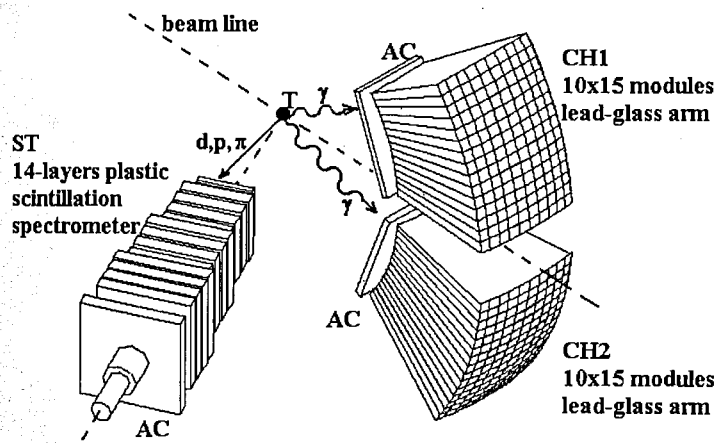


Fig. 1. A schematic view of the DELTA detector positions. T- polarized proton target; CH1, CH2 - two arms of the Cherenkov lead-glass spectrometer; ST - 14-layer opto-fiber scintillation telescope for multi-ΔE measurements of charged particles; AC - anticoincidence detectors.

The glass Cherenkov spectrometer is designed to determine energies and exit angles of $\pi^0$ and $\eta$ mesons coming from the used target. The applied experimental method consists in detecting two energetic photons, emitted in the decay of a neutral meson (the 99% probability for $\pi^0$ and 39% for $\eta$), in the array of Cherenkov lead-glass detectors.

The shoulders of the spectrometer (CH1 and CH2) are set in two blocks. The blocks are built from glass prisms (Fig. 2) made of F8-type Pb-glass with PbO 45% additions. The new principle is that the glass prisms are designed as cut pyramids with a cross dimension less than the Molier radius (400mm high, that is 12rad long). This allows one to improve the effective solid angle of the spectrometer by using "the center of gravity" method for avalanche coordinate measurements but without $\gamma$-converters and coordinate-sensitive detectors. The number of cells in each block is 150 (10 - along the horizontal line and 15 - the vertical line). Each cell is viewed by the photomultiplier tube of FEU-84 type.

Two anticoincidence (AC) detectors of plastic scintillators are located in front of the Cherenkov spectrometer units. The ACs serve to separate $\gamma$-quanta from the background charged particles. The thickness of each AC is 20mm, and ACs are observed through the two photomultipliers (FEU-84).

The scintillation telescope used to measure charge particles is represented as a 14-layer scintillation spectrometer assembled from plastic scintillator slices with optical conducting wires to collect light from the slices to the photomultipliers. To define the type and energy of the charged particles taken from the target, we used the technique of the repeated ionization loss measurements in the scintillator slices and also performed the time-of-flight measurements at a distance of 1m.

The Cherenkov spectrometer and scintillation telescope are fixed in some mechanical system that allows one to move and adjust their positions (Fig. 3). This system is mounted directly in the beam area and makes the detectors rotate in the vertical and horizontal planes independently. A remote computer controls the movements of the detectors.

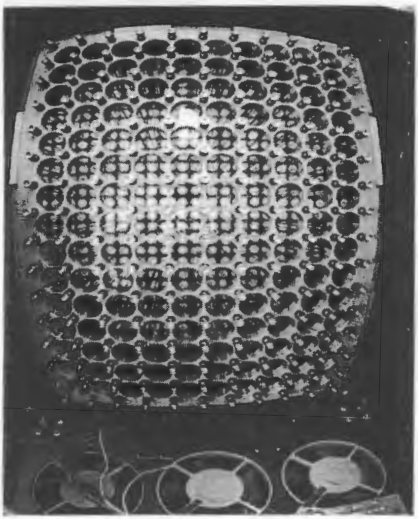

Fig.2. A rear side of the DELTA spectrometer's Cherenkov arm with removed photomultipliers.

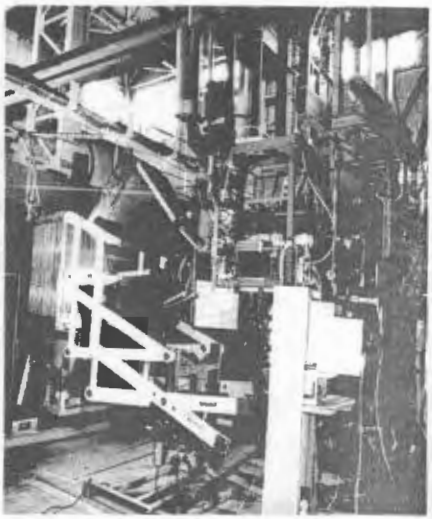

Fig 3. A mechanical system for the Cherenkov spectrometer and scintillation telescope.

**Data acquisition and control system**

The data acquisition is organized by the intelligent CAMAC crate controller (type CCPC5) containing compatible PC. The whole data acquisition system consists of 4 CAMAC crates organized in a branch. Crate 0 is controlled by the CCPC5 and contains a branch driver. The other crates are connected via standard branch crate controllers of type A1.

The pulses from PMTs are led to the analogue sum units Σ (Fig. 4). They are organized in such a way that allows one to work with whole rows or columns summed or with pulses from individual PMT on the output. The control program switches the sum units to the desired mode. The pulses from the sum units are transmitted to QDCs. The 16QDC-398 contains sixteen complete 10-bit integrating ADCs (QDCs) designed for DELTA spectrometer [3].

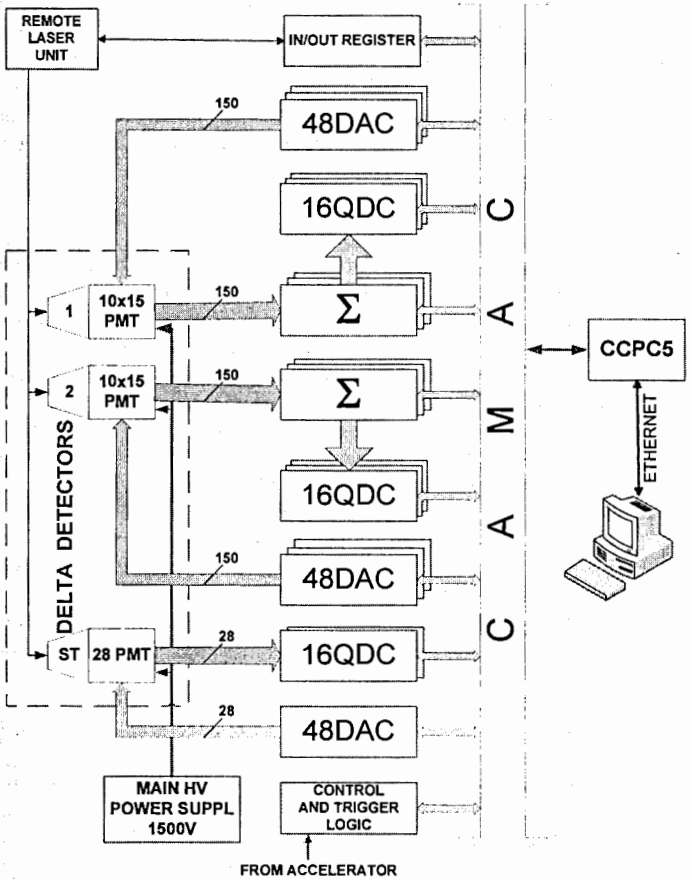


Fig. 4. The block diagram of the DELTA data acquisition and control system

The work of the data acquisition system is triggered by the signals from the accelerator or the laser [4]. These signals are worked out in logical modules [2], strobe the QDC conversion and are given to the CAMAC input-output register.

The data from QDCs are used to measure and compute the correction codes for DACs which set up the high voltages. The goal is to set the optimal working mode for photomultipliers and ensure the maximum stability during the experiments.

Every PMT has its own regulated high voltage provided in the following way. There is a common stabilized high voltage source of 1500V for all the detectors. The individual voltage source for every PMT is supplied in series with the common source. This 300 individual voltage sources are controlled by the program via DACs. They set up the individual correction voltages for every PMT in 255V region. The 48-channel Digital-to-Analog Converter module (48DAC-348) was designed for this purpose [3].

There are some main functionally complete subsystems on the low level. The modules of each subsystem are located in each CAMAC crate. The first crate controls the step motors to set the Cherenkov spectrometer shoulders CH1 and CH2, and to rotate the scintillating telescope ST. In the second crate the modules control the start counters and the start trigger can be programmed. In the third crate the electronics reads out some data from the scintillation telescope and stabilizes the electronic multiplier gain. The last crate reads out the data from Cherenkov spectrometer and stabilizes its modes.

**The DELTA software**

The DELTA software is another essential part of the DAQ system. The data acquisition software uses Client-Server architecture with sockets (TCP/IP protocol) for communication in LAN. It manipulates remotely the hardware units (controls high voltage sources, multiplier coefficients, changes the trigger logic parameters, switches on/off the laser). It also reads out the status from hardware units (the strobe signal from the accelerator, code tables), the data of the hardware parameters (mean value tables, high voltage dividers tables, QDC basement voltage) and also reads out the data from QDCs and TDCs.

The DELTA software consists of four parts – Server, Client, Setup and Viewer. The first one is DELTA Server which carries out CAMAC data readout, runs control and processes the data from the DELTA Client. The Server is placed in CAMAC CCPC5 controller and works as CAMAC Ethernet Crate Controller. The Client performs control functions, storage data and visualization of the histograms. Up to 10 histograms can be viewed simultaneously by the Client.

The Setup program helps to change various parameters of the DELTA DAQ: the station and channel numbers for control; the trigger logic parameters; the high voltages of the detectors; the operation mode of the sum units.

The graphical part of the program Viewer is fully user-friendly. There is an exhaustive number of various settings for limits, the color and display modes of selected tables and graphs.

The program is written in C++ under the Borland C++ Builder using the windows, network and other components. Some CAMAC functions are realized in the assembler.

The program is fully network oriented. It can operate in three modes: autonomous, client and server mode. All server functions can be remotely controlled over the network using TCP/IP protocol from the client.

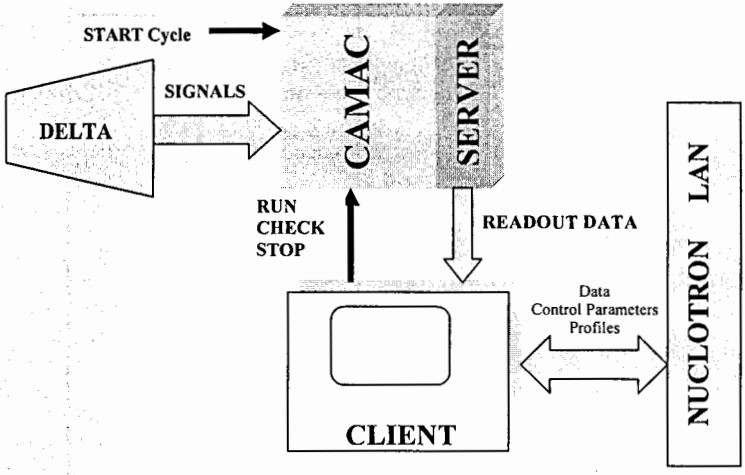


Fig. 5. The software structure

**Experimental results**

Some results have been obtained with the neutron beam and the carbon and polyethylene targets. About 2100 coincidence events appropriate to the $np \rightarrow \pi^0$ reaction on the polyethylene target and about 700 events on the hydrogen target, were recorded using the neutron beam with the intensity of $5 \times 10^6$ neutrons per burst and the energy of 1.5GeV. The level of random coincidence noise was at the order of 30% of hydrogen. As an example, Fig. 6 shows the spectrum of the restored values of the particle mass decaying info two gamma-quanta, with two gamma-quanta coincidences in the blocks of the spectrometer. The average restored value (for $2\gamma$ events) of the mass equals to 130MeV at the instrument resolution of 15%.

**Conclusions**

- The Data Acquisition and Control system for the DELTA spectrometer has been constructed and successfully tested on the beams of the LHEP JINR accelerator complex.
- The numerous electronic modules have been designed and produced.
- The special software package has been developed for the DELTA spectrometer.
- The experimental tests have demonstrated that the high-performance instrument has been manufactured now. Its capabilities open up numerous areas of research for abnormal pion production on the Nuclotron internal target.

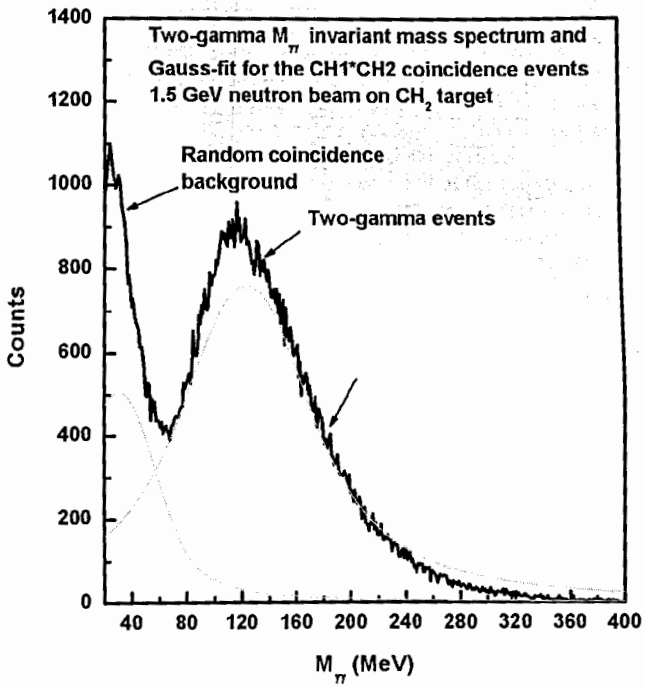


Fig. 6. Reconstructed invariant mass spectrum of pions. The solid lines are the result of the right peak Gaussian fitting.


## Acknowledgements

The authors are very grateful to: P. Maniakov, A. Malakhov, V. Ladygin, S. Reznikov, S. Gudkov, S. Bazilev, V. Slepnev (Laboratory of High Energy Physics, JINR, Dubna); S. Gmuca, J. Kliman, V. Matoushek, M. Morkhach, I. Turzo (Institute of Physics, SAS, Bratislava); A. Kurepin (Institute for Nuclear Research, RAS, Moscow) for their contributions to the reported activity.


## References


[1] Yu.S. Anisimov, S.N. Bazilev, J. Kliman et al., "Delta" Setup on the LHE Polarized Proton Target, Status and Preliminary Results. Proceedings of the International Workshop "Relativistic Nuclear Physics: from Hundreds MeV to TeV", Slovak Republic, Stara Lesna, June 14-18, 1999, JINR, Д1, 2-99-294, pp. 57-65.

[2] A.M. Ermolaev, P.K. Maniakov, A.V. Pilyar et al., Electronics of LHE JINR for detectors of experimental setups. Proceedings of the XVIII International symposium NEC'2001, Varna, JINR.

[3] A.V. Pilyar, Analog electronics for measurement and control. Proceedings of the XXI International Symposium NEC'2007, Varna, JINR, E10, 11-2008-37, pp. 382-389.

[4] A.I. Malakhov, Yu.S. Anisimov, S. Gmuca et al., The laser-based calibration system of DELTA spectrometer. NIM in Physics Research, Section A, Vol. 566, 2006, pp. 413-421.

# Electronic devices for constructing a multichannel data acquisition system

A. Kuznetsov, E. Kuznetsov
*"Tekhinvest" Ltd., Moscow, Russia*

## Introduction

Electronic registration systems at the Flerov Laboratory of Nuclear Reactions (FLNR) are mainly of the CAMAC standard. There is a great experience in developing amplitude spectrometer that is why the Laboratory uses its own devices. A number of such single-channel blocks was developed about 20 years ago. These blocks are still used in systems with small number of channels. In 80-90$^{th}$, according to an increase in the number of detectors in experimental setups, 4- and 8- channel amplifiers, multiplexer of spectrometric signals, blocks for multichannel measures, multichannel generators for testing of spectrometric section were developed. These devices are also used in modern spectrometers.

Since 2006 "Tekhinvest" together with the FLNR specialists have been developing devices for spectrometers with a number of channels of several tens, and in the future of several hundreds.

The basic principles of our developments are as follows:

- All devices are in the CAMAC standard or compatible ;
- Number of channels is multiple of 16;
- Devices are compatible with each other by the type of connector, signal levels, signal names;
- Similar functional nodes are made from the same components and can be used in different blocks.

## 1. Preamplifiers

Preamplifiers are made using a classical charge-sensitive circuit with low noise FET at the input. We have only changed feedback RC-circuit parameters for the registration of different type particles with low capacity semiconductor detectors (SCD).

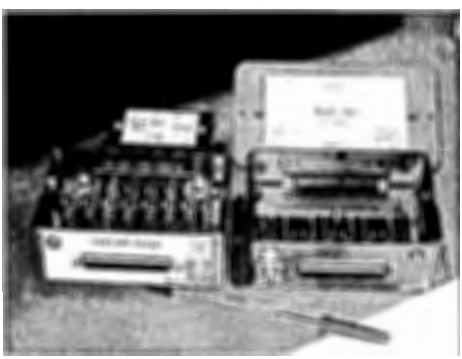

Fig. 1. 16- and 32-channel preamplifiers

For the fission fragments it is 56M and 2.2pf, for alpha particles – 100M and 1pf.

The 16- and 32- channel preamplifiers are made in the same way (Fig. 1).

Linear amplifiers with the gain of 10 in a steel case are additionally used in the case of x- and gamma- radiation registration.

The preamplifier' own noise is less than 4.5kev with a SCD and cable capacity of less than 50pf.

**2. Spectrometric amplifier (SA)**

SAs are also made with a number of channels multiple of 16.

To increase the signal dynamic range we produce our last SA version with 2 separate outputs, each one with its own base line restorer named "alpha" and "fission". The amplitude of these output signals is different precisely by a factor of 11.

The 16-channel SAs in a standard CAMAC (Fig. 2) are used in the "VASSILISSA" separator.

The 32-channel SAs in the original 19'' box have been used in the setup "COMPACT" of Munich Technical University in experiments on super heavy element synthesis since 2005 (Fig.3).

The 4-channel SA (Fig. 4) specially developed for obtaining the high energy resolution with an extra intensity of incoming signals in x- and gamma-spectrometers.

Special features of all our SAs:

"P – Z "( Pole –Zero cancellation), INL < 0.05% , TKG < 50 ppm / deg.C.

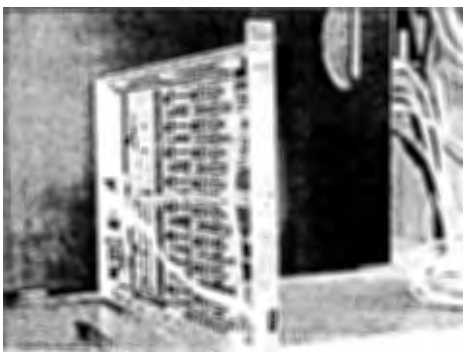

Fig. 2.

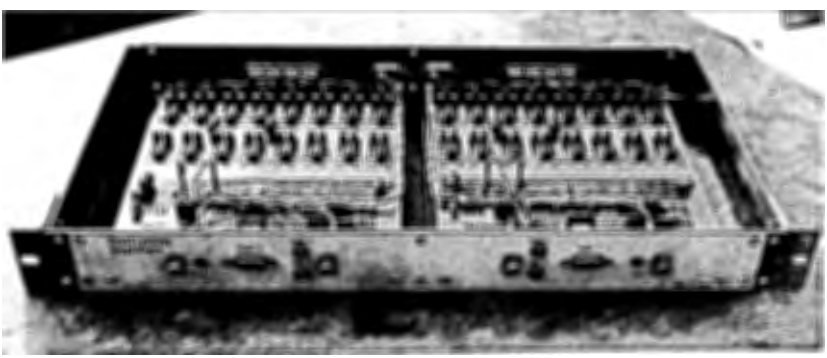

Fig. 3.

Fig. 4.

### 3. Analog to Digital converters

Fig. 5.

In all ADCs the input is connected with the linear gate and peak detector inputs. These are made as a single universal circuit for different applications and mounted on the "motherboard" as the second level.

A number of devices were made in a similar way:

- universal single-channel 12-bit ADC with memory for the channel number,
- 2-channel ADC for alpha particles and fission fragments (resolution of 13 and 12 bits, correspondingly),
- 3-channel ADC for a multichannel position-sensitive SCD (Fig. 5).

In the course of the registration of signals from a 16-channel SA with analog multiplexers the channel number code is memorized in a special ADC register using a clock from the "STROBE" SA signal.

Such ADCs were used for the registration of signals from 64-channels in two ranges (alpha and fission) in the set-ups "COMPACT" (TUM) and "VASSILISSA" (FLNR). A pulse coming moment was also registered with a 32-bit timer-counter with a resolution of 1us (Fig. 6). These modules can be joined in series using UNIBUS to increase the number of channels. There is a special synchronization system in these ADCs, in which all timers can be controlled by one ''master" whereas any of these ADCs or other devices can be set as "master".

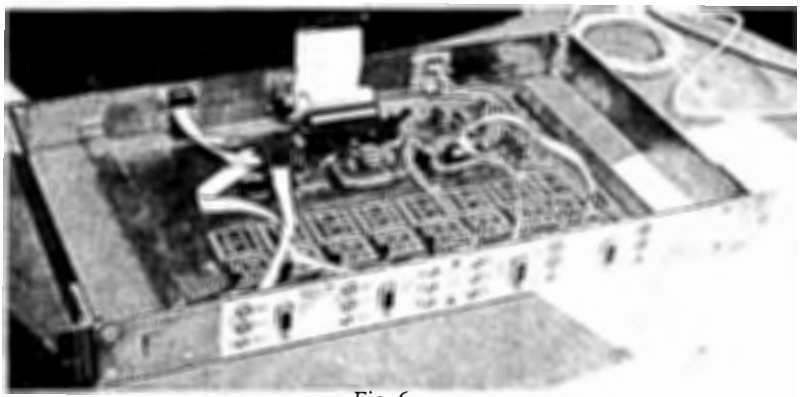

Fig. 6.

**4. Programmable analog-digital devices**

There is a need in a big number of analog and digital modules for additional signal processing in every data acquisition system. These modules are as follows: discriminators, level converters; counters, memory blocks, triggers, pulse shapers, logic and arithmetic device. A variety of combinations of such devices made it necessary to have a large set of special modules.

To decrease the amount of equipment in an experiment a special device was developed which can realize all the functions mentioned above. The device is the so-called "16-channel discriminator", (Fig. 7) based on ALTERA programmable logic devices (PLD). It has: 16 inputs(50 Ohm) of low level discriminators with polarity switch and manual threshold adjustment; 2 timers with regulators on the front panel; 4 timers with inside regulators; quartz generator; 2 programmable TTL inputs/outputs; 8 programmable TTL or NIM inputs/outputs

Input or output level selection is made via jumpers on the device printed circuit board (PCB). The module was used in the experiments at the "MASHA" setup (FLNR) as: 16-input discriminator for micro channel plate signals; signal counter on each input with different exposition time, adjustable by CAMAC; "master" in synchronization system of the whole setup; "gate" pulse former for coincidence schemes; event trigger.

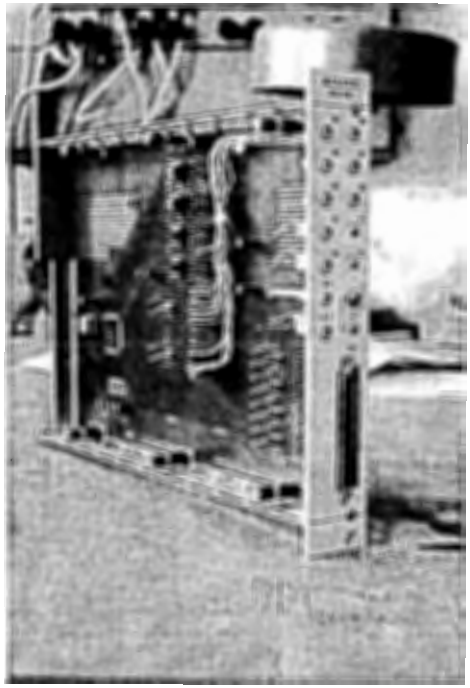

Fig. 7.

**5. Analog-digital signal simulator**

To provide fast checking of the spectrometry channel the Analog-digital signal simulator was developed (Fig. 8).

The device has 16 analog outputs with the signal shape similar to that of the preamplifier signal. Signal Amplitude and frequency are set in by software using internal DAC or by external voltage and synchronization sources.

There are 40 programmable logic input/output ports for the synchronization with external devices, digital circuit and signal imitation.

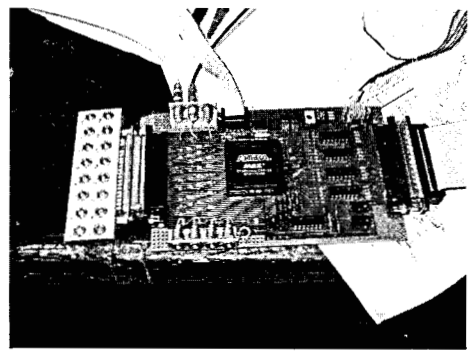

Fig. 8.

**Conclusion**

The developed devices have provided the construction of the data acquisition systems with a whole amount of channels of about several hundreds within a short time.

Below one can see some applications of our developments.

**Acknowledgements**

The authors express their thanks to V. Gorshkov, Yu. Semenov for the cooperation in workings out and their realizations and also to A. Artukh, P. Bondarenko, A. Yeremin, E. Kozulin, Yu., Sobolev, A. Fomichev, A. Yakushev for the constant attention and comprehensive support of works.

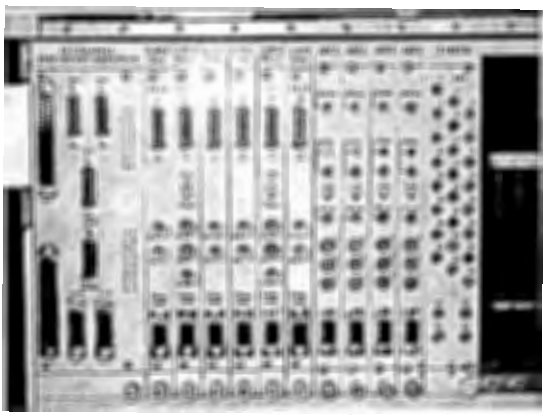

Fig. 9. GFS (FLNR JINR) – single crate

Fig. 10. GFS (FLNR JINR) – registration electronics

Fig. 11. FLNR JINR. Data acquisition system for the "VASSILISSA"

**References**


[1] А.Н. Кузнецов, В.Г. Субботин, Спектрометрические усилители, X Intern. Symp. on Nucl. Electronics, zfk-433, v.1, p. 148-151, Dresden, 1981.

[2] А.Н.Кузнецов, В.Г.Субботин, Аналого-цифровой преобразователь,ОИЯИ, 13-83-67, Дубна, 1983.

[3] А.Н.Кузнецов, Комплекс спектрометрической аппаратуры многодетекторных экспериментальных установок для регистрации продуктов ядерных реакций, ОИЯИ, Р13, 15-86-413, Дубна, 1986.

[4] А.Н. Кузнецов, Е.А. Кузнецов, Программно-управляемый многоканальный генератор для тестирования амплитудных трактов в системах регистрации экспериментальных установок, ОИЯИ, Р13-99-246, Дубна, 1999.

[5] A. G. Popeko et. al., Physics of Atomic Nuclei, 2006, Vol. 69, No. 7, pp. 1183-1187.

[6] J. Dvorak et. al., Phys. Rev. Lett. 97, 242501 (2006).

# Multichannel program-controlled spectrometer blocks in a standard CAMAC

A. Kuznetsov, E. Kuznetsov
*"Tekhinvest" Ltd., Moscow, Russia*

## Introduction

16-channel blocks of spectrometer amplifiers (SA) and analogue-digital converters (ADC) have been developed for spectrometers of nuclear reaction products in which various multichannel semiconductor detectors (SCD) are used for the registration of particles. A general problem in electronic registration systems of such spectrometers is the preservation of high-energy resolution at an increased intensity of signals in analogue paths. For several units of the spectrometer channels the problem has been solved by means of multipurpose single-channel SAs and ADCs, similar to those developed earlier/1, 2/. In modern registration systems with a number of channels of tens and hundreds it is necessary to reduce considerably the volume and cost of the equipment for one channel. The purpose of the work was an attempt by minimal technical resources to provide flexibility of inclusion of multichannel blocks in the general system of registration and to keep good spectrometer characteristics.

## I. 16-channel ADC (ADC16)

In the definition of the ADC16 functions we considered the following circumstances:

1. In many modern multichannel systems the events registration speed is basically defined by the necessity of data read-out from a large number of ADCs, among which the number of ADCs with the helpful information is small. For example, in a CAMAC system the reading of "empty" ADCs (or finding-out by the controller of the fact that the ADC is "empty") requires no less than 1 us.
2. A typical way of registration of the spectrometer information in multichannel spectrometers is a preliminary selection of events using rather fast schemes and then the start of the "master trigger" similar to that, for example, presented in /3/. The "Master trigger" generates a strobe to ADCs and controls a further data read-out process in the controller. Thus only part of fronts of the spectrometer impulses (see fig. 1) appear in the strobe, therefore it is desirable to have means of suppression of such signals in most ADCs.
3. Except spectrometer impulses it is often necessary to measure some slowly varying parametres of the system (practically direct current signals). It is useful to provide such a possibility using the existing ADCs in the presence of "free" inputs.

In connection with the above-mentioned, developed ADCs have possibilities of programmed on/off options of the signal selection on each channel individually and also adjustments of parameters of selection manually or by a program. We will consider these possibilities in more detail.

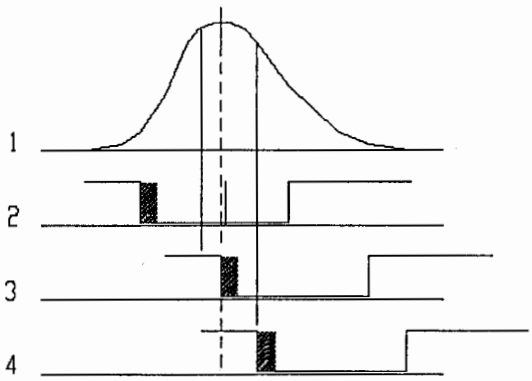


Fig.1. Selection of signals by the relative arrangement of the spectrometer impulse, a signal of the peak detector and the strobe.

1. Spectrometer impulse, the "true" top is shown by the dashed line.
2. The "true" strobe. The shaded area is the « mistrust interval», the heavy line is the signal of the peak detector.
3. The registration forbiddance occurs when a signal of the peak detector gets to «a mistrust interval».
4. The registration forbiddance occurs when a signal of the peak detector arrives after the strobe.

Programmed control by a common threshold of the low level discriminators (LLD) and a common threshold of the high level discriminators (HLD); programmed on/off options of LLD and HLD. LLD is switched off at the registration of signals of a direct current, for example, at the calibration of SA channels by the initial shift. When HLD is switched off and the signal exceeds the linear range of the ADC input, an output code of amplitude will contain all «1».

1. Hand control duration of the "suspicion" interval (0.2 – 2 us, the internal resistor). The fact that the signal of a spectrometer impulse top (from the peak detector in each ADC channel) appears in a short time of "suspicion" interval right after the beginnings of a strobe of "master trigger", means that the strobe appear at the back front of the spectrometer impulse (see fig. 1) and its registration can be forbidden.
2. The programmed on/off option of selecting the signals in presence of the top of an impulse inside the "master trigger" strobe.

ADCs block-scheme is presented in fig. 2. Each channel has a linear gate (LG) at the input, the peak detector (PKD) and a pair of discriminators (LLD, HLD). Control signals for LGs, thresholds to the LLDs and HLDs are common, whereas the output signals LLDs, HLDs and PKDs are individual. LGs and PKDs are made as separate modules located on "the second floor» over the "mother" board CAMAC.

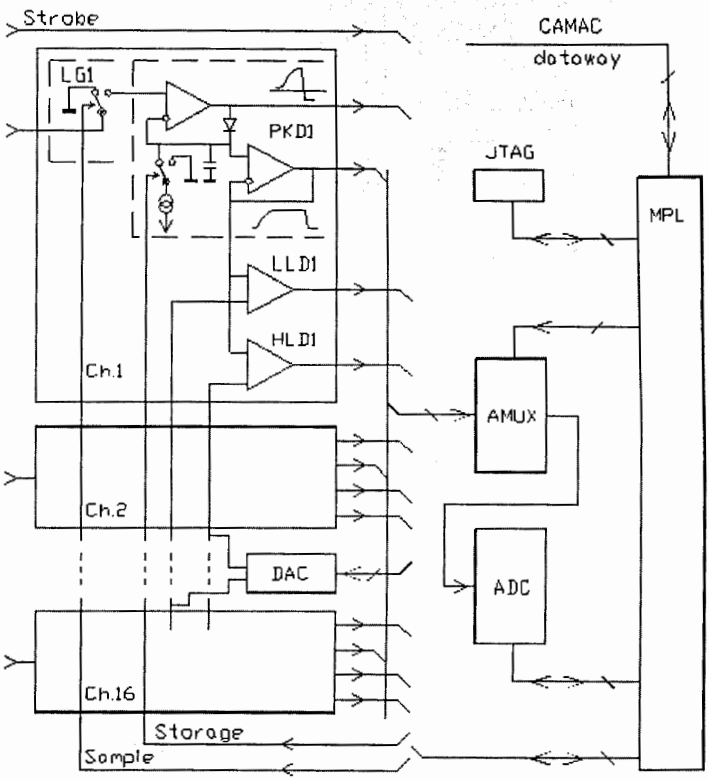


Fig.2. ADCs block-scheme

Comparators LLD, HLD and the elements common for the block are also located on the "mother" board CAMAC:

- analogue multiplexer AMUX,
- integrated ADC,
- digital-to-analogue converters (DAC) for setting the thresholds to the LLD and HLD,
- microcircuit of programmed logic (MPL),
- converters of levels and sources of secondary power supplies (in fig. 2 they are not shown).

The ALTERA make MPL does all the necessary logic functions for the block which provide the following:

- accepts all individual signals to the LLD, HLD, PKD, a general strobe,
- forms general signals of SAMPLE and STORAGE for the management of the linear gates and peak detectors,
- during the strobe defines "worked" channels according to the chosen criteria of selection,

- organizes serial connection of analogue signals "worked" channels to ADC, cycles of analogue-digital conversion and records results in its own memory,
- executes CAMAC commands the list of which is given below.

**CAMAC commands**

N A(0) F(8) - checking LAM; the answer X, Q – if LAM exists.
N A(0) F(10) - checking and reset LAM; the answer X, Q – if LAM exist.
N A(0) F(24) – interdiction L; ответ X.
N A(0) F(26) – permission L; the answer X.
N A(0) F(16) W1...W8 – writing LLD; the answer X.
N A(1) F(16) W1...W8– writing HLD; the answer X.
N A(0...15) F(18) W1...W3 – reset of criteria of selection by sub addresses (channels); W1=1 – reset selection by LLD, W2=1 – reset selection by HLD, W3=1 – reset selection by the top of pulses; the answer X. The initial condition is W1=0, W2=1, W3=1, so only HLD selection is reset.

**Data reading**

Depending on the features of a concrete registration system and the type of applied CAMAC controller there are two ways of the data reading, the difference is set by the program of the MPL.

1. Reading ADC in two stages. At first, at the command F (0) A (0) the position code of "useful" channels (in the presence of such) is read. Then by commands F(2) A(...) the "useful" channels are read, the block answers thus with signals X, Q. If the sub address is not correct, the answer is only X.
2. Reading from ADC only by commands F(0) A(0) or F (2)A (0) is consecutive. The block gives out codes of "useful" channels (in the presence of such) and signals Q, X. The absence of Q means that "useful" channels are not present any longer. 12 low bits of the output code present the amplitude, 4 main bits – a code of channel number.

**Short specifications of the block**

Quantity of analogue inputs – 16.
Input resistance of analogue inputs – 4.7 kOhm.
Amplitude of the input signals – from 0 to 5V.
Polarity of the input signals – positive.
Number of bits ADC – 12.
Time of conversion for 1 channel – < 2.5 us.
INL (50mV – 5V) < 0.05%.
DNL (50mV – 5V) < 1 %.

**II. Spectrometer amplifier SA-16**

Spectrometer amplifier SA-16 contains 16 identical channels, each of which includes (see fig. 3):

- input differentiating chain , the switch of polarity and the chain of "pole – zero cancellation": ("p-z");
- cascade of the fast amplifier-shaper (FAS) and the low-level discriminator (LLD);
- two cascades of identical active integrators;
- cascade with a programmed gain amplifier (PGA);

- passive base line restorer (BLR);
- output buffer.

The shaping corresponds approximately to the filter of 7th order on passive RC-chains, time constant is fixed, in various copies of blocks it is 0.5, 1.0 or 1.5 us.

BLR is made according to the scheme of "the strengthened diode» /3/ and provides satisfactory stabilization of level at the output at the intensity of signal of the order of 5 kHz.

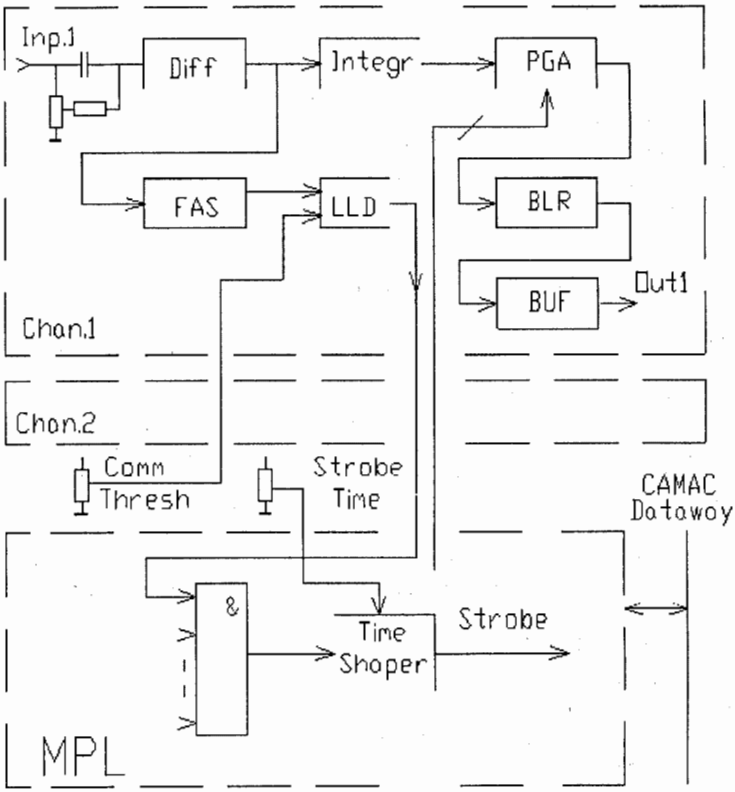


Fig. 3. SAs block-scheme

The minimal gains Kmin, as well as the shaper constant, are chosen in accordance with the application.

The current gain is defined by

$$K = Kmin \times 255/(255-N),$$

where N is the 8-bits binary code of gain.

At a shaper constant of 1 us it is recommended to limit a range of adjustment of gain by a range of about 80. It is connected with that fact that at the big gains at the expense of capacities of semi-conductor structure DAC (in a PGA) there is an additional shaping

(integration) of a signal. However, in spite of the fact that the justice of the above equality is broken, linearity of the gain remains in the entire range of the signals.

FAS and LLD form the fast channel of the shaper.

LLD signals are gathered by "OR" in a MPL, then their duration is formed and the signal arrives to logic out "strobe".

**Short specifications of the block**

Quantity of analogue inputs and outputs – 16,
Input resistance of analogue inputs – 1 kOhm,
Output resistance of analogue inputs – 50 Ohm,
Polarity of input signals – any,
Polarity of output signals – positive,
Amplitude of output signals – from 0 to 5V,
The threshold LLD levels are reduced to the input – from 1 to 100 mV,
INL (50mV – 5V) < 0.05%,
Temp. co. gain in a range of (10 – 40) C < 0.005%/C.

**The summary**

A short description and technical characteristics of 16-channel blocks of the spectrometer amplifier and the analogue-digital converter, used in multichannel spectrometers, has been presented. We tied to find an optimal compromise between functionality, volume and cost of the equipment.

The developed blocks have been used at the FLNR and other experimental laboratories since 2002 as a pair of basic spectrometer modules.

**Acknowledgements**

The authors express their thanks to P. Bondarenko, A. Yeremin, A. Fomichev, A. Yakushev for the constant attention and comprehensive support of works.

**References**

[1] А.Н. Кузнецов, В.Г. Субботин, Спектрометрические усилители, X Intern. Symp. on Nucl. Electronics, zfk-433, v.1, p. 148-151, Dresden, 1981.

[2] А.Н. Кузнецов, В.Г. Субботин, Аналого-цифровой преобразователь, ОИЯИ, 13-83-67, Дубна, 1983.

[3] R.L. Chase and L.R.. Poulo, A high precision dc restorers, IEEE Trans. on Nucl. Sci., 1967, v. NS-14, No.1, p. 83-88.

# Multichannel high voltage system for the detection system of LNS-project

**V.P. Ladygin, A.V. Pilyar, S.M. Piyadin, S.G. Reznikov**
*Joint Institute for Nuclear Research, Dubna, Russia*

A multichannel high voltage system with the individual control and monitoring of the voltage and current, is described. The system consists of 16-channels high voltage supplies from "Wenzel Electronik", 16-channels of the 12-bits Digital-to-Analog converters and 32-channels of the 14-bits Analog-to-Digital converters developed at LHEP JINR. The high voltage is adjusted and checked on-line by using a versatile DAQ system for middle range physics experiments MIDAS.

The system is used for the photomultipliers PMT-63 in the experiments at the Internal Target Station at the Nuclotron to study Light Nuclei Structure (LNS). The results on the time stability of the system during beam tests are presented.

## Introduction

The purpose of the Light Nuclei Structure experimental program is to obtain the information on the spin dependent parts of 2-nucleon and 3-nucleon forces from two processes: dp-elastic scattering in a wide energy range and dp- non-mesonic breakup with two protons detection at the energies from 300 to 500 MeV.

The dp breakup reaction will be investigated by using ΔE-E techniques for the detection of protons. Hardware bay consists of 4 vertical steel arcs. Each arc can move in the horizontal plane (see Fig.1). Two carriages for ΔE-E counters can take up a position on the arc. Counters move relatively to the arc in the vertical plane.

Fig. 1. The hardware bay for the detector with ΔE-E counters

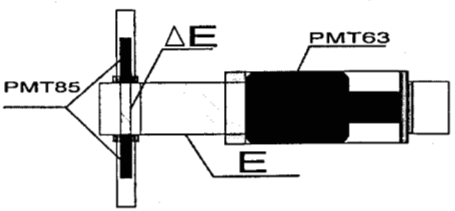


Fig. 2. The schematic view of the ΔE-E detector to study dp breakup reaction

Each detector consists of 2 scintillation counters (Fig.2): the first and the second ones are having scintillators 1 and 20cm long, respectively. The diameter of the E-counter scintillator is 10cm. The counter with a thick scintillator is used for the energy and time-of-flight measurements. The counter with a thin scintillator is used to reduce the number of

accidental events and ΔE measurements. The signal amplitudes for PMT-85, PMT-63 and correlation for the PMT-85 and PMT-63 obtained with cosmic muons, are shown in Fig.3.

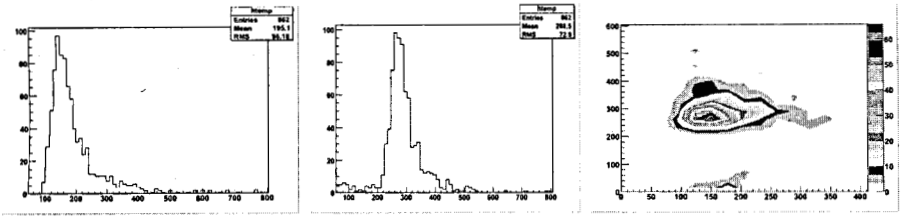

Fig. 3. The amplitudes for PMT-85 (a) and PMT-63 (b) and correlation of these amplitudes (c) obtained with cosmic muons

**Control system**

The PC performs independent setting and monitoring protocols for voltage and current. The high voltage (HV) is supplied by Wenzel N-1130 4-channel modules. The HV for each photomultiplier can be set to within 1.0V (stability of 0.5V) by the Digital-to-Analog converter 8DAC-12. The actual operating voltage and current can be monitored through the Analog-to-Digital converter module 8ADC-14 for each channel (Fig.4).

The **8DAC-12** [1] is a 8-channel 12-bit Digital-to-Analog converter, where the outputs are digitally programmable through CAMAC bus. The CAMAC W-lines are used to set a voltage value to be stored in one of eight DACs, selected by the subaddress A-lines. The values, stored in the DACs internal registers, can be read out back to the 12 CAMAC R-lines. Powering on or CAMAC resetting, lead to all output voltages going to zero until the corresponding channels are written by CAMAC functions. The module is implemented in a single width CAMAC unit.

The **8ADC-14** [1] is a 8-channel 14-bit Analog-to-Digital converter to sample analog signals, applied to the input connectors. Measurements start on the GATE signal, initiated by an external pulse from the front panel or by the CAMAC instruction that cause the signals to be stored into the "Track and Hold" circuits and converted by the ADCs. The obtained digital data codes, written down to the output registers, can be read out from the CAMAC R1-R14 bus lines. The module is implemented as a single width CAMAC unit.

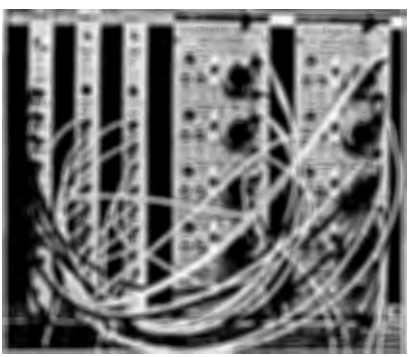

Fig. 4. The view of the LNS high voltage system for PMTs-63

The high voltage of the PMT-85 photomultiplier tube bases were controlled by the module connected with the computer through the RS232 bus. The module was designed at LHEP JINR [2].

The system demonstrated good time stability during the beam tests at the Nuclotron in June 2008. We obtained a high voltage drift not more than 0.5V per day.

**Software**

The software for HV system includes the test program and the main program. The test program is written in C++ using ROOT libraries [3]. It could control the CAMAC ADC and DAC modules and check the high voltages from Wenzel supplies.

The main program uses the MIDAS control software [4]. The drivers were written for the operation with CAMAC ADC and DAC modules under the MIDAS system. The system currently runs in LINUX operating system and can be ported easily to any operating system which supports TCP/IP sockets.

The MIDAS (Maximum Integration Data Acquisition System) has been used for implementing the control software. The MIDAS system was developed at PSI by Stefan Ritt. It has been developed as a general purpose data acquisition system for small and medium scale experiments. The main purpose of the MIDAS DAQ is to provide the following: data collection from local and/or remote hardware sources; data recording to common storage media; full data flow control. The integrated slow control system contains a fast online database and a history system. The framework can be extended by user code for front-end readout on one side and data analysis on the other side. The online data can be presented by PAW and ROOT as the histograms. A dedicated HTTP server gives fast Web access for experiment control and access to the slow control system including a graphical representation of variable trends (history display).

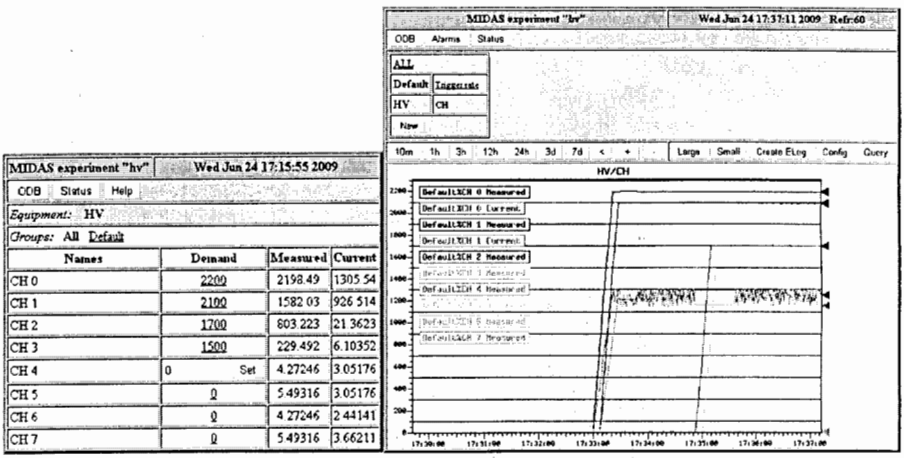


Fig. 5. HV values setup and monitoring window. The online voltage and current history window

The program for HV system provides the following main functions:

- driving ADC and DAC modules;
- set and check of HV for all channels;
- readout of the data from ADC modules;
- maintaining of online operation mode;
- writing the control data on disk;
- display the control results.

**Beam test results**

The beam test of ΔE-E counters and DAQ was performed at the Nuclotron in June 2008 using the 2.3 GeV deuteron beam and $^{12}C$ target. The signal amplitudes from the thin and thick plastic scintillators are shown in the left and right panels of the Fig.6, respectively. The results on the correlation of the energy depositions in two E- scintillation counters and their time-of-flight difference are given in Fig.7.

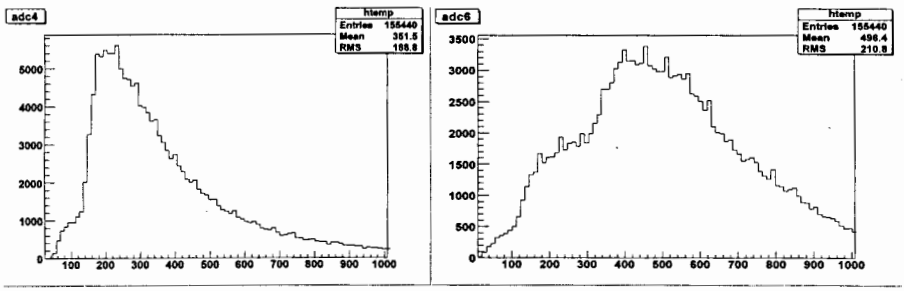


Fig. 6.The amplitude from one of the PMT-85 and the amplitude from PMT-63

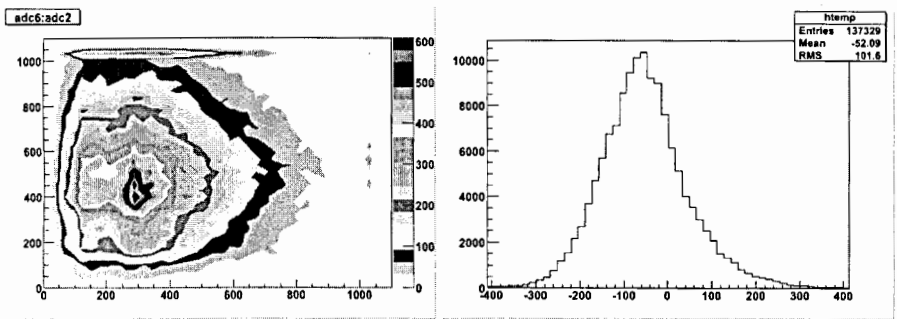


Fig. 7. The correlation of amplitudes from two E-detectors and their time-of-flight difference

**Conclusions**

- The 8DAC-12 and 8ADC-14 modules have been developed to control "Wenzel Electronik" high voltage supplies,
- The drivers have been written and compiled with the software package MIDAS to control the high voltage system,
- The test of the $\Delta E - E$ counters, the high voltage system and DAQ system have been performed by using cosmic muons and the beam at the Internal Target Station at the Nuclotron.

The work has been supported in part by the RFBR grant 07-02-00102a.

**References**

[1] A.V. Pilyar - Analog electronics for measurement and control, Proceedings of the XXI International Symposium NEC'2007, Varna, JINR, E10, 11-2008-37, pp. 382-389.
[2] http://hvsys.dubna.ru
[3] http://root.cern.ch/
[4] http://midas.psi.ch/htmldoc/index.html

# Pattern recognition methods for data handling of the CBM experiment

A. Lebedev[1,2], Semen Lebedev[1,2], G. Ososkov[1]
[1]*Joint Institute for Nuclear Research, Dubna, Russia*
[2]*GSI Helmholtzzentrum für Schwerionenforschung GmbH, Darmstadt, Germany*

Pattern recognition of particle trajectories and Cherenkov radiation rings is one of very important problems in such contemporary experiments as the Compressed Baryonic Matter (CBM) at the future FAIR accelerator at Darmstadt, Germany, with its extremely high rate and multiplicity of heavy ion collisions. Rigid requirements to the accuracy and computational speed of those recognition processes demand quite elaborated approaches to fulfill them which are described in the given talk. The application of pattern recognition methods for CBM data handling is expounded on examples of three important problems: (1) recognition of charged particle tracks in the Transition Radiation Detector (TRD), muon system (MuCH) and TOF detectors of the CBM; (2) recognition of rings registered in the Ring Image CHerencov detector (RICH); (3) handling invariant mass spectra with small signal to background ratio for finding small resonance peaks on a bulky background pedestal. Various pattern recognition techniques are described. A special attention is focused on speeding up all developed algorithms and their optimization by the time consumption and other computing resources.

## Introduction

The Compressed Baryonic Matter (CBM) experiment at the future FAIR accelerator at Darmstadt, Germany is being designed for a comprehensive measurement of hadron and lepton production in heavy-ion collisions from 8-45 AGeV beam energy, producing events with large track multiplicity and high hit density. Such experimental objectives require the collection of a huge number of events which can only be obtained by very high reaction rates (up to 10 MHz) and long data taking periods. Therefore a beam intensity of $10^7$ beam particles per second are expected while rare signals of interest are embedded in a large background of charged particles [1].

The CBM setup consists of several detectors (see. Fig. 1) It includes the silicon tracking system (STS) in a magnetic field designed for track and vertex reconstruction and momentum determination; then depending on two possible CBM modes (either reconstruction of electrons or muons) the Cherenkov radiation detector RICH together with the Transition Radiation Detector (TRD) are used for electron identification or, alternatively, the muon detector (MuCH) followed by the first TRD station are used for muon reconstruction. The setup will be completed by a time-of-flight (TOF) wall, an Electromagnetic CALorimeter (ECAL) and a Projectile Spectator Detector (PSD).

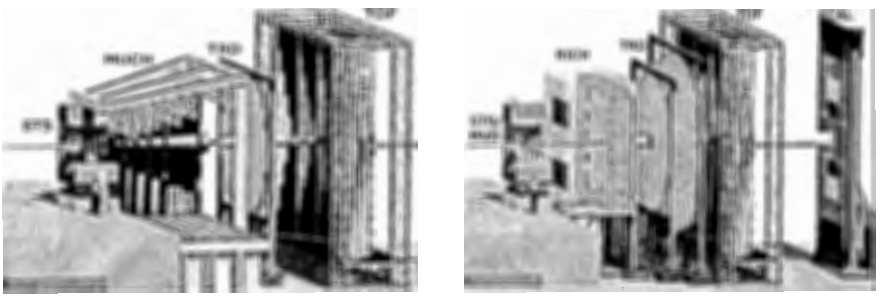

Fig. 1. Two alternative CBM setups: for measurements of muons (left) and electrons (right)

In this lecture the application of pattern recognition methods for data handling of the CBM experiment is expounded on the example of three important problems:

- recognition of charged particle tracks in TRD, MuCH and TOF detectors;
- recognition of Cherenkov radiation rings registered in the RICH detector in order to identify electrons and suppress pion background;
- handling invariant mass spectra with small signal to background ratio for finding small resonance peaks on a bulky background pedestal.

Various pattern recognition techniques are developed to solve these problems: an original modification of the Kalman filter method [2]; a rapid version of the Hough transform and neural net classification [3]; wavelet analysis with wavelets of continuous and discrete types [4].

Due to above mentioned high rate of data stream, data processing must also be extremely intensive, therefore a special attention is focused on speeding up all developed algorithms and their optimization by the time consumption and other computing resources. The detailed study has been carried out to evaluate the efficiency and accuracy of developed algorithms and corresponding software, after which they are included in the CBM framework and used to optimize the CBM setup.

## 1. Track recognition for TRD and MuCH detectors

Curve recognition on the large background with noise points and neighboring curves is a classic task of the pattern recognition in many important scientific and technical applications. This kind of problems is particularly difficult in high energy physics, where processing a very huge 3D set of measurements one has not only recognize the trajectory of the particle among hundreds of other trajectories, but also estimate its parameters as precise as possible. Such a joint procedure of the track recognition and their parameters estimation is named usually as **the tracking**. Although problems of tracking have more than half of century history, methods of tracking have considerably changed with the evolution of the experimental setups from bubble and spark chambers, which could register several tracks on a photograph, to modern heavy-ion experiments, producing thousands of particles, registered by electronic detectors directly in the computer memory as arrays of measured coordinates. These changes gave rise to new tracking algorithms based on such innovations as neural networks, cellular automata, elastic tracking etc (see, for example, survey [5]).

However, it must be pointed out that those methods are not directly applicable in the conditions of the TRD and MUCH detectors due to their very specific features. Both detectors have similar structures in which the detector is constructed as set of detector planes, which are able to produce space points from the detected particle. These planes alternate with so called absorbers, - thick material layers intended to either produce transition radiation as in the TRD or to suppress other particles except of muons in the Much detector. Besides there is a stray non-homogeneous magnetic field in the area of the MuCH detector.

The challenges for the tracking algorithms of this type of detectors are as follows: high multiplicity - about 800 tracks per each event, high hit density, significant distortions of particle trajectories due to multiple scattering and energy loss in absorbers, presence of the stray magnetic field, noise measurements, background tracks and detector measurement errors.

One of the most reliable tracking procedure which can meet these challenges is the track following. It begins with a stage of initialization in which the information on the tracks found in the vertex detector or on measurements in the first stations of the detector, is used to estimate initial parameter values of spatial tracks-elements on the basis of local model of a track. At the following stage these estimations allow to extrapolate each of tracks on the

following coordinate plane. If there in the area surrounding the predicted point (it names a validation gate) there is one measurement, it is added to a track-element, parameters are recalculated and process proceeds up to reaching the last coordinate plane. If several points occur in the validation gate, each of these points begins a track branch, continuing up to either this track breakage, or also till the end of the detector. Such process of track following with branching gives the highest tracking efficiency although it has such a drawback as rather big computer time consumptions.

Global tracking in CBM is based on track following using reconstructed tracks in the STS to provide initial track parameters in order to start the following track prolongation to the MuCH or TRD detectors and further up to the TOF detector to be able to merge TOF hits to a track. This track following is based on the standard Kalman filter technique as proposed in [6].

**Kalman filter.** The Kalman filter (KF) process works iteratively using the **state vector** $\vec{x} = (x, y, t_x, t_y, q/p)^T$ to predict a track position on the next station, then to recalculate a validation gate using the current value of covariance matrix. The main KF advantages over a common least square fit (LSF) of ***n*** measurements (hits) to a track model are widely known [6]: (i) KF is suitable for combined track finding and track fitting; (ii) only small ***5x5*** matrices of the state vector parameters have to be inverted instead of large ***nxn*** LSF matrices; (iii) KF is optimally suits to handle many measurements in the presence of multiple scattering and other energy loss effects. KF provides mathematical tools for the main tracking steps: track prolongation subsequently from one detector station to the next adding found hits in each detector to the track-candidate set, calculating the validation gates and then for track fitting.

However, in order to apply the KF formalism to CBM data from MuCH or TRD detectors, it was necessary to put substantial efforts to modify KF algorithms to satisfy the CBM specific conditions. The corresponding developed program was named the LIT tracking program.

**Track propagation.** One of the most important components of a track reconstruction procedure, which is used both in the track recognition and track parameters estimation is the track propagation. It is embodied in an extrapolation algorithm intended to predict the trajectory of the charged particle in terms of mean values of the track parameters and corresponding errors. Two models are implemented for the average trajectory and transport matrix calculation: (1) straight line in case of the absence of a magnetic field; (2) solution of the equation of motion for a charged particle in the magnetic field with the $4^{th}$ order Runge-Kutta method, with a parallel integration of the derivatives. Besides the magnetic field, which influences the average trajectory only, two more physics effects were taken into account during the propagation: Multiple Coulomb scattering, which affects error calculation only, and energy loss (ionization: Bethe-Bloch, bremsstrahlung: Bethe-Heitler, pair production), which influences both mean values and errors

Detailed description of the developed track propagation algorithm can be found in [8]. It is important to stress that this algorithm has been compared in detail to the GEANE track propagation package which is used in Geant3 [9] for the TRD and MuCH event simulations. Since GEANE package has different concepts of track parameterization, track modeling and multiply scattering simulation, it demanded considerable efforts to adopt GEANE's algorithms in our program. The simulation showed good agreement between developed track propagation algorithm and GEANE. The time consumption is approximately 2.5 times less for the LIT tracking program and was further improved.

**Track finding.** The track finding algorithm is based on the track following and the Kalman filter methods. It uses branching to take into account missing hits, to deal with detector

inefficiencies, but two more hit-to-track assignment methods were also considered and tested, both were without track splitting into branches and, therefore, less time-consuming. The first was the nearest neighbor method when the only hit closest by the Euclidean distance to the prediction point in the validation gate is assigned to track. The second method used a robust approach calculating weights of all hits in the validation gate to evaluate the most probable track position.

**Track selection.** The aim of the track selection algorithm is to remove clone and ghost tracks and to leave good ones. Clone tracks are tracks that consist of similar set of hits, ghost tracks are tracks that consist of some random set of hits. The algorithm works in two stages. First, tracks are sorted by their quality, which is defined by the track length and its $\chi^2$. Then the procedure is executed to check the shared hits of tracks. It loops over tracks starting from the highest quality tracks and checks all hits belonging to the track. The number of hits shared with other tracks is calculated and the track is rejected, if more than 15% hits are shared.

**Performance of the tracking algorithms.** Testing of the tracking algorithms was carried out on a set of simulated central Au+Au collisions at 25 AGeV beam energy with embedded signal particles, i.e. electrons in case of TRD and muons in case of MUCH tracking. The resulting momentum integrated efficiency value for the TRD tracking is 94.7% for all tracks, and 91.0% for electron tracks. The efficiency drop for electrons is due to more complex energy loss calculation for electrons because of the bremsstrahlung..

The comparative results of three developed method for MUCH tracking is given in Table 1.

Table 1. MUCH track finding efficiency

| MUCH tracking | Branching | Nearest Neighbor | Robust weights |
|---|---|---|---|
| muon track finding efficiency | 94.9% | 92.7% | 94.0% |

## 2. Cherenkov radiation ring recognition from the CBM RICH

The main challenge of the ring recognition in the CBM RICH detector results from the large multiplicity in heavy-ion collisions which leads to a high ring density in the RICH detector. Currently two different RICH designs are under discussion [10]. Both designs provide about 22 hits/ring, but differ in length due to different choices of radiator gas. The larger option with nitrogen has a radiator length of 2.25 m. The smaller option with $CO_2$ has a radiator length of 1.5 m. As it is depicted in Fig. 2, the ring density in this compact RICH is higher, which poses an additional challenge for the ring recognition.

Most measured electrons are produced in the STS detector or magnet yoke. This material budget significantly increases the ring density in the RICH detector and causes many overlapping rings. The ring resolution is determined by multiple scattering, distortions from the residual magnetic field and detector granularity. Besides rings are distorted to ellipses with about 10% difference in the length of major and minor half axis, because the at photodetector can only be approximately placed in the focal plane.

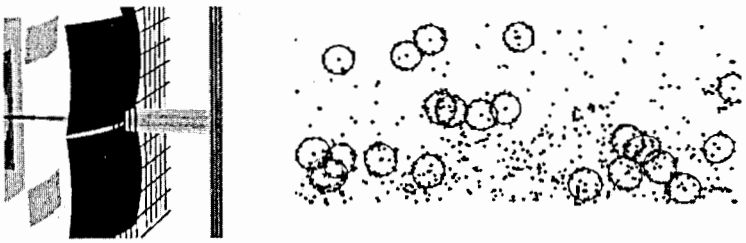

Fig. 2. Left: Sketch of the smaller CO2-RICH setup as used in simulations (outer gas box omitted). Right: Part of one typical event: RICH hits, found rings (continuous circles), track projections form the STS (separate dots).

The developed ring recognition algorithm is standalone, i.e the input data is only an array of RICH hits without information from other detectors. It consists of two steps. First, a local search of ring-candidates is performed. It is based on an original algorithm of local selection of hits and a special fast version of Hough Transform (HT) [10]. In RICH reconstruction both circle and ellipse fitter are used. Because of its simplicity and a very high computational speed the first one is used in the ring recognition algorithm. The algorithm which is known as COP (Chernov-Ososkov-Pratt) is used [12]. As the rings in the CBM RICH detector have a notable elliptic shape, therefore a direct and fast ellipse fitting method was implemented for more precise parameter determination [11].

The second step is a global search, in which mainly the quality of rings is determined using an artificial neural network (ANN). This step is used as filter: collecting information about all ring-candidates, the algorithm compares them and chooses only high quality rings, rejecting repeatedly found rings (clone rings) and wrongly found rings (fake rings). In order to reliably reject these fake rings, a set of ring characteristics had to be selected which have to differ significantly for wrongly and correctly found rings. After a statistical analysis nine parameters were selected: the number of hits per ring; $\chi^2$ of the ellipse fitting; the position of the ring in the RICH detector, etc. The ANN using these nine input parameters derives its output as the ring quality or probability, whether a ring-candidate was correctly found or not. With this information, the selecting algorithm compares the ring quality choosing good rings and rejecting wrongly found rings and clones, which were determined according to the rule: if a ring shares more than 30% of its hits with better quality rings it is rejected.

The performance of the optimized ring finding algorithm is quite satisfactory: its efficiency for electrons is 93% for the compact RICH design with higher ring densities. Overall, typically 4% of the approximately 100 found rings are fake rings and 2% clone rings.

The developed programs for the RICH ring reconstruction were embedded in the CBM framework and intensively used for the physics analysis and detector optimization studies. In particular, the compact RICH design was shown to be optimal from its efficiency and cost consideration.

### 3. Parallelism

Very fast event reconstruction is extremely important for the CBM experiment to process in on-line mode terabytes of input data produced in particle collisions. Therefore, the intensive efforts were put to speedup developed algorithms. A fast parallel event reconstruction algorithms which uses available features of modern processors were elaborated. These features enable parallel programming. The first allows to pack several data

items into one register and to operate on all of them in parallel thus achieving more operations per cycle. It was realized by the SSE (Streaming SIMD Extensions) technology, which is using SIMD (Single Instruction, Multiple Data) execution model. The second multicore CPUs feature enables the routines to exploit all available CPU cores and hardware threads. The parallelized version of the tracking algorithm, in particular, allows to achieve a speed up factor **2400** speed up factor for track fit and **487** for the track finder with 94% efficiency for the computer with two CPUs Intel Xeon X5550 at 2.67 GHz.

Both features have been also implemented in the ring reconstruction of the RICH detector giving the impressive results: if the initial implementation of Hough transform was on level of 80 s/event, then its parallel implementation performed in 3 ms/event achieving the speed up factor **26600** for the Intel Xeon X5550 (4 cores) CPU with 93% of ring finding efficiency.

## 4. Wavelet analysis application for handling invariant mass spectra

The invariant mass method as very effective one is, therefore, one of the most usable tools for data analysis in heavy ion physics. However there are serious problems with extracting rare or short lived particle resonances in question from invariant mass spectra because of the presence of bulky background, which dramatically increases when the event multiplicity grows. Two approaches are mostly used to overcome this problem: either to approximate the spectrum pedestal by some appropriate function (usually a polynomial) and then to subtract it from the spectrum or, more effective, but cumbersome, to simulate the pedestal by Monte Carlo as a combination of background particles contributing to the same event and then again to subtract it from the spectrum. An example of the $\gamma\gamma$ invariant mass spectrum in pC and dC interactions [13] is shown in Fig. 3(left).

Result of its handling by subtraction of combinatorial background is depicted in Fig. 3(right).

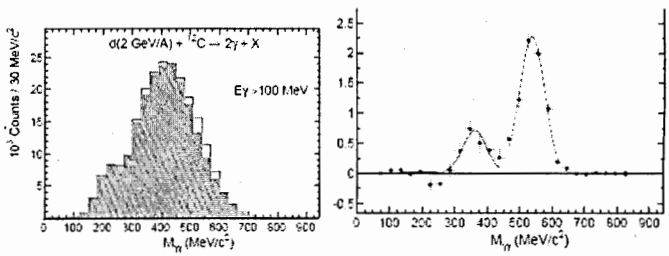


Fig. 3. Invariant mass distributions of $\gamma\gamma$ pairs without (left) and with (right) the background subtraction

As it is seen, the significant part of a physical background is cleaned by subtraction of a combinatorial background. Signal to background ratio is increased within the peak interval. However, this approach supposes adequate knowledges about particles, which are alternative to the particle of interest in studied events. Since it is not always the case, physicists have often to guess what kind of processes contribute to form the background.

Such an arbitrariness leads often to a stray background and worsen the accuracy of the peak position estimation. Therefore a method is needed that would be able to analyze signals of invariant mass spectra independently of their origin, i.e. of processes generating peaks and background. Such an approach alternative to above mentioned common methods is based on

the wavelet analysis [13]. Wavelets have particular advantages, which allows to skip the phase of background estimating and to make statistically proved assertion of the peak existing. Besides wavelets are robust, i.e. resistant to noise. Therefore new efficient algorithms on the wavelet basis are proposed below for recognizing and extracting resonance peaks from invariant mass spectra.

Wavelet transformation is known as an efficient multiscale technique to reduce the presence of statistical noise and then extract physical parameters from the obtained smoothed form [14]. The one-dimensional wavelet transform (WT) of a signal f (x) has a biparametric form. This allows WT to overcome the main shortcomings of the Fourier transform such as nonlocality, infinite support, and necessity of a broad band of frequencies to decompose even a short signal. The WT is defined as a convolution of invariant mass spectrum f(x) and a special biparametric wavelet function ψ((b-x) /a)

$$W_\psi(a,b)f = \frac{1}{\sqrt{C_\psi}} \int_{-\infty}^{\infty} \frac{1}{\sqrt{|a|}} \psi\left(\frac{b-x}{a}\right) f(x)dx,$$

The condition $C_\psi < \infty$ is, at the same time, the condition of the wavelet ψ existence. It holds, in particular, when the first n-1 moments are equal to zero:

$$\int_{-\infty}^{\infty} |x|^m \psi(x)dx = 0, \quad 0 \le m < n. \tag{1}$$

Due to freedom in the choice of the wavelet function ψ many different wavelets were invented [1, 2], but we use in this paper continuous wavelets with vanishing moments (WVM) because condition (1) always holds for it. One of the WVM families is a set of *Gaussian wavelets* (GW) which are normalized derivatives of the Gauss function

$$g(x, A, x_0) = A \exp\left(-\frac{(x-x_0)^2}{2\sigma^2}\right) \tag{2}$$

The most known in the GW family is the second order wavelet $G_2(x) = (1-x^2)e^{\frac{x^2}{2}}$ which is also known as "the Mexican hat". Despite of their nonorthogonality, in some cases gaussian wavelets are more suitable to evaluate peak parameters. One of these cases arises when a peak in question has a Gaussian shape (2). This makes it possible to use very simple analytical expressions in the continuous Gaussian wavelet transform for Gaussian peaks

$$w_{g_n}(a,b)g = \frac{A\sigma a^{n+1/2}}{\sqrt{(n-1)!s^{n+1}}} g_n\left(\frac{b-x_0}{s}\right), \tag{3}$$

where it is denoted $s = \sqrt{a^2+\sigma^2}$ It gives us a remarkable advantage to calculate the peak parameters directly in the wavelet domain instead of the time-space domain *without using the inversion*. Moreover, in real cases, when our signal shape is close to a Gaussian one and is considerably contaminated by an additive noise and, in addition, is distorted by binning to be input into the computer, one can also use the remarkable robustness of Gaussian wavelet filtering, as proved in [15]. Let us demonstrate this scheme by the $G_2(a, b)$ wavelet example.

According to (3), one can obtain the maximum (absolute) value of $G_2$ for a Gaussian (2) at the shift point $b = x_0$ as

$$\max_b W_{G_2}(a, x_0)g = \frac{A\sigma a^{5/2}}{(a^2+\sigma^2)^{3/2}}. \qquad (4)$$

In the wavelet domain of $G_2(a, x_0)$ this dependence looks like a simple curve with one maximum. The corresponding calculations give the position of maximum at the scale axis as $a_{max} = \sqrt{5}$. Since the maximum location in the $G_2$ domain is stable when the signal is contaminated by some noise (see [15]), one can use the obtained point $x_0$, $a_{max}$ to find the maximum of a real contaminated signal. Although it is inevitably blurred over some area in the wavelet space due to various distortions, it can nevertheless be used as a good starting point for iterations minimizing a fitting functional.

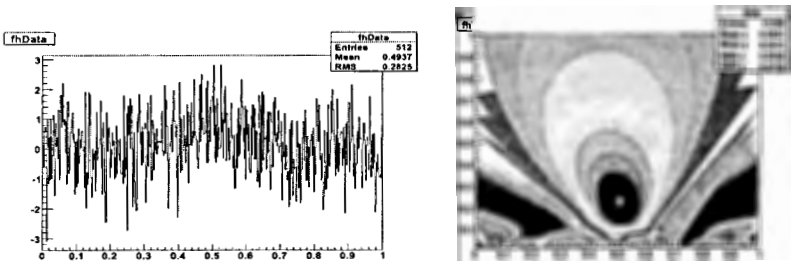


Fig. 4. Simulated example of a noisy i.m. spectrum (left) and its 2D wavelet surface (right) which maximum is marked by star

The following simplified algorithm showed quite satisfactory results.
Let us have a noisy invariant mass spectrum, as in Fig. 4 (left).

1. transform it by $G_2$ into wavelet domain Fig. 4 (right)
2. look for the wavelet surface maximum $b_{max}$, $a_{max}$ marked by star in Fig. 4 (right)

From the formula (4) one can derive analytical expressions for its maximum $x_0$ and $a_{max} = \sqrt{5}$, which should correspond to the found $b_{max}$, $a_{max}$. Thus we can use coordinates of the maximum as estimations of wanted peak parameters $\hat{x}_0, \hat{a}$, from which one can obtain such parameters of the peak in question, as its

halfwidth $\hat{\sigma} = \frac{\hat{a}}{\sqrt{5}}$, amplitude $\hat{A} = \frac{\max W}{a^{\frac{5}{2}}\hat{\sigma}}(\hat{a}^2+\hat{\sigma}^2)^{\frac{3}{2}}$ and even the integral $I = A\sigma\sqrt{2\pi}$

This technique was quite successfully applied in several experimental tasks. In particular, it was used to approve independently the results of study invariant mass distributions of $\gamma\gamma$ pairs for the reaction $dC \to \gamma + \gamma$ in the Photon-2 experiment [13]. One can see comparative results of the Gaussian approximation of experimental points in Fig. 3 (left) and the biparametric distribution of the GW of the 8-th order for dC interactions in Fig. 5 obtained without subtraction of background, which marked by ***a*** and ***b*** arrows.

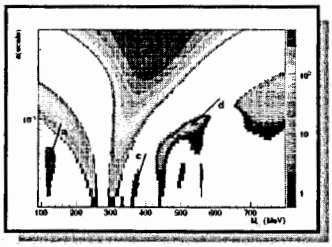

Fig. 5. 2D distribution of the GW of the 8-th order for $dC \rightarrow \gamma + \gamma$ interaction

Two wavelet surface maxima marked by arrows c and d correspond to sought peaks in Fig. 3 (right).

As it is shown in Fig. 6, despite of a quite jagged spectrum[1] (left panel), GW wavelets of the 4-th order could give visible peaks with $\sigma_1 = \sigma_3 = 0.013$, $\sigma_2 = 0.021$ (right panel).

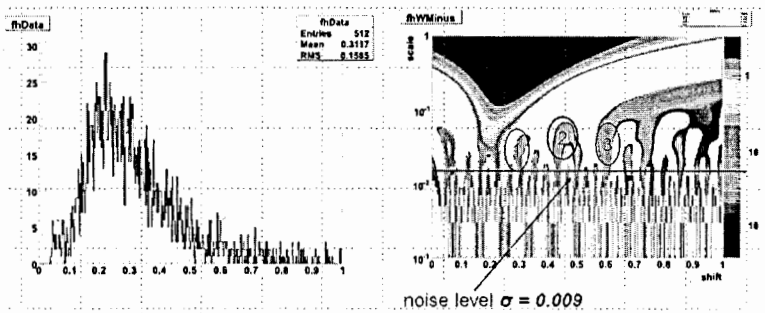


Fig.6. An original jagged spectrum (left) and its 2D wavelet surface (right)

Then this result was compared with the common method of obtaining a simulated background and subtracting it from the original spectrum, see Fig. 7 (left). It was very revealing to realize that the simulated background gives the wavelet surface without any significant peaks see Fig. 7 (right).

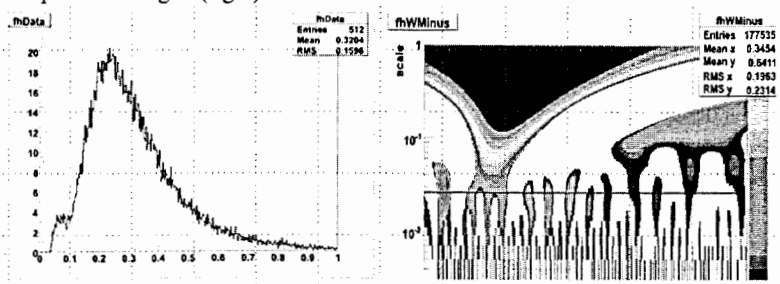


Fig.7. The simulated background spectrum (left) and its 2D wavelet surface (right)

[1] Results were obtained in [16] on the data provided from the FOPI experiment by the courtesy of Dr. N. Hermann

It should be noted that the spectrum obtained by background subtraction from the original looked rather disappointing to observe any peak on it (see Fig. 8, left), but on the wavelet surface (Fig. 8, right) one can clearly see three significant maxima in good correspondence with the wavelet surface maxima on Fig. 6 (right).

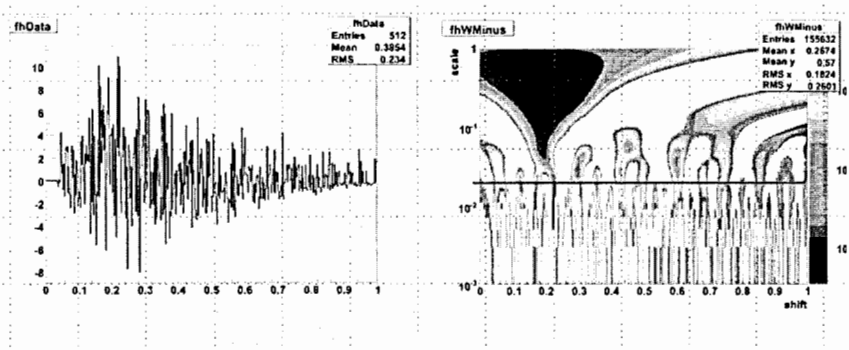


Fig. 8. The spectrum obtained by background subtraction (left) and its 2D wavelet surface (right)

Package of the programs for wavelet analysis has been implemented. It includes continuous and discrete wavelet transform. This package works under the ROOT and is available for the common use. Wavelet analysis has been applied to filter various invariant mass spectrums form high frequently noise, low frequently background, finding and estimation peak parameters.

**Summary**

1. Track and ring recognition methods for the CBM experiment were discussed, vital need of speeding up all recognition algorithms was stressed
2. The variation of reconstruction time depends on selected parameters in the track and ring finders trading efficiency vs. speed.
3. Corresponding algorithms were significantly optimized in terms of calculation speed without loosing any efficiency
4. All developed algorithms were tested on large statistics of simulated events, included then into the CBM framework and are intensively used now by CBM collaboration members
5. Possibilities to elaborate parallel versions of these algorithms look very promising, but need a more advanced computing systems

**References**

[1] CBM Collaboration, Compressed Baryonic Matter Experiment. Technical Status Report, GSI Darmstadt (2005).

[2] C. Lebedev, G. Ososkov, Fast Algorithms for Ring Recognition and Electron Identification in the CBM RICH Detector, Physics of Particles and Nuclei Letters, 2009, Vol. 6, No. 2, pp. 161–176.

[3] A. Lebedev, G. Ososkov , Track reconstruction in the CBM TRD, JINR Comm. E10-2008-3, Dubna, 2008.
[4] Kh.U. Abraamyan et al, A Resonance Structure in the γγ Invariant Mass Spectrum in pC- and dC-Interactions, PHYSICAL REVIEW C 80, 034001 (2009) 34pp.
[5] G.A. Ososkov, A. Polanski, and I. V. Puzynin, Current Methods of Processing Experimental Data in High Energy Physics, Physics of Particles and Nuclei, Vol. 33, No. 3, 2002, pp. 347–382.
[6] R. Fruhwirth, Application of Kalman filtering to track and vertex fitting, Nucl. Instrum. Meth. A262 (1987), pp. 444-450.
[7] The ROOT Users Guide (2009), ftp://root.cern.ch/root/doc/Users_Guide_5_24.pdf
[8] A. Lebedev, G. Ososkov, LIT Track Propagation for CBM, CBM note (2008), [QCD_CBM_SOFT-note-2008-002].
[9] GEANT - Detector Description and Simulation Tool, CERN Program Library Long Writeup W5013.
[10] C. Hoehne et al., 2008, Nucl. Inst. and Meth. A 595, 187.
[11] S. Lebedev et al., Proceedings to CHEP-09, March 21 - 27, 2009 (to be published).
[12] N. Chernov , G. Ososkov, 1984, Comp. Phys. Comm., 33, pp. 329-333.
[13] Kh.U. Abraamyan et al, A Resonance Structure in the γγ Invariant Mass Spectrum in pC- and dC-Interactions, PHYSICAL REVIEW C 80, 034001 (2009) 34.
[14] I. Daubechies, The wavelet transform, time frequency localization and signal analysis, IEEE Trans. Inf. Theory 36, 961 (1990).
[15] G. Ososkov and A. Shitov, Comput. Phys. Commun. 126, (2000), 149.
[16] G. Ososkov, P. Koczoń, S. Lebedev, Recent results of wavelet applications for handling invariant mass spectra, CBM Collaboration meeting, March 2009, https://www.gsi.de/documents/DOC-2009-Mar-118-1.pdf

# Internet evolution scenarios

O.H. Martin[1]
*ICTConsulting, Gingins (VD), Switzerland*

A review of the state of the Internet in terms of traffic and services trends covering both the Research & Education and the Commercial Internet will first be given with particular emphasis on green ICT and mobile technologies. The problematic behind the IPv4 to IPv6 migration will be explained, a short review of the ongoing efforts to re-design the Internet in a clean-slate approach will then be made. Last, an overview of the main organizations involved in Internet Governance will be presented

**Keywords**: Internet, GÉANT, FIND, FP7, GENI, IAB, ITU, IPv6, LTE, "clean-slate", "green ICT".

## 1. Introduction

This article attempts to address the evolution of Internet and, more generally, relevant ICT technologies with special emphasis on Mobile, Green, Grid and Cloud computing technologies.

One major concern is to keep the Internet together throughout this very complex and fast evolving technological process, hence some plausible evolution scenarios will be sketched.

As the exhaustion of the IPv4 address space is getting closer i.e. 2011-201, as the wide adoption of IPv6 is still lacking, as the Internet continues to grow at a annual rate greater than 20%,, the Internet is at a crossroad with two competing approaches, evolutionary or clean-slate.

While a clean-slate approach bears lot of promises it does not provide a realistic alternative in the short to medium term given the time to standardize new architectural proposals that both solves the numerous problems of today's Internet while also providing a more stable foundation for the "Internet of the Future" encompassing new needs and requirements (e.g. mobility, security, sensor networks, Radio Frequency Identification (RFID), Personal Area Networks (PAN), Vehicle Area Networks (VAN), etc.).

## 2. Main Sources

This article is an updated version of an article that was originally published in the NEC'2007 conference proceedings[2] and is also derived from the presentations I made at CHEP'2009[3] in Praha and at NEC'2009[4] in Varna.

## 3. Internet Traffic & Infrastructure

There are really two Internets branches that, apart from the fact that they are obviously interconnected, have very little in common namely, the Commercial Internet and the Academic & Research Internet exemplified, in Europe, by the pan-European GEANT backbone interconnecting National Research & Education Networks (NRENs), in the USA by Internet2[5], the Energy Science Network (ESnet[6]) and the National Lambda Rail (NLR[7]), etc.

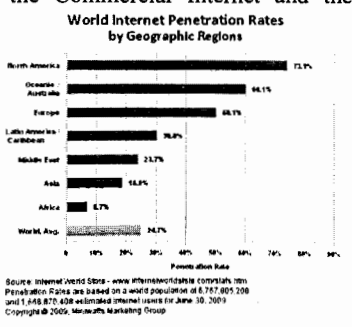


[1] Olivier.Martin@ictconsulting.ch
[2] www.ictconsulting.ch/reports/NEC2007-OHMartin.doc
[3] www.ictconsulting.ch/presentations/CHEP09-Final.ppt
[4] www.ictconsulting.ch/presentations/NEC2009.ppt
[5] http://www.internet.edu
[6] http://www.es.net/
[7] http://www.nlr.net/

### 3.1. Internet Traffic

Despite the numerous technical problems the Internet is faced with, all available statistics indicate that it is growing very rapidly and does not show any signs whatsoever of a brutal slowdown, indeed, the Internet is, in a sense, "victim" of his own success. According to Internetworldstats[8], the worldwide Internet user penetration is approaching 25%, i.e. 1.7 billion users off a world population of 6.8 billion persons mid-year 2009, with an increase in the number of Internet users of more than 200.000 since mid-year 2008, when the Internet penetration was only 21.9%.

Internetworldstats is monitoring the number of Internet users per world region and has also been tracking the development of the Internet since 2000.

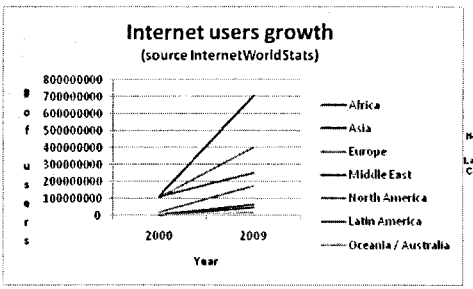


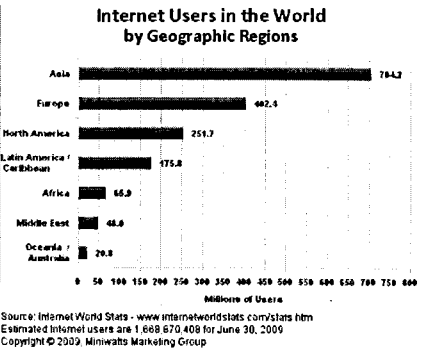


Not surprisingly, Asia with 650 Million users and Europe with 390 Million users are now well ahead of North America with only 247 Million users. However, these figures are somewhat different when one looks at the penetration of the Internet with respect to the population of the various regions with North America still being well ahead of Asia and Europe.

Another source of information is the Internet traffic studies conducted by Ipoque[9] in collaboration with 8 ISPs around the world and 3 universities, using deep packet inspection (DPI) techniques. In their last 2008-2009 report[10] covering 1.1 Million users (i.e. 0.7/1000 sample) producing 1.3 Petabytes of data, it is stated that "*BitTorrent and eDonkey downloads have been analyzed to classify the transferred files according to their content type. Some of the key findings are: P2P still produces most Internet traffic worldwide although its proportion has declined across all monitored regions – loosing users to file hosting and media streaming; regional variations in application usage are very prominent; and Web traffic has made its comeback due to the popularity of file hosting, social networking sites and the growing media richness of Web pages.*"

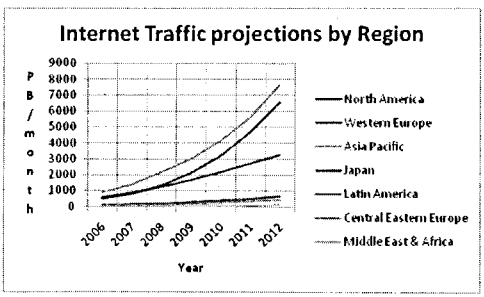


[8] http://www.internetworldstats.com/stats.htm
[9] http://www.ipoque.com/resources/internet-studies
[10] http://www.ipoque.com/resources/internet-studies/internet-study-2008_2009

The traffic projections made by Cisco in their Cisco Visual Networking Index[11] are also most interesting, however, they must be taken with a grain of salt as it is clearly in Cisco's own interest to predict too high rather than too low compound annual Internet growth rate; nonetheless the Cisco predictions appear to make a lot of sense as everyone can observe the clear move towards more access to multimedia content over the Internet.

Both Cisco and Ipoque agree that Peer to Peer (P2P) traffic is the dominant source of Internet traffic worldwide, up to 40-50% depending in some regions. So, one essential fact is that the Web traffic, that used to be the prevalent source of Internet traffic, is only representing 20% to 25% of that traffic today; however, due to the increasing popularity of Web 2.0 & social networks, Web usage appears to be growing again. In the longer term, Cisco predicts that by 2012, with a compound annual growth rate of 97%, "Internet video to PC" will surpass P2P traffic.

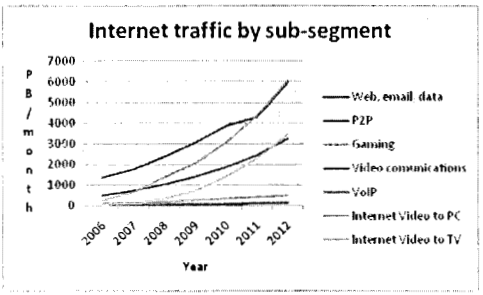


Given its high impact on the overall performance of the ISPs, in particular transit ISPs, the P2P traffic sometimes raises network neutrality issues, that is discrimination against specific types of traffic (e.g. encrypted, P2P, traffic) by using traffic shaping, also dubbed "traffic throttling", techniques, thus potentially causing major performance losses under high load conditions.

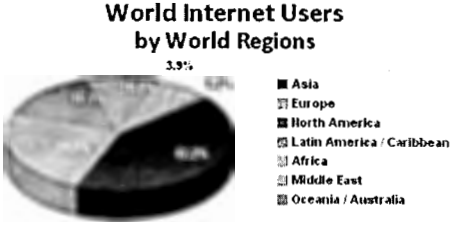


Source: Internet World Stats - www.internetworldstats.com/stats.htm
1,668,870,408 Internet users for June 30, 2009
Copyright © 2009, Miniwatts Marketing Group

### 3.2. Towards a "green" Internet

An unfortunate consequence of the high-penetration of the Internet into (almost) everybody's home, in particular, and, more generally, spectacular advances in Information, Communication and Computing Technologies is the impact on worldwide CO2 emissions. According to Bill St.Arnaud's "Green Broadband" Web site[12] "It is estimated that the CO2 emissions of the ICT industry alone exceeds the carbon output of the entire aviation industry."

So, "green computing" has thus become a major topic and is the subject of many conferences, reports and projects. Like with cars and many home appliances, energy-aware network ICT products bear a lot of appeal and low energy consumption coupled with smarter energy management strategies have become excellent selling arguments. In the not too distant future we are therefore likely to see a sharp increase in the use of self-powered sensors and renewable energy.

In any case, Information and Communication Technologies (ICT), in general, and the Internet, in particular, will, no doubt, become "Greener"; in other words, an energy aware, Internet will appear sooner rather than later as energy consumption of new data centers becomes both very expensive but also extremely problematic to deliver. Given the urgency as well as the potential savings, rapid progress can be expected.

[11] http://www.cisco.com/en/US/netsol/ns827/networking_solutions_sub_solution.html
[12] Green IT/Broadband and Cyber-Infrastructure: December 2007

### 3.3. The growth of ICT

The ITU has been tracking the growth of ICT technologies, in general, and the role of mobile technologies, in particular. On the occasion of Telecom World 2009[13], the ITU published a report titled "The world in 2009, ICT facts and figures[14]". As shown in the following diagram, ITU estimates that the total number of mobile cellular subscriptions will reach 4.6 billion by the end of 2009 and that the total number of mobile web users[15] also dubbed "mobinauts" grew past the total number of desktop computer based internet users for the first time in 2008.

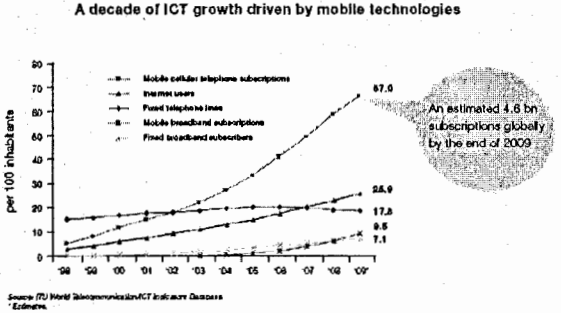


- Mobile cellular has been the most rapidly adopted technology in history. Today it is the most popular and widespread personal technology on the planet, with an estimated 4.6 billion subscriptions globally by the end of 2009
- Mobile broadband subscriptions overtook fixed broadband subscribers in 2008, highlighting the huge potential for the mobile Internet
- In 2009, more than a quarter of the world's population are using the Internet

### 3.4. Access and Backbone Technologies

Broadband access needs are increasing in order to support new applications, therefore wired as well as wireless access speeds will evolve from Mb/s to Gb/s and will become nearly ubiquitous in a very fast evolving technology framework, but fixed access will not disappear (ADSL, FTTH, GPON, Cable TV, leased lines, etc.).

Wide-scale commercial 40Gb/s deployments that really started in 2008 (e.g. ATT, NTT) are expected to continue, however, "commodity" 10Gb/s circuits will also continue to be increasingly widespread as 40Gb/s technology is still too expensive for most ISPs. Although it is too early to say, it could well be that 100Gb/s will overtake 40Gb/s technology as an interconnection technology (e.g. Internet Point of Presences (PoP), Internet Exchange Points (IXP), high performance LAN environments). Indeed, a number of 100Gb/s deployment have been announced, e.g. the deployment of CIENA's 100Gb/s equipment[16] during 2010 in the NYSE (New York Stock Exchange) Euronext data centers in New-York

[13] http://www.itu.int/net/TELECOM/World/2009/newsroom/index.aspx
[14] http://www.itu.int/net/TELECOM/World/2009/newsroom/pdf/stats_ict200910.pdf
[15] http://en.wikipedia.org/wiki/Mobile_Web
[16] http://www.ciena.com/news/news_nyse.htm

and London. This announcement comforts my long held belief that the commercial Internet is actually well ahead of the academic and research Internet despite the commonly held view.

There is, in fact, little doubt that the major evolutionary trend in the last years has been the pervasiveness and the ubiquity of wireless technologies, be it Wi-fi[17] or Cellular phones.

The first full internet service on mobile phones[18] was *"i-Mode"* introduced by NTT DoCoMo[19] in Japan in 1999 that immediately met an overwhelming success. Shortly afterward the *"Blackberry[20]"* (1999, 2002) was introduced. However, it is only after the extraordinary successful introduction of Apple's *"iPhone[21]"* in 2007 which features, among other things, a new ergonomic user interface with a touch sensitive screen, that a new category of mobile phones[22] called *"Smarphones[23]"* started to invade the mobile telephony and mobile Internet market. One reason behind the success of iPhone is the ability to download applications from a very large database called *Appstore*[24].

Thus, it is the iPhone "mania" that really paved the way to a whole new generation of "smart phones" and to a new, potentially "dangerous", way to access the Internet, in general, and live Internet services, in particular. The danger lies in the way Internet traffic is charged to users, as behind the apparently *"unlimited"* there are usually a number of "exception" clauses, e.g. *"roaming"* but also various ceiling in monthly and/or daily traffics that look line *"devious"* ways to re-introduce *"pay per view"* style services. In that respect a recent case with an Orange customer[25] in France is rather instructive.

Google could not stay inactive, of course, so it first made available a new *"open"* operating system for smart phones called Android[26] and it is also rumored that Google will soon launch its own smart phone dubbed *"Nexus One[27]"*. This is actually quite worrying as the dangers of living in a "Google" centric world may actually be even greater than those of a Microsoft centric world!

The following chart[28] was extracted from a Light Reading Webinar delivered on Thursday, September 10, 2009 and titled "LTE Technology & Components": CDMA[29], a

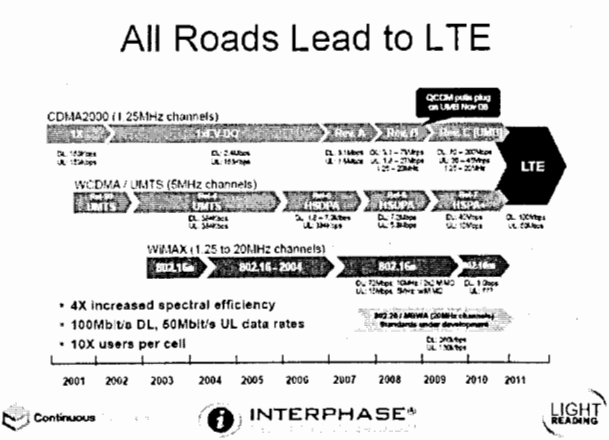


[17] http://en.wikipedia.org/wiki/Wi-Fi
[18] http://en.wikipedia.org/wiki/Mobile_phone
[19] http://www.nttdocomo.com/
[20] http://en.wikipedia.org/wiki/BlackBerry
[21] http://en.wikipedia.org/wiki/IPhone
[22] http://en.wikipedia.org/wiki/Mobile_phone
[23] http://en.wikipedia.org/wiki/Smartphone
[24] http://en.wikipedia.org/wiki/App_Store
[25] http://www.geekwithlaptop.com/french-customers-run-up-astronomical-bill-for-3g-internet-access
[26] http://en.wikipedia.org/wiki/Android_(operating_system)
[27] http://blogs.zdnet.com/BTL/?p=28432&tag=nl.e539
[28] http://www.iphase.com/downloads/LTETechandCompwebinar.pdf
[29] http://en.wikipedia.org/wiki/Code_division_multiple_access

proprietary standard designed by Qualcomm in the United States, has been the dominant network standard for North America and parts of Asia, whereas GSM[30] technology, that includes UMTS[31] and HSPA[32], is also known under the name WCDMA[33]. HSPA is a family of mobile telephony protocols including HSDPA[34] (up to 7.2 Mb/s downlink speed enhancement), HSUPA (up to 5.8 Mb/s uplink speed enhancement) and HSPA+[35] also known as Evolved HSPA with up to 40Mb/s downlink and 10 Mb/s uplink. Note that CDMA and WCDMA are incompatible.

Do all roads really lead to LTE in the short term, i.e. a convergence of CDMA and WCDMA? Some specialists, e.g. Dan Warren of the GSM Association, have doubts[36] "*With LTE set to become a short-term reality, rather than a long-term vision, it is easy to overlook the extraordinary impact of another young technology – HSPA. Now a standard feature in smartphones, netbooks and many laptops, HSPA is spreading mobile broadband services across the world and, in tandem with HSPA+, could ultimately emulate the longevity and widespread usage of GSM. For both GSM and CDMA mobile operators, all roads will eventually lead to LTE, but many will travel there via HSPA and HSPA+. The dilemma in the current economic climate is whether to move rapidly to LTE or focus near-term capital spending on HSPA and HSPA+.*"

### 3.5. Internet Infrastructures

A more extensive version of the following sections article is available from http://www.ictconsulting.ch/reports/CHEP2009.doc

#### *3.5.1. Academic & Research Internet*

Over time, DANTE (Delivery of Advanced Network Technology to Europe), thanks to massive European Union funding and continued support of European NRENs, successfully managed to build, mostly over leased dark fibers, the very impressive pan-European GEANT backbone with many interesting features and services, connections to the academic world in Africa, America, Asia, Caucasian (Black Sea) and Mediterranean countries.

It is interesting to note that thanks to the deployment of dark fibers and the resulting availability of cheap 10Gb/s light-paths, GEANT evolved from a single global pan-European backbone into multiple Mission Oriented Networks, e.g. DEISA, JIVE, LHC[37], i.e. back where the scientific community was some 30 years ago with mission oriented networks like HEPnet[38], MFEnet[39], NSI[40], which is actually a very good thing!

In the USA, Internet2 deployed a "High-Performance Data Transfer for Dynamic Circuit Networks" capability over its production network infrastructure dubbed PHOEBUS[41]. This new service can be activated from outside or inside the network; in the latter case it can be seen as a regular traffic engineering tool, the innovation being its automatic activation in the case of high bandwidth flows. While ESnet uses OSCARS[42] (On-demand Secure Circuits

---

[30] http://en.wikipedia.org/wiki/GSM
[31] http://en.wikipedia.org/wiki/Universal_Mobile_Telecommunications_System
[32] http://en.wikipedia.org/wiki/High_Speed_Packet_Access
[33] http://en.wikipedia.org/wiki/W-CDMA_(UMTS)
[34] High Speed Packet Access - Wikipedia, the free encyclopedia
[35] http://en.wikipedia.org/wiki/Evolved_HSPA
[36] http://www.rcrwireless.com/article/20090929/FRONTPAGE/909289993/reality-check-all-roads-lead-to-lte-eventually
[37] http://en.wikipedia.org/wiki/Large_Hadron_Collider
[38] High Energy Physics Network
[39] Magnetic Fusion Energy Network
[40] NASA Science Internet
[41] http://e2epi.internet2.edu/phoebus.html
[42] http://www.es.net/oscars/

and Advance Reservation System) to support production traffic. The main user community is the High Energy Physics (HEP) community with 21 out of 26 long term, i.e. static, virtual circuits[43] activated in October 2009, which is very similar to what can be seen in Europe over GEANT where the LHC community is, by far, the main user of dedicated "lambdas". What is more intriguing is the fact that short-term dynamic VCs have been used across ESnet on a "significant" scale, i.e. nearly 5000 successful VC reservations during the period between 1/2008 through 10/2009; however, most of these VCs have been initiated by BNL's TeraPaths[44] and FNAL's LambdaStation[45] with middleware that was precisely developed with the goal of demonstrating the use of dynamically established VCs. What is more "spectacular", in a sense, is that ESnet received ~$62M in ARRA[46] funds from the Department of Energy (DoE[47]) for an Advanced Networking Initiative (ANI) aiming at:

- building an end-to-end prototype network in order to address DoE's growing data needs while accelerating the development of 100 Gb/s networking technologies,
- providing a network test bed facility for researchers and industry.

While there is no doubt that there are classes of data intensive scientific applications that absolutely require large amount of bandwidth in order to operate successfully (e.g. HEP, astronomy, climate), while the availability of large amount of unallocated bandwidth in research infrastructures allows to develop and deploy new innovative Bandwidth on Demand (BoD) architecture and services, the question of whether these new type of services make real sense in a commercially driven Internet is, in my view, a sensible question to ask. Indeed, it is rather unclear whether there are sound commercial prospects for a mass market?

The answer maybe is to make an analogy with the commercial airplane industry where the cheapest way to fly is usually through hubs, i.e. local airport to hub, hub to hub and then hub to destination which is similar to the general purpose Internet; in contrast, direct, usually regional, flights allow shortcuts from local to destination airports, which is similar to end-to-end Internet circuits, whereas on-demand bandwidth solutions can be compared to private jet services. For once, the big science community would be travelling 1st class but are there real needs?

I contend that most needs can be satisfied with static circuits, either native, e.g. 10 Gb/s lambdas/optical circuits or emulated, e.g. with MPLS for fractional 10Gb/s circuits, i.e. typically 1Gb/s, above or below and my understanding is that this is the solution used by some research networks (e.g. RENATER) and commercial Internet Service Providers.

Whereas Grid computing was very fashionable some years ago, whereas funding agencies worldwide made considerable investments in Grid middleware and infrastructures, whereas a significant standardization effort has been put into defining open Grid protocols through the Open Grid Forum (OGF[48]), the commercial world, as exemplified by Amazon's EC2[49] service, is going into the direction of "cloud" computing. In an excellent article[50] authored by Judith M. Myerson[51] titled *"Cloud computing versus grid computing: Service types, similarities and differences, and things to consider"*, the author outlines the evolution of the grid towards cloud computing very well.

---

[43] 3 VCs for Climate related projects (GFDL, ESG), 2 VCs for computational astrophysics (OptiPortal)
[44] https://www.racf.bnl.gov/terapaths/
[45] http://www.lambdastation.org/
[46] http://en.wikipedia.org/wiki/American_Recovery_and_Reinvestment_Act_of_2009
[47] http://www.energy.gov/
[48] http://www.gridforum.org/
[49] http://aws.amazon.com/ec2/
[50] http://www.ibm.com/developerworks/web/library/wa-cloudgrid/
[51] jmyerson@bellatlantic.net

### *3.5.2. Commercial Internet*

The commercial Internet is faced with a number of very serious challenges that are threatening its long-term stability. By far the most serious problem is the IPv4 address space exhaustion which is predicted to occur within the next 2-3 years and the lack of IPv6 uptake by the commercial Internet; but there are also known DNS weaknesses (cache poisoning) that should be cured by the expected large scale deployment of DNSSEC in 2010, numerous security issues, lack of guaranteed Quality of Service (QoS), especially inter-domain QoS, poor mobility support and worrying growth of the routing table due to the fragmentation of the Internet and the increased use of Provider Independent (PI) addresses.

Lack of serious IPv6 operational deployment by commercial ISPs is clearly a direct result of the highly competitive Internet market situation with slimming profit margins; indeed, even assuming near-zero Capital Expenditures (CAPEX), the IPv6 deployment related Operational Expenditures (OPEX) will, no doubt, be fairly high.

While the common "wisdom" says that the academic and research community is still the major contributor to new major Internet technology innovations, I can only observe that, during the last decade or so, most innovations have actually come, in the form of new applications and services, through the commercial Internet, e.g. Web 2.0, sophisticated data dissemination techniques (e.g. Akamai, BitTorrent, Google, Yahoo), Web caches, content engines, network appliances, Network Address Translation (NAT[52]), Application Level Gateway (ALG), Firewalls, Intrusion Detection System (IDS), IP Telephony[53] (a complex mixture of IETF and ITU standards), Skype, Triple Play[54], Streaming media proxies, ultra sophisticated search engines like Google, Peer-to-peer[55], etc.

MPLS (Multi-Protocol Label Switched), IPSEC and SSL based VPNs (Virtual Private Network) are flourishing within the commercial Internet and are a major source of revenue in a market where, as already observed, profit margins are extremely low.

Internet TV over VDSL[56] is becoming increasingly popular and represents a serious threat to cable TV as well as terrestrial and satellite TV operators.

## 4. The predicted end of IPv4 and the long expected advent of IPv6

An IPv4 Address report is auto-generated by a daily script and is available from: http://www.potaroo.net/tools/ipv4/index.html

The report generated on 13 December 2007 predicted November 2010 as the date of the exhaustion of IANA's Unallocated IPv4 Address Pool and November 2011 as the date of the exhaustion of the RIR[57] (Regional Internet Registries) Unallocated IPv4 Address Pool. According to the December 14th report, these dates have now been pushed back to September 2011 and 2012 September respectively.

In a reason driven world the migration to IPv6 would appear to be unavoidable, however, the sad reality is that IPv6 deployment is still in its infancy and may even never happen as there is still a very strong resistance and alternative solutions/kludges, like carrier grade NATs, could extend the life of IPv4 indefinitely. In addition, translators providing a convenient way to interconnect the IPv4 and the IPv6 Internets will become widely available soon; even though it is rather obvious that a healthy Internet cannot rely on the massive use of translators, be they "carrier grade", these are likely to have a big impact.

---

[52] http://en.wikipedia.org/wiki/Network_address_translation
[53] http://en.wikipedia.org/wiki/Voice_over_IP
[54] http://en.wikipedia.org/wiki/Triple_play_(telecommunications)
[55] http://en.wikipedia.org/wiki/Peer-to-peer
[56] http://en.wikipedia.org/wiki/Very_high_bitrate_digital_subscriber_line
[57] http://en.wikipedia.org/wiki/Regional_Internet_Registry

One problem is that the time horizon of ISPs is much shorter that those of the Internet architects; indeed, Internet Service Provision is driven by short term economic incentives and the profit margins are very low due to the highly competitive business environment; hence, the business case for IPv6 seems to be nearly impossible to make and the proliferation of NATs (Network Address Translators) is likely to continue until the Internet becomes completely impossible to manage and the case for IPv6 becomes both appealing and compelling. In any case, very interesting new ideas are already emerging from the various clean-slate Internet initiatives around the world therefore on can reasonably expect that some of these more radical design approaches, e.g. a content-centric rather than a host-centric Internet using self-certifying names, can be fitted into the existing Internet.

Therefore, it is extremely difficult to predict whether real IPv6 uptake will happen in 2010, e.g. in Network World 20/3/09 *"Business incentives are completely lacking today for upgrading to IPv6, the next generation Internet protocol, according to a survey*[58] *of network operators conducted by the Internet Society (ISOC).", w*hereas the Special Network World Executive Guide sponsored by NTT (21/1/09) is titled ***"IPv6: Not If, When***[59]**?"**

Although one can only concur with the above prediction, the sad fact, however, is that large scale IPv6 deployment by major ISPs around the world did not happen in 2009, what about 2010?

In any case, there appears to be, at least, a growing consensus that the IPv4 to IPv6 migration will not happen as originally thought out back in 1994, if only because of the forthcoming shortage of IPv4 addresses that will make it increasingly difficult to comply with the "canonical" dual-stack[60] transition strategy.

In a recent IETF panel[61] it was admitted by Internet developers that the ***"Biggest mistake for IPv6: It's not backwards compatible"***:

*"Our transition strategy was dual-stack, where we would start by adding IPv6 to the hosts and then gradually over time we would disable IPv4 and everything would go smoothly," says IETF Chair Russ Housley, who added that IPv6 transition didn't happen according to plan. In response, the IETF is developing new IPv6 transition tools that will be done by the end of 2009.*

Similarly, when asked the question ***"are NATs for IPv6 a necessary evil?"*** Russ Housley answered: *"They are necessary for a smooth migration from IPv4 to IPv6 so that the important properties of the Internet are preserved...we need to be pragmatic!"*

The above statements are very welcomed signs that paradigms are changing in the right direction, e.g. "end to end" is no longer a dogma, NATs are no longer evils, communication between IPv4 only and IPv6 only hosts is no longer deemed impossible. One can therefore hope that the IETF will soon specify the much needed new standards that could greatly facilitate a graceful transition towards IPv6.

## 5. Short Review of Internet "clean-slate" initiatives

Given the "stalled/ossified" state of the Internet and its inability to move forward in a coherent manner, some of the key players, e.g. the US National Science Foundation (NSF) through GENI and FIND, the European Union (EU) through the "Future Networks[62]" and "Future Internet Research Experimentation (FIRE[63])", Japan's National Institute of

[58] http://www.isoc.org/pubs/2009-IPv6-OrgMember-Report.pdf
[59] ksc.exportcenter.go.kr/_common/download/download_file.jsp?fileSeq=9999989979692
[60] http://www.rfc-archive.org/getrfc.php?rfc=1671
[61] http://networking-world.blogspot.com/2009/03/developers-admit-biggest-mistake-on.html
[62] http://cordis.europa.eu/fp7/ict/future-networks/
[63] http://cordis.europa.eu/fp7/ict/fire/

Information and Communication Technology (NICT[64]) through the Akari[65] project, but also some of the prestigious Universities that contributed the most to the Internet concepts and architectural principles, e.g. Cambridge University (UK), MIT & Stanford University (USA), have launched their own Internet "clean-slate" design programs.

NSF's GENI[66] (Global Environment for Network Innovations) is basically a flexible and reconfigurable network "test-bed" allowing multiple slices to be allocated to different user groups to validate their new architectural proposals. The GENI Research plan[67] is an evolving document which is most interesting to read as it very well describes a number of new "disturbing" concepts like "buffer-less[68]" routers, for example. The FIND[69] (Future Internet Design) program solicits "clean slate process" research proposals in the broad area of network architecture, principles, and design, aimed at answering these questions. *"The philosophy of the program is to help conceive the future by momentarily letting go of the present - freeing our collective minds from the constraints of the current.".*

It is, in fact, very surprising to find that so few public results are coming out of the GENI and FIND initiatives, despite all the *"hype"* that accompanied their launch. It is also very disappointing to observe similar *"opacity"* from Stanford University and MIT's (Communication Futures Program[70]) clean-slate projects.

In contrast, the European Union FP7 programs like "The Network of the Future[71]" and "Future Internet Research & Experimentation (FIRE[72])" have not gained much visibility inside and outside Europe, despite the fact that these projects are not only very interesting but also very open, i.e. most deliverables are public. Indeed, the EU initiated a number of extremely challenging projects, e.g. 4WARD[73], ANA[74], Ambient[75], PSIRP[76], TRILOGY[77]. The 4WARD project is particularly interesting as it is driven by the Wireless World initiative (WWI[78]) that aims to contribute to a clean-slate Internet design from a global, including mobile and wireless, perspective.

## 6. Internet Governance

This chapter was originally developed in the "State of the Internet & Challenges ahead" article and then updated in "Where is the Internet heading to?"

This chapter was never meant to be exhaustive given the huge number of actors and its only intent was to clarify the roles of the Internet Corporation for Assigned Names and Numbers[79] (ICANN), the Internet Society[80] (ISOC), the Internet Architecture Board[81] (IAB)

---

[64] http://en.wikipedia.org/wiki/National_Institute_of_Information_and_Communications_Technology
[65] http://en.wikipedia.org/wiki/AKARI_Project
[66] NSF's GENI
[67] http://www.geni.net/GDD/GDD-06-28.pdf
[68] http://www.sigcomm.org/co-next2007/papers/papers/paper15.pdf
[69] NSF's Future Internet Design (FIND) Program
[70] MIT's Communication Futures Program
[71] http://cordis.europa.eu/fp7/ict/future-networks/
[72] http://cordis.europa.eu/fp7/ict/fire/
[73] http://www.wireless-world-initiative.org/Innovation%20Day%202007/FP%207%20plans%20pa3.pdf
[74] http://www.ana-project.org/
[75] http://www.ambient-networks.org/
[76] http://www.psirp.org/
[77] http://www.trilogy-project.org/
[78] http://www.wireless-world-initiative.org/
[79] http://www.icann.org/
[80] http://www.isoc.org/
[81] http://www.iab.org

the Internet Engineering Task Force[82] (IETF), the Internet Governance Forum[83] (IGF), the OECD[84], the ITU and the European Union. The ITU and EU sections being fairly new and having been updated recently are reproduced here.

Regarding ICANN there has been a major policy change in September 2009 where ICANN announced the signature of a new 'Affirmation of Commitments' allowing it to break free from the US Government and be that long-sought-after international body. However, ICANN has confirmed that it will continue to be based in the United States.

### 6.1. ITU

For various reasons the ITU does not have a very good image in the Internet community, maybe because of its role in establishing the IGF, maybe for other reasons, e.g. failed standards like X.400, I personally believe that this poor image is largely undeserved given that the ITU has been very active on many fronts, e.g. QoS, Next Generation Networks (NGN) and a simplified version of IETF's MPLS, i.e. without dynamic signaling, called T-MPLS which is currently being reworked by the IETF under the name MPLS-TP in order to meet ITU's transport network needs.

More recently, ITU has started an annual Kaleidoscope event[85] *"aiming to increase the dialogue between experts working on the standardization of information and communications technologies (ICTs) and academia"* and a new Focus Group on Future Networks (FG-FN[86]).

However, reusing acronyms can be very confusing! For example, ITU's NGN only refers to the migration of the legacy telephone network and the new cellular phone networks over an IP based infrastructure and, although it claims to be a step beyond the existing Internet because of the built-in QoS, which is obviously necessary in order to support real-time delay and packet loss applications, it is not meant to address the future Internet as rather clearly shown in the following figures extracted from Tomonori Aoyama's (Keio University, NICT) presentation[87] at ITU's Kaleidoscope event in Geneva[88] (June 2008). The same remark can also be made about T-MPLS.

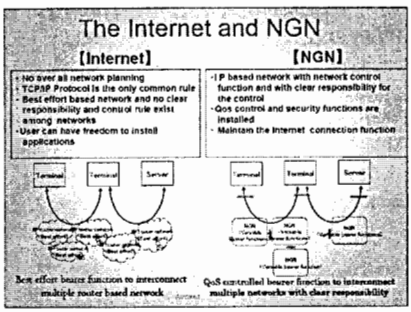


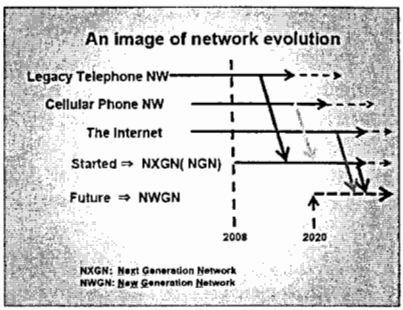


[82] http://www.ietf.org
[83] http://www.intgovforum.org/index.htm
[84] OECD's Science Technology and Industry Directorate http://www.oecd.org/sti/
[85] http://www.itu.int/ITU-T/uni/kaleidoscope/
[86] http://www.itu.int/ITU-T/newslog/Group+To+Track+Global+Future+Network+RD.aspx
[87] http://www.itu.int/dms_pub/itu-t/oth/29/01/T290100100010001PDFE.pdf
[88] http://www.itu.int/ITU-T/uni/kaleidoscope/2008/programme.html

### 6.2. European Union

The EU has made numerous, rather unsuccessful, attempts to influence directly or indirectly the deployment of Internet or stated differently to counterbalance the influence of the US government. However, a Future Internet Assembly[89] (FIA) that is due to meet twice a year has been successfully started under the auspices of the EU in Bled (Slovenia) and continued in Madrid (Dec. 2008), Praha (May 2009) and Stockholm (November 2009).

## 7. Internet evolution scenarios

The uncertainties around the wide adoption of IPv6 and the impact of the clean-slate programs are such that even the best Internet specialists are very unsure, but at least three scenarios are possible:

1. no changes (i.e. the Internet remains largely IPv4 based with increased use of NATs),
2. migration to IPv6 (for sure IPv6 use will continue to grow but how fast and when can one reasonably expect the Internet to become IPv6 based with only residual IPv4 islands?),
3. clean-slate (i.e. radical new design). Even the clean-slate proponents all agree, I think, that a clean-slate Internet will need to coexist and interwork for many years, if not for ever, with the existing Internet, be it IPv4 or IPv6 or both.

Likewise, campuses will have to choose between:

1. Full IPv6 migration (i.e. dual stack everywhere) which is, in practice, very difficult because of old legacy equipment,
2. Status quo (i.e. IPv4 as today) an unlikely though plausible scenario with connectivity to the IPv6 world through external gateways,
3. Mixed (i.e. partial migration), implies some partitioning of the campus, e.g. dual stack servers, desktop PCs, printers, etc. unchanged.

At first sight it looks like the deployment of IPv6 in the commercial Internet is somewhat easier, despite the fact that most, if not all, academic and research Internet backbone are already dual stack. Indeed, the commercial Internet is driven by commercial incentives, so, as soon as the business case becomes compelling, IPv6 deployment is likely to happen very quickly. In particular, it appears somewhat simpler to deploy new IPv6 aware ADSL routers with new firmware than converting very large campuses.

In any case, ICT, in general, and the Internet, in particular, will, no doubt, become "Greener".

Wired as well as wireless broadband access (i.e. Mb/s→Gb/s) will become nearly ubiquitous in a very fast evolving technology framework.

Use of MPLS will most certainly continue to increase. Although overly complex according to some, because of its connection oriented features and the associated signalling, MPLS has many interesting properties for Internet Service Providers, namely: traffic engineering, QoS delivery, provision of layer 2 or layer 3 Virtual Private Networks (VPN), departure from the destination based routing paradigm, implementation of the "routing at the edges, switching in the core" principle in order to remove complexity from the network core and push it at its edges. There are several MPLS variants: IETF's MPLS/VPLS including "Pseudo Wires" (PWE3), ITU's, a simplified version of IETF's MPLS without dynamic signalling, currently being reworked by the IETF under the name MPLS-TP in order to meet ITU's transport network needs, IEEE's PBB-TE (802,1Qay), Provider Based Transport, which was initiated by Nortel and is similar to T-MPLS but is Ethernet based.

Regarding streaming and QoS, will streaming technology overcome P2P technology or the other way round and will inter-domain QoS ever become a reality?

[89] http://www.future-internet.eu/

## 8. Concluding remarks

The conclusions of this article are essentially copied from the previously quoted "Where is the Internet heading to?" article.

There is little doubt that the most urgent problem is the exhaustion of the IPv4 address space. Strangely enough, this is not currently seen as a high priority item by most ISPs; however, IPv6 looks unavoidable some day, especially if one adopts the "conventional" view that all Internet capable devices, e.g. mobile phones, sensors, home appliances, RFIDs, etc., must be directly accessible, but, is this really desirable or even sound? In any case, the IPv4 Internet cannot continue to grow "as is" beyond 2012 or so, therefore, increased deployment of IPv6 looks "almost" unavoidable. What is much less clear, though, is the level of seamless interoperability that will really be achieved between these two Internets as well as their relative importance during the years to come. In the meantime, NAT like solution, even so considered as "kludges", are likely to continue to flourish and could even slow down considerably, if not prevent, the deployment of IPv6. Whether an IPv4 trading market will really develop and how it may impact the operational deployment of IPv6 is also impossible to assess at this stage.

The next most urgent problem is to solve the continuous growth of the routing tables that is endangering the growth and the stability of the Internet, but this should be much easier to handle as the core Internet routers market is still largely dominated by Cisco and Juniper. The proliferation of security threats and the associated "degeneracy" of the Internet, i.e. the deployment of patches/bandages, will no doubt continue as the time horizons of the Internet Service Providers and the clean-slate Internet architects are so different. Even though it is badly needed, the future of inter-domain QoS, remains very unclear!

The last major Internet architectural change was the introduction of MPLS, will it be the last one given the operational flexibility it brings, in other words will there ever be a "clean-slate" Internet? The increasing lack of "network neutrality" as well as the increase of copyright infringements and the related attempts to regulate the Internet in a lawful manner are also very preoccupying.

New business models will be necessary anyway, a mostly "free" Internet cannot go on forever, but are Internet customers ready to pay more?

## 9. Acknowledgments

Many thanks to Bill S[t] Arnaud (Canarie), Brian Carpenter (University of Auckland), Tomonori Aoyama (Keio University, NICT), Paulo Desousa (European Commission[90]) for their significant input to this article.

**Olivier Martin** was the Project Leader of the European Union DataTAG project. He received an M.Sc. degree in EE from École Supérieure d'Électricité (Supélec), Paris, France in 1962. He joined CERN in 1971, held various positions in the Software Group of the Data Handling Division, and then moved to the Communications Group of the Computing & Networks Division in 1984, where he has been Head of the External Networking Section from 1989 until 2004. Prior to the DataTAG project, he was involved in several European projects (including BETEL, BETEUS and STEN) in the framework of the RACE, ACTS and TEN programs. His research interests include next generation Internet, high-speed networking, transport protocols and Grids. Since August 2006, he is working as an independent ICT consultant.

[90] Information Society & Media, Directorate D "Converged Networks & Services/Future Networks"

# "Faster" LRC shaping circuit for NaI(Tl) scintillation detectors

G. Mitev, M. Mitev, L. Tsankov
*Technical University, Sofia, Bulgaria*

LRC shaping of the analogue output signal arising in the anode circuit of a photomultiplier tube (PMT) is rarely used as a processing method due to its very large dead time. An alternative approach is considered in the present work which allows a significant increase of the resonant frequency of the LRC circuit and thus the dead time is noticeably reduced. A schematic design is proposed based on the idea first to collect the total charge generated in the PMT into a free capacitor and then to adjoin an inductance to that capacitor using a quick electronic switch. Test results demonstrating the applicability of the method are presented and discussed.

**Keywords**: increased performance, RLC shaping, NaI(Tl) scintillation detectors.

## Introduction

Scintillation detectors are widely used to register the parameters of ionizing radiation due to the large variety of scintillators as well to the high sensitivity and the good stability of modern photomultipliers (PMT). In order to achieve high sensitivity, good energy resolution and high performance it is necessary to ensure full collection of the charge generated in the PMT anode, linear dependence between the output signal amplitude and the input charge in a wide dynamic range and fast recovery of the shaping circuit [1].

Adding an inductance in the PMT's anode chain deteriorates pulse shaping conditions by introducing slowly fading oscillations of the signal; so, measures are assumed to minimize the stray inductance.

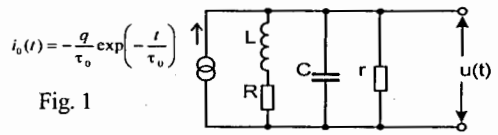


Fig. 1

Nevertheless, in the 1960's and 1970's several schemes have been proposed based on the idea to use PMT output pulses to generate fading oscillations into a LC circuit [2, 3, 4, 5]. The equivalent diagram of the anode chain with an added inductance is shown on Fig. 1. Its analysis [10] yields to the following conclusions which are important for an optimal signal shaping:

1. *u(t)* is strictly proportional to the charge *q*, generated into the PMT anode chain, i.e. to the energy deposited by the ionizing agent into the scintillator.
2. The transient process is due to the finite duration of the exciting current $i_0(t)$. It decays with a constant $\tau_0$ which is determined by the external conditions (decay constant of the scintillator and the transient characteristic of the PMT).
3. The stationary process is of oscillation type; it decays with a constant depending on the LRC circuit parameters.
4. No zero-level shift is observed after the end of the transient process. This is particularly important for the subsequent signal processing.

The requirement for a full charge collection limits the maximum resonance frequency of the LC circuit. As an example, 90% of charge can be collected if the period of the oscillations T is $T \geq 12\tau_0$, $\tau_0$ being the characteristic decay time of the scintillation pulse. For NaI(Tl) crystals $\tau_0 = 230ns$, so the resonance frequency is limited to $T^{-1} \leq 360kHz$.

Applying an amplitude discriminator, the free oscillations of the LC circuit can be converted into a bunch of rectangle pulses whose number is proportional to the logarithm of the energy deposited in the detector. Therefore, a logarithmic energy spectrum is obtained if the detector events codes are sorted into a histogram memory [8]. If a 256-channel spectrum

is used (which is comparable in spectrum details with a 1024-channel linear spectrum [9]) then the necessary processing time is extended up to 7ms. So, despite of its very attractive simplicity, the applicability of this pulse processing method is limited to low intensity radiations only.

The purpose of the present investigation is to find methods and circuit techniques aimed at a significantly increase of the working resonance frequency of the LC shaping circuit keeping the charge collection efficiency as high as possible.

## Method

### Signal processing using a RC-Sw-L (RC – switch – L) chain

In order to overcome the above mentioned restrictions we propose to collect the anode charge of PMT by a shaping capacitor $C_{in}$ and, after a time interval $t \geq 5\tau_0$ (which guarantees charge collection efficiency of more than 99%), a proper inductance $L$ to be adjoined to $C_{in}$. In this way the resonance frequency of the LC circuit is made independent of the decay constant of the scintillator $\tau_0$ and can be chosen considerably higher, thus reducing the dead time of the shaping circuit.

An analogue switch has to be used to configure the LC circuit at a proper time. The equivalent diagram of the PMT anode chain is shown on Fig.2. Its analysis can be divided into two phases. The charge is almost fully collected during the first phase (for a time interval $t \geq 5\tau_0$). Then the switch S is activated by the control electronics (not shown on the figure) and the inductance L is adjoined to the charged capacitor to form a LC circuit with freely fading oscillations. The resonance frequency of the LC circuit can be conveniently chosen because the whole signal (the PMT anode's charge) is already collected into C.

$$i_0(t) = -\frac{q}{\tau_0}\exp\left(-\frac{t}{\tau_0}\right)$$

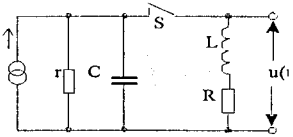


Fig. 2

### Problems, limitations, solutions

The realization of the described method meets the fact that any real switch has a finite resistance in on-state and a non-zero capacitance in off-state. Some charge is also being transferred between the control chain and the commutated chain during the switching process. Taking into account that the voltage across the capacitor can exceed 10V, the choice between the existing analogue switches is very limited. All these parameters have strong influence on the signal shaping quality; so, their effects have to be precisely analyzed and compensated as far as possible.

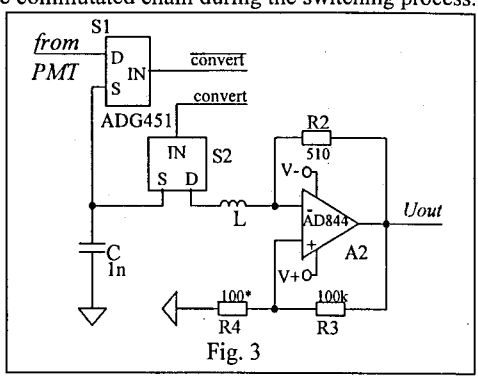


Fig. 3

### Principal diagram

The principal diagram is shown on Fig. 3. It includes a LC circuit, two analogue switches and an input amplifier. The switch S2 connects the inductance L to the charged capacitor C and thus configures a LC

circuit. The input chain of the amplifier A2 is also included in the LC circuit. A2 is realized as a trans-impedance amplifier with very low input impedance. A CFA of type AD844 is used due to its large output amplitudes dynamic range. An ADG451 is used as an analogue switch, having input impedance 4Ω and switch dynamics up to ±15V.

**Influence of the active resistance of the switch**

The active resistance of the analogue switch increases considerably the energy loss in the LC circuit. An effective 'increase' of the quality factor of the LC circuit can be achieved by returning a part of the energy back into it [5]. This cannot be done directly in the scheme of the input amplifier used since its output voltage simply repeats the LC current signal, i.e. it is shifted by $\pi/2$ towards the LC voltage. However, introducing a small positive feedback $\alpha=R4/R3$ in the input amplifier compensates partially the energy loss in the LC circuit. The amplifier output is shown on Fig.4 for different values of $\alpha$.

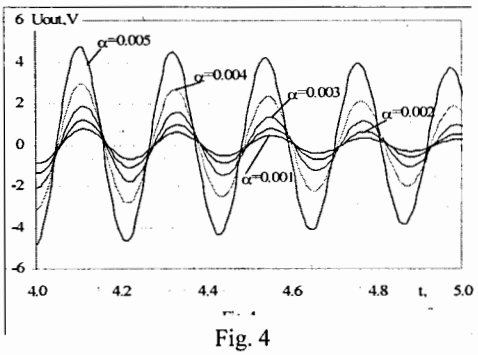

Fig. 4

The feedback depth $\alpha$ can be easily regulated, so, the channel-energy dependence can be precisely tuned according to the energy range of interest.

**Influence of the stray capacitance of the analogue switch**

The switch used AD451 has a stray capacitance of 37 pF in off-state. It is serially connected to the LC circuit's capacitance C. So, their equivalent capacitance and the inductance form always a LC circuit, whose resonance frequency is much higher at off-state of the switch.

Fig. 5. illustrates the work of the scheme showing the input current pulse $I_{IN}$, the voltage across the LC circuit's capacitor $U_C$ and the amplifier's output voltage $U_{OUT}$. It is seen that a very good charge collection efficiency is obtained ($U_C$ reaches a steady value). It is also seen that the period of the freely fading oscillations of the LC circuit (after switching the analogue switch 'on') is much smaller than the decay constant of the input signal. The LC circuit resonance frequency shown on the figure is 5 MHz.

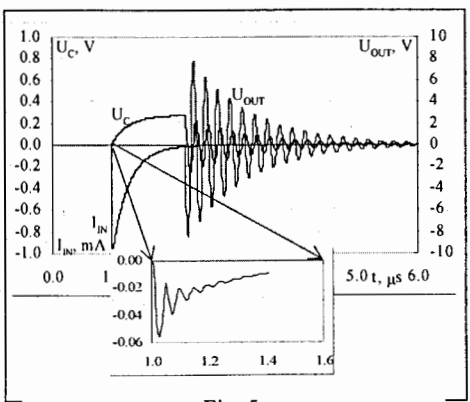

Fig. 5

The stray capacitance effect of the opened switch appears at the beginning of the charge collection process into the main capacitor - see the zoomed part of the diagram in Fig. 5. Then some high frequency and fast fading oscillations are generated at the amplifier's output (in that case with a frequency about 25MHz), which are imposed on the transient

process. The greater is the $C_{in} / C_{stray}$ ratio, the smaller is their amplitude. This parasitic signal is easily ignored in the next processing stage since it is out of the shaping time interval.

**The influence of the charge injection**

Another important parameter of the analogue switch is the amount of charge injected from the control chain into the commutated chain. This value for ADG451 is $20pC$. Unfortunately, that charge is injected directly into the LC circuit and is thus added to the useful signal. It leads to an increase of the minimum detectable charge (energy) of the input signal.

A possible way to compensate this effect is to add a second analogue switch into the charge injection point. The outputs of both switches are connected together and the control of the compensating switch S1 is realized by a signal in anti-phase with that controlling the basic switch S2. Commutating both switches simultaneously the charges injected by them are approximately equal but with opposite signs; so, the equivalent charge injected into the LC circuit should be much smaller.

As a compensating switch in our diagram is used S1, which separates the anode chain of the PMT from the shaping circuit during the signal processing. S1 and S2 are driven in anti-phase in order to partially compensate the charge injected into the LC circuit.

**Conclusion**

A method for signal processing by RLC shaping of the scintillation detectors signals is proposed. It overpasses the limitation for increasing the LC circuit resonance frequency imposed by the decay constant of the scintillator. The processing time for a code 256 is 54 μs at 5MHz and it can be made twice smaller by using both positive and negative half-waves of the fading oscillations. Taking into account the fact, that a 256-channel spectrum with a logarithmic energy scale is equivalent in respect to the spectrum details to a 1024-channel linear spectrum, the performance of the proposed solution approaches that of the multi channel analyzers of Wilkinson type.

**Acknowledgements**

This work is supported by the Bulgarian National Science Fund under contracts ВУНЗ - 01/06.

**References**

[1] A.G. Wright, Amplifiers for use with photomultipliers – who needs them?. Nuclear Instruments and Methods in Physics Research, A 504 (2003), pp. 245-249.

[2] J.C. Barton, A. Cripin, Simple logarithmic pulse height analysers, Nuclear Instruments and Methods, 16 (1962), pp. 39-43.

[3] А. Гадалов, Ю. Минеев,И. Рапопорт, Логарифмический амплитудно-числовой преобразователь на колебательном контуре с демпфирующим устройством. ПТЕ №5 1966г., с.144-146.

[4] В. Степанов, Логарифмический преобразуватель амплитуды импульсов, ПТЕ №3 1969 г., с. 115-118.

[5] J.C. Barton, A.F. Munas, A.G. Wright, Improved Ringing Coil Pulse Encoders, Nuclear Instruments and Methods, 92 (1971), pp. 89-91.

[6] M. Mitev, Ch. Lenev, Charge to Digital Logaritmic Resonanse Converter, Proceedings of the National Scientific Conference "Electronics '99", 1999, book III, pp. 28 -33.

[7] M.G. Mitev, T.B. Lenev, L.T. Tsankov, An Improved Resonant Charge-Code Trnsducer, Proceedings of the Tenth International Scientific and Applied Science Conference "Electronics ET'2001", 2001, book 1, pp. 111 – 124.

[8] M. Mitev, L. Tsankov, Ch. Lenev, A Spectral Analyser With a Logarithmic Energy-Code Characteristic - Nature, Features, Advantages and Drawbacks, Proceedings of the 12 International Scientific and Applied Science Conference "Electronics ET'2003", 2003, book 2, pp. 30 - 35.

[9] L. Tsankov, M. Mitev, Ch. Lenev, LC circuit as a pulse-height analyser for NaI gamma spectrometry. Nuclear Instruments and Methods in Physics Research, A 533 (2004), pp. 509-515.

[10] M. Mitev, L.T. Tsankov, Optimization of a RLC shaping circuit for NaI(Tl) scintillation detectors, Proceedings of the 14 International Scientific and Applied Science Conference "Electronics ET'2005", 2005, book 2, pp. 199 – 204.

# New proposals for Zeno effect study

L. Nadderd[1], A.N. Polyakov, K. Subotic[1], Yu.S. Tsyganov, V.B. Zlokazov
*Joint Institute for Nuclear Research, Dubna, Russia*
*[1] VINČA, Belgrade, Serbia*

The general considerations of problem of decay of the unstable systems demonstrated that decay rate of a quasi-stationary state does obey exactly exponential law [1]. In continuation of reported preliminary measurements [2] on the $^{220}Rn \rightarrow {}^{216}$ Po alpha-active system, the new $4\pi$ detector pair method is proposed for checking of assumed exponential decay law. In addition to this main task this set up will be used to study the statistical properties of pair correlated signals, arising from genetic links to CN produced in heavy ion nuclear reactions.

## 1. Introduction

The consideration of general problems of the unstable systems by Khalfin **[1]** demonstrated that the decay rate of a quasi-stationary state does not obey exactly the exponential law. The evidence of the non-exponential decay of a quasi-stationary state was performed on the basis of the general quantum-mechanical presumptions. The decay rate deviations from the exponential law were expected for very short and very long times after the set up of the quasi-stationary states **[2].**

Fonda et al. **[3]** have analyzed a decay model and showed that in some circumstances significant deviation from the exponential decay law could occur at about 10 lifetimes and the inverse power-law domination could occur at about 25 lifetimes.

As it concerns the relatively short lifetime range, observation of $^{220}$**Rn** $\rightarrow$ $^{216}$**Po** chains is a good model to study these effects due to the relative short $^{216}$**Po** lifetime what means that there is no need of any beam time **[4].** In connection with the mentioned above, the goal of the present paper is the developing of mathematical approach to the case of lifetime estimation in a short time region.

## 2. Measurements: present status

Most of the measurements were performed with the surface-barrier **n-Si(Au)** detectors pair (~80% from $4\pi$ geometry). Schematic of the measurement process is shown in the Fig. 1.

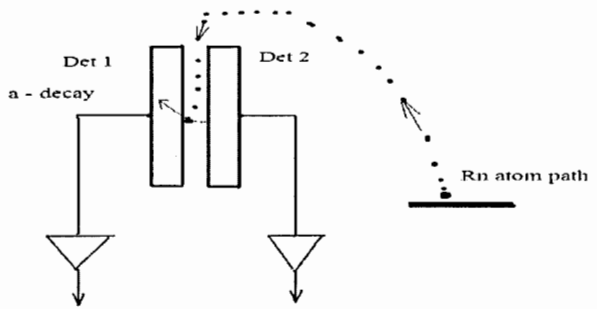


Fig. 1. Way for **Rn** atom to reach the active detector area is shown by dots

**Results**: Several decay curves were measured for $^{220}$**Rn**→$^{216}$**Po** decays (Fig. 2 e.g.)

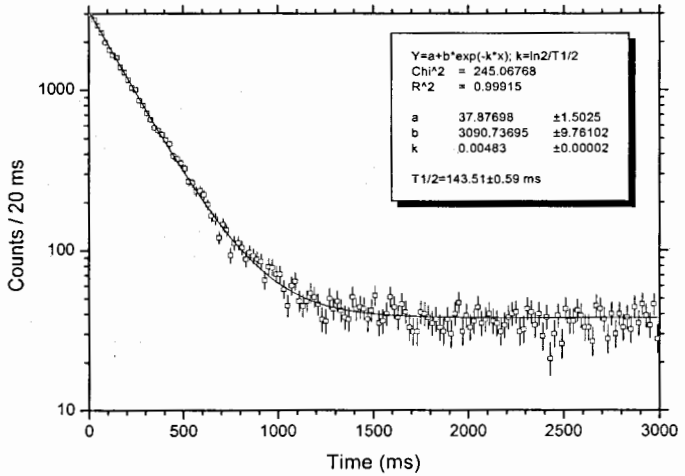


Fig. 2. Decay curve for $^{220}$**Rn** →$^{216}$ **Po** α-α correlated sequences **[3]**

Result: within ~ +/- 15% error interval no difference in $T_{1/2}$ for main region and in the vicinity of 1/5 half-life region.

**3. Nearest future developments: proposals**

We ***plan*** to improve experimental method by:

a) Using position sensitive PIPS (CANBERRA NV) detector (also, efficiency **~85%** from 4π if one use signals from he side detector)

b) Probable, a part of decaying **Rn** atoms may stop in the surface layer of the first detector→ therefore, one can measure direct α-α energy-time-position correlation and this provide radical random event background suppression due to position sensitivity and good resolution of PIPS detector (Fig. 3). To a first approximation this effect (additional recoiling Po atom adhesion) may take place due to non -uniformity of the detector surface.

c) An alternative way to use detector (PIPS) pairs with extra thin dead layer and geometry much close to 4π.

d) *Application of more perfect mathematical algorithm* to measure half-life value under condition of indefinite "Mother-daughter" relation [4].

(On this item see also *report of V.B. Zlokazov* at the present **NEC 2009** Symp.)

Main goal: to increase the efficiency of $T_{1/2}$ estimate.

(!) And of course, this approach can be applied for nuclear reaction study, especially if one detects EVR-alpha sequences with PIPS detector.

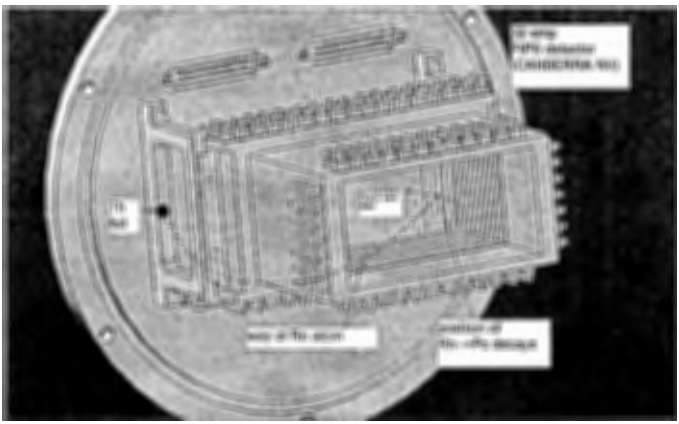

Fig. 3. Schematic of new series of measurements with 32 strip PIPS detector

## 4. Summary

1) First test measurements with the mentioned detection system and data processing are in progress now. We plan to finish the tests during 2009 – beginning of 2010.

2) Additionally, $^{220}Rn \rightarrow ^{216}Po$ correlation sequences measurements are a good beam-less tests for any mathematical models aiming to the calculation of probability parameters.

## References


[1] A. Khalfin, Zh. Eksp. Teor. Fiz. 33 (1958) 1371.

[2] L. Nadderd, Yu. Tsyganov, K. Subotic et al., in Proc. of NEC'2007 Symp., Sept. 2007, Varna.

[3] L. Nadderd, Yu. Tsyganov et al., in Proc. of NEC 2007. Sept., Varna, p. 362.

[4] V.B. Zlokazov, Yu.S. Tsyganov, submitted to Nucl. Instrum, and Meth, in Phys. Res.

# A possibility of the use of an avalanche photodiodes in spectrometry systems for ore measurement

Nguyen Manh Shat[1], Nguyen Minh Son[2], Phung K.N. Ho[2]
[1] *Joint Institute for Nuclear Research, Dubna, Russia*
[2] *VAST, Vietnam*

## Introduction

In recent years, due to changes in economic conditions, growing interest is the fast qualitative determination of metals in the laboratory and field conditions, especially gold and silver ores, but with a high-metal content.

Usually, for measuring the quality of gold and silver ores one uses activation method with semiconductor detector, which requires cooling with liquid nitrogen. However, this technique not suitable for use in field conditions.

The authors therefore suggested a more convenient method of measurement using combination of scintillate and avalanche photodiode instead of a semiconductor detector, and it is much easier to use, has lesser cost, and also it possible to use in any sites makes.

## Facility

How in the world and so in Vietnam the feature of measuring of a quality of gold and silver ores is important and necessary procedure for extraction of these expensive metals. For the past few decades, the technique used activation method with a semiconductor detector, which requires cooling with liquid nitrogen. In laboratory conditions it is well made, but it troubles exploitation and increases a value of cost of work. From the analysis of publications for the past few years relating to the issue of avalanche photodiode, it should be noted some interest in a more convenient method of measurement using a combination of scintillate and avalanche photodiode.

We have been tasked to develop methodology for the nuclear-electronic extraction gold and silver ores. It is else called the X-ray fluorescent method (in the future and silver group metals) from ore samples with subsequent determination of their concentrations using X-ray fluorescence device.

X-ray radiometric method of analysis is based on the excitation of atoms of the analyzed elements with the help of the primary study of the radioactive isotope and the subsequent registration of the characteristic radiation of atoms excited by special radiometric equipment.

Scientific and technical basis for the creation of X-ray radiometric method of analysis have been major advances in the field of obtaining radioisotope sources of nuclear radiation, as well as successes in the field of radiometric methods for the registration of various types of ionizing radiation, in particular the soft $\gamma$-and X-rays.

Schematic diagram of measurement of radiation and schematic crossection of this tripod is shown in Fig. 1.

PC using for data processing of X-ray fluorescence spectrometers, as well as for processes of control and measurement of accumulation, resulting to a significant improvement in quality and quantity of information an a composition of matter, provided a qualitatively new level of analytical definitions.

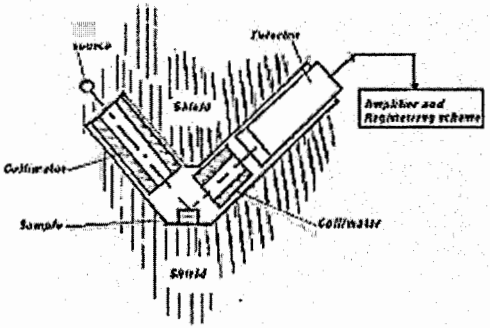


Fig. 1. The principle scheme of the measurements of the radiation and present schematic cut of the stand

Using radioisotope source Cd - 109, or Fe - 55 initiated X-ray radiations L - A series of gold and silver, which is measured by the combination of scintillate and avalanche photodiode and a multichannel analyzer (based on a PC notebook, and ADC, which is connected separately to the PC).

The resulting spectrums were processed on the PC with the original program (AN- MCA). The program can analyze the basic characteristics of the spectrum:

- To calculate the centroids of the peaks, the energy resolution (at the half and 1 / 10 the height of the peak), as well as cause other statistical data on the spectrum. There are 3 areas of the allocation of interest (areas);
- Measurement of the spectrum;
- Resulting spectrum of the given magnitude scale of energy;
- Identification and computation of the background in the work area;
- Fit the reference Peak L - A series of gold and silver in the points of the spectrum in the windows. Then the calculated the peak of the L-A and L-B areas of gold are resulted to the same peaks of silver. The average of the relation was used as an analytical parameter. Treated spectrums of gold and copper are shown in Fig. 2a, b. Here has used combination of scintillate NaI and ADP of the company Hamamatsu.

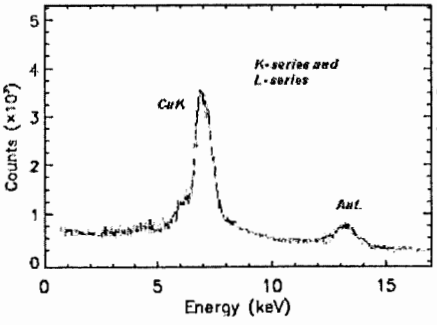


Fig.2a

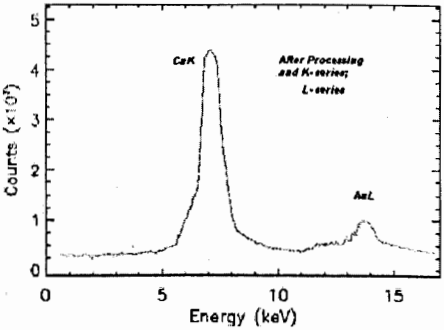


Fig.2b

* The Gold ~ 20 Mkg on Copper and Ceramic pacrage.

In the device are included:

- Detector (combination of scintillate and avalanche photodiode);
- Tripod (screen, collimator, holder for a sample, radioactive source);
- Preamplifier and spectrometric amplifier;
- Block of power conversion;
- Block ADC;
- Portable PC.

The basic element is an integral plate, on which are placed low voltage transformers, high voltage transformer, ADC-converter, thermo-controller board, timer and batteries. The system is designed for use in industrial and laboratory environments.
To process the spectrums is developed by AN-MCA, which is a 32 bit application running under control of operating systems Windows-95/98, NT.

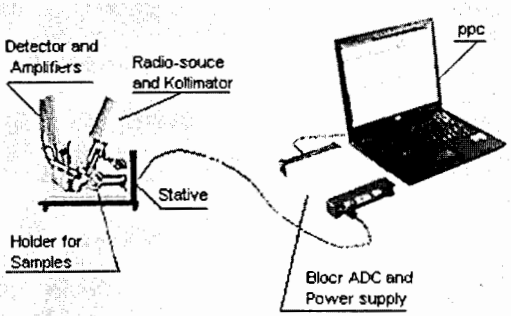


Fig. 3

The spectrometric system with scintillates and avalanches' photodiodes used for the control of technological processes of extraction and control of ore of the Geology Ministry and VAST in Vietnam (Fig. 3).

**Conclusion**

Spectrometric analyzer system with scintillate and avalanche photodiode is designed to convert the quanta of X-ray and gamma-radiation in proportion to the amplitude of electrical signals.

It can be used in spectral analysis and applied in the fields of geological dubiety of ore quality to determine the elemental composition of materials, monitoring of the ore quality. In the latter as of a unit and its earlier prototypes will be used by VAST-inspectors for a number of same future years in Vietnam.

**References**

[1] M. Moszyński, M. Kapusta, M. Balcerzyk, M. Szawlowski, D. Wolski, Large area avalanche photodiodes in x-rays and scintillation detection, Nucl. Instr. and Meth. A, 442(2000)230.

[2] M. Moszyński, M. Szawlowski, M. Kapusta, M. Balcerzyk, D. Wolski, Large area avalanche photodiodes in x-rays and light detection, IEEE Trans. on Nucl. Sci., 47(2000)1297.
[3] M. Kapusta, M. Moszyński, M. Balcerzyk, K. Leśniewski, M. Szawlowski, Avalanche photodiodes in scintillation detection for high resolution PET, IEEE Trans.on Nucl. Sci. (in press).
[4] M. Moszyński, M. Kapusta, M. Balcerzyk, M. Szawlowski, D. Wolski, I. Węgrzecka, M. Węgrzecki, Comparative study of avalanche photodiodes with different structures in scintillation detection, IEEE Transactions on Nuclear Science (in press).
[5] M. Moszyński, M. Kapusta, M. Balcerzyk, M. Szawlowski, D. Wolski, I. Węgrzecka, M. Węgrzecki, Comparative study of avalanche photodiodes with different structures in scintillation detection, IEEE Nucl. Sci. Symp. Lyon, Francja, 15-20.10.2000.
[6] M. Balcerzyk, M. Moszyński, M. Kapusta, Timing properties of LuAP:Ce studied with large-area avalanche photodiodes, 31-st Crystal Clear Meeting, Gandawa, Belgia, 23-24.03.2000.
[7] M. Moszyński, Avalanche photodiodes in X-ray and scintilation detection, FZR Rossendorf, Germany, 15 March, 2000.
[8] M. Moszyński, Avalanche photodiodes in scintilation detection, Working meeting of ICANOE Polish group, IPJ Warsaw, 21 Febr., 2000.
[9] К.Н. Мухин, Экспериментальная ядерная физика, том I, Физика атомного ядра, М: Энергоатомиздат, 1983.
[10] К. Клайнкнехт, Детекторы корпускулярных излучений М: Мир, 1990.
[11] Ю.П. Гангрский, Б.Н. Марков, В.П. Перелыгин, Регистрация и спектрометрия осколков деления, М: Энергоатомиздат, 1982.
[12] К. Групен, Детекторы элементарных частиц, Новосибирск, Сибирский хронограф, 1999.
[13] Ю.К. Акимов, О.В. Игнатьев, А.И. Калинин, В.Ф. Кушнирук, Полупроводниковые детекторы в экспериментальной физике, М: Энергоатомиздат, 1989.

# Software for organizing the information & data support for scientific community activities

E.G. Nikonov, D.A. Oleynik, A.Sh. Petrosyan, A.V. Prikhodko, R.N. Semenov
*Joint Institute for Nuclear Research, Dubna, Russia*

The main aim of this work is the design and development of the all-purpose multiplatform software based on .NET technology for information & data support for scientific community activities as well as for holding scientific events (conferences, meetings, workshops, etc). Work with this software doesn't require any special Internet technology skills and can be distributed among different members of the community.

**The software includes:**

- specialized databases,
- set of libraries,
- deferent variants of customized web-interface which enable further project management:
  - online members registration;
  - initial document submission and upload of files of various formats;
  - web-site structure (dynamic creation of sections and subsections) and its files management;
  - forming mailing lists and setting up e-mail distribution service;
  - keeping the news bulletins;
  - extracting and sorting information on members and their publications;
  - extracting and sorting information on current events and connected documents;
  - providing access of different level for work with database (for the web-site administrator and members of the community);
  - events, the news, documents posting;
  - etc.

**A new community member registration**

Application form is formed dynamically by the web-site administrator on the base of application form sample that is provided in the administrator interface. Unnecessary positions can be removed; necessary ones can be added. The positions can get a status of obligatory filling-in. Filling-in of these positions is automatically checked by the software.

When the application form is signed up the web-site administrator as well as the new member receives an e-mail notification on the registration. All the information is automatically uploaded to the database.

**File upload to the site**

For site publication of community members' works as well as other documents of various formats the software supports a possibility to unload files to the site. On default only the site administrator and community members have an access to the file upload interface.

The interface allows review/editing of uploaded file catalogue as well as deleting some of them. Each of the uploaded files is associated either with the member who uploaded it or with the site section where it was placed.

**Web-site structure management**

CMS (Content Manage System) is integrated into the site. It enables management of the web-site structure and context. There is a possibility not only to build up the site structure as a whole (add pages/sections) but also work with the content of each page separately.

User-friendly interface is analogous to the ones of MS Office. It enables easy content handling of already existed pages as well as filling in new site pages. The offered CMS can partially interpret MS Office text formatting, bullets and numbering, tables, etc. This facilitates work for such administrators who don't have basic HTML skills. Still there is a possibility to edit HTML code for each page separately.

Plus to this there is a possibility to keep the news bulletins where the news of current and coming events can be published, e.g. meetings, conferences, new orders, announcements, etc. All the news announcements can be presented on specially provided place on the site.

**E-Mail distribution service**

Signed-up members of the community get a possibility to distribute different information messages through e-mail. Announcements of all the news published on the site are automatically distributed among all the signed-up members. Individual mailing lists can be formed, too.

**Sorting information on members and their documents**

To facilitate the work of the community members there is a possibility to sort database information for various purposes:

- **Forming the list of the members based on alphabet/e-mail/country/organization sorting;**
- **Forming the list documents based on titles/authors sorting;**
- **Forming the event/news list.**

**Different level access to the database**

The software enables giving different level access through the web-interface to the data and work with it. On default only the site administrator has the full access (reading/editing/deleting) to the site. All other site users have read-only access. Still there is a possibility to give administrator rights to separate users.

**Used software**

- **.NET Framework (ASP.NET),**
- **MS Windows Server,**
- **MS SQL Server.**

**This software was used in the following projects:**

- **http://icd.jinr.ru/** (International Cooperation Department),
- **http://innovation.jinr.ru/** (Science – Education - Innovation),
- **http://sid.jinr.ru/** (Scientific Information Department),
- **http://sod.jinr.ru/** (Science Organization Department),
- **http://nec2009.jinr.ru** (XXII International Symposium on Nuclear Electronics & Computing),
- **http://mmcp2009.jinr.ru** (Mathematical Modeling and Computational Physics).

# Detection of rare alpha decay events in the reaction $^{226}Ra + ^{48}Ca \rightarrow ^{270}Hs + 4n$ with PIPS 12 strip position sensitive detector

A.N. Polyakov, V.G. Subbotin, A.M. Sukhov, Yu.S. Tsyganov, A.A. Voinov
*for an FLNR, JINR Dubna - LLNL Livermore-TU Munich-VINĆA Belgrade collaboration*[1]

Experiment aimed to the synthesis of Hs isotopes in the heavy ion induced complete fusion reaction $^{226}Ra + ^{48}Ca \rightarrow ^{270}Hs + 4n$ [1,2] is considered from the viewpoint of detecting of rare decays. Description of the PC-based data acquisition system of the Dubna Gas Filled Recoil Separator, as well as its E-TOF detecting module precedes the discussion of the experimental details. Specific character of the background that prevents in part the application of active correlation technique [3] is considered too.

## 1. Introduction

Recently, more than 30 new nuclides with atomic numbers Z between 104 and 118 have been synthesized at the Dubna Gas-filled Recoil Separator (DGFRS) [4,5]. It should be noted that some of these experimental results have been clearly confirmed in independent experiments [6-9] involving the study of the chemical properties of the synthesized atoms.

In this connection reaction of $^{226}Ra+^{48}Ca$ is required by experimenters to provide more wide knowledge about heavy nuclei formation, including direct measurement of the production cross section for different de-excitation reaction channels. This parameter, undoubtedly, can be effectively used for rough extrapolations to higher Z, including those beyond Z=118 (Fig.1).

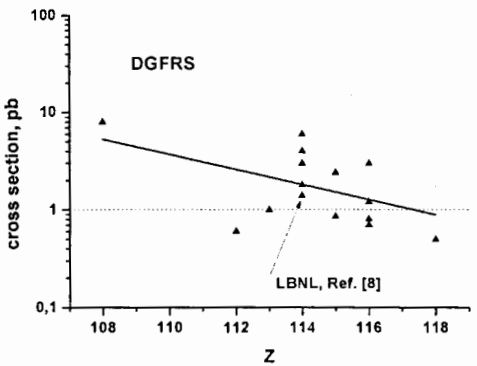


Fig 1. The simple parameterization (trend) of effective cross section parameter for reactions with $^{48}Ca$ projectile. (Experimental points given for only 3 and 4n channels). Level of 1 pb is shown by dotted line.

## 2. Experimental details of the ER –α-SF detecting procedure

The $^{48}Ca$-ion beam was accelerated by the U400 cyclotron of the FLNR, JINR. The Dubna gas-filled recoil separator [4] was used for transmission of evaporation residues (ER)

[1] Sci. Leader- Prof. Yu.Ts.Oganessian

to the detectors and their separation from $^{48}$Ca beam ions, scattered particles and transfer-reaction products. ERs passed through a time-of-flight system (TOF) and were implanted in a 4-cm×12-cm semiconductor detector array with 12 vertical position-sensitive strips surrounded by eight 4-cm×4-cm side detectors without position sensitivity, forming a box open to the front (beam) side. The position-averaged detection efficiency for full-energy α particles emitted in the decays of implanted nuclei was 87%.

The detectors were tested by registering the recoil nuclei (ER) and α or SF decays of known isotopes of No, Th, and their descendants produced in the reactions $^{206}$Pb($^{48}$Ca,2*n*) and $^{nat}$Yb($^{48}$Ca,*xn*), respectively. The FWHM energy resolutions were 50-110 keV (depending on strip) for α particles absorbed in the focal-plane detector and 130-310 keV for α particles that escaped this detector with a low energy release and registered by a side detector. Fission fragments from the decay of $^{252}$No implants were used for the total kinetic energy (TKE) calibration. The measured fragment energies were not corrected for the pulse-height defect of the detectors or for energy losses of escaping fragments in the detectors' entrance windows, dead layers, and the pentane gas filling the detection system. The mean sum energy loss of fission fragments of $^{252}$No registered by both the focal-plane and side detectors was about 20-25 MeV. The FWHM position resolutions of correlated ER-α and ER-SF signals were 1.1-1.9 mm and 0.6-1.6 mm respectively. For α particles detected by both the focal-plane and side detector, the ER-α position resolution depends on the energy deposited in the focal-plane detector and was on average 2.0-3.5 mm and 3.4-5.8 mm for energies larger and lower than 3 MeV, respectively.

For detection of the daughter nuclides in the absence of beam-associated background, the beam was switched off after a recoil signal was detected with implantation energy $E_{ER}$=9-15MeV expected for complete-fusion evaporation residues, followed by an α-like signal with an energy of 9.0 MeV≤ $E_\alpha$ ≤9.38 MeV in the same strip, within a 2.2-mm wide position window and a time interval of $\Delta t$≤8 s. However, for reducing the number of beam interruptions and collecting larger beam dose the most part of the first experiment (about three fourth) at $E_{lab}$=233.5 MeV with 0.23-mg/cm$^2$ target was performed without switching the beam off. Other part of experiment at $E_{lab}$=233.5 MeV, as well as both experiments at $E_{lab}$=228.5 MeV were performed with 3-min beam-off intervals. In the experiment at high $^{48}$Ca energy duration of beam-off time interval was 1 min, but if an α particle with $E_\alpha$=8.5-9.1 MeV was registered in any position of the same strip, the beam-off interval was automatically extended to 3 minutes.

Note, that specific of background in this experiment is the presence of Rn alpha-radioactive gas in the PIPS detector vicinity that partially prevents application of the "active correlations" method.

For data storage/visualization process the PC based (CAMAC, CC202 autonomous controller, CC012 controller, C++, Builder C++) data acquisition system is used [10, 11].

## 3. Summary

The detection system of the Dubna Gas Filled Recoil Separator has been applied in the experiment aimed to the synthesis of Hs isotopes in $^{226}$Ra+$^{48}$Ca nuclear reaction. Few events attributed to the 4n de-excitation channel were detected. Method of "active correlations" was applied to minimize beam-associated background contribution to the stored data.

In the nearest future we plan to provide an upgrade of the detection module of the DGFRS.

**References**


[1] Yu.Ts. Oganessian et al., to be submitted to Phys. Rev. C.

[2] Yu.S. Tsyganov et al, Presentation at IOP Conference, April (2009), Univ. of Birmingham, UK. http://www.np.ph.bham.ac.uk/iop09/iop_talks/07_04_09_Parallel_2/07_04_09_Parallel_2.htm

[3] Yu.S. Tsyganov et al., Nucl. Instrum. & Meth. In Phys. Res. A525 (2004)213.

[4] K. Subotic et al., Nucl. Instrum.&Meth. In Phys. Res. A 481(2002) 71-80.

[5] Yu.Ts. Oganessian, J. Phys. G. 34, R165(2007).

[6] R. Eicher et al., Nature, Letters (2007) 447, 72.

[7] S. Hofmann et al., Eur. Phys. A32 (2007) 251.

[8] L. Salvestra, K. Gregorich, J. Dvorak et al., Phys.Rev. Lett. 103 , 132502(2009).

[9] C. Duelman et a; TASCA-2009, Oct. 14 (2009), GSI, Germany, www.gsi.de/tasca

[10] Yu.S. Tsyganov, A.N. Polyakov, V.G. Subbotin et al., in Proc. of HPC-ASIA'97 Conference, Seoul, Korea, May 02. IEEE Comp. Soc. Press, California. (1997)651.

[11] A.M. Sukhov, Yu.S. Tsyganov et al., JINR comm. P12-96-371. Dubna, 1996 (in Russian).

# Parameter-control system of the Dubna Gas-Filled Recoil Separator

A.N. Polyakov, A.M. Sukhov, Yu.S. Tsyganov
*Joint Institute for Nuclear Research, Dubna, Russia*

PC-based (CAMAC, KK012) one-crate control system of the Dubna Gas Filled Recoil Separator (DGFRS) is considered. It is developed for the long-term experiments at the U400 FLNR cyclotron and is aimed at the synthesis of super heavy nuclei in heavy ion induced complete fusion reactions. Parameters related to:

a) beam and cyclotron,
b) separator by itself,
c) detection system,
d) target and entrance window,

are measured and stored in the protocol file of the experiment. Special attention is paid to generating the "alarm" signals and implementing further the appropriate procedures.

## 1. Introduction

During the long term experiments aimed to the sinthesys of superheavy elements at the Dubna Gas-filled Recoil separator (DGFRS) the system to measure technological parameters of the experiment and to provide a definite response to some abnormal (alarm) situations is strongly required [1,2 ].

Usually, a list of parameters/signals includes the following:

- *Dipole, quadruples current values measurements as well as setting of alarm thresholds;*
- *Rotation speeds both entrance window and radioactive target wheels;*
- *Pressure value in working area of the DGFRS and pentane pressure value in the TOF (time-of-flight module);*
- *Temperature parameters;*
- *Beam associated parameters;*
- *Vacuum parameters;*
- *Pressure of saturated vapor of pentane in liquid pentane volume;*
- *Photo-diode rotation target output signal amplitude;*
- *..others.*

***The Dubna Gas-Filled Recoil separator (schematics)***

## 2. Schematics of the system

In the Fig. 1 the system schematics is shown.

Design in brief: CAMAC, one (digital) crate, KK012 controller (modified, see Ref. [3]), program (Windows XP, Borland's Builder C++ , v.6 ).

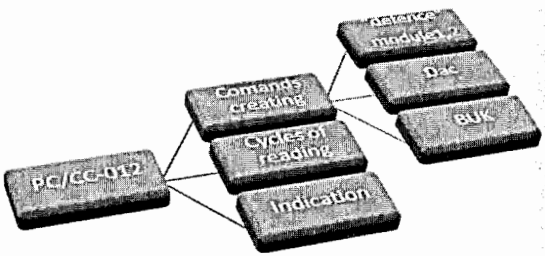


Fig. 1. Schematics of the system

**Main CAMAC modules in the digital apparatuses crate:**
**BUK01** – CAMAC-1M (to create time intervals window to measure parameters, **NF16A0** (3 in parallel, 0.02,02 or 2 s interval) + (three independent outputs) **NF16** (A2/A3, A4/A5, A6/A7).
**BZ01** ("alarm" modules ( 2 mod 2M) each one 8 inputs and 1 output to switch the beam OFF) ; **F24/26( A0-A7)** – off/on "defense" mode, **NF2**(read), **NF10** (to reset alarm's register).
3 16 bit counters KS019,
1 ADC PA 01 (8 inp dc, design by A.N. Kuznetsov -in reserve use now),
2 ADC PA-24K (10 bit, target control, TOF U400 (in reserve use),
5 KS022 rate meters (~rotation control, +some others),
1 KV009 1M - DAC → thresholds setting for low Dipole magnet current and Wobbler current.

**Gauges**(sensors): **MCS** Baratrons (N=4), vacuum gauges **"Pfiefer"** (N=7, long scale!), Target (entrance window) - el.Motors(N=2) **"Siemens"** asynchronous AC.

- ***Basic dc parameters*** *measurements: voltage-frequency-code conversions.*
- Main code **Builder Timers** – 5 (CAMAC, calibration, visualization, imitation of rotation, protocol writing.. etc…).

In the Fig. 2 user interface is shown. Picture (Prt Scr) corresponds to real SHE experiment with $^{48}$Ca ion as a projectile.

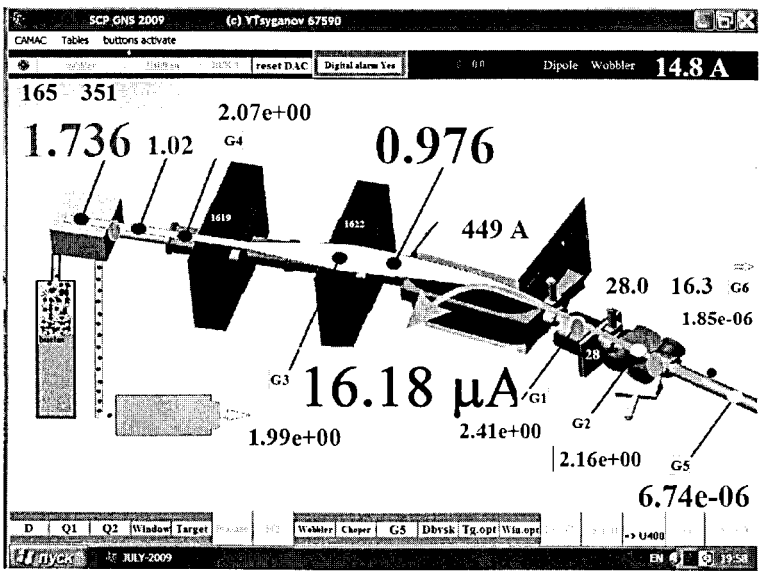


Fig. 2. Schematic of the system interface (three monitors- near the separator, in the control room and near PC)

1) **(examples of values meanings):**
   a) green field means the parameter under control, if alarm will occur- color will red. Action – beam is turned off;
   b) **16.18**- value (~ add 10%) of projectile beam at the target;
   c) **1.736** (Tor) – pentane pressure;
   d) **28.0 and 16.3** – target and entrance window wheel rotation speed (1/s)// double control: rotating itself+ optical pairs light source-photodiode;
   e) **0.976** – $H_2$ pressure in the separator;
   f) **6.74-06** - cyclotron vacuum value in the point before the separator window;
   g) **449**, 1622, 1619 A – current values in Dipole magnet and in the lenses;
   h) **165 351** at yellow field (left-upper corner) – rates of DAS events (focal plane PIPS + side detector) and TOF camera operation; if **165 351** then it means, that rate of events is under control using low limit ( dblClick in Edit area, ~5 events in ~ 10 s)
   i) **14.8 A** (right-upper corner) – wobbler current
   j) Green button in the left-upper corner: start spectrum measure from additional detector( p-i-n, 8x8 $mm^2$) located close to rotating target in order to estimate it's state
   k) "buster" – pressure of saturated pentane vapor ( in progress)

As examples, graphs for pentane pressure, beam intensity and U-400 $^{48}Ca$ ions energy against time are shown in the Fig. 3a-c.

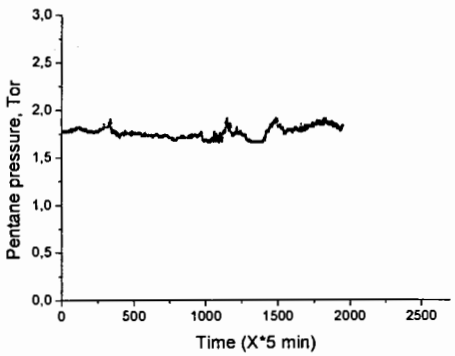


Fig. 3a. The dependence of the pentane pressure in the TOF module against time (no any feed back!)

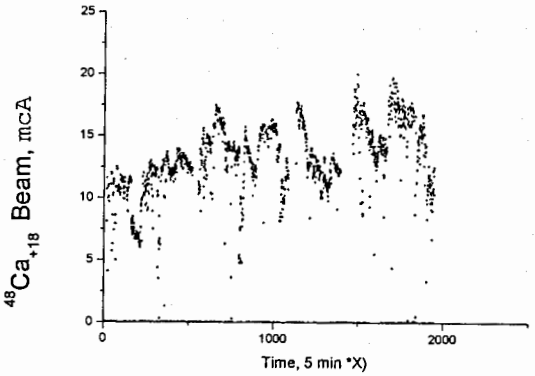


Fig. 3b. The dependence of the bean intensity against time

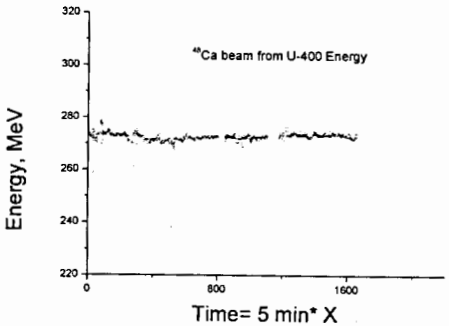


Fig. 3c. Energy against time dependence
(modules to convert pic-Up electrodes signals into spectroscopy codes:
ORTEC fast preamps VT **120**, ORTEC CFD **584**, TAC **567**, KV **005** (JINR))

**3. A view at the U-400 cyclotron staff room from the system**

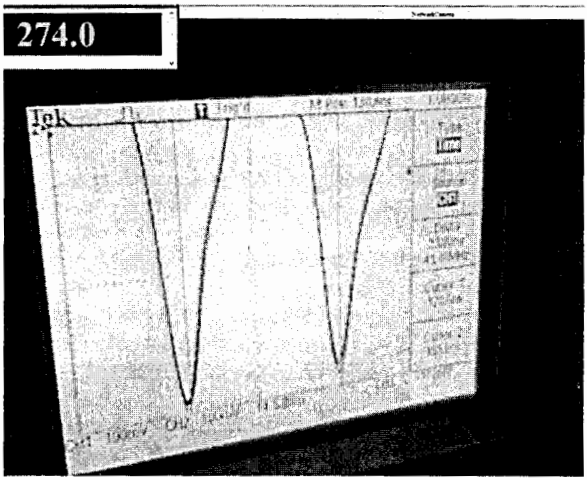


Fig. 4a. A view at the cyclotron operator working place PC. It is shown a beam energy (MeV, $f_{refresh} \sim 1\ c^{-1}$) and "quality" of beam tuning signals from two picUp electrodes located before the separator (oscilloscope picture - via net-camera).

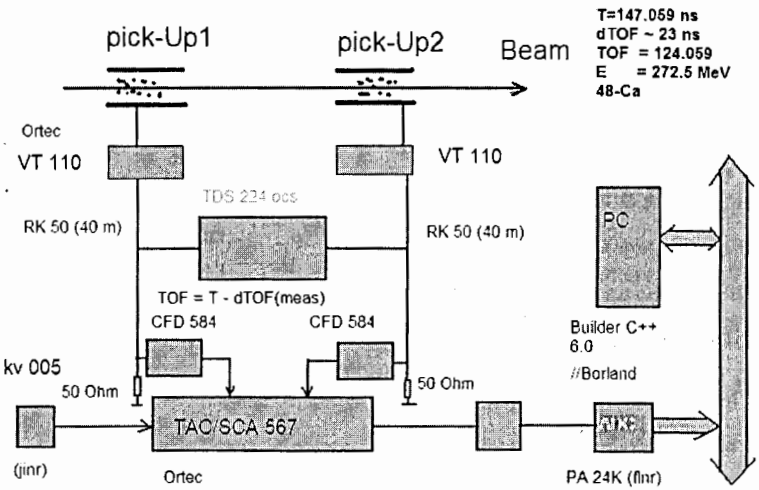


Fig. 4b. TOF U400 system block-diagram

## 4. Chopper beam OFF operation

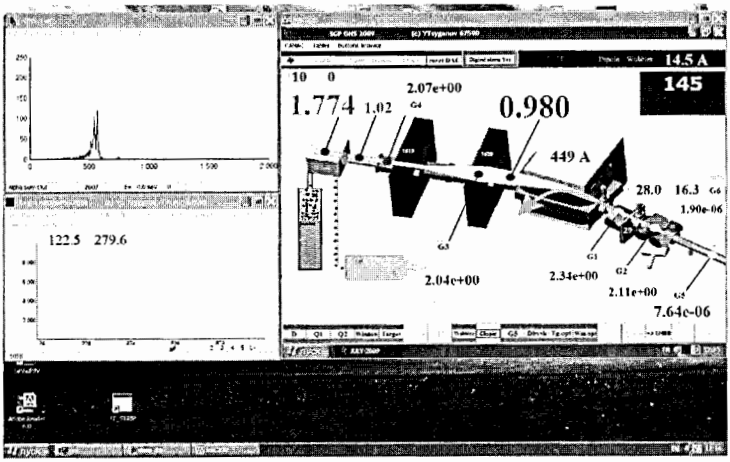


Fig. 5. Beam - Off phase. Right upper red square – number of delay seconds for beam chopper operation. Yellow color of "chopper" button indicates an active phase for beam chopper device. $I_{beam}$=0. Rate ~ 10 $s^{-1}$ (left upper corner – in yellow). It can be easily seen perfect spectrum in beam off phase.

Note, that namely due to beam interruption in the Dubna Gas Filled recoil Separator long term experiments it has become possible to provide a radical suppression of backgrounds related with a cyclotron operation [4-6].

### Summary

New PC based control parameter system of the DGFRS has been designed and after testing in the reactions with relatively high cross section formation of the products under investigation, has been applied in real long term experiments aimed to the synthesis of SHE. Development of the system is in progress now.

*We would like to express our gratitude to the personnel of the U400 cyclotron for obtaining intense $^{48}Ca$ beams; to Dr's V. Zhuchko, F. Abdullin and V. Shirokovsky for their support in the system calibration and Dr. V. Bashevoy for his help in the program interface design development.*

### References

[1] Yu.S. Tsyganov et al., in Proc. of SCP'2005 Conf. St. Ptbg., 29.06.2005-01.07.2005, Russia. Ed. By D.A. Ovsyannikov, Vol.1 (2005)236-244.
[2] A.N. Polyakov, Yu.S. Tsyganov and A.M. Sukhov, in Proc. Of NEC'2007 Symp., Varna, Bulgaria. Sept. 10-17, 2007. Dubna (2008)390-392.
[3] Yu.B. Semenov, V.E. Zhuchko, in Proc. of NEC'2005 Symp. Varna , Bulgaria (2005).
[4] Yu.S. Tsyganov, J. Phys. G.: Nucl. And Part. Phys., vol.25, no.4 (1999)937-940.
[5] Yu.S. Tsyganov et al., Nucl. Instrum. And Meth. In Phys. Res. A 513 (2003)413-416.
[6] Yu.S. Tsyganov et al., Nucl. Instrum. And Meth. In Phys. Res. A 525 (2004) 213-216.

# Monte-Carlo calculations for increasing of very cold neutrons flux

E.P. Shabalin, A.E. Verhoglyadov
*Joint Institute for Nuclear Research, Dubna, Russia*

**Concept of the conical reflector**

Neutron scattering methods need high fluxes of cold (CN, wavelength from 4Å to ~20Å) and very cold (VCN, wavelength higher than 20Å) neutrons. Such neutrons can be produced by using the cold (cryogenic) moderators. Low rate of these neutrons even in Maxwellian spectrum forces us to look for ways of increasing their intensity. Mirror neutron guides with multiple coating are usually used for neutron transport from reactor to samples and cannot be placed close to a reactor core because of radiation damage. One can place special reflector near the surface of a moderator for the purpose of increasing neutron flux in the direction of the sample. This reflector should consist of irradiation stable material and efficiently reflect CN and VCN.

Such neutron reflector is the object of our work. We research properties of reflectors contained nanodispersed diamond powder with particle size between 1 and 10 nm. As we know from theoretical and experimental [1] investigations, the reflection coefficient of cold and very cold neutrons from nanodispersed material is much higher than from solid material and close to unity. Moreover, good reflection is reached with low thickness of nanopowder, about several millimeters. It is caused by the fact that the size of diamond particles is close to wavelength of very cold neutrons. Neutrons coherent scatter on particle as a whole, and cross section of scattering is very high because it is proportional to number of atoms in the particle squared, but absorption cross section is still low as in solid material. Despite the primary forward scattering, reflectivity is found to be high. Because of this and because of irradiation stability of the nanodispersed diamond, this material is seems to be much suitable for using in the source of VCN.

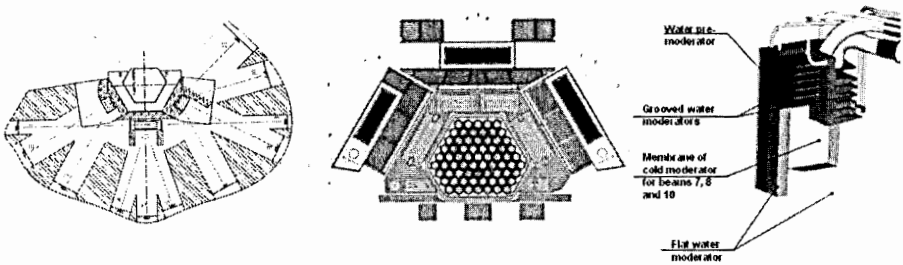


Consider a flat source of VCN which is presented by limited surface in the form of the circle with fixed diameter, its plane is orthogonal to axis of neutron beam. Over the source there is a reflector presented by the hollow truncated cone as we see on the Fig. 1. Inner walls of the cone are covered by a layer of the diamond nanopowder; the height of the cone is limited. Thickness of the nanopowder layer is considered sufficient for VCN not to penetrate through it, but scattering cross-section of neutrons with small wavelength (thermal and CN) to be low (aluminium, carbon) . Then reflector would not reduce fluxes on spectrometers located at the oblique angles.

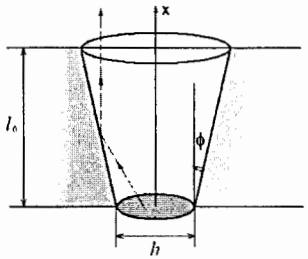

Fig. 1

Let's define *the directed flux* as the number of neutrons crossing the plane orthogonal to the axis of the beam to the positive direction in a unit of time inside the infinitesimal solid angle and reduced to unity of solid angle. Without reflector, directed flux will be constant along the beam axis. In the presence of the cone reflector, neutrons with direction which is not parallel to the axis, have possibility to get to the wall, reflect and fly out to the right direction. Correspondingly, the directed flux will be increased along the axis right up to the big base of the cone.

Especially high reflection is to be expected for neutrons which get into surface of the cone at the angles close to the angle of small-angle coherent scattering on powder particles. Neutrons fly out the source plane according to the cosine law and this lead to existence of the optimal angle of cone opening. At this angle the directed flux has maximum value (at the fixed cone height).

The main point of our work was computation of the gain in the directed flux as function of parameters of reflector (angle of cone opening, cone length and thickness of nanopowder walls). Also dependences of total and differential (angular) albedo from hade in the case of flat surface of nanopowder were investigated.

**Calculation of the VCN transport**

If reflector is used then straight directed flux sums up from the flux directly from the source (call it as $G_s$) and reflected flux from the walls of the cone ($G_r$). Gain factor of the directed flux will be:

$$G = \frac{G_r + G_s}{G_s} = \frac{G_r}{G_s} + 1. \qquad (1)$$

Calculating of the very cold neutrons transport was done by Monte Carlo statistical test.

In the nanopowder material, VCN mainly have coherent elastic scattering on particles as a whole. At the scattering on the particle with size close to neutron wavelength, incident wave diffracts on the particle, cross section is proportionate to number of atoms in the particle squared, and angle of scattering is small (small angle scattering). Capture cross section on carbon nuclei $C^{12}$ is low ($\sigma_a$ = 0,01b), but it was taken into account in our calculation. Inelastic scattering didn't consider because of assumption that material has low enough temperature, so that, VCN can't accelerate. In principle, scattering on the set of particles is also exist, but Dr. Artemiyev pointed out [2] that so called "structure factor" of this process is close to unity at such condition.

Calculated in perturbation theory with the Born approximation differential section of neutron scattering on spherical particle with radius $a$ is given by expression [3]:

$$\frac{d\sigma}{d\Omega}(\Omega) = a^2 \frac{u^2}{q^4}\left(\cos(qa) - \frac{\sin(qa)}{qa}\right)^2. \qquad (2)$$

Here are $q = \frac{4\pi}{\lambda}\sin\theta$, $\theta$ – angle of deviation, $u = 4\pi N_0 b_C$, $b_C$ = *0,627 ·10$^{-12}$cm* – scattering length (the characteristic of the $C^{12}$ nuclei), $N_0$ = *1,76 ·10$^{23}$cm$^{-3}$* – nucleus concentration in solid diamond.

Created program of Monte Carlo method allows calculating the gain factor of directed VCN flux for reflector with conical and parabolic forms and also differential albedo of VCN from the flat wall.

**The results**

Reflection from the flat wall

Obtained dependences of the total reflectivity of incident flux from the polar and azimuth angles (differential albedo) are listed here (Fig. 2). One sees that strong dependence of all characteristics from the polar angle is typical for VCN. Angular distribution of reflected neutrons , both for azimuth angle $\varphi$ and polar angle, is strongly elongated forward at small incident polar angle. In particular, for the polar angle $89^0$ the forward reflected flux is two-order higher than the orthogonal reflected one and single-order higher at the polar angle $45^0$. This is consequence of the fact that angle of deviation in each scattering act is small (see the differential section formula (2)). Also this explains behavior of dependence of the total albedo from the polar angle (Fig. 3); it comes near unity at the polar angle about $90^0$ (i.e. when flux is almost parallel to the wall).

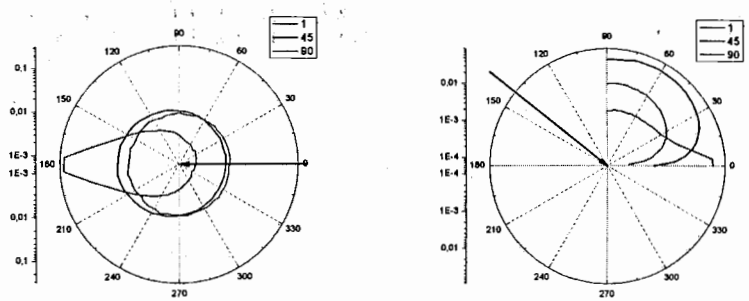


Fig. 2

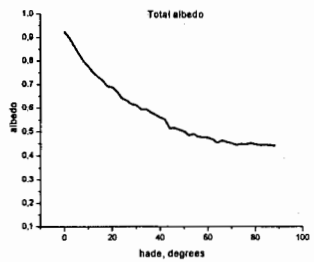


Fig. 3

Gain factor

In calculating of the gain factor G in the directed flux and of optimal angles $\varphi$ of the cone opening, we considered diameter of the round source equal to 10cm, neutron wavelengths has Maxwellian distribution between 1-10nm, nanopowder particles was spheres with known distribution of their diameter (see Fig. 4).

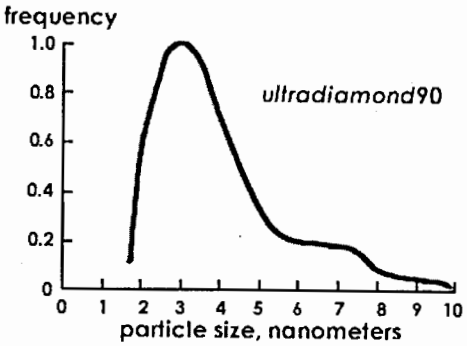


Fig. 4

Calculating was done for three values of the cone length: $l$ = *20, 30, 40*cm. The $G(\varphi)$ dependence at $l$=*30cm* is shown on the Fig. 5.

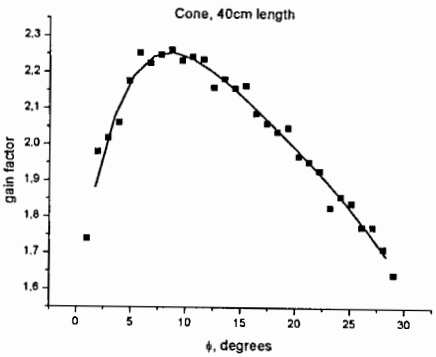


Fig. 5

The $G(\varphi)$ curves are similar at $l$=*30, 20* and *40cm*, all of them have maximum at $\varphi$ between 10-30$^0$.

The parabolic reflector was also investigated and its gain factor didn't differ from gain factor of the conic reflector.

## Conclusion

As was found from the Monte Carlo computation of the VCN transport, addition of the conical reflector to the cold moderator raises forward directed VCN flux about twice. This is consequence of high reflectivity of nanopowder.

Maximum gain factor of the flux is obtained at angles of cone opening about 15-30 degrees, this confirm initial supposition. Obviously, because of the anisotropy of differential albedo value of optimal angle must depend on distribution of the neutrons flying out from the source.

Because of the scale invariance of neutron transport inside the reflector, this estimation of directed flux gain factor can be used for reflector and moderator of any size.

Nowadays we investigate so called *grooved type* reflectors with nanodispersed diamond powder layers to reach more gain in VCN production.

## References


[1] V.V. Nesvizhevsky, E.V. Lychagin, A.Yu. Muzychka, A.V. Strelkov, G. Pignol, K.V. Protasov, The reflection of very cold neutrons from diamond powder nanoparticles, Nuclear Instruments and Methods in Physics Research A 595 (2008), pp. 631–636.

[2] V.A. Artem'ev, Atomic energy 101, 901 (2006).

[3] V.K. Ignatovich, E.P. Shabalin, Nuclear Physics 7, 2 (2007).

# Job monitoring for the LHC experiments

I. Sidorova[1,2] on behalf of the Dashboard group
[1] *CERN, Geneva, Switzerland*
[2] *Joint Institute for Nuclear Research, Dubna, Russia*

With LHC startup expected later this year job processing and data transfer are the two main activities present on the Worldwide LHC Computing Grid. Taking into account a complexity of heterogeneous distributed infrastructure which includes 140 computing centers in 33 countries Job Monitoring is an important challenge. Experiment Dashboard [1] gathers information about job processing and data transfer from the multiple sources, aggregates it and represents in different ways according to a particular user use case.

The Large Hadron Collider (LHC) [2] is preparing for data taking later this year. The volume of data produced by the LHC will be hundred times greater than in previous accelerators. 15 PetaBytes of data is expected to be generated every year. Access to this data has to be provided to 7000 physicists all over the world. In order to provide necessary resources Grid infrastructure in Europe, the USA and Asia were brought together by the Worldwide LHC Computing Grid (WLCG) [3] collaboration.

Data distribution and data processing are two main computing activities for Virtual Organizations (VOs) running on the WLCG infrastructure. Quality of job processing provides the estimation of the quality of the infrastructure in general and defines the overall success of the computing activities of the VOs. On the other hand, detailed and reliable job monitoring helps to improve the computing models of the LHC VOs.

Considering the complex heterogeneous distributed infrastructure which includes 140 computing centers in 33 countries job monitoring is a very difficult and important challenge.

**Existing job monitoring applications**

To have a possibility to create physics tasks, to submit them for execution and then to follow their progress on the grid LHC experiments developed the experiment-specific workload management systems. The job monitoring task depends on workload management system, where it was submitted and on what infrastructure it was executed.

Job processing in ALICE and LHCb experiments is organized through central queue. The queue keeps track of the jobs progress. In this case job monitoring is quite simple because workload management system can provide also job monitoring functionality. This task is more complicated in CMS and ATLAS experiments. Different workload management systems are used for analysis and production by the experiments. Therewith their jobs can be run on different grid infrastructures like gLite[4], NDGF[5] and OSG[6]. So there is no any central point which contains all the information about jobs processing. There are some job monitoring applications available in ATLAS and CMS which are combined with workload management systems. These are PANDA monitoring for ATLAS or ProdAgent monitoring in CMS.

Experiment Dashboard was developed as generic monitoring framework which is used by all four LHC experiments. It offers the solutions which are working in the scope of a single experiment. The reason is every experiment has VO-specific data. If the source of the data is not VO-specific then Dashboard offers common monitoring solutions. To provide complete view of job processing both from the Grid and application point of view the VO jobs submission tools should be instrumented to report job's status information. For the

moment Dashboard Job Monitoring for CMS is the most advanced one since all CMS submission tools are well instrumented for the Dashboard reporting.

**Overview of the Dashboard job monitoring applications**
**ATLAS ProdSys Monitoring**

Monte-Carlo production is a well-organized activity performed by a group of experts. Managers which are responsible for that large-scaled activity need a tool to monitor the processing of the production jobs. The ATLAS production system is based on a central database, holding information about the job status (e.g. waiting submission, scheduled in a resource, running, being aborted and some others).

The Experiment Dashboard provides a user interface to the data. The main goals of the interface are to permit:

- shifters to identify failing tasks and jobs so that they can reschedule them for execution or send a ticket to Global Grid User Support,
- site administrators to see how ATLAS production is performing on their sites,
- people running executors to follow the execution of the instances they are responsible for, quickly find out the reason of the failures, browse the detailed data of tasks and jobs,
- production managers to get the daily/weekly/monthly statistics of the system.

**Central repository for the CMS ProdAgent monitoring data**

In case of CMS situation is different. Every production agent (ProdAgent) has its own database keeping track of the jobs processing. Experiment Dashboard was requested to create a central repository for the job monitoring data. And it was implemented along with the collector to retrieve data from CMS ProdAgent instances some time after.

At the moment the Experiment Dashboard database plays the role of the central repository for the production monitoring data, while the user interface is developed by the CMS production development team.

**Generic job monitoring**
**Monitoring of user analysis jobs**

Contrary to monitoring of the production system monitoring of user analysis is much more complicated task. User analysis is a chaotic data processing running by members of the huge distributed physics community.

As it was already mentioned the organization of workload management systems of the LHC experiments differs from one experiment to another. And in case of ATLAS and CMS the job submission instances are distributed and there is no central point of control as in ALICE or LHCb. These facts say that job monitoring of CMS and ATLAS computing activity is not that trivial.

Experiment Dashboard covers a wide range of activities on the Grid. Usually Dashboard starts to develop a new application by request of one of the experiments. But if non experiment-specific information sources are used, this application can be reused for other experiments. One of the most used applications is Dashboard Job Monitoring. This tool is a generic one and it's developed for the all experiments. The application has the same user interface but uses different information sources to collect data about job processing.

This figure explains the data flow for Dashboard Job Monitoring application.

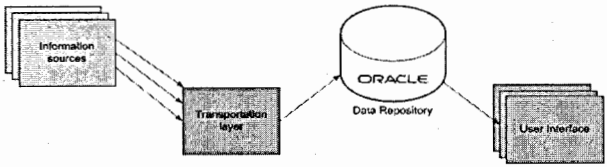


Fig. 1. Data flow for Dashboard Job Monitoring

The Dashboard retrieves job status information from different sources. In case the jobs are submitted via the gLite Workload Management System (WMS) the Logging and Bookkeeping (LB) [7] service keeps full track of the job processing. The LB provides the notification mechanism which allows to subscribe to the job status changes event and to be notified when the event happened.

But LB does not keep track of jobs submitted directly to the Computing Resource Execution And Management (CREAM) computing element (CE). The CEMon service plays the same role as the LB for jobs submitted to the CREAMCE. A CEMon listener component was developed in order to enable job status changes publishing to Messaging System for the Grid (MSG). It subscribes to CEMon for notifications and then republishes the information to MSG.

Jobs submitted to Condor-G [8] do not use the WMS service and correspondingly do not leave a trace in the LB. The job status changes publisher component was developed in collaboration of Condor and Dashboard teams. The publisher reads new events from standard Condor event log, extracts essential job attributes and publishes them to MSG. The publisher runs as a Condor job. In this case, Condor itself takes care of publishing status changes.

Finally, the jobs themselves are instrumented for the runtime reporting of their progress at the worker nodes. It was done to compensate the lack of information from the Grid-related sources.

At the moment MonALISA monitoring system [9] is used for transporting data about jobs processing to Dashboard Data repository. This functionality of MonALISA will be replaced by more elaborated messaging system which can collect data from the most of available job submission tools which is not the case with MonALISA. Experiment Dashboard information can be displayed using HTML. So it can be viewed in any browser. Moreover, Dashboard framework also provides the functionality to retrieve information in various formats (XML, CSV, JSON or image formats) in response to requests sent by different user interfaces.

Dashboard Job Monitoring is designed as common solution to use by any virtual organization. To provide complete view of job processing both from the Grid and application point of view the VO jobs submission tools should be instrumented to report job's status information. For the moment Dashboard Job Monitoring for CMS is the most advanced one since all CMS submission tools are well instrumented for the Dashboard reporting.

**Dashboard job monitoring functionality**

Standard job monitoring application provides two types of user interfaces. The first one shows what's going on the Grid now. The interactive UI [10] represents the distribution of active jobs and jobs terminated during a selected time window by their status. Jobs can be sorted by various attributes, for example, the type of activity (analysis, production, etc.), site or CE where they are being processed, job submission tool, input dataset and many others. The information is presented in a bar plot or in a table.

To reduce time of access to the data information in Dashboard repository is being regularly aggregated in the summary tables. The second interface called Historical View [11] shows job statistics distributed over time. The data requested from it is being retrieved from these summary tables, which keep aggregated data with hourly and daily time bin granularity.

The interfaces are widely used by different categories of users like VO managers, computing shifters, Monte-Carlo production teams, Site commissioning or LHC physicists running their jobs on the Grid.

To serve the needs of the analysis community and of the analysis support team, the Dashboard Task monitoring application [12] has been developed on top of the CMS job monitoring repository. The application provides a comprehensive view of the task processing. It demonstrates the progress of the task, helps to detect problems and provides information for debug.

The Task Monitoring information includes the job status of individual jobs in the task, their distribution by site and over time, the reason of failure, the number of processed events and the resubmission history. The application offers a wide variety if graphical plots that visually assist the user to understand the status of the task.

The development was driven by user's feedback. Close collaboration with several CMS users resulted in a tool being focused on their exact monitoring needs. It has become very popular among the CMS users. According to our web statistics [13], more than one hundred distinct analysis users are using it on the every day basis. It is also widely used by analysis support team and site administrators.

## Conclusions

Distributed user analysis on the WLCG infrastructure is currently the main challenge of the LHC computing. After LHC start up the number of analysis users will dramatically increase. Hence the significance of job monitoring will also increase. Due to user-friendly, complete and reliable monitoring of the analysis task processing is an important factor for successful organization of the distributed analysis.

Experiment Dashboard creates the applications focused on the exact needs of the users regarding job monitoring, providing complete views of how the distributed infrastructure is used by the LHC experiments, and covering different areas of their activities.

## References


[1] Dashboard home page, http://dashboard.cern.ch/
[2] LHC home page, http://lhc.web.cern.ch/lhc/
[3] WLCG home page, http://lcg.web.cern.ch/lcg/
[4] gLite home page, http://glite.web.cern.ch/glite/
[5] Nordic Data Grid Facility (NDGF) home page, http://www.ndgf.org
[6] Open Science Grid (OSG) home page, http://www.opensciencegrid.org
[7] LB home page, http://egee.cesnet.cz/cz/JRA1/LB/
[8] Condor-g home page, http://www.cs.wisk.edu/condor/condorg
[9] MonALISA home page, http://monalisa.cern.ch/monalisa.html
[10] Job Monitoring Interactive UI,http://dashb-cms-job.cern.ch/dashboard/request.py/jobsummary
[11] Historical View UI, http://dashb-cms-sam.cern.ch/dashboard/request.py/dailysummary
[12] Task Monitoring page, http://dashb-cms-sam.cern.ch/dashboard/request.py/taskmonitoring
[13] Dashboard statistics page, http://lxarda18.cern.ch/usage.html

# A micropower phase-locked loop (PLL) IC for processing the signals of silicon detectors

A.S. Silaev, Yu.A.Volkov
*Moscow Engineering Physics Institute (State university) MEPhI, Moscow, Russia*

The results of designing and manufacturing a micropower PLL IC are presented. Different structures of the PLL are compared. The advantages of the Delay-locked Loop (DLL) structure are grounded. The circuit schematics and chip layout of DLL are presented. The IC has been implemented with the 0.18u CMOS technology, the corresponding design being carried out with the Cadence Design System. Chip area makes up 970u*610u, out of which 650u*210u is occupied by a 100pF capacitor. The test results of the IC are presented. Current consumption of the "core" is within 100uA at a supply voltage of 1.8V and an output frequency of 100MHz.

It is well known, that the principles of building PLL systems have been founded in the times of vacuum valve electronics, but then they had a rather limited application (precise measuring systems). Since the advent of semiconductor technology their application has considerably expanded [1, 2].

The PLL systems are used mainly for high-speed clock generators particularly for the reason of being capable to multiply frequency. The PLL systems have several disadvantages, which complicate the generation of a precise clock signal in a noisy environment, such as the noises of supply sources and substrate. The PLL system has at least two poles, what imposes limits on the stable working mode and makes the design complicated. The PLL uses a voltage controlled oscillator (VCO), the frequency of which is checked by a filter (feedback loop). The variation delay, accumulated under the influence of supply noise, can not be immediately corrected, therefore the output jitter is accumulated by all oscillator cycles. The Delay locked loop (DLL) system has several advantages comparing to PLL. Thus the DLL is a single-pole system and therefore it is much more stable, as well as simple in design. The DLL system uses an open delay line loop, where jitter is accumulated only by a unity delay element. Besides that, the DLL has a lesser power consumption, lesser area on chip and faster loop locking, comparing to PLL. However the DLL is not able to multiply frequency as the PLL, but there exist other circuits, capable of multiplying frequency [3, 4, 5].

Fig. 1 shows the structure diagram of the DLL developed, which consists of: a phase-frequency detector (PFD), a charge pump (CP), a filter, delay line (VCDL), phase multiplier (Multiphase), multiplexer, starting circuit and an input buffer.

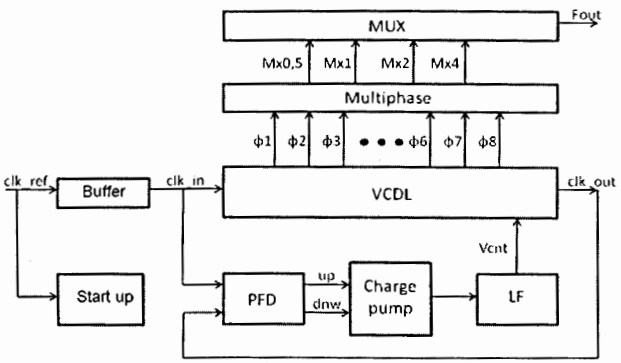


Fig. 1. Structural diagram of a PLL with frequency multiplication

The PFD's zone of insensibility causes the emergence of a phase error in the output signal. Therefore the CP will not charge the filter's capacitance and that will entail the emergence of noise. The PFD uses a dynamic system including additional digital blocks, what permitted to achieve a phase error less then 20ps.

The principal criterion of the charge pump operating correctly is the correspondence of "UP" and "DNW" currents. The correspondence of currents was achieved by using switches so, as to obtain a minimal static phase error. The switches are placed so that the output node is isolated from switch noises. The CP is designed for charging and discharging the filter capacitance and shaping the control voltage across that capacitance – Vcnt. The control voltage makes the line's propagation delay constant. In order to minimize the phase error, a fixed current is fed into the filter, what helps to keep the loop gain and phase margin constant. The filter serves as an integrator since being a first order one, using a large capacitance.

The voltage controlled delay line consists of sixteen cells. A single-phase delay line, as distinct from a differential one, has a lesser power consumption and a lesser area on chip. Besides that, a solitary delay line has a noise characteristic better, than a fully differential one, since the single-phase delay line does not have any dc consumption. The given delay line generates sixteen phase signals which allow us to obtain an output frequency multiplied by up to eight times (Mx0,5; Mx1; Mx2; Mx4; Mx8) [6, 7].

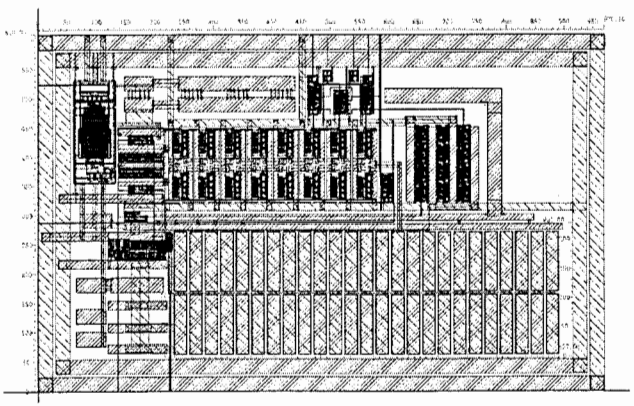

Fig. 2. Layout of the DLL system

The DLL system has been implemented by the 0.18u CMOS technology. The supply voltage is 1.8V, the output frequency range – 22.5...400 MHz, phase error ~ 20ps. At an output frequency of 200MHz the signal's period to width ratio is 50±0.2%, and the current consumption equals 148uA. At a frequency of 400MHz the current consumption does not exceed 340uA. The designed DLL is fully laid out within a chip of 970x610u² (see Fig. 2), thereat the area of the 100pF capacitor makes up 650x210u².

**References**


[1] Alan B. Grebene, Analog integrated circuit design. VNR Company, NY, 1972, 256P.

[2] A.D. Artym, S.V. Trifonov, Frequency domain means of PLL system analysis and synthesis, M., 1976, p. 160.

[3] Ro-Min Weng, Tung-Hui Su, and Chuan-Yu Liu, A CMOS 2.4GHz Delay-Locked Loop Based Programmable Frequency Multiplier, 2006 IEEE, pp. 371-372.

[4] Md Ibrahim Faisal, Magdy A. Bayoumi, A Low-Area, Low-Power Programmable Frequency Multiplier for DLL based Clock Synthesizers, 2008, IEEE.

[5] Byung-Guk Kim, Le-Sup Kim, A 250MHz – 2GHz Wide Range Delay-Locked Loop, 2004, IEEE.

[6] David J. Foley, Michael P. Flynn, CMOS DLL Based 2V, 3.2ps Jitter, 1GHz Clock Synthesizer and Temperature Compensated Tunable Oscillator, 2000, IEEE.

[7] A Low Power Small Area, 7.2ps Jitter 1GHz DLL Based Clock Generation, 2007, IEEE.

# Silicon microstrip detector model for read-out electronics

A.S. Silaev, Yu.A. Volkov
*Moscow Engineering Physics Institute (State university) MEPhI, Moscow, Russia*

A model of the silicon microstrip detector for read-out electronics of physical experiments is presented. The analysis of silicon detector Spice models is discussed. The detector model based on a resistive-capacitive chain is defined. The DC characteristics of a microstrip detector are determined.

It is well known, that the microstrip detectors at present are widely used in physical experiments [1,2]. Thus, the detector laboratory of RINF MSU for many years has been developing silicon detectors, particularly, for the "Nuclon" experiment of Roskosmos [3].

The further improvement of such detector structures is imagined as their preliminary analysis and design using the most advanced CAD systems. One of the aims of the given paper is to clarify the capabilities of the TCAD system of the American Synopsys Company in the field of simulating the basic characteristics of microstrip detectors.

In the course of this work there were used the following software tools:

- DIOS, an 1D and 2D system of simulating the technological process of semiconductor devices manufacture; it can simulate the full sequence of technological operations, such as etching, ion implantation, diffusion, material deposition, oxidation.
- MDRAW, a tool of 2D editing of the grid (boundaries) and dopants of the arrangement; it also can create and edit semiconductor devices; MDRAW uses the DF-ISE file format and transfers data to other simulation means of TCAD.
- DEVICE (DESSIS), an instrument capable to simulate the electrical, thermal and optical characteristics of silicon and compound semiconductor devices in 1D, 2D and 3D.
- TECPLOT, a tool visualizing the results of simulating 2D and 3D devices, such as electric field, current densities, distribution of dopant concentration and so on.
- INSPECT, a program analyzing the designs, visualizing the dependences (graph plotting). INSPECT offers the opportunity to work with data in an interactive mode, using both the graphic interface and the programmation language (script).

The TCAD supports such widely spread and used technological file formats, as GDSII *.gds and CIF *.cif.

Having prepared first the layout of the microstrip detector (Fig. 1), it is necessary further to define the route of technological operations (see Table 1).

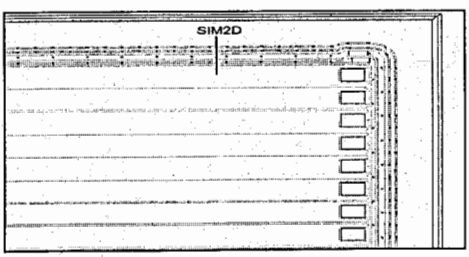


Fig. 1. Layout of the microstrip detector

The comparison of simulation results with measurement data allows us to conclude, that they agree satisfactory. Thus, for instance, the breakdown voltage is 400...500 V (experiment) and 450...550V (simulation) (Fig. 2), bedding depth of p-region 2...4 um (experiment), 2...4.5um (simulation), bedding depth of n+-region 5...10um (experiment) and 7...12um (simulation).

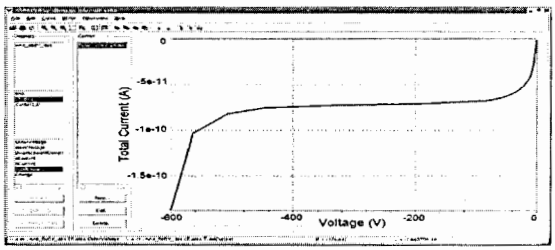


Fig. 2. Calculating VI characteristic of microstrip detector

Table 1

| № | Name of technological operation | Parameters of technological operation |
|---|---|---|
| 1 | Choice of environment | DIOS simulator, substrate thickness 100 um, orientation <111>, simulation region SIM2D (2D-simulation) |
| 2 | Choice of substrate | Dopant Phosphorus concentration 1e12/cm², surface resistance 5kOhm/cm |
| 3 | Anneal 1 | Time 30 min, temperature 950°C |
| 4 | Anneal 2 | Time 60 min, temperature 1000°C |
| 5 | Mask A deposition | Polarity – dark field, thickness 1 um |
| 6 | Oxide etching | Thickness 0.5um, etching type anisotropic |
| 7 | Oxide etching (lower side) | Thickness 0.5um, etching type anisotropic |
| 8 | Ion implantation 1 (upper) | Boron, dose 1e13/cm², energy 60 keV |
| 9 | Ion implantation 2 (lower) | Arsenic, dose 1e13/cm², energy 70 keV |
| 10 | Photoresist A etching | Thickness 1um, etching type anisotropic |
| 11 | Dopant 1 annealing | Time 15 min, temperature 950°C |
| 12 | Dopant 2 annealing | Time 30 min, temperature 1000°C |
| 13 | Dopant 3 annealing | Time 45 min, temperature 1050°C |
| 14 | Mask B deposition | Polarity – dark field, thickness 1 um. |
| 15 | Material (upper and lower sides of substrate) deposition | Metal, thickness 1um. |
| 16 | Mask B deposition | Polarity – light field, thickness 1um |
| 17 | Metal etching (upper and lower sides of substrate) | Thickness 1um, etching type anisotropic |
| 18 | Photoresist B etching | Thickness 2um, etching type anisotropic |

Other useful results of the conducted studies consist in refining the values of elements of the microstrip detector SPICE-model. There have been published several SPICE models of microstrip detector [4, 5], one of which is presented in Fig. 3.

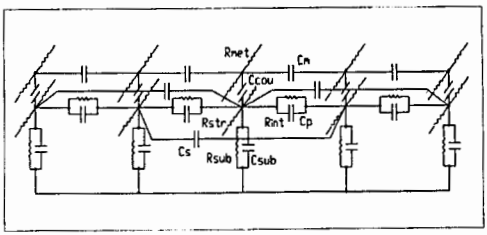


Fig. 3. SPICE model of microstrip detector

Using the simulation techniques of TCAD, it is possible to optimize those models, what would be much useful for solving the problem of matching optimally the microstrip detector with front-end electronics.

**References**


[1] G. Bagliesi et al., A double sided readout silicon strip detector: a new device for vertex detection in high energy experiments, INFN PIAE, 1986.

[2] W. Adam, E. Berdermann et al., Microstrip sensors based on CVD diamond, NH Elsevier, 2000, pp. 141-148.

[3] www.roscosmos.ru/Docs/Conkurs-Plan-2009.doc

[4] N. Baccetta, D. Bisello at al., A SPICE model for Si microstrip detectors and read-out electronics, IEEE, June 1996, Vol. 43, pp. 213-1219.

[5] N. Baccetta, D. Biselo, HSPICE simulations of Si microstrip detectors, NH Elsevier, 1998, pp. 142-146.

# Radiation hardness research of the strip and ELT transistors manufactured on submicron (0.18 microns, UMC, Taiwan) technologies for CBM experiment

A.B. Simakov
*Moscow Engineering Physics Institute (State University- MEPHI), Russia*

Moscow Engineering Physics Institute is official member of International Scientific Collaboration CBM (Compressed Baryonic Matter) experiment in GSI. MEPHI is responsible for IP-blocks design of front-end electronics for new VLSI type SoC (System on a Crystal) for STS (silicon tracker station) of CBM. This electronics will be placed in inner part of heavy ions accelerator – FAIR and should have very high radiation hardness. A manufacturing of integrated SoC is planning on silicon factory UMC (Taiwan), using KMOS technology with resolution factor 0.18 micron. Experimental data of radiation tests of different NMOS transistors are given in this report. Two different topologies of test NMOS transistors are shown on Fig. 1.

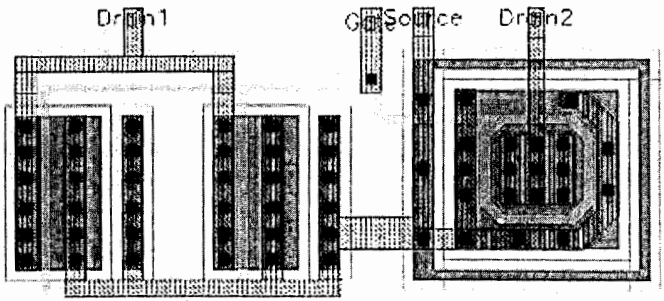


Fig. 1. Different topologies of NMOS transistors

The left transistor has traditional stripe topology (Two-edge layout). The right transistor is so-called ELT structure (Enclosed Layout Transistor). Here the drain region is completely surrounded by source ring. This design has to have essentially less value of leakage current especially under radiation action. Both structures were designed in MEPHI's design center (Cadence and Mentor Graphics CAD platforms). The main design task is getting similar electrical characteristics for both transistors. For calculation of ratio W/L (W – width, L – length of the NMOS channels) of ELT we break common structure on three parts, as it is shown on Fig. 2.

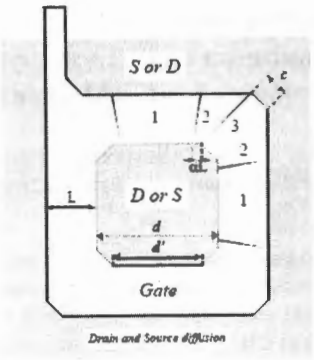


F

Fig. 2. Topology ELT (part 1 – horizontal, part 2 – diagonal, part3 – angular)

The joint W/L is calculated as sum of all small transistors.

$$\left(\frac{W}{L}\right)_{eff} = a \cdot \frac{2\alpha}{\ln\frac{d'}{d'-2\alpha L_{eff}}} + b\frac{1-\alpha}{\frac{1}{2}\sqrt{\alpha^2+2\alpha+5}\ln\frac{1}{\alpha}} + c\frac{d-d'}{2L_{eff}}.$$

Here, *a, b, c* – amount of corresponding types of small transistors. Coefficient α – doesn't depend on topology and equals 0.05.

So, transistors on Fig. 1 have effective length 0. 18 μ and effective width – 7.2 μ. The test transistors were manufactured on UMC with help of "EUROPRACTICE".

The static characteristics were measured in control-testing division of MEPHI's design-center. The test board is shown on Fig. 3.

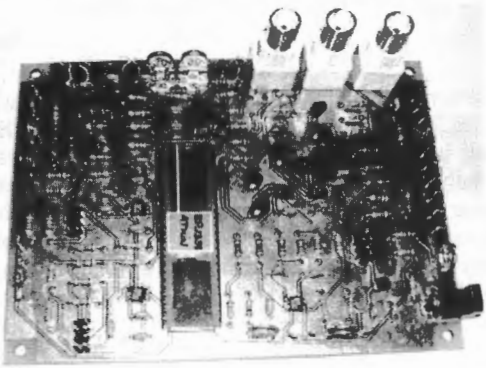

Fig. 3. Test board for static characteristics measurements

The input and output voltage-current characteristics are shown on Fig. 4, and Fig. 5.

After this, the transistors were irradiated by linear electron beam accelerator with energy 8 MeV (width of spectra – 30%) and consequently total doses: 100 krad; 1 Mrad; 3 Mrad.

The 100 krad didn't change static characteristics of the transistors. But at doses more than 1 Mrad essential leakage current arise between source and drain of traditional stripe topology.

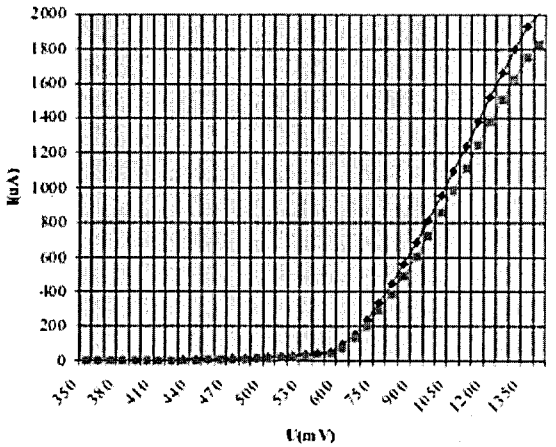


Fig. 4. The input characteristics of test transistors (dark line –ELT)

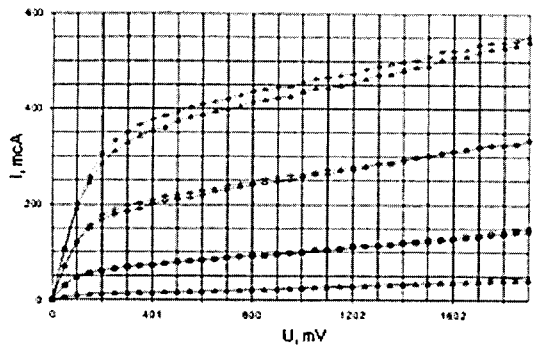


Fig. 5. The output characteristics of test transistors (Δ –ELT)

The 0, 1 μA leakage currents have appeared in strip transistors at the doze 1 Mrad. At the doze 3 Mrad it increased up till 1μA. In ELT leakage currents were not observed. In both types of transistors the maximal shift of the threshold voltage was 200 mV at the doze

3 Mrad and at nominal threshold voltage 400 mV. Fig. 6 demonstrates this on example of changes of transfer characteristics.

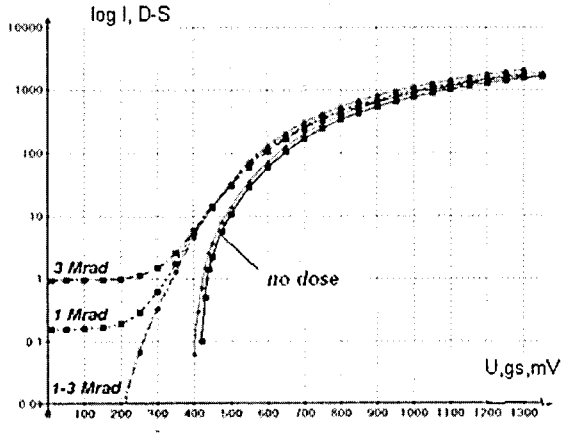


Fig. 6. Transfer characteristics of the pair transistors

The ELT has no leakage current even at 3 Mrad dose. Both transistors have shift of threshold voltage about 200 mV (original – 400 mV).

The carried out experiments have evidently shown the advantages of the ELT structures in comparison with the stripe at designing of radhard integrated microcircuits for CBM experiment.

# SPEEDUP - optimization and porting of path integral MC Code to new computing architectures

V. Slavnić, A. Balaž, D. Stojiljković, A. Belić, A. Bogojević
*Scientific Computing Laboratory, Institute of Physics Belgrade, Serbia*

Path integral formalism presents the concise and flexible formulation of quantum theories at different levels, providing also simple description of many other complex physical systems. Recently introduced analytical approach that systematically improves convergence of numerically calculated path integrals of a generic theory leads to a significant speedup of Path Integral Monte Carlo algorithms. This is implemented in the SPEEDUP code. Here we report on optimization, porting and testing of the SPEEDUP code on new computing architectures: latest Intel, and IBM POWER6 and PowerXCell CPUs. We find that the code can be highly optimized and take substantial advantage of the features of new CPU types.

## 1. Introduction

Path integral Monte Carlo code SPEEDUP [1] is used for various calculations mainly for studies of Quantum Mechanical systems and investigation of global and local properties of Bose-Einstein condensates. Porting of this code to new computing architectures will enable its use on a broader set of clusters and supercomputer facilities. The purpose of the code optimization is to fully utilize available computing resources, eliminating bottlenecks that may be located in different parts of the code, depending on the details of hardware implementation and architecture of the CPU. In some situations even compiling, linking or choosing more appropriate (optimized) libraries can lead to significant reduction in program execution times. However, the optimization must be performed carefully and the new code has to be verified after each change by comparison of its numerical results with the correct reference values.

In addition to obtaining highly optimized code, the above procedure can be also used to benchmark different hardware platforms and to compare their performance on a specific application/code. Such application-specific benchmarking, based on the assessment of hardware performance for the chosen set of applications, can be also used for the proper planning of hardware upgrades of computing centers supporting several user communities.

## 2. SPEEDUP code

Functional formalism in quantum theories naturally introduces Monte Carlo simulations as a method of choice for numerical studies of relevant physical systems. The discretization of the phase space (necessary in any numerical calculation) is already built in to the functional formalism through the definition of continuous (path) integrals, and can be directly translated into the Monte Carlo algorithm. A detail study of the relationship between discretization of different coarseness in the case of a general quantum theory leads to substantial increase in convergence of path integral to its continuum limit [2-4]. This study resulted in an analytic procedure for deriving a hierarchy of effective actions up to an arbitrary level $p$. We will illustrate the use of higher-level effective actions for calculation of the transition amplitude $A$ for a quantum system that evolves from the initial state $i$ to the final state $f$ in time $T$. In the path integral formalism, this amplitude is given as $N\to\infty$ limit of the $(N-1)$-fold integral expression:

$$A_N(i;\, f;\, T) = \left(\frac{1}{2\pi\epsilon_N}\right)^{N/2} \int dq_1 \cdots dq_{N-1} e^{-S_N},$$

where $S_N$ is the discretized action of the theory and $\epsilon_N=T/N$ is the discrete time step. Using naively discretized action, the transition amplitude would converge to its continuum limit as

slow as $1/N$. Numerical simulations based on the use of effective action of the level $p$ have much faster convergence, approaching the continuous limit as $1/N^p$. The effective discretized actions up to level $p$=18 are implemented in the Path Integral Monte Carlo SPEEDUP code [1] in C programming language. It is used for efficient calculation of transition amplitudes, partition functions, expectation values, as well as low lying energy spectra.

The algorithm of a serial SPEEDUP code can be divided to the following steps:

1. Initialize variables; allocate memory; set input parameters of the model, number of time and MC steps, and random number generator (RNG) seed.
2. Main Monte Carlo loop, which accumulates contributions of sampled trajectories to intermediate variables; each loop step consists of the following steps:
   a. Generate trajectory using bisection method [5]. The number of time steps is $N=2^s$, where $s$ is the discretization level (input parameter),
   b. Calculate effective action for a generated trajectory and each sub-trajectory with smaller discretization level ($s$-1, ..., 1),
   c. Accumulate variables used to calculate observables and their error estimates at each discretization level,
3. Calculate observables and associated errors by averaging variables accumulated in the previous step at each discretization level,
4. Print the results, deallocate memory and exit the program.

Parallelization of the above Monte Carlo algorithm is very simple, since each loop step 2 is independent. Therefore, the total number of Monte Carlo steps can be easily and evenly divided to a desired number of CPU threads or parallel processes (in MPI or in other available parallelization environment).

The SPEEDUP code generates large numbers of random trajectories and relies on the MC theory to achieve no correlations between the generated trajectories. This necessitates high-quality RNG, able to produce large numbers of uncorrelated random numbers from the uniform probability density distribution, in a form suitable for parallel simulation. For the SPEEDUP code we have used SPRNG - Scalable Parallel Random Number Generator [6], which is verified to satisfy all of the above criteria. SPRNG can generate large numbers of separate uncorrelated streams of random numbers, making it ideal for parallel applications.

### 3. Tested hardware architectures

The hardware platform used for the testing reported in this paper was IBM BladeCenter with 3 kinds of servers within the H-type chassis commonly used in high performance computing:

- HX21XM blade Server based on Intel Xeon technology. It features two Intel Xeon 5405 processors that run on 2.0 GHz with front side bus of 1333MHZ and level two cache (L2) of 12MB with support for Intel SSE2, SSE3, SSE4.1 extensions. Along with standard GCC (GNU Compiler Collection) compiler (gcc version 4.1.2), Intel C++ Compiler Professional Edition 11.1 by Intel Corporation (ICC) [7] that includes advanced optimization, multithreading, and processor support, as well as automatic processor dispatch, vectorization, and loop unrolling was used for testing in this paper.
- The BladeCenter JS22 server is a single-wide, 4-core, 2-socket with two cores per socket, 4.0 GHz POWER6 [8] SCM processors. Each processor includes 64 KB I-cache and 32 KB D-cache L1 cache per core with 4 MB L2 cache per core. Processors in this blade server are based on POWER RISC instruction set architecture (ISA) with AltiVec, a single-instruction, multiple-data (SIMD) extensions. IBM provides XL C/C++ compiler solution (XLC) [9] that offers automated SIMD capabilities for application code that can

be quite help for programmers. Beside GCC compiler IBM XLC/C++ is used for benchmark purposes in this paper.

- The IBM BladeCenter QS22 is based on 2 multi-core IBM PowerXCell 8i processors, based on Cell Broadband Engine Architecture (Cell/B.E.) [10]. The Cell Broadband Engine is a single-chip multiprocessor with nine processors specialized into two types:
    1. The PowerPC Processor Element (PPE) is a general-purpose, dual-threaded, 64-bit RISC processor fully compliant with the 64-bit PowerPC Architecture, with the Vector/SIMD Multimedia Extension operating at 3.2 GHz. It is intended primarily for control processing, running operating systems, managing system resources, and managing SPE threads.
    2. The SPE (Synergetic Processing Element) is core optimized for running compute-intensive applications. SPEs are single-instruction, multiple-data (SIMD) processor elements that are meant to be used for data-rich operations allocated to them by the PPE. Each SPE contains a RISC core, 256 KB software-controlled locale storage (LS) for instructions and data, and a 128-bit, 128-entry unified register file. The SPEs provide a deterministic operating environment. An SPE accesses both main memory and the local storage of other SPE's exclusively with DMA commands. They do not have caches, so cache misses are not a factor in their performance and programmer should to avoid branch intensive code.

    The Cell Broadband Engine has one PPE and eight SPEs.

Such a heterogeneous multi-core architecture of the Cell CPU requires that a developer adopts several new programming paradigms in order to fully utilize the full potential of Cell B/E processor. In addition to the GNU tools (including C and C++ compilers) which are provided with the Software Developer's Kit for Multicore Acceleration [11], one can also use IBM XL C/C++ Compiler [9] for Multicore Acceleration, specialized for Cell Broadband Engine solution.

## 4. Results

Here we describe the performed optimization and the obtained benchmarking results. In all benchmarks in this paper we have executed the code with $Nmc$=5120000 MC samples for the quantum-mechanical amplitude of the quartic anharmonic oscillator with the boundary conditions $q(t=0)=0$, $q(t=T=1)=1$, with zero anharmonicity and with level $p$=9 effective action. We always used the same seed for SPRNG generator so that the results can be easily compared. Section 4.1 gives results for a serial SPEEDUP code on each platform with different compilers. These results are later used as a reference in benchmarking and in verification of the optimized code. Section 4.2 gives results for SPEEDUP MPI code tested on Intel platform and Section 4.3 presents the threaded SPEEDUP code and results obtained with Intel and POWER architectures. In Section 4.4 we give results for the Cell SPEEDUP code, and in Section 4.5 we compare all obtained results.

### 4.1. Serial SPEEDUP code

For Intel Blade server we compiled the serial code with GCC C compiler using optimization flags *O1* and *funroll-loops* which give the best performance (better than the *O3* flag, with or without loop unrolling). Along with GCC, we also used ICC compiler with maximal optimization flag *O2*.

On POWER6 and Cell Blades the code was compiled with both GCC and IBM XLC compilers. On Cell Blade we used the flags *O3*, *funroll-loops*, *mabi=altivec*, and *maltivec*

with GCC, and *O5*, *qaltivec* and *qenablevmx* with XLC. Appropriate versions of GCC and XLC binaries were used (ppu-gcc and ppuxlc). On POWER6 Blade the *O5* flag was used with XLC and *O3* and *funroll-loops* with GCC. Results for serial program testing are presented in Table 1.

Table 1. Average time of execution of a serial SPEEDUP code on all tested platforms with different compilers

| Compiler / Platform | GCC | ICC | XLC |
|---|---|---|---|
| Intel | (13760±50) s | (10160±30) s | - |
| POWER6 | (17000±10) s | - | (1900±10) s |
| Cell | (49410±50) s | - | (14020±20) s |

Table 1 demonstrates the significant increase in the speed of the code when platform-specific compiler is used. We also see that in this specific case the POWER6 platform in combination with the XLC compiler shows order of magnitude improvement in the speed compared to the Intel platform. On the other hand, it is clear that Cell version, running only on the PPE is no match for other two platforms. Real utilization of the Cell platform can be achieved only when SPEs are used.

### 4.2. MPI SPEEDUP code

On the Intel Blade multicore, we tested the performance of the SPEEDUP code with MPI implementation, compiled with GCC and ICC compliers. The results are shown in Fig. 1.

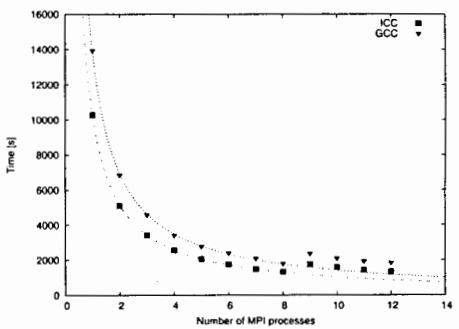


Fig. 1. Average times of execution of the MPI SPEEDUP code on Intel platform compiled with ICC (*O2* flag) and GCC (*O1* and *funroll-loops*). The curves give fits to the expected dependence $A + B$ / (Number of MPI processes).

As we can see, the MPI version of the code shows excellent scalability with the number of MPI processes. When the number of MPI processes exceeds the number of physical cores in the system, the operating system is trying to distribute the load among

already fully loaded cores, which creates additional overhead. This implementation gives minimal execution time of 1320s.

### 4.3. Modified SPEEDUP code

To fully optimize the parallel SPEEDUP code, instead of using MPI API we implemented its threaded version using POSIX threads (pthreads). Each thread calculates *Nmc/Nth* of Monte Carlo samples where *Nth* is the number of threads. Also, some minor additional modifications of the code were performed, focusing on specific improvements for $p$=9 effective action. The Intel version was compiled with ICC, while the POWER version was compiled with XLC. The obtained numerical results are shown in Fig. 2.

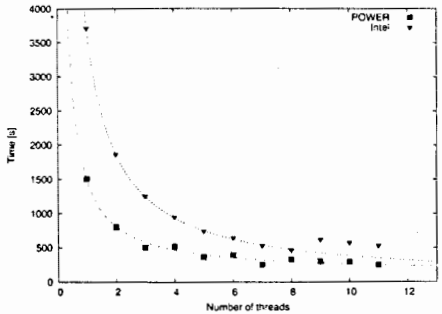


Fig. 2. Average times of execution of the threaded SPEEDUP code on Intel and POWER platforms

With the threaded code we obtained a significant increase in the speed of the code, even without implementing specific vector instructions (AltiVec on POWER6 or SSE on Intel). Again, POWER6 Blade in conjunction with XLC compiler was faster than Intel Blade. However, the relative increase in the speed of threaded code was larger on the Intel platform. The minimal execution time was 460s on Intel and 250s on POWER Blade. This gives relative increase in the speed of the code of 2.8 (threaded vs. MPI) for Intel and 1.3 (one thread vs. serial) for POWER6 platform.

We also note an interesting scaling issue on POWER6 system. While the threaded code scales perfectly on Intel Blade, POWER6 Blade shows strange behavior for even number of threads, where execution times are slightly higher than expected. When the code is compiled with GCC, the same behavior is observed for odd number of threads. Such throttling may be related to low-level hardware details that are not properly implemented in different compilers.

### 4.4. Cell SPEEDUP code

The heterogeneity of the Cell architecture required the slight rearrangement of the SPEEDUP code. We used MPI version of the code as a basis, and modified it so as to separate parts that are executed on the PPE and parts that are executed in parallel on SPEs. Our implementation was to create a number of pthreads on the PPE that will pass control and start execution of the code on the dedicated SPE for each pthread. Each SPE performs *Nmc/Number_of_SPEs* MC steps, running the same code, only with different parameters passed by the PPE. After all SPEs finish their work, the final processing of gathered data is done on the PPE.

The main problem in a proper porting of the SPEEDUP code to the Cell architecture was missing Cell SPRNG code that can be compiled for the SPU. For this reason, we have compiled SPRNG for the PPE and performed all RNG operations only on the PPEs. This was done in parallel through several pthreads, distributed between both PPU processors of a QS22 Blade. Each pthread is associated with one of SPEs and synchronizes with it using mailbox technique, one of the simplest, hardware based, ways of communication within Cell CPU. The PPE mailbox checking is implemented through the interrupt, without active waiting (such as polling through the loop). Access to the main memory by all SPEs is realized through the Direct Memory Access (DMA) transfers. We have one initial transfer where control data from the PPE are received, one final transfer where computation results are sent back to the main memory and intermediate transfers of generated random numbers for each MC step. The XLC-compiled code was superior in the performance compared to the GCC-compiled code. The results for the XLC-compiled code are shown in Fig. 3.

As we can see, the fact that only PPEs are used for generation of random trajectories leads to a saturation of the performance when we increase the number of used SPEs to around 4. In the ideal case, when PPEs would be able to produce enough random trajectories for all SPEs, the simulation execution time would be around 250s, as can be seen in Fig. 3 for the code without random number generation). We also tested the code with the communication part disabled (no DMA memory transfers). From Table 2 we see that the communication does not have significant impact on the execution time and does not represent a bottleneck. To confirm this, we tested also the code that only generates random trajectories on PPEs, and observed the saturation in its performance at about 750s for the given *Nmc* number. This clearly corresponds to the minimal execution time for the full version of the Cell code in Fig. 3.

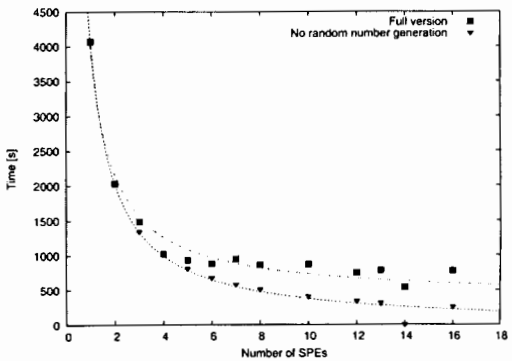


Fig. 3. Average times of execution of the Cell SPEEDUP code (full version) and for the code without generation of random numbers

Table 2. Average times of execution of the Cell SPEEDUP code without random trajectories generation and without PPE-SPE communication

| Number of SPEs | No random trajectories generation | No communication |
|---|---|---|
| 1 | (4040±5) s | (4020±5) s |
| 2 | (2020±5) s | (2010±5) s |
| 4 | (1010±5) s | (1000±5) s |
| 6 | (675±5) s | (670±5) s |
| 8 | (505±5) s | (500±5) s |
| 10 | (405±5) s | (400±5) s |
| 16 | (255±5) s | (250±5) s |

Therefore, as we can see, the missing implementation of the SPRNG library was limiting factor in fully utilizing the capabilities of all SPEs of the Cell Blade. This would not be the case if individual MC step calculation would require more time to complete, since then PPEs would be able to generate random trajectories at a sufficient rate. Such situation can be easily achieved e.g. if one uses higher effective action level $p$ code. We have demonstrated similar situation in Fig. 4, where we have used unoptimized Cell SPEEDUP code, and where we observe perfect scaling of the code with the number of SPEs. Note that we used only 5120 MC samples for these tests since the code is now executed much slower.

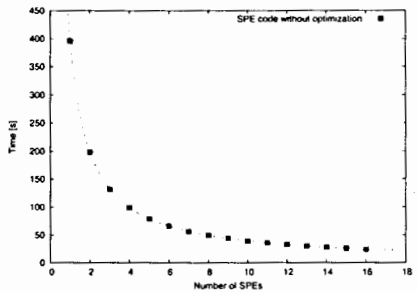


Fig. 4. Average times of execution of the Cell SPEEDUP code compiled without optimization

### 4.5. Comparison of hardware performance results

The overview of the obtained performance results for all tested hardware platforms is presented in Table 3. For Intel and POWER6 platform we give the results for the fully optimized threaded SPEEDUP code. For the Cell platform we give the minimal obtained execution time, as well as the execution time obtained with random trajectories generation disabled, which corresponds to the full utilization of all SPEs.

Table 2. Average times of execution of the Cell SPEEDUP code without random trajectories generation and without PPE-SPE communication

| Number of SPEs | No random trajectories generation | No communication |
|---|---|---|
| 1 | (4040±5) s | (4020±5) s |
| 2 | (2020±5) s | (2010±5) s |
| 4 | (1010±5) s | (1000±5) s |
| 6 | (675±5) s | (670±5) s |
| 8 | (505±5) s | (500±5) s |
| 10 | (405±5) s | (400±5) s |
| 16 | (255±5) s | (250±5) s |

Therefore, as we can see, the missing implementation of the SPRNG library was limiting factor in fully utilizing the capabilities of all SPEs of the Cell Blade. This would not be the case if individual MC step calculation would require more time to complete, since then PPEs would be able to generate random trajectories at a sufficient rate. Such situation can be easily achieved e.g. if one uses higher effective action level $p$ code. We have demonstrated similar situation in Fig. 4, where we have used unoptimized Cell SPEEDUP code, and where we observe perfect scaling of the code with the number of SPEs. Note that we used only 5120 MC samples for these tests since the code is now executed much slower.

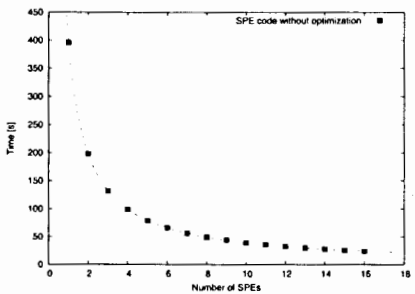


Fig. 4. Average times of execution of the Cell SPEEDUP code compiled without optimization

### 4.5. Comparison of hardware performance results

The overview of the obtained performance results for all tested hardware platforms is presented in Table 3. For Intel and POWER6 platform we give the results for the fully optimized threaded SPEEDUP code. For the Cell platform we give the minimal obtained execution time, as well as the execution time obtained with random trajectories generation disabled, which corresponds to the full utilization of all SPEs.

Table 3. Minimal average execution time per Blade of the fully optimized SPEEDUP code for each tested platform

| Intel | POWER6 | Cell | Cell Ideal |
|---|---|---|---|
| 460s | 250s | 750s | 250s |

## 5. Conclusion

We have ported and optimized Path Integral Monte Carlo SPEEDUP code to three different computing architectures (Intel, POWER6 and Cell) and used the obtained code for benchmarking of these hardware platforms. For Intel and POWER6 platforms full optimization was obtained with the straightforward threaded version of the code, while the Cell platform required more complex changes of the code (implementation of separate PPE and SPE parts of the code). For benchmarking purposes we have also used different available compilers for each of architectures, and our results clearly show that platform-specific compilers always give much better performance.

The SPEEDUP code was most easily optimized on the POWER6 platform, where it also achieves superior performance (per Blade server) compared to all other hardware platforms. The Cell platform is demonstrated to be able to achieve the same level of performance in the case when individual MC steps take more time to complete. In the current implementation, due to the missing Cell SPRNG library, SPEEDUP code can fully utilize all Cell SPEs only for higher effective action levels $p$. The Intel platform shows also very good performance and excellent scalability, without any glitches for certain (odd or even) number of cores, observed on other platforms.

The plans for further development and testing include porting of SPRNG library to SPEs and implementation of platform-specific instructions (vectorization) for each tested platform.


## Acknowledgements

This work was supported in part by the Serbian Ministry of Science, under project No. OI141035, and the European Commission under EU Centre of Excellence grant CX-CMCS. Numerical simulations were run on the AEGIS e-Infrastructure, supported in part by FP7 projects EGEE-III and SEE-GRID-SCI. The authors also acknowledge support by IBM Serbia.


## References


[1] SPEEDUP, https://viewvc.scl.rs/viewvc/speedup/
[2] A. Bogojevic, A. Balaz, A. Belic, Phys. Rev. Lett. 94 (2005) 180403.
[3] A. Bogojevic, I. Vidanovic, A. Balaz and A. Belic, Phys. Lett. A 372 (2008) 3341-3349.
[4] A. Balaz, A. Bogojevic, I. Vidanovic and A. Pelster, Phys. Rev. E 79 (2009) 036701.
[5] D. M. Ceperley, Rev. Mod. Phys. 67 (1995) 279.
[6] http://sprng.cs.fsu.edu/
[7] ICC, http://software.intel.com/en-us/intel-compilers/
[8] POWER, http://www-03.ibm.com/technology/power/
[9] XLC, http://www-01.ibm.com/software/awdtools/xlcpp/
[10] Cell B/E, http://www-03.ibm.com/technology/cell/
[11] IBM SDK for Multicore Acceleration, http://www.ibm.com/developerworks/power/cell/

# Commissioning of the ATLAS Liquid Argon Calorimeter

A. Talyshev[1]
*on behalf of the ATLAS Liquid Argon Calorimeter Group*
[1] *Budker Institute of Nuclear Physics, Novosibirsk, Russia*

The ATLAS liquid argon (LAr) calorimeter system consists of an electromagnetic barrel calorimeter and two end-caps with electromagnetic, hadronic and forward calorimeters. Since the installation of the LAr calorimeter in the ATLAS cavern, the electronic calibration of the readout system has been continuously exercised in the commissioning phase. The large amount of collected calibration data allows careful studies of the stability of constants, like pedestals and pulse shapes. The analysis of the large cosmic muon data samples and of the beam splash events that occurred on September 2008 has allowed to measure the in-situ calorimeter performance that was found to be close to the expectations.

## 1. Introduction

ATLAS [1, 2] is a general purpose detector built for operation at the Large Hadron Collider (LHC). The collider will produce proton-proton collisions at a center-of-mass energy of 14TeV at a design luminosity of $10^{34}$ $cm^{-2}s^{-1}$.

The Liquid Argon calorimeter (LAr) is a key detector component in the ATLAS experiment at the LHC. It provides precision measurements of electrons, photons, jets and missing transverse energy produced in the LHC proton-proton collisions. The LAr calorimeter has been installed in the ATLAS cavern and filled with liquid argon since 2006.

Since then, the calibration and readout systems have been extensively used by taking very frequent calibration runs. Physics data coming from cosmic muons (since summer 2006 up to now) and from the first LHC beam events (September 10 to 12th, 2008) were analyzed and used to measure the calorimeter in-situ performance.

## 2. The Liquid Argon Calorimeter

The ATLAS LAr calorimeters consist of four sub-detectors located in three cryostats filled with liquid argon which acts as active medium [3]. The central cryostat houses the electromagnetic barrel calorimeter (EMB), while each end-cap cryostat contains an end-cap electromagnetic calorimeter (EMEC), a hadronic end-cap wheel (HEC) and forward calorimeter (FCAL).

The EMB and EMEC provide a precise measurement of electron and photon positions and energies up to a pseudo rapidity of 3.2. Their absorbers are made of lead, achieving a minimal radiation length of 22 $X_0$. Their specific accordion geometry ensures a full hermeticity, a uniform and fast response. They are segmented in three longitudinal compartments (called the strip, middle and back samplings) to extract the shower shape, with an additional presampler layer in order to estimate the loss due to the dead material in front of the calorimeter. The resolution is expected to be $E/E = 10\%/\sqrt{E} \oplus 0.7\%$ after noise subtraction.

The HEC is a classical sandwich calorimeter with copper as passive material. Its pseudo rapidity coverage ranges from 1.5 to 3.2 with a minimal interaction length of 10 $\lambda$. It is segmented in depth in four longitudinal compartments. The resolution for hadrons is expected to be $E/E = 50\%/\sqrt{E} \oplus 3\%$.

The FCAL detects the particles in the forward region with pseudo rapidity coverage between 3.2 and 4.8. Due to the high particles occupancy in this region, a specific geometry with very thin liquid argon gaps (between 250μm and 500μm) has been adopted to limit the

space charge, which could induce detection inefficiencies. The absorbers are made of copper (in the first compartment) or tungsten (in the second and third compartments), with a depth equivalent to 11 $\lambda$. The resolution for hadrons is expected to be $\Delta E/E = 100\%/\sqrt{E} \oplus 10\%$.

### 2.1. Detector readout and calibration

The choice has been made to develop common readout electronics for all LAr sub-detectors (the HEC nonetheless uses cold preamplifiers). The LAr readout electronics is divided into a Front-End system [4] of boards mounted in custom Front-End crates (FEC) placed directly on the cryostat feedthroughs inside the ATLAS detector, and a Back-End system [5] of VME-based boards housed in the main services cavern (USA15), located 70 m away from the detector.

The signal induced on the electrodes has a triangular form. It is first routed to the front-end boards (FEB) [6] hosted in FEC. The raw signal after the preamplification is split into three linear gain scales with the ratio ~1/10/100. To optimize the signal-to-noise ratio, the signal is shaped by a bipolar $CR-(RC)^2$ filter. The resulted pulse is then sampled with the LHC bunch crossing frequency of 40 MHz and stored in analog pipelines during the L1 latency (2.5 μs). When the L1 trigger decision arrives, the optimal gain scale is selected. The pipelined samples are then digitized at a 5 MHz rate in 12-bit ADC which, together with the gain selection procedure, ensures the required 17-bit dynamic range over the whole energy interval. The FEB data are finally sent via the 1.6 Gbit/s optical link to the Read Out Driver (ROD) of back-end electronics. Typically five samples per channel are transmitted during LHC standard running and up to 32 samples can be readout for commissioning studies. The ROD processor unit applies an optimal filtering algorithm to the samples in order to compute the energy and time of the pulse for every calorimeter cell and also $\chi^2$ - like quantity characterizing the quality of the waveform.

An electronics calibration system is used to monitor the electronics response and to compute the electronic gain. The dynamic range of the calibration board [7] is 16 bits and the observed non-linearity is less than 0.1%. However the pulse shape differs in calibration and physics modes because the injected calibration signal has an exponential shape and the ionization one is triangular, and because they are injected at different points - mother boards instead of electrodes (Fig.1).

### 2.2. Energy computation

Based on the sample values $s_i$ (in ADC counts), after pedestal $p$ subtraction, the maximum amplitude of the pulse $A_{\max}$ as well as the time shift of signal maximum $\Delta t$ is obtained by Optimal Filtering (OF) technique [8]:

$$A_{\max} = \sum_{i=1}^{N_{samples}} a_i (s_i - p), \quad \Delta t = \frac{\sum_{i=1}^{N_{samples}} b_i (s_i - p)}{A_{\max}}.$$

The $a_i$ and $b_i$ are the Optimal Filtering Coefficients (OFC) determined while minimizing the dispersion in $A_{\max}$ and $\Delta t$ arising from electronics and pile-up noise, taking into account the time autocorrelation of noise. Using 5 samples, the electronic noise is reduced by a factor of 1.7 with respect to the readout with only one sample.

The following formula presents the steps needed to get the cell energy from the amplitude $A_{\max}$:

$$E_{\text{cell}} = F_{\mu\text{A}\to\text{MeV}} \cdot F_{\text{DAC}\to\mu\text{A}} \cdot \frac{1}{M_{\text{phys}} / M_{\text{cali}}} \cdot R \cdot A_{\text{max}},$$

where $F_{\mu\text{A}\to\text{MeV}}$ and $F_{\text{DAC}\to\mu\text{A}}$ are two conversion factors. The first one depends on the sampling fraction and is estimated with simulations and results from testbeams. The second one takes into account calibration board specificities. The $R$ factor transforms ADC into DAC values. As $R$ is determined on calibration pulse and not directly on ionization pulse, the difference between those two pulses has to be taken into account. The energy is corrected for the ratio of the two pulse maxima $1/(M_{\text{phys}}/M_{\text{cali}})$, the ionization pulse being predicted by factorisation of the readout response [9]. All the constants in the formula for $E_{\text{cell}}$, except the first two factors, are determined by calibration runs [10].

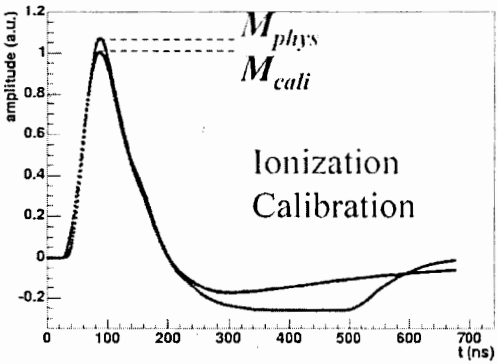


Fig. 1. Typical pulse shapes from calibration and ionization signals in the barrel EM calorimeter

### 2.3. Calibration runs

There are three different types of calibration runs: *pedestal*, *ramp* and *delay*.

The *pedestal* run consists of reading the detector with no input signal. It provides pedestal information from the average, noise from the RMS and noise autocorrelation from the timing correlation of the samples.

During the *ramp* run, current signals of different amplitude are injected by means of calibration board. The gain slope $R$ is extracted from a fit of the DAC versus ADC curve with a first order polynomial.

For a *delay* run the signals of constant amplitude are used. The calibration pulse is shifted by steps of 1.04 ns along 25 ns in order to reconstruct the pulse shape.

### 2.4. The constant stability

Frequent sets of calibration data are taken in order to test the stability of the different constants. An automatic processing has been put in place to reconstruct the data and prepare new sets of constants to be ready for loading into the ATLAS databases. The validation of those data is done with respect to a reference run. Databases are updated only if it is needed.

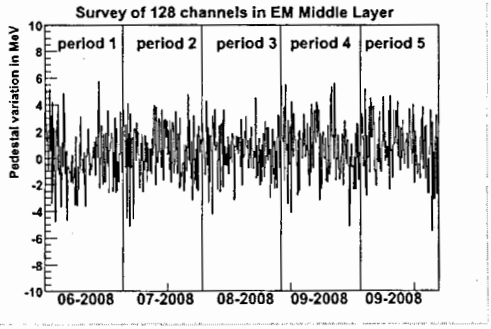


Fig. 2. Pedestal variation in MeV for different time periods, for a random set (1 FEB) of channels in the EM calorimeter

From recent measurements, it has been observed that in stable conditions (stable temperature, cooling, etc.) the parameter variations are small. As shown in Fig. 2, the pedestal variation is of the order of a few MeV, which is below noise level. The relative maximum amplitude difference of the calibration pulses is at the per mil level (Fig. 3). In such a case, the databases do not need to be updated.

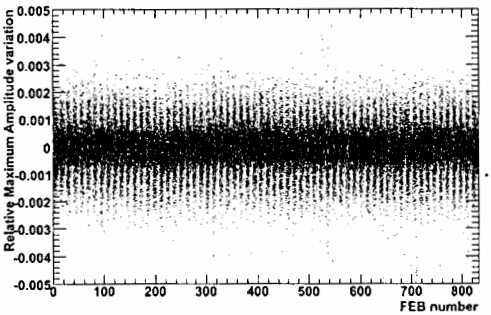


Fig. 3. Relative maximum amplitude variation of the calibration pulses in the barrel EM calorimeter

### 3. Cosmic data taking

Cosmic muon data are taken in ATLAS regularly for commissioning purposes since 2006. Events with large energy deposition in calorimeter cells were selected to compare with predictions [11].

32 samples were recorded, allowing to see the complete pulse shape. The measured signal (in ADC counts) is plotted in red as a function of the time (Fig. 4). The black dots represent the ionization pulse prediction. A nice agreement between the two can be observed (<2%) as shown by the green dots which represent the difference between data and calculation, normalized to the maximum amplitude of signal; the corresponding axis is given on the right part of the figure.

The length of the under-shoot of the pulse is related to the drift time and the rising at the end of the pulse is sensitive to a shift of the electrode with respect to its nominal central

positioning. Stable cosmic data runs taking at the end of the summer and during autumn of 2008 allowed to measure accurately the drift time of ionization electrons (Fig. 5). Data agree well with the expected values derived from the structure of the absorbers. The contribution of the gap variation to the barrel calorimeter response non-uniformity is no larger than 0.3%.

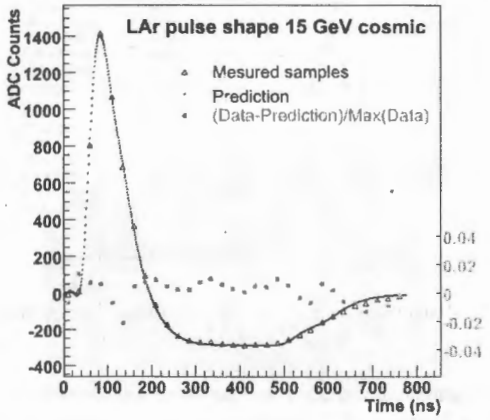


Fig. 4. Typical pulse for cosmic muon in the LAr EM Barrel

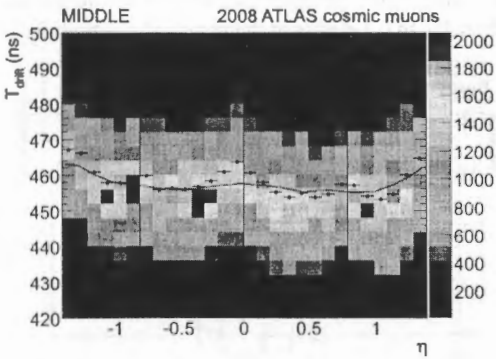


Fig. 5. Drift time as a function of η in the middle of LAr EM Barrel, in bins of 0.1. The black dots correspond to the mean values and the brown line illustrates the prediction from calorimeter geometry.

Muons, as minimum ionizing particles (MIP), deposit few hundreds of MeV on average in the electromagnetic calorimeter. Depending on the trigger conditions (the trigger was derived from the tile calorimeter signal or from the muon detectors signal), the recorded event rate was observed to be around 0.1 Hz - 1 Hz, with a signal well above the noise level. A selection on the minimal distance to ATLAS interaction point was applied in order to extract a sample of approximately 10000 pseudo projective muons and study detector uniformity. Fig. 6 displays the reconstructed energy of clusters located in the pseudo-rapidity range [0.3, 0.4]. The distributions are shown for two different clustering algorithms [12].

LArMuID is a variable size cluster algorithm better suited for normal LHC running, while the 3x3 cluster is less sensitive to out-of-cluster energy loss for non-projective muons.

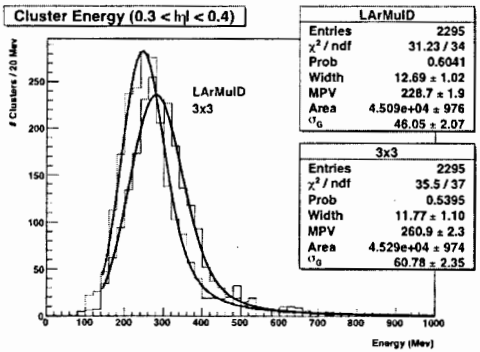


Fig. 6. Measured LArMuID and 3x3 cluster energy distributions in the range $0.3 < |\eta| < 0.4$

The Fig. 7 represents the variation of the fitted most probable value (MPV) of the Landau distribution as a function of the pseudo rapidity for both the data and Monte Carlo simulation. The variation of the energy deposition along $\eta$ is due to the different cell depths: since the muon energy deposition is proportional to the path length in the calorimeter, the Landau MPV naturally follows the cell depth variations. The energy response non-uniformity was shown to be less than 2% in 0.1 $\eta$ bins in the region $-0.8 < \eta < 0.8$.

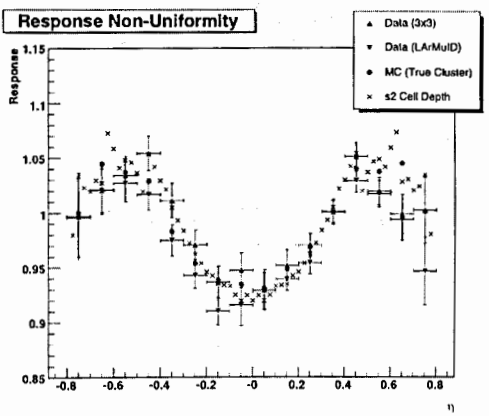


Fig. 7. Normalized $\eta$ dependence of the energy response of the EM barrel calorimeter to cosmic muons. Two cluster algorithms, Monte-Carlo results and cell depth evolution of the main EM layer are presented.

## 4. LHC beam data

During the first week of LHC operation in September 2008, with first single beams circulating in the LHC, events resulting from dump of the beam on collimator, located 140 m away from the ATLAS interaction point, called later 'splash events', were recorded. As a

consequence, a huge particle flow, mainly muons and pions, went through the detector and several hundreds of TeV were deposited over the whole coverage of each of LAr calorimeter samplings. Fig. 8 presents the accumulated energy per cell in the middle sampling of the EM calorimeter as a function of the pseudorapidity and azimuthal coordinate. In order to select signal, only cells with energy greater than 5 sigma of noise were summed.

The observed φ modulation, with eight energy dips, is due to the presence of the toroid endcap magnet located between the collimators and the LAr detectors. The lower energy deposit in the φ region [-2;-1] (corresponding to the lower part of the detector) can be explained by the LHC tunnel geometry, with an enhanced screening of particle flow in this region.

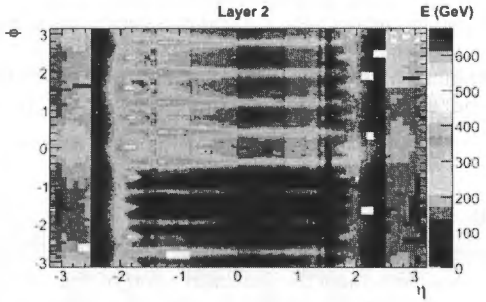


Fig. 8. (η, φ) map of energy deposited in the middle layer of the EM calorimeters (accumulated over 86 "beam splash" events)

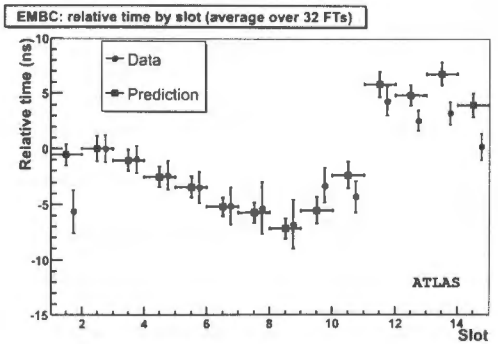


Fig. 9. Comparison between the predicted (black squares) and measured (red dots) cell timings for each FEB slot in the front-end crate, averaged over all front-end crates

The coherent arrival of particle flow through the whole detector, induced by beam splash events, allows one to study the timing of the whole LAr calorimeter. Fig. 9 shows the comparison between the predicted and measured cell timings averaged over all front-end crates as a function of the FEB slot in the crate. The measured timings are obtained using the optimal filtering coefficients and are corrected by a time-of-flight correction applied as if the particles were coming from the collision point. The predicted timings are derived from the calibration timings taking into account the different cable lengths involved in the readout path. The agreement between the two timings is better than 2 ns for most of the slots. The residual discrepancies can be corrected using a programmable delay on each FEB.

## 5. Conclusions

The LAr calorimeter has been installed in the ATLAS cavern and filled with liquid argon since 2006. The electronic calibration of the readout system has been continuously exercised in the commissioning phase, resulting in a fully commissioned calorimeter with its readout and a small number of problematic channels. A total of only 0.02% of the read-out channels are dead beyond repair and 0.2% need special treatment for calibration. Regular calibration runs show the good stability of constants. The energy response non-uniformity measured in cosmic muons is less than 2% in the region $-0.8 < \eta < 0.8$. The particle flow occurred during the beam-collimator splash allowed to verify the timing alignment at the level of 2 ns.

The commissioning of the ATLAS LAr calorimeter has shown that the detector, calibration system and signal reconstruction infrastructure are fully ready for the LHC collisions.

## 6. Acknowledgments

The work presented here has been performed within the ATLAS LAr collaboration. It would not have been possible without the dedicated effort of many people in our LAr detector group and the ATLAS collaboration over many years. I would like to thank all the people who built, integrated and installed the LAr detectors in the ATLAS cavern and those who operate the detector on a daily basis.

## References

[1] ATLAS Collaboration, ATLAS: Technical design report, CERN-LHCC-99-14/15, 1999.
[2] ATLAS Collaboration, G. Aad et al., The ATLAS Experiment at the CERN Large Hadron Collider, JINST 3 S08003, 2008.
[3] ATLAS Collaboration, ATLAS liquid argon calorimeter: Technical design report, ATLAS-TDR-002, CERN-LHCC-96-41, 1996.
[4] N.J. Buchanan et al., ATLAS liquid argon calorimeter front-end electronics, JINST 3 P09003, 2008.
[5] The Liquid Argon Back End Electronics collaboration, ATLAS liquid argon calorimeter back-end electronics, JINST 2 P06002, 2007.
[6] N.J. Buchanan et al., Design and implementation of the Front End Board for the readout of the ATLAS liquid argon calorimeters, JINST 3 P03004, 2008.
[7] J. Colas et al., Electronics calibration board for the ATLAS liquid argon calorimeters, NIM A593 (2008), pp.269-291.
[8] W.E. Cleland, E.G. Stern, Signal processing consideration for liquid ionization calorimeters in a high rate environment, NIM A338 (1994), p. 467.
[9] D. Banfi at al., Cell response equalisation of the ATLAS electromagnetic calorimeter without the direct knowledge of the ionisation signals, JINST 1 (2006), P08001.
[10] C.Collard on behalf of the ATLAS Liquid Argon Calorimeter Group, Electronic calibration of the ATLAS LAr calorimeter, ATL-LARG-PROC-2009-001.
[11] C.Collard et al., Prediction of signal amplitude and shape for the ATLAS electromagnetic calorimeter, ATL-LARG-PUB-2007-010.
[12] M. Cooke et al., In situ commissioning of the ATLAS electromagnetic calorimeter with cosmic muons, ATL-LARG-PUB-2007-01.

# Detecting low level signal for digitization method used in ATLAS Tile Calorimeter

V. Tsiskaridze
*Iv. Javakhishvili Tbilisi State University, Tbilisi, Georgia*

Detecting low level signal in a noisy environment requires detailed information on the noise statistical parameters. There are well-known methods for solving this problem when the noise is Gaussian. The raw data analysis shows however that in some cases the distribution of ATLAS Tile Calorimeter (TileCal) digitizer samples noise definitely differs from Gaussian. This motivates studying possible causes of this difference and the method allowing effective detection of a low level signal over such a noise.

One reason for a non-Gaussian distribution may be nonlinearity of the measuring device, such as an analog-to-digital converter (ADC). Digitizing system used in TileCal allows a programmable shift of the baseline using internal DAC settings. Under the assumption that outside noise does not correlate with this adjustment a method for measuring samples distribution and detecting the low level signal is proposed.

## 1. Introduction

The ATLAS Hadronic Tile Calorimeter (TileCal) is one of the subdetectors in ATLAS experiment 0. TileCal is a sampling calorimeter made of steel and plastic scintillating tiles which are grouped by cells. The light produced by the particles in cells is routed to photomultiplier tubes (PMTs). Information is read out from PMT through corresponding channel.

Raw data analysis shows that noise distribution, which comes from the channel, in some cases definitely differs from Gaussian. One can try to fit the data using more complex distribution function for a noise (for example such as Double Gaussian distribution 0) as well as study possible reasons of such distribution.

In this paper we focus on effects, which may come from ADC nonlinearity side. For signal digitization and reconstruction we use the method used in TileCal 0.

## 2. Front-end Electronics

The signal in each channel is measured by a PMT. A 3-in-1 card which is attached to each PMT amplifies and shapes the PMT pulse by means of a shaper 0. Shaped PMT signals are produced with two linear outputs with relative gain of 64 and are sent to high-gain and low-gain digitizing 10-bit ADCs. Each ADC digitizes signal in 7 time slices of 25 ns.

In case of the auto-gain mode the front-end electronics automatically defines which gain to use and sends 7 samples with an additional 1 bit gain information to the back-end electronics. In the bi-gain mode both sets of the samples are sent to the back-end.

For a noise study we may use the TileCal digitizer's properties. One digitizer contains 2 TileDMU chips, each of them controls 3 PMTs (both gains). TileDMU allows us to shift the pedestal levels for high and low gain ADCs separately, using DAC settings. Three ADC for each gain use the same DAC property, so we cannot change pedestal of ADCs independently. We suppose that the noise which comes to the ADC input does not correlate with the DAC settings.

## 3. ADC Characteristic

In a TileCal digitizer the AD9050 10-Bit 40 MSPS ADC is used 0. At the input, the analog signal is buffered by a high speed differential buffer and applied to a track-and-hold (T/H) that holds the analog value present when the unit is strobed with an ENCODE command. The two stage architecture completes a coarse (5-bit ADC) and then a fine (5-bit ADC) conversion of the T/H output signal. This means that the fine 5-bit ADC nonlinearity (32 ADC counts) will repeat periodically with coarse 5-bit ADC shifts.

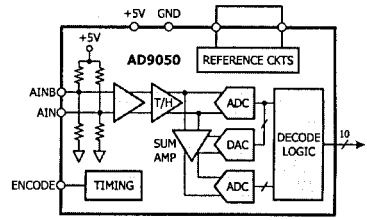

**Block Diagram of AD9050**

In our ADC model we suppose, that coarse ADC is ideal. So, we have only fine ADC nonlinearity with 32 counts periodicity.

We assume, that each of the ADC values has its own acceptance width $w_k$, $k = 0,\ldots,1023$.

In case of ideal ADC these widths are $w_k = 1$.

For each value $k$ we can define

$$v_0 = 0 \text{ and } v_{k+1} = v_k + w_k .$$

The periodicity of ADC (32 ADC counts) means, that $v_{k+32} = v_k$.

The ideal coarse ADC means, that $v_{32\cdot k} = 32$ ADC counts.

By definition, for an input value $x$ our ADC returns $k = \mathrm{ADC}(x)$, such that $v_k \le x < v_{k+1}$.

## 4. Signal Reconstruction

The amplitude of the signal is reconstructed using Optimal Filtering Coefficients (OFC) $a_i$ ($i = 1, \ldots, 7$) and represents a linear combination of the samples $s_i$ ($i = 1,\ldots,7$) 0,

$$A = a_1 \cdot s_1 + \ldots + a_7 \cdot s_7 .$$

If we assume that without a signal the $s_i$ samples are not correlated and are distributed according the Gaussian law we can expect that the reconstructed amplitudes should also have the Gaussian distribution.

Actually digitized samples are integers from [0..1023] interval. Even approximately, for RMS ~ 1.5, it cannot be considered as Gaussian distributed. Thus, we should take into account the ADC rounding effects.

## 5. Monte Carlo Simulation

The input noise is considered to be Gaussian-distributed i.e. $x_i$ = Gauss(*ped*, *rms*), where Gauss(*mean*, *sigma*) – is a function which returns random value with given *mean* and *sigma*. We also assume that we have no correlation between $x_i$. Digitized samples $s_i = \mathrm{ADC}(x_i)$, reconstructed amplitude $A = a_1 \cdot s_1 + \ldots + a_7 \cdot s_7$. For different values of pedestal and RMS we checked whether the amplitude is normally distributed.

## 6. Simple ADC Model

The simplest model is the ideal ADC, when all $w_k = 1$. The Monte Carlo (MC) simulation has shown that for any pedestal value for RMS ~ 1.5, the distribution of the amplitude resembles Gaussian. This means that here the contribution to non-Gaussianity is negligible.

## 7. Nonlinear ADC Model

For a nonlinear ADC model we take the values of $w_k$ randomly

$$w_k = \text{Gauss}(1, 0.3), \text{ for } k = 0, 1, ..., 31$$

and scale them so that to get a period 32 ADC counts. An example of such random ADC nonlinearity is shown below.

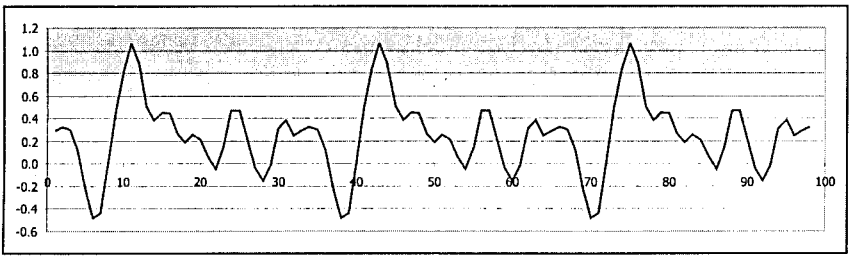


**Residuals of ADC nonlinearity**

The MC simulation has shown, that for the most of the pedestal levels, the distribution of amplitude is Gaussian, but there is some exceptional region, where the distribution is non-Gaussian. It lasts about 9 % of the ADC nonlinearity period (32 ADC counts interval) and the placement of the exceptional region within the period changes from channel to channel. The distributions of amplitude for these pedestals are shown below.

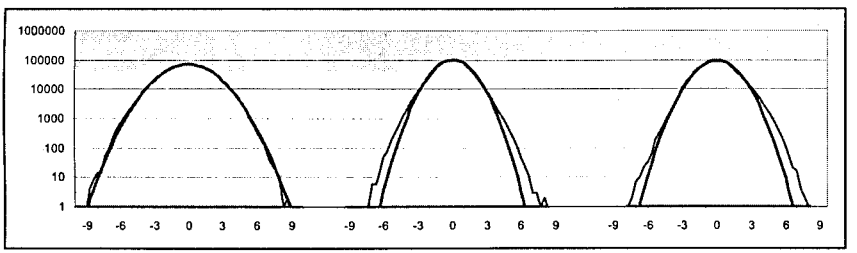


**Distributions of Amplitude (Log Scale)**

To avoid such non-Gaussian distribution we can choose individual DAC settings for each channel, which are outside the exceptional region. For the TileCal digitizer, due to the TileDMU design, a DAC setting simultaneously affects 3 channels. So, in the worst case we may get an undesirable area covering about 27 % of the ADC period. Nevertheless remaining 73 % are more than enough for choosing appropriate DAC settings, avoiding exceptional areas for each of these 3 channels.

## 8. Distribution of Samples

Direct measurements of the sample distributions cannot give satisfactory results due to the ADC nonlinearity. The MC simulation shows that the distribution of samples changes, when we change the DAC settings (which means that nonlinearity starts to play a role).

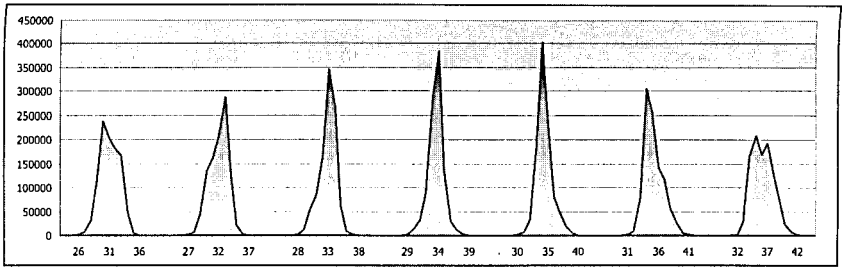


**Distributions of Samples for different DAC settings**

With such variable distributions it is very difficult to make any precise measurement or conclusion. So, we should find a way to measure the sample distribution which is insensitive to the ADC nonlinearity.

## 9. DAC Scan

The proposed DAC scan method is insensitive to the ADC nonlinearity and allows to measure the samples distribution.

First of all we fix some ADC value $u$. Then for each DAC setting we make a set of measurements and calculate the ratio of samples which are equal to $u$. A function $f$ created by this way will be proportional to the distribution of samples.

For a different ADC value $u'$, we will have a different distribution $f'$, which is proportional to $f$ i.e. $f' = c \cdot f$, where $c$ is a scale coefficient and depends on the ADC nonlinearity. The shape of $f$ does not depend on ADC nonlinearity. Here we significantly use the fact that DAC scan linearly changes the pedestal value.

For each ADC value $u$ distribution $f_u(x) = c_u \cdot f(x)$, where $c_u$ depends on $u$ (i.e. on ADC nonlinearity). The coefficient $c_u$ corresponds to the sensitivity of a particular ADC value (width of bin for the value $u$) and has the same period as the ADC. When the amplitude of ADC nonlinearity is around 1.5 ADC counts, the amplitude ratio between neighboring shapes may reach ~2.5.

For TileCal digitizer the scan step for 1 DAC = 0.6 ADC counts. This means, that using the DAC scan, we can more precisely measure the distribution.

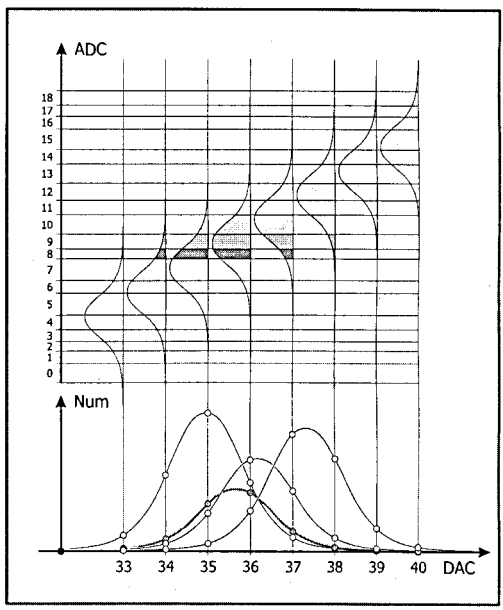


**DAC Scan Results for Different ADC Values**

## 10. Conclusions

The proposed method of DAC scanning allows to measure the distribution of samples with 1 DAC count step. It does require any preliminary information about the ADC nonlinearity. The ADC nonlinearity may be one of the reasons of samples non-Gaussianity. With the default DAC setting, only from the ADC side, we expect ~9% of channels with non-Gaussian distribution of noise. The solution is to choose an individual DAC setting for each digitizer. After shifting all channels from non-Gaussian regions to Gaussian ones, it is possible to use standard tools for data processing. When all other sources of non-Gaussianity are removed, the one coming from the ADC nonlinearity can be eliminated by an optimal DAC setting for every digitizer.

## References


[1] ATLAS Tile Calorimeter Technical Design Report, CERN/LHCC 96-42.

[2] L. Fiorini, B. Martin, Status of the Noise Description, http://indico.cern.ch/getFile.py/access?contribId=3&resId=0&materialId=slides&confId=61346, Tile Calibration Meeting, 2009.

[3] S. Berglund, C. Bohm, M. Engström , S-O. Holmgren, K. Jon-And, J. Klereborn, B. Selldén, S. Silverstein, K. Anderson, A. Hocker, J. Pilcher, H. Sanders, F. Tang, H. Wu, The Atlas Tile Calorimeter Digitizer, hep.uchicago.edu/atlas/tilecal/notes/Digitizer_LEB99.pdf

[4] K. Anderson, J. Pilcher, H. Sanders, F. Tang, S. Berglund, C. Bohm, S-O. Holmgren, K. Jon-And, G. Blanchot, M. Cavalli-Sforza, Front-end Electronics for the ATLAS Tile Calorimeter, Fourth Workshop on Electronics for LHC Experiments, Rome 1998.

[5] Analog Devices, AD9050 10-Bit, 40 MSPS/60 MSPS A/D Converter, http://www.analog.com/static/imported-files/data_sheets/AD9050.pdf

[6] E. Fullana et al., Optimal Filtering in the ATLAS Hadronic Tile Calorimeter, CERN-ATL-TILECAL-2005-001 (2005), http://cdsweb.cern.ch/record/816152/files/tilecal-2005-001.pdf

[7] B. Salvachua et al., Algorithms for the ROD DSP of the ATLAS Hadronic Tile Calorimeter, Technical Report, JINST 2 T02001 (2007).

# On some specificity of spontaneous fission detection of the implanted nuclei with a silicon radiation detector

Yu.S. Tsyganov
*Joint Institute for Nuclear Research, Dubna, Russia*

Specific features of the detection of spontaneous fission (SF) with a PIPS detector are considered. Such specificity arises from the fact that the implantation depth of the evaporation residues in silicon of the order of units of microns for different nuclear reactions induced by heavy ions. Results obtained in the test reaction $^{206}Pb+^{48}Ca \rightarrow ^{252}No+2n$ are compared with the computer simulation of SF spectra both for focal-plane and side detector of the Dubna Gas Filled Recoil Separator. Additional comparison is made for SF events measured at SHIP velocity filter (GSI). Small correction of the absolute energy scale when using heavy projectiles for calibration procedure is considered too.

## 1. Introduction

Typically, when one studies decays of superheavy elements (SHE), detection system registers a multichain event consisting of recoil signal amplitude (ER), alpha-decay signal amplitudes and, sometimes, amplitude of signal of one or more fission fragments (FF, SF). Of course, the main part of every detected multichain event, are alpha-decays, according two reasons – it is possible establish precisely energies of α-decays and then using this information to provide an indication to a nuclide's Z number [1]. Nevetherles, the registered amplitude of signals of ***ER*** and ***SF***, which have significant pulse height defect value (***PHD***) are also of interest in order to make the identification process more complete. A specific moment of implanted nuclei detection with the PIPS detector is that main (focal plane detector) detects a sum of the fist fragment and part of the second one, whereas the side detector registers only a part of the second fragment with some definite geometrical efficiency.

## 2. Amplitude analysis

The systematical shift of the data with respect to each other can be explained by some systematic errors in the ***FF*** registered energy scale which are caused by different experimental conditions. For this reason, let us consider a dimensionless value ***k*** equals to the ratio $E_{esc} / (E_{esc} + E_{main})$, where ***esc*** and ***main*** subscripts denote detection by side and main detectors, respectively. Such ratio can diminish the systematic shift of scales and can be introduced as a specific parameter for comparing the data.

For complete-fusion reaction products, for which the implantation depth into the main silicon detector can be easily estimated, the ***k***-parameter should decrease with increase of the implantation depth. Dependence of the ***k***-parameter on implantation depth for simulations and experimental data is plotted in Fig.1a,b. As it is seen the values corresponding to the experiment are outside of the theoretical main trend[1].

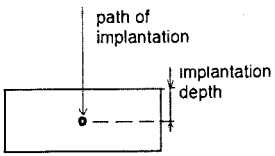


Fig.1a) Implantation of nuclide into a silicon PIPS detector (Usually, implantation depth is about ~1- 6 μm for typical complete fusion HI-induced nuclear reactions).

[1] Nuclear properties reported in [21] are not supported at anytime in any independent research

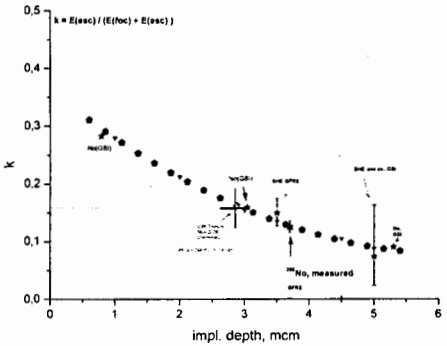


Fig. 1b. Dependence of ***k***-parameter against ***ER*** implantation depth. Circles correspond to the simulation. Stars denote the values extracted from measurements at different facilities. [2] (cross – see [7]).

**3. On the possible small systematic error if one use heavy ion projectile for *FF*- scale calibration** (*basing on the "surface recombination" concept*)

Let us consider a $^{40}Ca$ projectile[2] with the energy about 240 Mev as a candidate for fission-scale calibration process. Being considering this particle with the small ***PHD*** we can create some small systematic crror in the value of the registered energy signal.
Let us estimate the mentioned value approximately.
Using the "surface recombination concept" one can state the following:

$$PHD = \Delta_w + \Delta_n + \Delta_R, \qquad (1)$$

where ***PHD*** – pulse height defect, $\Delta_w$- losses in dead layer (entrance detector window, [3]), $\Delta_n$- nuclear stopping losses [4] and $\Delta_R$ – recombination component [5].

For the calculations let's believe:
E=240 MeV, range in silicon about 64 μm, dead layer ~ 0.2 μ (Si)[3], effective surface recombination parameter $S_{eff}$~$10^3$ cm/s and plasma time according to ***Seibt*** et al. $T_p$~80 ns and form-factor parameter $k_{geom}$ ~1, one can easily to obtain ***PHD***=0.59+0.468+2.98 =4 MeV. The value of the electric field strength value is taken as 2.3E+3 Volt/cm.

In the above example the relative value of the recombination component was calculated as:

$$\lambda \approx k_{geom} \cdot \frac{S_{eff} T_p}{R} \qquad (2)$$

Therefore, the approximate value of systematic correction should be estimated by 4/240~ 1.7%.

[2] Close to $^{48}$Ca ion fro the tables by Northcliffe and Shiling [].
[3] Last versions: ~ 500 Å !

Note, that in [ 6] ***PHD*** of $^{48}$ Ca 110 to 223 MeV has been studied. Slightly greater value of the recombination component ($\lambda$=2.6 % , $^{48}$Ca ion, see Fig.2) was measured.

The reasonable scenario for a small difference is a difference in the effective recombination parameter for the detectors and dead layer values from the Ref. [6].

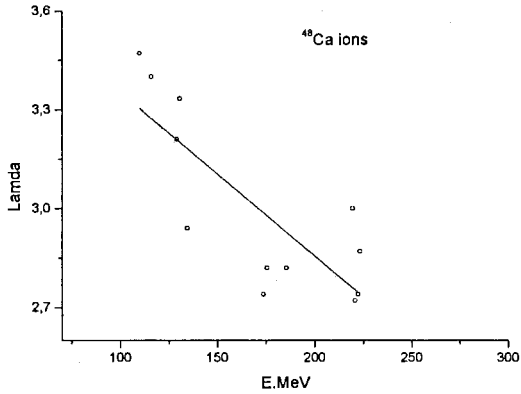


Fig. 2. Dependence of the relative recombination loss of $^{48}$Ca ion against energy from [6] for ion implanted Si detectors . $\lambda$ (250) = 2.6 %

## 4. Summary

SF measured energy signal value can be used for complete amplitude analysis of signals detected with a silicon radiation detector for decay of implanted nuclei. Of course, it should be considered together with ER signal and, probably, with some other information. Reasonable value of systematic shift in absolute energy value scale is considered to be small as about ~2% for PIPS detector.

## References

[1] V.E. Viola, G.T. Seaborg, J.Inorg. Nucl. Chem., V.28 (1996)161.
[2] Yu.S. Tsyganov, Nucl. Instrum. And Meth. In Phys Res. A 582/2 (2007) 696-670.
[3] V.F. Kushniruk, JINR comm., P13-11933, Dubna, 1978.
[4] B.D. Wilkins et al., Nucl. Instrum. And Meth. In Phys. Res. Sect A,Vol.92, (1971)381.
[5] Yu.S. Tsyganov, in Proc. of NEC'2007 Symp., Sept. 2007, Varna, pp. 421-429.
[6] V.F. Kushniruk et al., Instr. And exp. Techn., Vol.47, No.4, (2004), pp. 444-450.
[7] C. Dulman, Report at TASCA 2009 Workshop, GSI, Darmstadt, Germany; submitted to Phys. Rev. Lett.

# Half-Life estimation under indefinite "Mother-Daughter" Relation

Yu.S. Tsyganov, V.B. Zlokazov
*Joint Institute for Nuclear Research, Dubna, Russia*

An algorithm for estimating the half-life of decaying nuclei, when the time at which the parent is created is unknown ("indefinite start time"), is presented. There are two fields of its possible application. One of them is the studying of Zeno effect [1]. Another one is the estimation of the half-life of related recoil-alpha sequences in heavy-ion induced nuclear reactions.

**Keywords**: Rare statistics, Zeno effect, Half-life.

## 1. Introduction

The consideration of general problems of unstable systems by Khalfin [1] demonstrated that the decay rate of a quasi-stationary state does not obey exactly the exponential law. A possibility of the non-exponential decay of a quasi-stationary state follows from the general quantum-mechanical presumptions. The decay rate deviations from the exponential law were expected for very short and very long times after the set up of the quasi-stationary states [2].

Fonda et al. [3] have analyzed a decay model and showed that in some circumstances a significant deviation from the exponential decay law could occur in a time range of about 10 half-life periods and the inverse power-law domination could occur in a range of about 25 half-life periods.

As it concerns the relatively short time range, the observation of $^{220}Rn \rightarrow {}^{216}Po$ chains is a good model to study these effects due to the relatively short $^{216}Po$ half-life what means that there is no need of any beam time [4]. For these reasons, the goal of the present paper is the developing of a mathematical approach for the case of half-life estimation in a short time region.

## 2. Mathematical method

Let us consider a situation when a relatively constant concentration of $^{220}Rn$ undergoes alpha-decay and the resulting 'daughters' - $^{216}Po$ - do the same with an unknown half-life. The energies of alpha particle signals are also registered, so that isotopic references of the decays may be established well but it is not known whose 'daughter' is the appearing nucleus. The start values of decays remain unknown, and, therefore, we can't evaluate the half-life by usual statistical estimators.

Let us arrange the sequence of m $^{220}Rn$ decays and n ones of $^{216}Po$ in a time-increasing order and assume that the $^{220}Rn$ decay distribution is uniform in a range [0; Tm] and that of Po is $F(t)= 1- \exp(-at)$ within each $[t_j ; t_{j+1}]$, $j = 1,\ldots,m$, where $t_j$ are the $^{220}Rn$ decay instants, $a = 1/\tau$ or $a = \ln(2)/T_{1/2}$, and $T_{1/2}$ is the half-life of $^{216}Po$, which should be evaluated.

Let us analyze the registered m decays of $^{220}Rn$ and n ones of $^{216}Po$. Then the average time between the two Rn decays is $T_d = T_m/m$. The "average" probability of Po decay during this time is $\exp(-a\cdot (T_d - t_0))$, and if this quantity is substantially smaller than 1, then the majority of decays of both isotopes will be chaotically intermingled with each other.
To solve the problem the following approach is proposed.

### 2.1. Estimator 1 – trivial approach

If, for some reasons, we assume that the Po half-life is substantially smaller than $T_d$, and it means that the probability of decay during this time is however close to 1, then the

relation 'mother daughter' is built very simply: the 'mother' for any given 'daughter' is a nucleus, whose decay instant is closest to that of Rn on the left, and having assigned any 'daughter' $t_i$ to its 'mother' $t_{ji}$, we then build a set of differences $t_i - t_{ji}$ and their mean

$$\hat{\tau} = \sum_{i=1}^{n} \frac{t_i - t_{ji}}{m}, \tag{1}$$

will be the usual least square estimator of $\tau$, and $\ln(2)\cdot\tau$ – that of $T_{1/2}$.

### 2.2. Estimator 2

The estimator 1 will work well only in a particular case of extremely small $\tau$, so that $T_d$ is several times greater than $\tau$ ; in other words, if Po decays during the time length $T_d$ with a very large probability. Otherwise, the decay instants of Rn and Po will be intermingled chaotically, and the estimate of $\tau$ will be very lowered.

We can determine a measure of such decay disorder, or, decay correlatedness of both the isotopes, and it can be done by various ways, e.g., so

$$h_1 = \sum_{i=1}^{m-1} \frac{|k_i - \frac{2n}{m+n}|}{m},$$

where $k_i$ - the number of Po decay instants, which are between the i-th and i+1-th decays of Rn nuclei. In the case when, on the average, $2n/(m + n)$ Po decays get into this time interval, the measure $h_1$ will be close to zero, and vice versa the more it differs from zero, the more chaotically the decays are mixed together.

The second measure of decay disorder is $h_2$ - difference of the unit and the ratio of the number of registered Po decays and the number of Rn decays: the further it is from zero, the more chaotic is the decay mixture.

Using $h_1$ and $h_2$ we can estimate chances of (1) for success, and if they are both closer to 1 than to 0, we need another estimator.

Let us try the following one. First suppose that the Po half-life $\tau$ is known to us. For any given Po decay instant t we don't know what Rn nucleus has produced this decay, but we can determine the probability of the Po decay at the time instant t, if we assume that every Rn nucleus which has decayed before t has equal chances of being the 'mother' of this Po.
This probability is

$$\sum_{i=1}^{n_t} \exp(-a \cdot (t - t_i)), \tag{2}$$

where $t_i$ - the instant of the Rn decay, such, that $t_i \le t$, and $n_t$ is their total number.

Using randomization concept, we can now consider (2) as a relation "mother - daughter" for our case, and, in principle, build an estimator for $\tau$:

$$\hat{\tau} = \sum_{i=1}^{m_t} \frac{w_i (t - t_i)}{m_t}, \tag{3}$$

where the weights $w_i$ are equal to

$$w_i = \exp(-a(t-t_i)), \quad i = 1 \ldots m, \tag{4}$$

and normalized by their sum for each t.

This sum averaged over all Po decays will give us the final estimate of $\tau$ parameter. Of course, in order to build the weights (4) we already need the value of $\tau$, and it is to be found. Here we can use a method, which is usual for such cases: taking some a priori estimate of $\tau$, e.g., (1) (it doesn't depend on $\tau$), we can use an iteration process of $\tau$ refinement, and in the case of its convergence take the result as the estimate searched for.

## 2.3. Efficiency of estimate

The efficiency of this estimator is substantially higher than that of the foregoing one for large $h_1$, $h_2$, and less depends on the relation of Rn and Po τs. Nevertheless, the assumption of equal probability for any foregoing Rn to be "mother" of Po is unlikely. It is more appropriate to interpret the quantities (4) as generalized weights for the iteration procedure based on (3) and select these weights on the basis of true a priori information about the Po half-life, or taking $T_d$ into account.

The following approach can be recommended as the simplest one for the selection of weights:

$$w_{mi} = 1,\ w_i = \exp(-a(t_{i+1} - t_i));\ i = 1,2\ldots m_i - 1. \qquad (5)$$

Here $t_i$ - Rn decay instants preceding the decay of Po, and all $w_i$ are normalized by their sum, and the meaning of each $w_i$ is the probability for Po to decay in a time span $[t_i; t_{i+1}]$, and not to decay before.

Accordingly, the estimator of τ is built as a normalized sum of all weighted sums over all decays of Po

$$\hat{\tau} = \sum_{j=1}^{n} \sum_{i=1}^{m_j} \frac{w_i(t_j - t_i)}{m}, \qquad (6)$$

Here $t_j$ – the Po decay instants and $t_i$ - those of Rn, which precede the Po decay $t_j$.

The elements of the subjective arbitrariness while selecting the weights and thereby setting up the relation «mother - daughter» do not allow us to build a conventional measure of statistical accuracy (bias, variance) of the estimate (6). Still, we can build a conditional formal measure of accuracy according to the rules of error propagation in the formula (6).

In this formula the $w_i$ and $t_j - t_i$ quantities are sources of errors. The accuracy of the 2nd quantity is the usual variance of $t_j - t_i$, equal to

$$\vartheta_r^2 + \tau^2\ , \qquad (7)$$

where $\upsilon_r^2$ is the variance of the Rn decay instants.

The accuracy of the 1st quantity - $w_i$ - depends on the same quantities (7), but in a rather sophisticated way. We'll try to trace all the chain of forming of this accuracy.

First, let us derive the formula of the distribution of $t_j - t_i$ on condition that they are positive (since the instants are arranged in an increasing order). Actually, we need a formula for the distribution of the absolute value of a random quantity.

Let a random quantity ξ have a continuous distribution function F(x) in [-∞, +∞]. We have to find the mathematical expectation and the variance of |ξ|.

Apparently, the distribution function P( |ξ |) is as follows

$$P(|\xi|=x) = \begin{cases} 0 & \text{if } x<0; \\ F(x)+F(-x) & \text{if } x>0; \\ F(0) & \text{if } x=0. \end{cases}$$

The event $|\xi| < x$ is equivalent to the event $\xi \in [-x, +x]$, and, therefore, the distribution function of absolute value is F(x) - F(-x).

Next, let the quantity ξ have an exponential distribution in [0, ∞] with a density function a ·exp(-at). We have differences of this quantity and are interested in the distribution function of these differences.

Let us divide the set of all the values of ξ into 2 parts - the minuends and subtrahends - and consider them as independent, equally exponentially distributed quantities $\xi_1$ and $\xi_2$. Then we have the difference $d = \xi_1 - \xi_2$. Let us calculate the characteristic function (CF) of d.

$$f_d(t) = f_\xi(t) \cdot f_\xi(-t),$$

$$f_\xi(t) = \int_0^\infty \exp(ixt)a \cdot \exp(-ax)dx = \frac{a}{-a+it}.$$

From this we conclude that the CF of d is equal to

$$f_d(t) = \frac{a}{-a+it} \cdot \frac{a}{-a-it} = \frac{a^2}{a^2+t^2}. \quad (8)$$

But the expression (8) is a result of the Fourier transform of a function 0.5a·exp(-a|x|), and, therefore, the latter is the density function of d.

Let us derive the distribution function of the absolute value of d. We have seen above that the distribution function of a continuous random quantity with a distribution function F(x) is F(x) - F(-x). Therefore, the density function of |d| is as follows

$$p(x) = \frac{\partial F(x)}{\partial dx} - \frac{\partial F(-x)}{\partial dx} = \frac{1}{2}a \cdot \exp(-ax)\,|_{x\geq 0} + \frac{1}{2}a \cdot \exp(ax)\,|_{x\leq 0},$$

that is: a·exp(-ax) if x≥0, and 0 otherwise.

So the distribution function of absolute value of differences of an exponentially distributed random quantity will coincide with the initial distribution.

Now let us consider the distribution function of ξ = exp(-bx), where x is distributed according to an exponential law 1- exp(-at). We can show that

$$P(\xi<t) = \begin{cases} 1 & \text{if } t>1, \\ t^{(a/b)} & \text{if } 0\leq t\leq 1, \\ 0 & \text{if } t<0. \end{cases}$$

Indeed, if $0 \leq t \leq 1$, $(\exp(-bx) < t) \equiv (-x < \ln(t)/b) \equiv (x >= -\ln(t)/b)$.

The probability of the last event is

$$1 - (1 - \exp(-(-a \cdot \ln(t)/b))) = \exp(\ln(t^{(a/b)})) = t^{(a/b)}.$$

Accordingly, the density of this probability is

$$\frac{a}{b}t^{\frac{a-b}{b}}$$

From this we find the expectation and the variance

$$\hat{E}\xi = \int_0^1 \frac{a}{b}t^{(a-b)/b+1}dt = \frac{a}{a+b} \qquad \hat{E}\xi^2 = \int_0^1 \frac{a}{b}t^{(a-b)/b+2}dt = \frac{a}{a+2b}$$

$$\hat{V}\xi = \frac{a}{a+2} - \frac{a^2}{(a+b)^2} = \frac{ab^2}{(a+2b)(a+b)^2}; \qquad \hat{\sigma}\xi = \sqrt{\frac{a}{a+2b}} \cdot \frac{b}{a+b} \quad (9)$$

In a particular case, when b << a the expression (9) can be written as follows

$$\hat{V}\xi = \frac{z^2}{(1+2z)(1+z)^2}; \qquad \hat{\sigma}\xi = \sqrt{\frac{1}{1+2z}} \cdot \frac{z}{1+z},$$

where z = b/a. From this we see that while $z \to 0$ the limit of the variance (and the sigma) is equal to

$$\lim_{z\to 0} \hat{V}\xi = \lim_{z\to 0} \frac{z^2}{(1+2z)(1+z)^2} = 0. \quad (10)$$

Accordingly, we can write the variance (6) in this way

$$\hat{V}(\hat{\tau}) = \frac{1}{m^2}\left(\sum_{j=1}^{n}\sum_{i=1}^{n_j} \hat{V}(w_i)\cdot(t_j - t_i)^2 + w_i^2\hat{V}(t_j - t_i)\right). \quad (11)$$

If b << a takes place, it follows from (10) that the random quantity $w_i$ can be regarded as approximately a constant one and then (11) can be simplified

$$\hat{V}(\hat{\tau}) = \frac{1}{m^2}(\sum_{j=1}^{n}\sum_{i=1}^{n_j} w_i^2 \hat{V}(t_j - t_{ij}).$$

Assuming that in the described situation the decay of nuclei is observed only in the range $[0, T_d]$, we can define for the estimate (1) an approximate bias on the basis of formula (3) in [5].

$$B = \frac{T_d \cdot \exp(-T_d/\tau)}{1 - \exp(-T_d/\tau)}.$$

For the case (6) the reliability of the bias estimate decreases, since the reliability of the $T_d$ estimate decreases, and $T_d$ is a virtual average time length within which we observe cumbersome combinations of decays of Rn and Po.

Table 1

| $T_{Po}$ | $T_{pile\text{-}up}$ | $\tau$ | $P_{decay}$ |
|---|---|---|---|
| 15 | 10.21 | 15.20 | 0.8647 |
| 30 | 15.54 | 29.67 | 0.6321 |
| 100 | 22.00 | 75.66 | 0.2592 |
| 200 | 28.12 | 130.24 | 0.1393 |

Table 1 contains the results of the application of the algorithm to the simulated data. Here 100 nuclei of Ra and 100 nuclei of Po were taken, the quantity $T_d$ being equal to 30 time units(tu).

$T_{Po}$ is the half-life of Po (in tu); $T_{pile\text{-}up}$ is the averaged simple estimate, and $\tau$ is the averaged estimate, given by the described algorithm; $P_{decay}$ is the probability of the Po decay within the time length $[0, T_d]$.

One can see that the estimate $T_{pile\text{-}up}$ is too low. The $\tau$ estimate is good, if the probability of the decay in $[0,T_d]$ is greater than 0.5; otherwise, the $\tau$ estimate can be considered only as lower bound (still better than $T_{pile\text{-}up}$).

## 3. Summary

A method for half-life estimation on condition of indefinite "mother-daughter" nucleus relation has been presented. The described approach is appropriate for the half-life $\tau$ estimation, if the latter doesn't exceed substantially the $T_d$ quantity. Otherwise, the obtained $\tau$ estimates will be much lowered. In this case they can be regarded as estimates of lower bounds of the half-life of the nucleus. And, of course, this method can be applied in heavy-ion induced complete fusion nuclear reactions if one detects rare recoil-alpha (or/and spontaneous fission) sequences and there are more than one statistically significant recoil candidates for these events.

The authors express their deep gratitude to Drs. Yu.V. Lobanov, V.I. Chepigin, and A.N. Polyakov (FLNR, JINR) and Drs. K. Subbotic and L. Nadderd (INS VINČA, Belgrade, Serbia) for their help in this work.

## References

[1] A. Khalfin, Zh. Eksp. Teor. Fiz. 33 (1958) 1371.
[2] D. Novcovič, L. Nadderd, A. Kandič et al., Nucl. Instrum. And Meth in Phys. Res. A, 566(2006), pp. 477-480.
[3] L. Fonda et al., Rep. Prog. Phys. 41(1978) 587.
[4] L.Nadderd, Yu. Tsyganov et al., In Proc. Of NEC'2007 Int. Symp. 10-17 Sept, 2007, Varna, Bulgary. ISBN 5-9530 -0171-1, Dubna 2008. pp. 362-366.
[5] V.B. Zlokazov, ACAT05, VIII Congress on Advanced Computation and Analysis Techniques, Berlin, Germany, 23-27 May 2005.

# Serbian participation in Grid computing projects

D. Vudragović, A. Balaž, V. Slavnić, A. Belić
*Scientific Computing Laboratory, Institute of Physics Belgrade, Serbia*

Pan-European EGEE, regional SEE-GRID, and Serbian AEGIS eInfrastructures have a common aim - provision of processing and storage services for eScience research. Serbia participates in these projects, by developing new applications, providing computing and storage resources and advanced services to scientific, research and development communities, fostering collaboration, and attracting a wide range of new users to the Grid. We give an overview of our activities and main achievements in Grid computing projects.

## 1. Introduction to Grid computing

Science is becoming largely digital - it needs to deal with ever increasing amounts of data and computational needs. Numerical simulations become more detailed, experimental science uses more sophisticated sensors to make precise measurements, and shift from the tradition of individuals-based science work towards more collaborative models now starts to dominate.

Computing resources and services able to support needs of such a new model of scientific work are available at different layers: local computing centers, national and regional computing centers, and European supercomputing centers. The gap between needs of various user communities and computing resources able to satisfy their requirements is addressed by introduction of Grid technology on the top of pan-European academic network.

Computing Grids are conceptually not unlike electrical grids. In an electrical grid, the wall outlets allow us to link to and use an infrastructure of resources, which generate, distribute, and bill for electrical power. When we connect to the electrical grid, we do not need to know details on the power plant currently generating the electricity we use. In the same way Grid technology uses middleware layer to coordinate and organize into one logical resource a set of available distributed computing and storage resources across a network, allowing users to access them in a unified fashion. The computing Grids, like electrical grids, aim to provide users with easy access to all the resources they need, whenever they need them, regardless of the underlying physical topology and management model of individual clusters.

Grids address two distinct but related goals: providing remote access to information technology (IT) assets, and aggregating processing and storage power. The most obvious resources included in Grids are processors (CPUs), but Grids also can encompass various sensors, data-storage systems, applications, and other types of resources. One of the first commonly known Grid initiatives was the SETI@HOME project [1], which solicited several millions of volunteers to download a screensaver, which was able to use idle processor time to analyze the astronomical data in the search for extraterrestrial life.

Europe has played a leading role in Grid technology development, starting with the EU DataGrid project [2] and related efforts under the Framework Programme 5. After this proof of concept, demonstrating the potential impact of Grid technologies on European science and industry, a first large scale production Grid infrastructure was deployed by the Enabling Grids for E-SciencE project [3] (EGEE), and its operation was further consolidated in its second phase (EGEE-II). Current phase of EGEE programme, EGEE-III project in close collaboration with pan-European network provided by GÉANT2 [4], National Grid Infrastructures (NGIs), and the European Grid Initiative Design Study project [5] aims to

prepare the transition towards a sustainable Grid infrastructure after the current set of short-term projects is completed.

In the past five years the European Commission has funded through a number of targeted initiatives activating of new user communities and enabling collaborative research across a number of fields in order to close existing technological and scientific gaps, and thus bridging the digital divide, stimulating research and consequently alleviating the brain drain in the less-developed regions of Europe. This was especially successful in the South-East Europe (SEE), where a number of such initiatives show excellent results. The SEEREN [6] (SEE Research and Education Networking initiative) project, through its two phases, established the SEE segment of the pan-European GÉANT network and successfully connected the scientific communities in the region. Currently, the SEE-LIGHT project is working towards establishing a dark-fibre backbone that will interconnect most national research and education networks in the region. In the Grid arena, the SEE-GRID [7] (South-East European GRid eInfrastructure Development) project, similarly through its two phases, has established a strong human network in the area of scientific computing and has set up a powerful regional Grid infrastructure, attracting large number of applications from diverse fields from countries throughout the South-East Europe. The third phase of SEE-GRID programme (SEE-GRID-SCI) aims to have a catalytic and structuring effect on a number of SEE user groups, with a strong focus on the key seismological, meteorological, and environmental communities.

Inline with the European and regional vision of paving the way towards a long-term sustainable European Grid Initiative, Academic and Educational Grid Initiative of Serbia [8] (AEGIS) is bringing together under one umbrella at the national level all interested parties involved in provisioning and using of Serbian research computing infrastructure. Institute of Physics Belgrade [9] (IPB) coordinates AEGIS initiative through its Scientific Computing Laboratory [10] (SCL). AEGIS and IPB participate in pan-European EGEE and regional SEE-GRID programmes, integrating Serbian research and education communities to European Research Area (ERA), and promoting and implementing European and regional Grid activities at the national level.

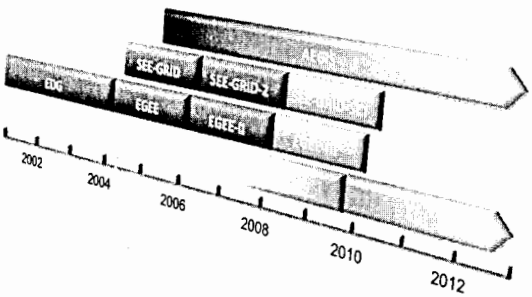


Fig. 1. Roadmap to a sustainable Serbian Grid infrastructure

## 2. Grid projects relevant for Serbia

Pan-European EGEE, regional SEE-GRID, and Serbian AEGIS eInfrastructures have a common aim - provision of processing and storage services for eScience research. Serbia actively participates in these projects (Fig. 1.), sharing national computing and storage resources with other countries from the SEE region and from the Europe, fostering

collaboration and providing advanced computing services and capabilities to Serbian researchers, as well as to other researchers using the shared Grid eInfrastructure.

## 2.1. EGEE programme

The EGEE programme, which is built on top of national and thematic Grid efforts, as well as the pan-European network provided by GÉANT2 and the NRENs (National Research and Education Network), aims to deliver Grid technology to many scientific disciplines and to users with widely varying levels of computing expertise located all over the globe. Since the beginning of EGEE, there has been a substantial expansion in the use of the infrastructure by a broad range of scientific applications. Scientists are clustered into Virtual Organizations (VOs), a framework to conduct collaborative research and gain access to shared computing and data resources. EGEE provides a variety of services to scientists, ranging from training and user support, to the software interfaces and APIs necessary to access the resources. The number of EGEE VOs supported now exceeds 250, and about 150,000 jobs/day are routinely executed worldwide on the eInfrastructure comprising more than 280 sites in over 55 countries. These applications deal with more than 100 PB of data made available on the EGEE data storage resources, which sees routine aggregated data transfers of more than 1GB/sec. The number of scientists benefiting from EGEE has grown to over 15,000.

Life Sciences and High Energy Physics now depend on the EGEE Grid infrastructure, which is an essential and crucial part of their large-scale data processing. Other disciplines, notably astrophysics, earth sciences, computational chemistry, and fusion (to name but a few) are also increasingly using EGEE resources for production and processing of data. Close relations are established with a number of collaborating projects extending the infrastructure and applications support to more disciplines. Through these collaborating projects and interoperability efforts with related non-European infrastructures, EGEE contributes to the establishment of a seamless worldwide computing infrastructure. Continuous advancements of EGEE's relations with business have contributed significantly to the growing uptake of Grid technologies in the commercial sector, with first prototype service providers appearing on the market and several sectors deploying enterprise Grid infrastructures.

Given the success of the EGEE programme, it is essential to build on its achievements and prepare the transition towards a sustainable infrastructure in the future. EGEE-III project, undertaken in close collaboration with National Grid Infrastructures (NGIs) and the European Grid Initiative Design Study (EGI_DS) project are designing a conceptual set-up of a new organizational model, based on NGIs such as the UK National Grid Service [11] (NGS), D-GRID [12] in Germany or AEGIS in Serbia for a sustainable pan-European Grid infrastructure. EGEE-III and all NGIs work closely with EGI_DS to transfer their experience in operating large-scale international Grid infrastructures, ensuring the development of a viable model in EGI_DS. Based on the plans to be produced by EGI_DS, EGEE-III will, in its second year, start implementing the required structural changes to allow a seamless transition to the European Grid Initiative (EGI) model, while ensuring the continued provision of the Grid service.

## 2.2. SEE-GRID programme

The SEE-GRID programme through its two phases has established a strong regional human network in the area of scientific computing, has set up a powerful regional Grid infrastructure, and attracted a number of applications from diverse fields from countries throughout the South-East Europe. Current phase of SEE-GRID programme, SEE-GRID-SCI (SEE-GRID eInfrastructure for regional eScience) involves three strategic international

scientific communities (seismology, meteorology, environmental protection) and thus further stimulates the use and expansion of the existing regional eInfrastructure and its services, and capitalize on the existing human network to further strengthen scientific collaboration and cooperation among participating SEE communities in the area of eInfrastructures.

The inclusion of the new scientific communities and the expansion of the infrastructure in terms of both size and geographical spread, together with a set of coordinated actions aimed at strengthening the National Grid Infrastructures in the region, will ensure that at the end of the project each country in the region will be ready to join the long-term, sustainable European Grid Initiative as a full-fledged peer.

### 2.3. AEGIS programme

Academic and Educational Grid Initiative of Serbia (AEGIS) was established in 2005 to coordinate efforts on developing academic and educational high performance computing facilities (e.g. computers, storage, networks, instruments, and visualization resources) in Serbia, and help to integrate them in the AEGIS infrastructure. One of the major AEGIS tasks is dissemination and training activities organization, and help to Serbian research communities in developing and production use of applications on the AEGIS eInfrastructure.

AEGIS is also focal point in Serbia for facilitation of wider participation of AEGIS members in Framework Programme 7 and other international Grid projects, coordination of fund raising efforts to improve AEGIS infrastructure and human resources, creation of national Grid development policy, and lobbying for its position within an overall research agenda.

## 3. Serbian Grid resources – AEGIS eInfrastructure

The Serbian Grid infrastructure [13] consists of nine Grid sites (Fig. 2.), comprising from tens to hundreds of computing nodes and disk-based storage elements ranging from several hard disks to tens of terabytes. Apart from computing and storage resources, core Grid services which enable seamless access to all resources are provided to national users. AEGIS sites are running Scientific Linux operating system [14] and the latest version of the EGEE gLite middleware. Beside standard serial tasks, sites are optimized and heavily tested for parallel processing mode using MPICH framework [15]. The resources are fully dedicated to national and international Grid communities within AEGIS, SEE-GRID and EGEE projects.

The first Grid site in Serbia **AEGIS01-IPB-SCL** is installed at the Scientific Computing Laboratory of the Institute of Physics Belgrade. This Grid site is a set of 89 worker nodes (2 x quad core Xeon E5345 on 2.33 GHz with 8GB of RAM) and 15 service nodes (Xeon based nodes). AEGIS01-IPB-SCL, as the largest, is the Tier-0 site in the Serbian Grid infrastructure, providing all core services and managing national AEGIS Virtual Organization. All computing and core services nodes at AEGIS01-IPB-SCL Grid site are interconnected by the star topology Gigabit Ethernet network through three stacked high-throughput Layer 3 switches, each node being connected to the switch by two Gigabit Ethernet cables in channel bonding. In terms of storage resources, AEGIS01-IPB-SCL provides 27 TB of disk space to the Grid community.

Belgrade University Computer Centre [16] (RCUB) hosts **AEGIS02-RCUB** grid site. The site consists of 14 nodes with 2.0 GHz AMD Sempron CPUs with 1GB of RAM. The Storage Area Network (SAN) cluster is connected to the storage element via NFS. The Laboratory for Electronic Design Automation [17] (LEDA) of the Faculty of Electronic Engineering, University of Nis has deployed **AEGIS03-ELEF-LEDA** site. The site capacity

is currently being extended to 64 CPUs (Intel Xeon Quad-core 2.4GHz, with 12MB L2 cache and 4GB RAM per node), and the site storage capacity is 2TB.

The site **AEGIS04-KG** is installed at the Bioengineering Research and Development Center [18] of the University of Kragujevac since June 2006. It consists of 42 CPU cores with the total RAM of 40GB. The School of Electrical Engineering [19] of the University of Belgrade hosts **AEGIS05-ETFBG** Grid site. It consists of 30 nodes (AMD 2600+ Sempron CPUs), with 1GB RAM and 80 GB of disk space at the storage element.

**AEGIS07-IPB-ATLAS** is the second site hosted by the Institute of Physics Belgrade, and is based on 128 Intel Xeon processors with 32-bit architecture and the total of 96GB of RAM. The site supports several virtual organizations, but is mainly dedicated to the ATLAS VO community of the CERN LHC experiment. Another site at Institute of Physics Belgrade, **AEGIS08-IPB-DEMO,** is used purely for educational/training purposes. It is based on Xen virtual machines deployed on a single node with two Intel Xeon Quad-core CPUs with 16 GB of RAM. It is used in various training events for demonstration of installation and configuration of different Grid services.

With the support of the GRINKO project [20], **AEGIS09-FTN-KM** Grid site has been established in Kosovska Mitrovica at the Faculty of Technical Sciences [21] of the University of Pristina. This site consists of four Quad-core CPU computing nodes.


Fig. 2. Overview of the Serbian Grid infrastructure

## 4. AEGIS applications

Apart from establishing a reliable national Grid eInfrastructure, one of the most important results of Serbian Grid activities is the production use of the pan-European EGEE, regional SEE-GRID and national AEGIS infrastructures by a large number of diverse applications developed by Serbian researchers. The user activities drive the evolution of Grid

technology through specific, challenging applications, and demonstrate that these infrastructures provide viable computing services for many scientific communities. AEGIS applications require, in particular, that the Grid middleware performance and core Grid services scale with the growth of the infrastructure, and have additional requirements for high-level services. Here we will describe the most used applications, developed and gridified by the Serbian Grid community.

The grid-enabled **Volumetric Image Visualization Environment (VIVE)** is an interactive analysis tool for 3D medical images, facilitating diagnosis, surgical planning, therapy evaluation, and remote 3D examination. It improves understanding of complex anatomies by providing an interactive three-dimensional environment with simple Web-based user interface. The lightweight Java/VRML client enables user interaction and 3D rendering within a Web browser. The user interacts with the visualization server running on the grid through the specialized portal responsible for job submission and communication with server jobs. The grid provides computing and storage resources, as well as access methods required for volumetric data processing.

Grid-based computational model of realistic blood flow in a section of artery - **Parallel Blood Flow Simulation (PBFS)** - improves diagnosis and treatment of health problems such as aneurysms and wounds to artery vessel walls. Systems of equations describing fluid and wall behavior are numerically simulated in Center for Scientific Research of Serbian Academy of Science and Art and University of Kragujevac with parallel computational software environment for solving equations using finite element analysis. These systems include Navier-Stokes and incompressible fluid equations coupled through boundary conditions to the deformable wall motion using fluid-structure interactions.

Gridified version of the Path Integral Monte Carlo **SPEEDUP** code presents efficient and reliable tool for calculating basic properties of matter, such as free energy, energy spectra, probability amplitudes, low and high temperature properties etc. Until recently the best available result for partition functions of a generic N-fold discretized theory led to a $1/N^4$ convergence. In a series of papers developers fro SCL have investigated the dynamical implications of stochastic self-similarity by studying the relation between discretization of path integrals with different coarseness. This has resulted in a systematic analytical procedure that is used to reduce path integral error to $O(1/N^p)$ for integer $p$ as high as 35 for one-dimensional theories and 10 for general many-body models. This reduction of error brings about a substantial increase in the speed of calculation of path integrals.

The grid-enabled simulation of planetary system formation - **SOLAR** - presents an effective model of planetary accretion. It provides possibility to simulate the formation of planetary systems starting from as many as $N=10^{12}$ initial particles, and to investigate properties of condensates, including the distribution of their masses, spins, and radial distributions. It is also possible to investigate evolution of these properties during the condensation process, and to uncover sensitivity of key features of such systems on initial conditions.

Grid-based simulation of the compaction of granular materials – **COMPACTION** - is event driven method to simulate compaction processes in two-dimensional vibrating boxes. Event driven method is modification of molecular dynamics approach since the simulation increments from collision event to collision event rather than incrementing at a specified time. Inelastic hard-sphere model is used, and in the event driven approach the particles follow an undisturbed Newtonian motion, under the influence of gravity, until an event occurs. An event is either the collision of two particles or the collision of one particle with the wall. The time

during which two particles are in contact is implicitly zero. The hard-particle collision model uses momentum conservation laws and the definition of the coefficient of normal and tangential restitution to determine the states of particles after a collision.

**Parallel Analog and Logic Electronic Simulation System (PALESS)** presents Grid-enabled simulation of modern electronic circuits and systems which are very complex (tens of millions of transistors), and can be applied in complex surroundings including sensors, actuators and other devices not directly connected to electronics, but whose behavior can be described in a different non-electrical natural domain (such as mechanical, chemical, biological etc.).

The proper elements of asteroids are used to classify asteroids into families, and to study the dynamical and collisional evolution of the asteroid belt, and of the Solar system as a whole. Their calculation is made possible in an efficient way by the gridified version of **Asteroid Proper Elements Calculation (PROPEL)** application. This application in the Grid environment presents a powerful tool to study the problems of the stability of motion, resonant and chaotic phenomena.

Grid-based Visual interactive general purpose discreet event simulator – **SLEEP** – simulates digital circuits made in VLSI technique for educational purposes and verification of business process integration. Simulator is able to use set of independent basic elements connected with single target simulation. The appropriate tools implemented within this simulator should be able to help end users to write their own simulators easier.

## 5. Grid training activities

The training activities are seen as one of the crucial tasks within AEGIS community, as well as by EGEE-III and SEE-GRID-SCI project. Such activities are effective way of introducing new users to the world of Grid. At the same time, even the experiences users are regularly informed about new developments and improvements in Grid technology, in available computing and storage resources, and also in available software environments and libraries in the national, regional and pan-European eInfrastructures. The organized training events serve two purposes: to develop and validate the shared pool of best practices, training materials and resources, and to initiate direct contact of users, developers and system administrators.

The Grid training courses are mainly organized by SCL at the national and regional level in Serbia, with strong participation and support in co-organizing training events in other countries in the region. The courses cover a wide range of competences and skills from induction-level courses focusing on newcomers to Grid computing, to more advanced courses aimed at application developers working on porting of their applications to the Grid. Many courses are also designed for site administrators responsible to operate Grid sites.

## 6. Conclusions

AEGIS Grid eInfrastructure provides more than 1000 CPUs and 30 TB of data storage to all user communities through a distributed set of Grid sites hosted by major research institutes and universities. This eInfrastructure is fully utilized by a number of scientific high-performance applications, developed Serbian researchers and adapted for optimal use on the Grid with the support of the Scientific Computing Laboratory of the Institute of Physics Belgrade. Such support is provided either directly for specific applications, or through advanced training activities for application developers.

Serbia has long-standing strong participation in European Grid projects and has established a reliable and extensive national Grid eInfrastructure, which provides advanced computing services not only to national research community, but also to other researchers from user communities supported by EGEE and SEE-GRID programmes. The AEGIS eInfrastructure also stimulated further collaboration of Serbian and European researchers, and helped in bringing the issue of providing support for research infrastructure to the agenda of Serbian policy makers. For these reasons, AEGIS also actively participates and works with other NGIs on establishing a sustainable European Grid Initiative, which should provide stable environment for scientific communities with high-performance computing requirements.

**Acknowledgements**

This work was supported in part by the Serbian Ministry of Science under project No. OI141035, and the European Commission under EU Centre of Excellence grant CX-CMCS. Described Grid applications were developed and deployed on the AEGIS e-Infrastructure, supported in part by FP7 projects EGEE-III and SEE-GRID-SCI.

**References**

[1] SETI@HOME, http://setiathome.ssl.berkeley.edu/
[2] European DataGrid project (EDG), http://eu-datagrid.web.cern.ch/
[3] Enabling Grids for E-sciencE (EGEE), http://www.eu-egee.org/
[4] Pan-European GÉANT network, http://www.geant.net/
[5] European Grid Initiative Design Study project (EGI_DS), http://web.eu-egi.eu/
[6] SEE Research and Education Network (SEEREN), http://www.seeren.org/
[7] SEE-GRID eInfrastructure for regional eScience (SEE-GRID-SCI), http://www.see-grid-sci.eu/
[8] Academic and Educational Grid Initiative of Serbia (AEGIS), http://www.aegis.rs/
[9] Institute of Physics Belgrade, http://www.ipb.ac.rs/
[10] Scientific Computing Laboratory (SCL), http://www.scl.rs/
[11] UK National Grid Service (NGS), http://www.grid-support.ac.uk/
[12] The German Grid Initiative (D-Grid), http://www.d-grid.de/
[13] GStat Grid information system monitoring tool for the AEGIS Grid eInfrastructure, http://goc.grid.sinica.edu.tw/gstat/aegis/
[14] Scientific Linux (SL), https://www.scientificlinux.org/
[15] MPICH Implementation of MPI, http://www.mcs.anl.gov/research/projects/mpi/
[16] Belgrade University Computer Centre, http://www.rcub.bg.ac.rs/
[17] Laboratory for Electronic Design Automation (LEDA) of the Faculty of Electronic Engineering, University of Nis, http://leda.elfak.ni.ac.rs/
[18] Bioengineering Research and Development Center of the University of Kragujevac, http://www.csk.kg.ac.rs/
[19] School of Electrical Engineering of the University of Belgrade, http://www.etf.bg.ac.rs/
[20] GRid e-Infrastructure and Networking with KOsovo (GRINKO), http://www.grid.bas.bg/site/index.php?page=grinko
[21] Faculty of Technical Sciences of the University of Pristina, http://www.ftnkm.info/

# Single-photon detector for telecom wave-lengths

A.I. Klimov, K.N. Kozlov, S.P. Kulik[1], S.N. Molotkov[2], I.E. Ostashev, V.I. Zaitsev

*Russian Research Center Kurchatov Institute, Moscow, Russia,*
*[1]Moscow State University, Moscow, Russia,*
*[2]Institute of Solid State Physics, Moscow Region, Chernogolovka*

The detector of single - photon pulses w as developed for application in quantum communication systems (Qc systems) based on transmission of unique key through fiber -optic communication lines. The detector provides a noise-free operation in mode of single photon detection at the 1550 nm wave-length (the minimum of attenuation in optofibers). Detectors are the unique avalanches photodiodes (APD) based on InGaAs/InP heterostructures with three-stage cooling by Peltier elements down to -50° C temperature. The software controls the Peltier cooler temperature as well as bias voltage; discrimination threshold; amplitude, duration and delay of strobe - signals about a clock pulse.

The noise counts included dark pulses and afterpulses were measured, and the dependence of noise counting rate on the strobe-pulse duration was extracted. At the small duration of strobe – pulses, the main contribution to noise counting is caused by dark pulses of APD. For the 1 MHz repetition rate and 2 ns strobe - pulses duration, the number of noise counts was around 200 for 10 s acquisition time. Thus, the number noise counts per one strobe-pulse was of the order of $2 \times 10^{-5}$. The analysis of literature and carried out assessment ($2 \cdot 10^{-5}$ 1/pulse) demonstrate that the low noise detector can be applied in QC systems, spectroscopy and telecommunication diagnostics.

## Single - photon detectors

The solution of the problem of quantum communication systems based on transmission of unique key through fiber - optic communication lines dependents on ability of single-photon detection. This can be accessed, using different detectors, so as PMT, silicon APDs, of NbN superconducting detectors [1], germanium photodiodes et. al. Photo-multiplier tube (PMT) has spectral response up to 1700 nm. However, their quantum efficiency in this range does not exceed the parts of percent. For photon detection on wave-length 1300 nm avalanche germanium photodiodes were studied [2]. For receipt of low dark counts rate these detectors should be cooled. They are cooled by the liquid nitrogen, below 150 K, that makes them impractical for most applications. Avalanche photodiodes operated in the so-called Geiger mode currently represent the best solution to detect single-photon beyond 900 nm [3]. Ideal detector must content to following requirements:

- High quantum efficiencies for detecting single-photons in specified spectral range;
- Small dark counts (in the absence of light);
- Sub-nanosecond timing resolution, time between single-photon detection and drawing-up pulses should be constants;
- The small dead time for getting of high counting rate.

The convenience for most applications is very important factor for practical implementation of system. The single–photon detectors (germanium or superconducting), which need to be cool down to liquid nitrogen or helium are not considered as a basic tool. Avalanche photodiodes EPM 239 InGaAs/InP APD manufactured by the Epitaxx division of JDS-Uniphase are mostly used for the content of listed conditions. If attached to APD voltage insignificantly exceeds the threshold of breakdown, then absorbed photon stimulates electronic avalanche. In order to restore photo diode, this macroscopic current should be extinguished: if the charge emission breakes/cut off, photodiode will be recharged. There are three abilities to break/cut off avalanches:

- the mode of passive extinguishing of the avalanche;
- the mode of active extinguishing of the avalanche;
- the strobe mode.

The strobe mode is the best one in the schematics for application in quantum communication systems based on weak laser pulses, when arrival time of the photon is defined with good accuracy: the strobe, resolving registration of the photon, is attached to APD only in that moment, when photon reaches the detector [5]. An incoming photon is absorbed and creates an electron–hole pair. The charge carriers are then swept through the junction and accelerated by the strong electric field applied to the active area. They can gain enough energy to generate secondary electron–hole pairs by impact ionization. These pairs are in turn accelerated and can generate new electron–hole pairs. If the field is high enough, impact ionization can yield a self-sustaining current pulse. This multiplication phenomenon is known as an avalanche. The avalanche produced by electron-hole pairs may be produced not only b y coming photon but also due to other effects. These processes can be triggered temperature fluctuations, tunneling between zones or emission from traps, etc. First two processes are called «dark» counts – they are result in the pulse appearance on output APD even in absence photons. The third process depends on the parameters of preceding avalanche, this effect is called afterpulsing. For optical communication wavelengths 1310 nm and 1550 nm are used, since namely at these lengths of waves there is small absorption in optical fiber (Fig. 1).

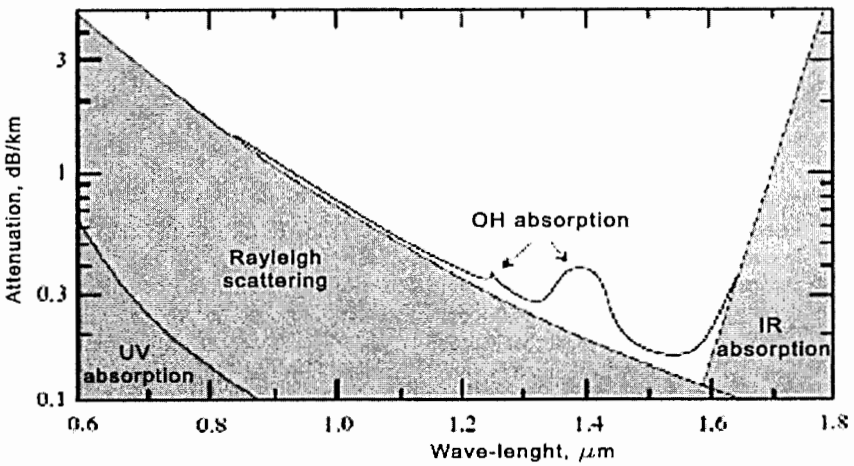


Fig. 1. Absorption in optical fiber

The logic diagram of the single-photon detector present on Fig. 2. Detector consists of three modules:

- Shaper of strobe pulse,
- Discriminator pulses of the APD,
- Power supply.

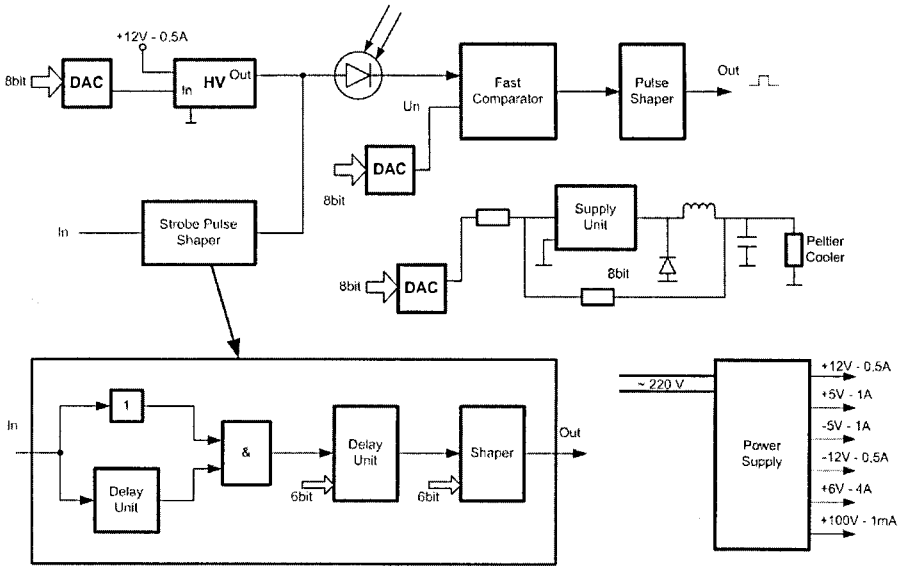


Fig. 2. Diagram of single-photon detector

**The shaper of strobe pulses**

The shaper unit comprises:

- USB interface for connection with computer,
  The microcontroller C8051F021 (Cygnal Integrated Products, Inc., USA). The software controls the Peltier cooler temperature; bias voltage; discrimination threshold; amplitude, duration and delay of strobe - signals about a clock pulse;
- Programmed logic integrated circuit on EPM7256AETC100-10 (PLD -programmed logical device). PLD counts with high rate sequence of strobe-pulses and the pulses of avalanches photodiode, and transmit data flow to computer through USB during exposition. PLD produces test signals and the signals for suppression of unwanted events. The strobe pulse shaper produces positive pulses, which amplitude can be changed in the range from 2 V up to 7V on 50 Ohm (Fig. 3).

The duration of the strobe-pulse can be varied from 2 ns up to 12 ns with resolution 40 ps, the delay pulse with respect to start pulse also can be changed from 2 ns up to 12 ns with resolution 40 ps. The programmable delay chips MC10EP195, (ON Semiconductor, USA) are used as elements adjusting duration and delay of the strobe pulses. Delay chip consists of cell array OR and multiplexer. MC10EP195 has the 10-bit counter allowing one to install the delay in the range between 2 and 12 ns with resolution 10 ps. The amplitude of the strobe pulse is performed in 3 stage ultrahigh speed current feedback amplifier (AD8009, Analog Devices). High voltage for avalanche photodiode is produced by the DC-DC converter TS-01P (Matsusada Precision Inc., Japan).


Fig. 3. The strobe pulse for APD

**Fast discriminator**

Dual ultrafast voltage comparator SPT 9689 (Fairchild Semiconductor, USA) is used to discriminate pulses of APD. The comparator operation threshold is determined by the two-channel DAC. Second cascade of the comparator is controlled by delayed strobe pulse in order to decrease photon detection probability caused by noise pulses. The duration of comparator pulses are shaped by chip MC10EL31 (D - trigger) and fast transistors. The single photon detector is placed inside refrigerator (dimension 80x80x60 mm) allocated on same board based on Peltier elements, which are controlled by N-Channel Power MOSFETs switch (IRF540, Harris Semiconductor, USA).

**Events identification**

PLD are processing pulses and passing data flow to computer after starting exposition. If USB computer does not have time to accept data or computer sends executive instruction, PLD is aborts exposition with saving combined data.

Quartz generator supports the accuracy of exposition time, it is setting to a high accuracy – 25 ns. The counts of strobe – pulses, of pulses from APD can be read as soon as the exposition finishes. Signal processing arises in the following way (see Fig. 4, the simulations diagrams of PLD). The bits of shift register (on graph – **data _ sh**) are shifted from entry by each strobe pulse (on graph - **strobe**). If the pulse from APD (on graph - **diode**) comes then contents of shifted bit accepts meaning to equal 1. Sequence of eight bits (on graph **_ data_buf**) is transmitted on the circuit of interface USB as the signal of write-in (on graph **_ wr_data**), and then in computer.

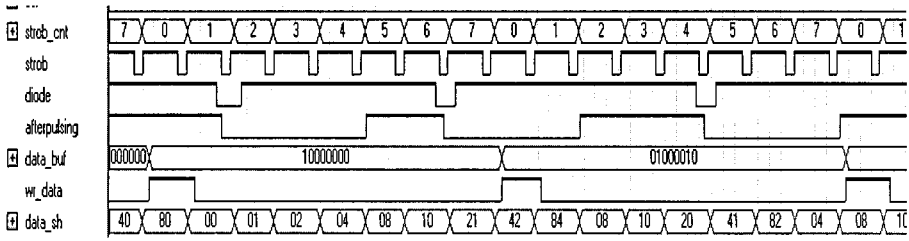


Fig. 4. Timing chart of the identification system

During the exposition PLD are composed signals from strobe and APD pulses. The signals come into the counters of microcontroller and may be read as to finish expositions.

**Afterpulsing suppression**

Logic for the suppression of the appearance of unwanted events is contained in PLD. Single-photon detector is switched off for a time exceeding the time of resorption charge localized to entrap after registration of helpful event. The suppression time is specified in number of missing strobe-pulses prior to the next exposition. On graph (Fig. 4) afterpulsing waveforms are presented which become by null on the specified number of clock cycles after the registration of APD pulse. PLD also comprises logic for production of the test-signals allowing to the control equipment without connection to APD. The test-signal parameters can be changed to form a command of the computer. The results of testing of the equipment display that essential indicators were achieved providing its operability and reliability:

- select single-photon detector - avalanche photodiode (APD) based on InGaAs/InP heterostructure providing the best level of ratio dark counts (***R***) to quantum efficiency($\eta$);
- noise equivalent power (***NEP***). This value is determined as optic power demanded for the measurement of single ratio signal/noise:

$$NEP = \frac{h\nu}{\eta}\sqrt{2R},$$

where $h$ – Planck constant, and $\nu$ - central frequency of photons dropping on detector. It is $10^{-15}\frac{W}{Hz^{1/2}}$ for best detectors on the length of wave 1.55 nm in temperatures about -100 °C;

- the long-term stabilization of temperature (≤ 1 degree) is provided in range +20°C – 50°C. Such accuracy of the temperature of APD maintenance must provide the level of noise about 0.00001 pulses/strobe, what ensures the allowable level of the errors of receiver system.

The reliability of the work of system is testing within ~ 100 hours. The modules are allocated in Eurocrate (Fig. 5, 6).

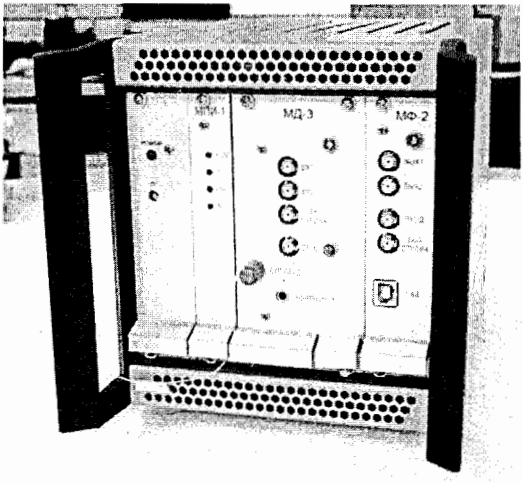

Fig. 5a. The general view of modules

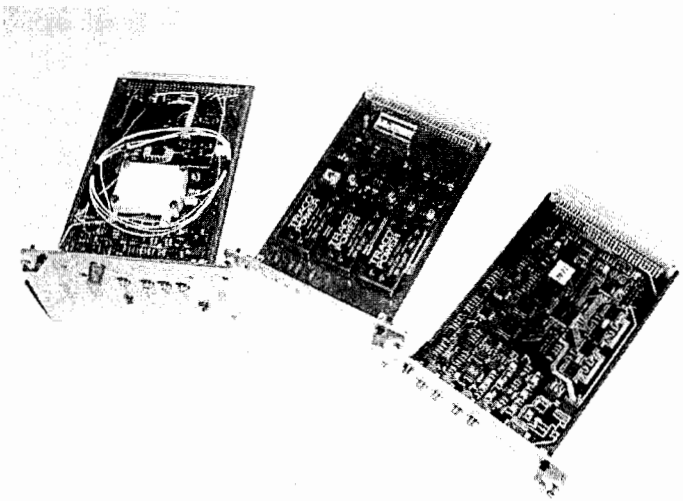

Fig. 5b. The modules of single-photon system

Fig.6a, 6b present the responses of the APD signal on the threshold of discrimination and numbers «dark» counts versus the duration of strobe-pulse.

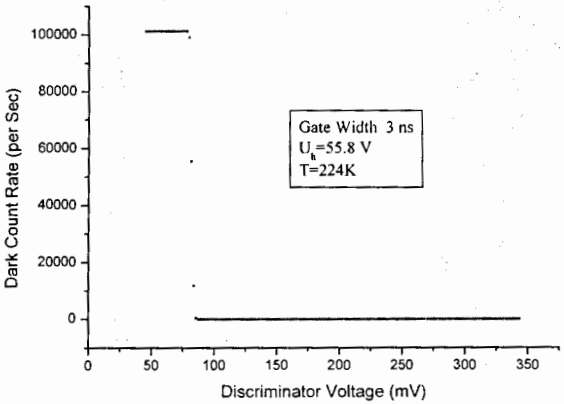


Fig. 6a. The APD «dark» count rate vs threshold

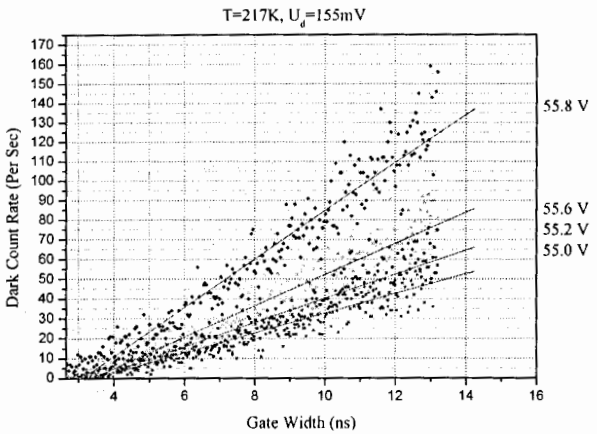


Fig. 6b. Responses «dark» rate of gate width strobe pulse

## References


[1] A. Goltsman, P. Korneev, V. Kouminov et.al., Appl. Phys. Lett. Vol. 84, N. 26, 2004.

[2] A. Lacaita, P. A. Francese, F. Zappa, S. Cova, Appl. Optics, 33, 6902, 1994.

[3] G. Ribordy, N. Gisin, O. Guinnard et.al., J. Mod. Opt., 51, 1381, 2004.

[4] D.S. Bethune, W.P. Risk, G.W. Pabst, A high-performance integrated single-photon detector for telecom wavelengths, DARPA report, 2002.

[5] S.N. Molotkov, S.P. Kulik, A.I. Klimov, Patent № 2339919, Arrangement for the registration of weak optic pulses, 15.06.2007.

# Control systems of neutron beam choppers at the physical instruments of the IBR-2 reactor

V.V. Zhuravlev, A.V. Nikul'nikov, A.P. Sirotin
*Joint Institute for Nuclear Research, Dubna, Russia*

**Introduction**

In different experiments, neutrons of different energies are required to be directed towards the sample. Since the time of flight of a neutron beam through a chopper is proportional to the neutron energy, the time of opening of a window determines the energy of neutrons incident on a sample. These problems are solved by means of mechanical systems (choppers) that permit the passage of neutrons for strictly specified time (approximately 1-10 ms).

In the Frank Laboratory of Neutron Physics two types of neutron choppers /1,2,3/ are used basically – drum (1) and disk (2) neutron choppers.

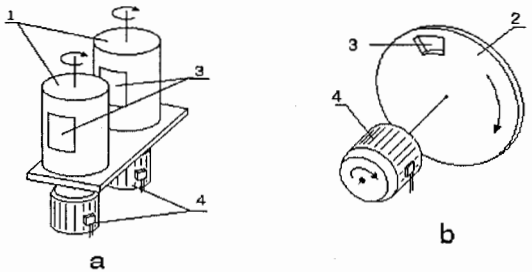


Fig. 1. 1) – drum chopper, 2) – disk chopper, 3) - window, 4) - motor

The drum type chopper rotates along the vertical axis. The neutron beam is opened in the form of a special window, two times per turn. The "drum" is filled with a special material, which is nontransparent for the neutron beam.

The disk-type chopper rotates along the horizontal axis. If the disk has one window, the disk window opens one time per turn. The disk is made of a material, which is nontransparent for neutrons.

A specialized controller /4/ made on the basis of micro-controller M167 is used as main element of chopper phase regulating system.

1. Processing of input signals of chopper period and phase stabilization system

The system has the following input signals:

- - reactor starts, which are synchronous with neutron bursts, are a generator for chopper control system;
- - selector pulses, which are synchronous with a turn of neutron beam chopper.

Continuous adjustment of the mutual arrangement of reactor start pulse and selector pulse is achieved by means of software-hardware delays of start and selector respectively. The initial delay value is set by 15-digit controller switch with a resolution of 10 μs.

Reactor/selector delay can be changed during the experiment. For this purpose, a corresponding parameter in ROM of the block should be changed either on the front panel or by means of PC program.

In order to be able to increase the chopper turn number, the parameter of selector pulse number per one turn is introduced. The latter allows, if necessary, to proceed to a higher number of chopper turns by means of the software.

2. Real-time registrations of selector and start

Real-time clock and its overflow pulses – 210|420 ms are used to determine the location of starts and selectors on the real-time scale.

At arrival of reactor start or selector, the registers/locks fix their location in the real time tr and ts. Based on data received, the start and selector registration system defines the sequence of their appearance and calculates the period of starts Tr and selectors Ts, as well as the mismatch of start and selector – the phase (tr-ts).

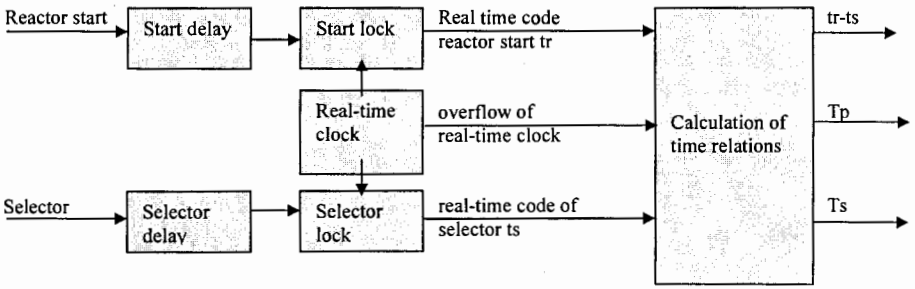


Fig. 2. Block diagram of processing of control system input signals

3. Block diagram of period and phase PID- regulators

At speed-up stage, the output voltage increases linearly until reactor period and chopper period are equal. Period stabilization regulator functions in a range of greater deviations, and phase stabilization regulator works in a range of smaller mismatches.

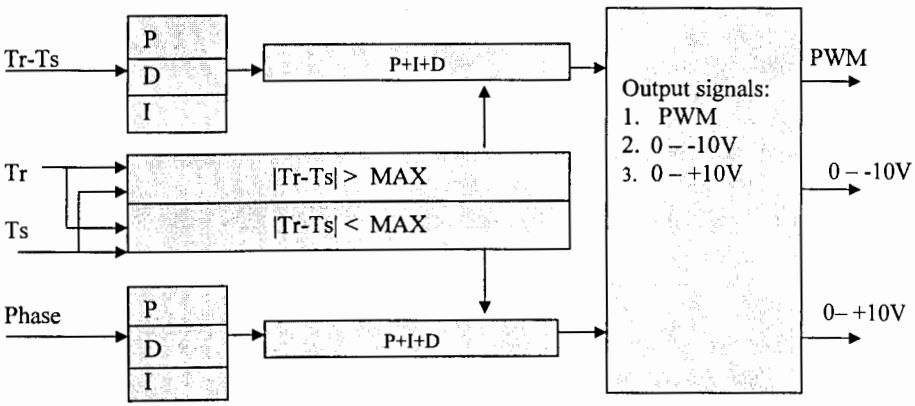


Fig.3. PID – regulators block diagram for chopper period and phase stabilization system

The input mismatch of chopper period regulator is the mismatch (Tr-Ts). The input signal of chopper phase regulator is the phase (tr-ts).

4. P and D components of phase regulation PID - law

The factors before PID-components of regulation law are broken functions, which change the slope depending on the mismatch. The value of control voltage has a limit, and it has a linear dependence in the smaller deviations range.

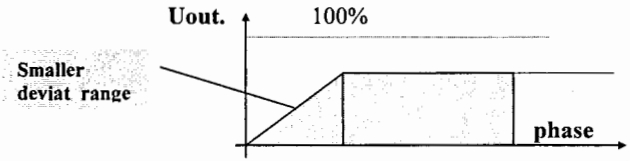


Fig. 4. P and D as a function of phase of components of PID –regulation law

5. Integral component of phase regulation of PID - law

In greater deviations range, the integral component changes with a constant velocity in order the phase changes slowly and gradually.

In smaller deviations range, the factor before the integral component is constant in order to provide for better sensitivity and to decrease the static phase error.

In medium deviations range, the linear factor dependence before integral component versus mismatch provides for the time reduction of entrance into smaller deviations range.

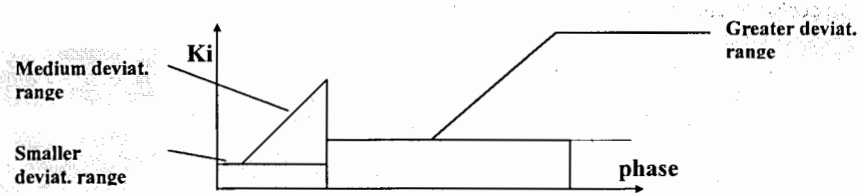


Fig. 5. Dependence of factor before integral component of PID-regulation law on phase mismatch

6. Pulse integral component of PID "phase" regulation law

To improve the accuracy of chopper phase maintenance on the background of a constant integral component, the pulse {**P+D+I** (pulse component)} with a duration of about 10% of a period is formed, which increases the resolution of control by 10 times and upgrades the accuracy of stabilization.

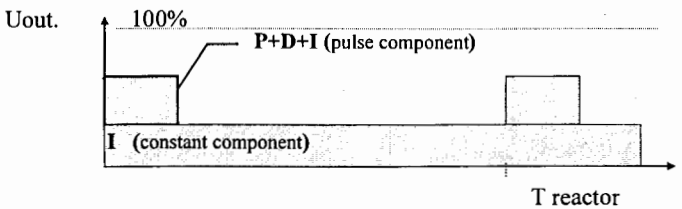


Fig. 6. Output voltage diagram of PID regulation law

7. Pulse-width modulator (PWM) and amplifiers

The control impact is programmed as pulse-width modulator with a resolution of – 50 ns and a number of regulation channels equal to 4096:

- PWM (external source – up to 100V, switching current – up to 10A, frequency – 5kHz);
- Analog signals from 0 up to +10B and from 0 up to -10V.

8. Block adjustment for a particular chopper

The block has its serial number (0-99) in order it can be addressed, if several choppers are connected to one PC port.

Each chopper has its serial number (0-15) of control parameters array in the ROM block. Thus at the start of the block, the program employs the parameters of an object, which were preselected during adjustment.

**Conclusion**

The chopper controller has the following features:

1. Simple control by the operator;
2. Accumulation of statistics on the quality of system operation:
   - chopper phase distribution diagram;
   - maximal deviations of chopper phase;
   - number of starts, which have been lost for accumulation etc.
3. An access to chopper control functions from the side of experiment control routines:
   - control of starts or selector delays;
   - change of chopper rotation velocity etc.
4. Control from the front panel is possible;
5. All blocks are interchangeable (the parameters for control program are selected from the ROM by the set number of a chopper);
6. Accuracy of stabilization is:
   - 25-30 μs at the chopper rotation rate of 300 Hz and 600 Hz;
   - 2-7 μs at the chopper rotation rate of 1500 Hz and 3000 Hz.

The control system of the neutron beam chopper presented in the given paper has been in service over a long period of time on channels 2, 4, 5, 7, 8, 9, 10, 11, 12 and 6b of the IBR-2 reactor.

**References**


[1] A.K. Popov et al., Relay system of phasing for a rotating disk selector driven by asynchronous motor, JINR communication, 13-10640, 1977, Dubna, 16p.

[2] V.N. Kriyuchkov et al., Microprocessor system for neutron beam chopper, JINR communication, 11-84-794, Dubna, 1984, 8p.

[3] V.M. Morozov et al., Twinned rotating collimator system for spectrometer DIN-2K, IPPE communication, IPPE-2506, Obninsk, 1996, 8p.

[4] JSC "KASKOD", Airborne and industrial electronics, Moscow, 1996.

## INDEX of REPORTERS

| | | | |
|---|---|---|---|
| Prikhodko Alexey | JINR | alexey@weblabpratory.ru | 227 |
| Rukoyatkina T.V. | JINR | rukoyt@sunse.jinr.ru | 134,144 |
| Russsakovich Nikolai | JINR | main@jinr.ru | 162 |
| Sedykh George | JINR | eg0r@bk.ru | 134,144 |
| Shiyakova Mariya | JINR | maria@jinr.ru | 111 |
| Sidorova Irina | JINR | irina.sidorova@gmail.com | 243 |
| Silaev Alexey | MEPhI, Russia | allx14@ya.ru | 54,247,250 |
| Simakov Andrey | MEPhI, Russia | simakov@mephi.ru | 253 |
| Sirotin A.P. | JINR | sirotin@nf.jinr.ru | 301 |
| Slavnic Vladimir | IP, Belgrade, Serbia | slavnic@scl.rs | 257,286 |
| Stetsenko Mikhail | JINR | mike@intergraphics.ru | 49,70 |
| Talyshev Alexey | INP, Novosibirsk, Russia | talyshev@inp.nsk.su | 265 |
| Tarasov Vladimir | JINR | tarasov@sunse.jinr.ru | 134 |
| Tikhonenko Elena | JINR | eat@cv.jinr.ru | 129 |
| Tsiskaridze Vakhtang | SU, Tbilisi, Georgia | vakhtang.tsiskaridze@cern.ch | 273 |
| Tsyganov Yuri | JINR | verbilky@list.ru | 220,229,232, 278,281 |
| Verhoglyadov Alexandr | JINR | verhoglyadov_al@mail.ru | 238 |
| Voinov Alexey | JINR | voinov_2000@mail.ru | 229 |
| Volkov Yury | MEPhI, Russia | volkov@eldep.mephi.ru | 247,250 |
| Vudragovic Dusan | IP, Belgrade, Serbia | dusan@scl.rs | 286 |
| Zager Valery | JINR | valery@jinr.ru | 29 |
| Zhuravlev V.V. | JINR | zhur@nf.jinr.ru | 84 |
| Zlokazov Victor | JINR | zlokazov@nf.jinr.ru | 220,281 |
| Zrelov Petr | JINR | zrelov@jinr.ru | 111 |
| Zhuravlev V.V. | JINR | zhur@nf.jinr.ru | 301 |

Научное издание

**Nuclear Electronics & Computing (NEC'2009)**

*Proceedings of the XXII International Symposium*

**Ядерная электроника и компьютинг (NEC'2009)**

*Труды XXII Международного симпозиума*

E10,11-2010-22

Сборник отпечатан методом прямого репродуцирования
с оригиналов, предоставленных оргкомитетом.

Ответственная за подготовку сборника к печати *Е. А. Федорова.*

Подписано в печать 08.04.2010.
Формат 60 × 90/16. Бумага офсетная. Печать офсетная.
Усл. печ. л. 19,0. Уч.-изд. л. 33,11. Тираж 200 экз. Заказ № 56110.

Издательский отдел Объединенного института ядерных исследований
141980, г. Дубна, Московская обл., ул. Жолио-Кюри, 6.
E-mail: publish@jinr.ru
www.jinr.ru/publish/